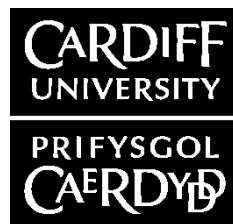


Ryanodine receptors: next generation of insecticide targets

Submitted as a part of PhD degree (Medicine)

Bartłomiej Jakub Troczka

December 2013



DECLARATION

This work has not previously been accepted in substance for any degree and is not concurrently submitted in candidature for any degree.

Signed Date

STATEMENT 1

This thesis is being submitted in partial fulfillment of the requirements for the degree of PhD.

Signed Date

STATEMENT 2

This thesis is the result of my own independent work/investigation, except where otherwise stated. Other sources are acknowledged by explicit references.

Signed Date

STATEMENT 3

I hereby give consent for my thesis, if accepted, to be available for photocopying and for inter-library loan, and for the title and summary to be made available to outside organisations.

Signed Date

Abstract/ Summary

Ryanodine receptors (RyRs) are calcium channels located on the endo(sarco)plasmic reticulum of muscle cells and neurons. They are the largest ion channels known made up of four monomers, each 565kDa in size. Mammals have 3 different RyR isoforms, encoded by different genes, while insects express only one isoform of the receptor, which is only 46% similar (at the amino acid level) to its mammalian counterpart(s). RyRs function to regulate the release of luminal Ca^{2+} stores into the cell cytoplasm and play a key role in muscle excitation-contraction coupling (ECC). The plant alkaloid ryanodine, from which the receptor derives its name, has been investigated extensively as a potential pest control agent, but to date no commercial products have been identified. Recently two synthetic insecticides selectively targeting pest RyRs were introduced to the market. These compounds belong to the novel group of insecticides called diamides.

In this study two insect ryanodine receptors were isolated sequenced and cloned into suitable expression vectors from economically important pests *M. persicae* and *P. xylostella* to identify protein site of interaction for the novel compounds. Both proteins were expressed in HEK 293 cells and Sf9 cells and analysed for evidence of function using ryanodine binding assays and calcium release imaging. In the case of *M. persicae* RyR the expression level was not sufficient to obtain any functional data. However the expression of *P. xylostella* RyR showed evidence of function in both HEK and Sf9 cells.

Functional studies showed that expressed *P. xylostella* RyR can bind [^3H] ryanodine and respond to various caffeine concentrations; the protein was also sensitive to both diamide compounds. DNA sequencing of RyR from field evolved diamide resistant strains of *P. xylostella* identified a mutation causing amino acid change G4946E. Functional analysis of modified RyR construct in Sf9 cells showed significantly reduced sensitivity to both diamide compounds while retaining caffeine and ryanodine sensitivity comparable to the expressed WT form.

Acknowledgments

Completion and submission of this doctoral thesis would not have been possible without the help and support of the kind people around me. Primarily I would like to thank my partner Hannah Davies for her unconditional support and great patience. I also want to thank my parents, who were always there for me during the last four years.

My gratitude goes to my excellent supervisory team; Prof. Lin Field and Martin Williamson at Rothamsted, Prof. Alan Williams and Dr. Christopher George at Cardiff university and Dr. Peter Luemen and Dr. Ulrik Ebbinghaus-Kintscher at Bayer CropScience. Their knowledge and experience was invaluable. Above all I would like to thank my co-supervisor at Rothamsted Research Dr. Emyr Davies for his time and patience during the last four years, without his support I would not have been able to complete this work.

I would like to acknowledge the technical, financial and academic support provided by Rothamsted Research and Cardiff University. And I would like to thank the BBSRC and Bayer CropScience for providing the funding.

I also would like to thank all current and former members of the Insect Molecular Biology group in Rothamsted; particularly Dr. Joanna Amey for looking after me during my first steps in the lab, Dr. Chris Bass for help and advice with qPCR techniques and Dr. Joel Gonzalez for technical advice. I also want to thank members of Alan Williams' group in Cardiff University; especially Lowri Thomas, Sam Mason and Cerdric Viero for their support during my visits to the Cardiff laboratories. The same thanks go to members of the Bayer CropScience team, who provided great support during my time in Monheim.

Last but not least I have to mention my friends and fellow PhD students Steph Heard, Jen Postles, Tristan Eagling, Helen Carter, Joe Helps, Trish Wells, Laura Erdmanis, Alix Blockley and Selcan Alptekin, for many great laughs and excellent Friday nights in the Rothamsted Pavilion.

Any short-comings and errors that remain in this work are solely my responsibility.

Table of Contents

| | |
|--|-------|
| List of Figures | XIII |
| List of tables..... | XVIII |
| Chapter I | 1 |
| 1.1 Global pest control and food security | 1 |
| 1.2 Insect control and synthetic insecticides | 2 |
| 1.2.1 Diamide insecticides | 4 |
| 1.3 Vertebrate ryanodine receptors – genes, proteins, distribution, function and role in calcium homeostasis | 8 |
| 1.3.1 Overview of Ca ²⁺ homeostasis in cells | 8 |
| 1.3.2 Overview of RyR isoforms | 11 |
| 1.3.3 Excitation contraction coupling (ECC)..... | 12 |
| 1.3.4 Role of RyRs in disease | 13 |
| 1.3.5 RyR protein structure and function..... | 15 |
| 1.4 Modulation of RyRs..... | 20 |
| 1.4.1. Ryanodine receptor macro molecular complex components | 20 |
| 1.4.2. Low molecular weight modulators | 25 |
| 1.5 Invertebrate RyRs | 28 |
| 1.5.1 Gene | 28 |
| 1.5.2 Functional studies | 29 |
| 1.6 Aims of this project..... | 32 |
| Chapter II: General methods | 33 |
| 2.1 General..... | 33 |
| 2.2 Insect material..... | 33 |
| 2.3 RNA extraction | 34 |
| 2.3.1 E.Z.N.A® mollusc RNA kit..... | 34 |
| 2.3.2 Isolate RNA mini kit..... | 35 |
| 2.3.3 TRiazol® reagent RNA extraction..... | 35 |
| 2.4 Synthesis of cDNA | 36 |

| | |
|--|----|
| 2.4.1 SuperScript® III..... | 36 |
| 2.4.2 RevertAid™..... | 36 |
| 2.5 Polymerase Chain Reaction (PCR)..... | 37 |
| 2.5.1 Primer design..... | 37 |
| 2.5.2 PCR with proof reading enzymes..... | 37 |
| 2.5.3 Colony PCR..... | 38 |
| 2.5.4 Analytical agarose gel electrophoresis..... | 38 |
| 2.6 Purification of PCR products..... | 39 |
| 2.6.1 Gel purification..... | 39 |
| 2.6.2 Column purification..... | 40 |
| 2.6.3 Phenol-chloroform purification..... | 40 |
| 2.6.4 Precipitation with NH ₄ OAc..... | 41 |
| 2.7 Molecular cloning and Bacterial transformation..... | 41 |
| 2.7.1 pCR-XL TOPO kit..... | 41 |
| 2.7.2 CloneJET™ PCR cloning kit..... | 41 |
| 2.7.3 Bacterial transformations..... | 42 |
| 2.7.4 Propagation of expression vectors..... | 42 |
| 2.8 Analysis of transformants..... | 43 |
| 2.8.1 Plasmid purification (mini-preps)..... | 43 |
| 2.8.2 Restriction digests..... | 44 |
| 2.8.3 Sequencing..... | 44 |
| 2.8.4 Maxi preps..... | 45 |
| 2.9 Site-directed mutagenesis..... | 46 |
| 2.10 Insect cells..... | 47 |
| 2.10.1 Starting insect cell cultures from frozen stocks..... | 47 |
| 2.10.2 Propagation of insect cell cultures..... | 47 |
| 2.11 Propagation of HEK 293 cell cultures..... | 48 |
| Chapter III: Molecular cloning and characterization of insect ryanodine receptors..... | 49 |
| 3.1 Introduction..... | 49 |

| | |
|---|----|
| 3.2 Methods and results | 50 |
| 3.2.1 Creation of databases of available RyR protein and cDNA sequences..... | 50 |
| 3.2.2 Amplification of <i>Myzus persicae</i> RyR gene fragments | 52 |
| 3.2.3 Sub-cloning <i>M. persicae</i> RyR fragments | 54 |
| 3.2.4 <i>M. persicae</i> RyR fragment assembly | 55 |
| 3.2.5 Sub-cloning and analysis of <i>M. persicae</i> RyR PCR fusions | 56 |
| 3.2.6 Assembly and propagation of the <i>M. persicae</i> RyR in pcDNA 3.1(-) | 57 |
| 3.2.7 Modification of pcDNA 3.1(-) to insert eGFP sequence | 61 |
| 3.2.8 Modification of <i>M. persicae</i> RyR and assembly of eGFP fusion in pcDNA 3.1(-) | 62 |
| 3.2.9 Assembly of eGFP tagged <i>M. persicae</i> RyR construct in a vector for expression in insect cells..... | 63 |
| 3.2.10 Quantitative RT-PCR..... | 65 |
| 3.2.11 Amplification and cloning of <i>Plutella xylostella</i> RyR fragments | 66 |
| 3.2.12 Obtaining <i>P. xylostella</i> RyR gene ends by RACE | 70 |
| 3.2.13 Amplification and sub-cloning fragments of full-length <i>P. xylostella</i> RyR..... | 71 |
| 3.2.14 Modification of sub-cloned <i>P. xylostella</i> RyR fragments | 74 |
| 3.2.15 Assembly of <i>P. xylostella</i> RyR in expression vectors..... | 75 |
| 3.2.16 Deletion mutants of the <i>P. xylostella</i> RyR..... | 77 |
| 3.3 Discussion..... | 78 |
| 3.3.1 <i>M. persicae</i> RyR | 78 |
| 3.3.2 <i>P. xylostella</i> RyR..... | 81 |
| 3.3.3 General remarks | 84 |
| Chapter IV: Functional expression of insect ryanodine receptors | 85 |
| 4.1 Introduction..... | 85 |
| 4.2 Methods..... | 86 |
| 4.2.1 Transfections..... | 87 |
| 4.2.2 Optimization of transfection methods..... | 88 |
| 4.2.3 Analysis of transfected cells | 89 |
| 4.2.4 Microscopy | 93 |

| | |
|---|-----|
| 4.2.5 Membrane solubilisation and sucrose gradient purification | 96 |
| 4.2.6 Single channel recordings | 97 |
| 4.3 Results and Discussion | 97 |
| 4.3.1 Expression of the <i>Myzus persicae</i> RyR..... | 97 |
| 4.3.2 Expression of the <i>P. xylostella</i> RyR..... | 101 |
| 4.3.3 Modification of the <i>P. xylostella</i> RyR constructs | 108 |
| 4.3.4 Expression of untagged modified <i>P. xylostella</i> RyR in HEK 293 | 109 |
| 4.3.5 Expression of untagged modified <i>P. xylostella</i> RyR in Sf9 cells..... | 110 |
| 4.3.6 General remarks | 118 |
| 4.4 Conclusions..... | 119 |
| Chapter V: Characterization of diamide insecticide resistance in <i>P. xylostella</i> | 120 |
| 5.1 Introduction..... | 120 |
| 5.1.1 <i>Plutella xylostella</i> | 120 |
| 5.1.2 Insecticide resistance in <i>P. xylostella</i> | 121 |
| 5.2 Methods..... | 122 |
| 5.2.1 <i>P. xylostella</i> strains | 122 |
| 5.2.2 Sequencing of TM region of <i>P. xylostella</i> RyRs..... | 122 |
| 5.2.3 DNA extractions and <i>TaqMan</i> assay..... | 123 |
| 5.2.4 Modification of the WT <i>P. xylostella</i> untagged constructs..... | 125 |
| 5.2.5 Expression of G-E <i>P. xylostella</i> RyR in Sf9 cells | 125 |
| 5.3 Results and discussion | 125 |
| 5.3.1 Bioassays..... | 125 |
| 5.3.2 Sequencing of transmembrane region..... | 126 |
| 5.3.3 <i>In silico</i> characterization of the RyR G4946E substitution..... | 129 |
| 5.3.4 <i>TaqMan</i> assay | 132 |
| 5.3.5 Expression of the <i>P. xylostella</i> RyR G4946E in Sf9 cells | 134 |
| 5.3.6 Ryanodine binding assay | 136 |
| 5.4 General remarks | 137 |
| Chapter VI: General Discussion | 139 |

| | |
|--|-----|
| 6.1 Identification, cloning and analysis of insect RyRs | 139 |
| 6.2 <i>In vitro</i> expression of insect RyRs | 141 |
| 6.3 Emergence of resistance to diamides, identification of the diamide binding site and implications for resistance management | 142 |
| 6.4 Future work..... | 144 |
| Appendix A: Media and buffers recipes | 146 |
| 1. Bacterial media recipes | 146 |
| 2. Calcium phosphate transfection solutions..... | 147 |
| 3. Hypo-osmotic buffer (per 1 litre)..... | 147 |
| 4. Western blots gel/buffers | 147 |
| 5. [³ H] Ryanodine binding assay buffers | 148 |
| 5.1 Filter disc assay binding buffer (per 1litre)..... | 148 |
| 5.2 96 well filter plate assay buffers | 149 |
| 6. Solubilisation and gradient buffers | 150 |
| 7. Electrophoresis buffers | 150 |
| 8. Calcium imaging solutions | 151 |
| Appendix B: Vector maps..... | 152 |
| Appendix C: Primer sequences | 154 |
| 1. Vector and eGFP tag specific primers | 154 |
| 2. <i>M. persicae</i> RyR sequencing primers | 154 |
| 3. <i>M. persicae</i> RyR mutagenesis and cloning cassette primers | 155 |
| 4. <i>P. xylostella</i> RyR sequencing primers | 156 |
| 5. <i>P. xylostella</i> mutagenesis and modification primers..... | 157 |
| References..... | 158 |

List of Figures

| | |
|--|----|
| Figure 1 Global sales of insecticides showing market share for different chemical classes [16] (Original Source: Agranova, Orpington, Kent, United Kingdom, http://www.agranova.co.uk/awa10.asp)..... | 4 |
| Figure 2 Chemical structures of diamide insecticides: A: Flubediamide (phthalic diamide), B: Chlorantraniliprole, C: Cyantraniliprole (anthranilic diamides)..... | 5 |
| Figure 3 Diagrammatic representation of the main components involved in free Ca ²⁺ entry into, and removal from, the cell cytosol. NCX –sodium calcium exchanger, VOCs- voltage gated channels. PMCA – plasma membrane calcium pump, ER/SR-endoplasmic / sarcoplasmic reticulum, cADPr - cyclic adenosine diphosphate ribose..... | 10 |
| Figure 4 Progress of TM helix prediction in mammalian RyR from (1) the four transmembrane helices in Takeshima <i>et al.</i> 1989 [99] (2) much less stringent TM helix assignment in Zorzato <i>et al</i> [100] (3) the most complex model in Du <i>et al.</i> [98] (4) High-resolution electron microscopic images of single channels identified 5 main TM helices in the channel [87, 96]. TM1 is inconsistently predicted in various models..... | 18 |
| Figure 5 Ryanodine receptor macromolecular complex (adapted from Song <i>et al</i> [90]) showing the predicted sites of protein interaction with the closed rabbit RyR1 superstructure (seen from the side). PP1/SP- Protein phosphatase 1/Spinophilin; DHPR – dihydropyridine receptors, CLIC2 -Chloride intracellular channel 2. D1-D3 represent divergent regions associated with RyR channelopathies, red numbering indicate individual domains, described in detail in Song <i>et. al.</i> The TA indicates transmembrane domain. For further information on proteins not mentioned in the text (PR130, CLIC2, HRC, Homer, SA100A1, mAKAP, PP1/SP, Calumenin) see [90]..... | 21 |
| Figure 6 Chemical structure of ryanodine..... | 27 |
| Figure 7 left- Five overlapping PCR fragments of the <i>M. persicae</i> RyR run on a 1% (w/v) TAE-agarose gel. Lanes: A) GeneRuler™1Kb DNA ladder, 1) N6a 2) N6b 3) C4Kb 4) LNK1 5) LNK2 right – N6Kb overlap extension PCR. Lanes: A) GeneRuler™ 1Kb DNA ladder, 1) N6kb. | 53 |
| Figure 8 1% (w/v) TAE agarose gel of 4 overlap extension PCR products (as described in Table 2). | 56 |
| Figure 9 Summary of the cloning strategy used for assembly of full-length <i>M. persicae</i> RyR in the expression vector pcDNA 3.1(-). | 60 |
| Figure 10 Summary of techniques used to remove the Kozak sequence and generate a short linker between the <i>M. persicae</i> (mRyR) START codon and eGFP sequence in the pcDNA-eGFP fusion construct..... | 63 |

Figure 11 Summary of the strategy used to introduce insect RyRs into a modified pIZ vector for expression in insect cell lines. The NruI site had to be engineered into the empty pIZ vector. 64

Figure 12 Summary of the amplification of *P. xylostella* RyR in order to obtain sequence of the receptor to devise cloning strategy. Top: The 3 initial small fragments amplified by degenerate PCR, which were cloned and sequenced to provide information for gene specific primer design for. (Bottom) 2 large fragments spanning the gaps between the initial small fragments. The extreme 5' and 3' ends missing approximately 100bp were obtained through RACE. 69

Figure 13 Diagram of the sequencing strategy for the two large *P. xylostella* RyR fragments. Fragments were first cloned and initially sequenced using vector specific primers. All subsequent overlapping primers were designed based on collected information for the sequencing results using upstream (for the 5' end) and downstream (for the 3'end) primers, until entire fragment have been sequenced. 70

Figure 14 Summary of *P. xylostella* RyR fragments used for the full-length assembly. Nterm and Cterm fragments were generated as initial sub-fragments fused together using overlap extension PCR to give the final product. Gel images: L - GeneRuler 1Kb ladder. Gel 1: lanes 1 and 4 = positive controls (REDtaq®), lane 2 = fragment M1, lane 3 = fragment C2. Gel 2: lane1 = fragment M2, lane 3 = fragment C1, lane 5= fragment N1, lane 6 = fragment N2..... 73

Figure 15 Summary of the restriction enzymes used to recover *P. xylostella* RyR fragments from the pJET1.2 vector (table) and a gel image of a ligation of all 4 fragments with the pcDNA-eGFP vector..... 76

Figure 16 Summary of the construction of *P. xylostella* RyR deletion mutants containing 963bp of the N-terminus (N-term) of *P. xylostella* RyR fused to the transmembrane (Tm) domain, using digestion with XbaI. 77

Figure 17 Summary of the relative expression of the RyR gene in different life stages of *M. persicae* clone 4106A. The apterous adult stage was used as a reference. There was no significant difference observed between all tested life stages. The data is presented as a mean of 3 biological and technical replicates with 95% confidence intervals. 81

Figure 18 Sequence alignment (using Geneious v6.05) of all of the *P. xylostella* RyR fragments generated for RyR cDNA assembly versus the initial sequencing results obtained early in the project. Gray bars represent sequence covered; names of individual cloned fragments are shown on the left. Black vertical lines represent individual SNPs, some of these could be attributed to the errors made by a low fidelity taq used to generate the reference sequence. Black horizontal lines represent individual splice sites. Top bar shows the scale numbering individual positions every 1000bp. 83

| | |
|---|-----|
| Figure 19 Graphical representation of known diamide sites of interaction on the model insect ryanodine receptor based on <i>B. mori</i> RyR expression. | 86 |
| Figure 20 Perfusion chamber setup with a glass U-tube applicator for recording of multiple agonist applications. Black arrows indicate flow of Ringer’s solution, which allows for a constant replacement of solution in the perfusion chamber. Agonist solutions are applied via the glass U-tube, where flow is controlled by recording software (VisiView®) or the electrical switch on the the peristaltic pump. When the U-tube flow is stopped, agonist present inside the tube diffuses over the cells by seepage through the application hole. | 95 |
| Figure 21 Low magnification images, using a Zeiss Axio Vert microscope (x10 objective), showing HEK 293 cells calcium phosphate transfected with A: human e-GFP-RyR2 fusion plasmid and B <i>M. persicae</i> eGFP-RyR plasmid. Images on the right are of the bright field view..... | 99 |
| Figure 22 Low magnification images, using Zeiss Axio Vert microscope (x10 objective), showing HEK 293 cells Effectene® transfected with A: human eGFP-RyR2 fusion plasmid B: <i>M. persicae</i> eGFP-RyR fusion plasmid. Images on the right show the bright field view. | 100 |
| Figure 23 Western blot of membrane preparations from HEK 293 cells expressing 1) the <i>P. xylostella</i> eGFP-RyR deletion mutant transfected with calcium phosphate, 2) <i>M. persicae</i> eGFP-RyR transfected with calcium phosphate 3) <i>P. xylostella</i> eGFP-RyR 4) human eGFP-RyR2 transfected with calcium phosphate (positive control). Ladder markers are indicated with arrows. The result shows a large molecular weight band in lane 3, similar in size to the human RyR2 control and the expected molecular weight for the deletion mutant protein in lane 1. 50µg of mixed-membrane preparation was loaded onto each lane. | 102 |
| Figure 24 <i>In vivo</i> , high magnification, images, obtained using x63 lenses on a Leica SP5 microscope, of HEK 293 cells expressing A) <i>P. xylostella</i> eGFP-RyR fusion protein, B) <i>M. persicae</i> eGFP-RyR fusion, C) human eGFP-RyR2 fusion (kindly provided by Dr Lowri Thomas, Cardiff University) (pictures on the right show bright field view of imaged cells). The eGFP signal is excluded from the nucleus (white arrows) in all 3 images; however the cells expressing insects RyRs do not exhibit the “spider-web” like pattern of expression seen with the human RyR2 construct (C). | 103 |
| Figure 25 Low magnification images of transfection experiments for the expression of the <i>P. xylostella</i> eGFP-RyR fusion protein in Sf9 cells (bright field view showed on the right). Panels: A) control plasmid carrying only the eGFP sequence (1µg of DNA), B) large amounts (15 µg) of plasmid DNA were required to achieve good transfection efficiency, C) addition of PLUS™ reagent improved the efficiency and decreased (8 µg) the amount of plasmid DNA needed. White square indicate the size of the imaged used for counting the efficiency..... | 105 |

Figure 26 High magnification in vivo images of Sf9 cells expressing the *P. xylostella* eGFP-RyR fusion protein, using a Zeiss 780LSM microscope (x63 lens). Arrows indicate two populations of cells with (1) a diffused cytosolic signal and (2) a more reticular globular signal distribution. The image on the right shows a fluorescent-bright field overlay showing that the expression efficiency is good, with approximately 46% of cells containing eGFP signal..... 107

Figure 27 Responses in individual HEK 293 cells transfected with *P. xylostella* - untagged RyR and loaded with Fluo-3 AM dye, after addition of 20mM Caffeine dissolved in DMEM. Data collected from a single experiment represents one field of view using x63 lenses..... 109

Figure 28 Activation of individual Sf9 cells expressing modified *P.xylostella* RyR using 20mM caffeine. Cells were loaded with FLUO-3 AM and the spike in fluorescent 20mM caffeine dissolved in Sf-900 II media was added to the dish. Like HEK cells cells did not show fast return of the signal to the baseline level. Data collected from a single experiment represents one field of view using x63 lenses..... 111

Figure 29 Fluorescence ratios measured over time in single calcium release experiment using Fura 2 AM. Panels A-D show mean \pm standard error responses of the same cells (n=8) to A 10mM caffeine, B 30 μ M diamide analogue, C 10 μ M flubendiamide and D 30mM caffeine - application of flubendiamide abolishes further caffeine responses, suggesting an irreversible binding. The picture on the left shows a snapshot of cells during fluorescence ratio measurement, using x40 lens and an excitation wavelength of 380nm..... 114

Figure 30 A single channel trace obtained from a bi-layer experiment showing a 'ryanodine receptor-like' channel incorporated into a membrane. The recording was done in a 4:1 KCl (~850:210mM) gradient between cis and trans chambers when a mixed membrane preparation from Sf9 cells expressing WT *P. xylostella* RyR was applied. The currents seen are due to the chemical gradient rather than holding potential, no agonists were tested. Histogram analysis of the trace indicated that the channel was mostly in a closed state with no visible sub-conductance states. Graph represents a single experiment. No further studies were attempted. The graph represents a single experiment; no further replications were conducted..... 116

Figure 31 Binding saturation curve for WT *P. xylostella* RyR (expressed in Sf9 cells) challenged with titrated ryanodine. Each point on the graph represents the average of 3 replicates \pm S.E.M..... 117

Figure 32 *P. xylostella* life cycle. Photographs provided by Mark Mallot. 120

Figure 33 Nucleotide alignments of the TM region around the mutation site (altered coding triplet highlighted in black) from 4 strains of *P. xylostella*, using the Wang *et al* [165] RyR sequence (GenBank: AET09964.1) as a reference. The alignment highlights individual SNPs - it is clear that the SNP profile is different for the Sudlon and ThaiR strains. 128

Figure 34 Amino acid alignments of the region of the RyR channel spanning the resistance-associated mutation G4946E (marked with an arrow). GenBank accession numbers for each sequence can be found in Chapter III section 3.2.1. For the purpose of clarity the alignment does not include the alternatively spliced isoforms and protein sequences available in the DuPont patent (US2007/0105098A1) and other mammalian RyRs. The glycine (G) residue is found in all species apart from nematodes and crustaceans. 130

Figure 35 *P. xylostella* RyR TM domain topology map, predicted using a hidden Markov modelling approach [220]. Individual TMs are labelled as in the cryo-EM images of the pore and TM region of RyR1 [87]. The amino acid residues at each end of the helices are numbered according to the RyR cDNA sequence described in this study. The location of the resistance-associated mutation is indicated with an arrow. 132

Figure 36 Representative *TaqMan* traces for the ThaiS strain showing the homozygous WT allele (blue), heterozygous resistant allele WT/resistant (green), and homozygous resistance allele (red). 133

Figure 37 Normalized A340/A380 nm fluorescence intensity ratios measured for Sf9 cells expressing *P. xylostella* RyR G4946E in a single Ca²⁺ release experiment using FURA 2 AM. Panels A-C show mean ±standard error responses of the same cells (n=8) 72h post transfection to A 30mM caffeine, B 10µM flubendiamide, C 30mM caffeine. Binding of flubendiamide appears to be abolished by the presence of the mutation. 135

Figure 38 Normalized A340/A380 nm fluorescence intensity ratio measurements for Sf9 cells expressing *P. xylostella* RyR G4946E in a single Ca²⁺ release experiment using FURA2 AM, 96h post transfection. n=8 cells. Panel A. 100µM chlorantraniliprole, Panel B. 30mM caffeine after exposure to chlorantraniliprole. A high dose of chlorantraniliprole is able to induce a response in cells expressing the G4946E channel and abolish subsequent release of calcium by caffeine. 136

Figure 39 Saturation curve fitted to data obtained for the binding of ryanodine to *P. xylostella* RyR G4946E expressed in Sf9 cells. Each data point is a mean of 3 replicates± S.E.M 137

List of tables

| | |
|--|-----|
| Table 1 Summary of low molecular weight pharmacological modulators affecting RyRs ... | 25 |
| Table 2 Comparison of RyR protein sequences of various insects shown as % identity..... | 29 |
| Table 3 List of species with available RyR protein and DNA sequence | 51 |
| Table 4 List of primers used for amplification of <i>M. persicae</i> RyR fragments | 53 |
| Table 5 Summary of <i>M. persicae</i> RyR fusion PCRs | 56 |
| Table 6 <i>M. persicae</i> qPCR primers..... | 65 |
| Table 7 List of degenerate primers used for amplification of <i>P. xylostella</i> RyR fragments .. | 67 |
| Table 8 List of RACE primer sequences | 70 |
| Table 9 List of sequenced splice sites..... | 74 |
| Table 10 SNPs in the <i>M. persicae</i> RyR sequence (DuPont data versus experimental results) | 78 |
| Table 11 Composition of transfection reactions | 89 |
| Table 12 summary methods of individual transfection experiments done for <i>M. persicae</i> constructs in HEK 293 cells..... | 97 |
| Table 13 Results for individual filter discs titrated [³ H] ryanodine binding assay | 115 |
| Table 14 Primer pairs used for amplification and sequencing of TM and N-terminal regions of <i>P. xylostella</i> RyR | 123 |
| Table 15 <i>TaqMan</i> assay probe and primer sequences..... | 124 |
| Table 16 Log-dose probit-mortality data for two diamide insecticides tested against 2 nd /3 rd instar larvae of <i>P. xylostella</i> in a leaf-dip bioassay (72h) as presented in [19]..... | 126 |

Chapter I

1.1 Global pest control and food security

There are many challenges facing modern agriculture today, for example, an estimated increase in the global population to 9 billion by 2050, climate change and limited arable land and water supplies. Historically, the major problem for agriculture was insufficient yields leading to food shortages. However, a series of research initiatives and technology transfer programmes in the second half of 20th century, commonly referred to as the Green Revolution, not only introduced new practices in how food is produced but also shifted the perception of agriculture as a subsidiary sector to a highly commercial one. In developed countries this resulted in a steady surplus in food production and removed the threat of food shortages. It was also one of the contributing factors which led to the sustained increase of the human population since the 1960's to over 7 billion today [1, 2]. However, according to the FAO (Food and Agriculture Organisation), the continued sharp increase in population growth and dietary changes in emerging economies (high meat and milk demand) will require a further 70% increase in overall food production by 2050. This means that we will need to increase cereal production by one third from today's 2.1 billion tonnes to 3 billion tonnes worldwide [3]. Additionally, the expansion of biofuels as an alternative energy source and the decrease in quality of arable land due to climate change and pollution are problems which will need addressing [2]. It is believed that we are at the dawn of a second Green Revolution, which will increase the productivity and sustainability of agriculture not only by improving crop yield but also by decreasing losses and minimizing adverse environmental impacts, resolving the issue of world hunger and closing the income gap between urban and rural areas [4]. It is hoped that these ambitious goals are going to be achieved by optimising the management and use of current technologies, and by the introduction of new technologies through continuous research and development driven by private sector and government programmes [4].

Effective pest control is one of the interventions currently employed to minimize crop losses and increase agricultural output. Since the Green Revolution there has been a big increase in the use of synthetic pesticides to control insects, weeds and

fungi and this, together with improved agricultural practices and crop varieties, has resulted in more than a doubling in crop production in the last 50 years [4]. Despite the increased use of crop protection methods, yield losses to pests remains one of the main challenges for agriculture. The exact percentage of yield loss is dependent on the region and the type of crop planted, with the average potential loss being 35% [5]. It was estimated that in 2007 the global pesticide market was worth \$29 billion US dollars with insecticides making up approximately 28% of this total. It was also noted that the demand for biologically active chemicals was likely to rise [6]. A recent market forecasting report by BCC research (<http://www.bccresearch.com/report/download/report/chm029d>) estimates that the global pesticide market was worth \$37.5 billion in 2011 and \$46.1 billion in 2012, with the total market value expected to reach \$65.3 billion in 2017 [7]. One of the main drawbacks of increased chemical pesticide usage is the associated risks for adverse environmental impacts. Unintended environmental consequences can often not be predicted or foreseen, as in the case of early synthetic insecticides such as DDT [8]. The second problem for pesticide sustainability is the development of resistance in target pests due to a high selection pressure imposed by frequent (and in many cases misapplied) spraying. For insecticides, it is estimated that around 600 insect and mite species are resistant to at least one class of currently used commercial compound [9]. Thus there is a need for the development of novel methods of pest control and for the discovery of new and safer insecticidal chemistries with improved efficacy and toxicological profiles. In the meantime, an understanding of insecticide resistance mechanisms and of the mode of action of approved pesticides can often lead into development of useful diagnostic tools for monitoring resistance in the field and thereby provide opportunities to enhance and sustain pest management strategies globally, by giving updated advice to farmers and growers on which chemicals they should deploy to best effect.

1.2 Insect control and synthetic insecticides

The two major strategies currently deployed to control insect pest populations are biological control agents and synthetic insecticides. Biological control includes the use of the insects own natural enemies to reduce population size and / or the

introduction of pathogens to kill the insect [10]. One of the most successful biological agents used to control some lepidopteran species is a gram positive bacteria, *Bacillus thuringiensis*. This produces *cry* toxins which are the main source of its insecticidal activity and can be used as a supplement or alternative treatment to synthetic insecticides [11]. Over the past ten years, genes for the production of *cry* toxin have been successfully engineered into crops such as tobacco, cotton or maize for better protection against insect pests, reducing the need for insecticide treatment [12, 13]. Despite some notable successes achieved by utilizing biological agents, by far the most widely used control measures at present still involve deployment of synthetic compounds. The discovery of the insecticidal properties of DDT in the early 1940's [14, 15] subsequently led to the large scale use of chemical insecticides to control pests in agriculture. Today, most commercially available insecticides on the market act on one of 5 main targets: chitin synthesis, mitochondrial respiration, the voltage-gated sodium channel, the nicotinic acetylcholine receptor and the γ aminobutyric acid (GABA) receptor. Of these, only 4 classes of insecticides targeting the latter 3 sites have managed to achieve major commercial success. The current bestselling insecticides belong to the neonicotinoid, pyrethroid and organophosphate classes of chemistry (Figure 1). All 3 groups exploit different targets on the insect nervous system [16].

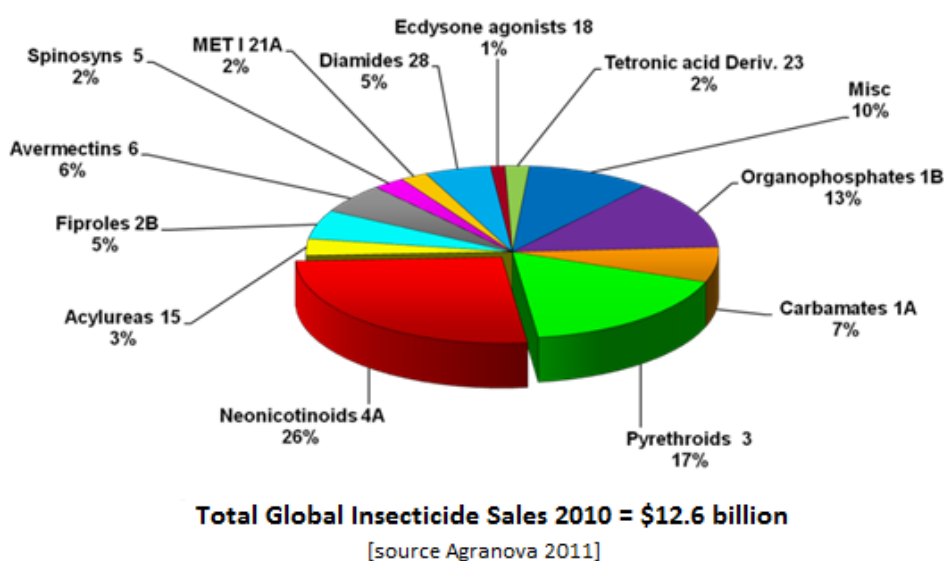


Figure 1 Global sales of insecticides showing market share for different chemical classes [16] (Original Source: Agranova, Orpington, Kent, United Kingdom, <http://www.agranova.co.uk/awa10.asp>).

1.2.1 Diamide insecticides

Diamides are a relatively new class of synthetic insecticides which cause an uncontrolled calcium release within insect muscle cells and disrupt the insect's intracellular calcium homeostasis through selectively targeting and activating ryanodine receptors (RyRs), giving symptoms of poisoning including feeding cessation, muscle paralysis and death [17, 18]. The 3 main compounds belonging to this class are flubendiamide, chlorantraniliprole and cyantraniliprole (Figure 2).

Since their recent introduction to the market in 2007, diamides have been a great commercial success (Figure 1), with sales of chlorantraniliprole alone reaching \$500 million US dollars in 2011 [19]. Up until the introduction of diamides, there has been no successful commercialisation of insecticides targeting the RyR or any other aspects of cell calcium signalling and homeostasis [17]. Ryanodine, a plant alkaloid extracted from the South American shrub *Ryania speciosa*, has been used as a botanical insecticide for almost 60 years. However, its high toxicity to mammals makes it unsuitable for wide-scale use [20] (<http://www.epa.gov/oppsrrd1/REDS/factsheets/2595fact.pdf>) (A more detailed description of the mode of action of ryanodine on the RyR channel is described in section 1.7.2). Attempts to create commercial compounds based on ryanodine [21], with an improved toxicological profile towards vertebrates, have had only moderate success. Ryanodol and 9,21-didehydroryanodol have low vertebrate toxicity, but did not become economically important chemicals [22]. 9,21-didehydroryanodol, unlike ryanodine, does not cause muscle contraction but rather inhibits contraction through the modulation of potassium channels [21]. Another unrelated compound, Verticilide (isolated from *Verticillium sp*), has 10x higher affinity towards cockroach RyR over a mouse RyR1 isoform; however the nature of the interaction with RyR is unknown [23].

The successful commercialisation of flubendiamide by Nihon Nohyaku and Bayer Crop Science in 2007, followed by chlorantraniliprole by DuPont a year later [24],

led to the creation of a new mode of action group (Group 28) by the Insecticide Resistance Action Committee (IRAC) [22].

Since the introduction of these novel insecticides to the global market a number of other diamide derivatives have been developed such as anthranilic isophthaloyl amides and anthranilic diamides containing alkyl ether group, some showing high insecticidal potency [24-26].

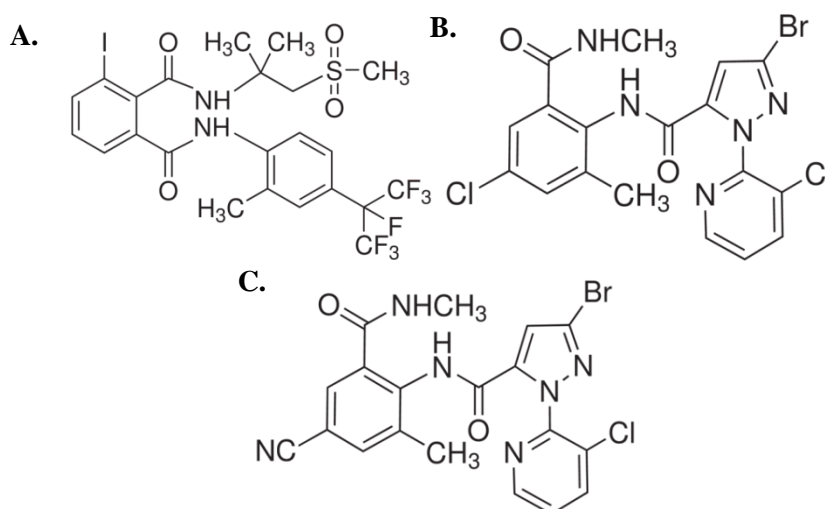


Figure 2 Chemical structures of diamide insecticides: A: Flubendiamide (phthalic diamide), B: Chlorantraniliprole, C: Cyantraniliprole (anthranilic diamides)

The exact site of interaction of flubendiamide, chlorantraniliprole and cyantraniliprole with the RyR is unknown but it is thought that they compete for the same binding site [27]. However, a radio-labelled binding study of flubendiamide and chlorantraniliprole on muscle membranes isolated from the house fly, *Musca domestica*, suggested binding to two distinct but allosterically coupled sites [28]. Neither insecticide negatively interferes with ryanodine binding, implying a different site of interaction for this well-known pharmacological probe [29]. Analysis of binding of flubendiamide to *Bombyx mori* (silk worm) RyR identified a region close to the N-terminus (between amino acids 183-290) important for channel sensitivity to flubendiamide; however the actual binding site was identified as being somewhere within the C-terminal transmembrane region, between amino acids 4111–5084. This was confirmed by construction of a chimeric RyR containing an insect cytosolic region and a rabbit transmembrane region, which did not show responses to flubendiamide in calcium release assay but could be activated by caffeine [30].

One of the most interesting features of the diamides is their exceptional activity against insects and their very low mammalian toxicity. Studies performed on cell lines expressing mammalian RyR isoforms showed a lack of, or very limited, response even to high doses of diamides [17, 29, 31]. Both classes of diamides (phthalic acid and anthranilic diamides) also exhibit very good eco-toxicological profiles, posing only small risks to beneficial insects such as parasitic wasps, ladybirds, predatory mites and pollinators at field application rates [32, 33]. Up to date individual case studies looking into impact of chlorantraniliprole on non-target organisms showed little or no effect [34]. However more in-depth studies are needed of the sublethal effects, of these new insecticides, on the non-target organisms including economically important beneficial insects such as pollinators (bees and bumblebees). Side effects of insecticidal sprays became important due to recent research results into the detrimental sublethal effects of neonicotinoid class of insecticides and their potential involvement in colony collapse disorder in honey bee *Aphis mellifera* [35]. Since the introduction of these novel compounds to the worldwide market, a number of field studies analysing the efficacy of diamides have been reported [36]. Also baseline susceptibilities in some target pest species, including *Plutella xylostella* (diamondback moth) [37], *Tuta absoluta* (tomato leafminer) [38] and *Spodoptera litura (lis)* (cotton leafworm) [39] have been established. Despite the great success of diamides, their use now appears compromised in some situations where there have been reports of resistant insect populations. In China, 20 populations of *P. xylostella* were reported to show decreased sensitivity to diamides and 6 populations showed a level of resistance as high as 2000-fold when compared to a susceptible laboratory strain [40]. The first published report of a strain of *P. xylostella* with a target-site mutation associated with a high level of diamide resistance is detailed in chapter V.

1.2.1.1 Flubendiamide

The initial lead to the discovery of flubendiamide (a benzenedicarboxamide or a phthalic acid diamide) came from the pyrazinedicarboxamide herbicide program of a Japanese company, Nihon Nohyaku [18]. The compound was then co-developed by them and Bayer CropScience, after it displayed excellent potency towards a broad range of lepidopteran species. Initial studies of the symptoms of poisoning disclosed

gradual contraction of the lepidopteran insect body without convulsions, suggesting a novel mode of action manifested outside of the central nervous system and similar to symptoms observed for ryanodine [41]. Flubendiamide also demonstrated good control of lepidopteran populations already resistant to existing classes of insecticides, with bioassays on *P. xylostella* larvae resistant to pyrethroids, organophosphates, carbamates and benzoylphenylurea (chitin synthesis modulator) giving a level of control equal to the susceptible strain, with no cross resistance apparent. The novel compound also exhibited very low mammalian toxicity, with an acute LD₅₀ in rats of >2000 mg/kg and a consistent lack of mutagenic properties [41]. More detailed investigation of the mode of action of flubendiamide, by analysis of its effects on isolated gut muscles from the tobacco budworm *Heliothis virescens*, showed no muscle contraction in response to stimuli, whilst maintaining nervous system activity. The molecular target was identified to be the RyR through fluorescent calcium release assays done on (i) single *H. virescens* neurons [29, 31] and (ii) CHO cells (Chinese Hamster Ovary) expressing *Drosophila melanogaster* RyR [29, 31]. Additionally, flubendiamide was shown to have a stimulating effect on Ca²⁺ pump activity, revealing a close relationship between luminal calcium concentration and activation of calcium pumps, and the negative effect of insecticide binding on cellular Ca²⁺ homeostasis [42]. The high specificity of flubendiamide towards insect channels was also confirmed by calcium release assays on different mammalian cell lines naturally expressing various isoforms of the receptor [31]. There are no reported flubendiamide effects on plants in literature found up to date. However since higher plants do not have direct homologues of RyRs [43]; it is unlikely any obvious negative effects could be predicted. Thus, flubendiamide became first the commercial synthetic insecticide with a novel mode of action targeting RyRs, and it entered the market in 2007 [16, 24].

1.2.1.2 Chlorantraniliprole and Cyantraniliprole

Chlorantraniliprole (an anthranilicdiamide), developed by DuPont Crop Protection, shows broader insecticidal activity in comparison to flubendiamide, giving good control not only of Lepidoptera but also Coleoptera (beetles), Diptera (flies) and Isoptera (termites) species [18]. Like flubendiamide, chlorantraniliprole has an excellent toxicological profile, with an LD₅₀ value of acute oral toxicity of

>5000mg/kg of body weight for vertebrates, and has a high efficacy on insects resistant to other classes of insecticides [18]. In cellular assays it was not active against mammalian RyR1 and RyR2 isoforms and showed up to 2000-fold decreased potency towards RyR2 in comparison to insect channels [18]. Apart from the high potency of chlorantraniliprole towards larval stages of many important lepidopteran pests it also exhibits mating disruption at sub-lethal doses, as demonstrated in the codling moth *Cydia pomonella* L. Male insects exposed to the insecticide's residues exhibited significantly reduced activity leading to smaller number of successfully mated females [44]. Identification of the molecular target of chlorantraniliprole was described in detail by Cordova *et al* [17]. The dorsal vessel (heart) and skeletal muscles from *Manduca sexta* (tobacco hornworm) showed an adverse contractility effect on exposure to diamides. Plasma membrane calcium channels were ruled out as a potential diamide target by analysis of the change in intracellular Ca^{2+} concentrations in *Periplaneta americana* (American cockroach) neuron preparations in calcium-free conditions during exposure to anthranilamides. The RyR was identified as the actual target by calcium release imaging done on Sf9 cells expressing *D. melanogaster* RyR and by radiolabeled ryanodine and diamide binding studies on *P. americana* leg muscle membrane preparations [17, 45].

Cyantraniliprole belongs to the same family of compounds as chlorantraniliprole but its insecticidal activity is much broader, affecting both chewing and sucking pests from the Orders Coleoptera, Lepidoptera and Hemiptera [46]. Its modified structure improves its mobility through the plant xylem, so it can be applied as a systemic insecticide [24, 47]. Both chlorantraniliprole and cyantraniliprole bind to a site on the RyR distinct from the binding site for ryanodine and their presence increases the likelihood of ryanodine binding [28].

1.3 Vertebrate ryanodine receptors – genes, proteins, distribution, function and role in calcium homeostasis

1.3.1 Overview of Ca^{2+} homeostasis in cells

Maintenance of low levels of free Ca^{2+} in the cell cytosol is crucial in maintaining normal cell function (Figure 3). In mammalian cells at normal resting state the free cytosolic Ca^{2+} concentration is approximately 100 nM and cells use a lot of energy, and a number of specialized proteins, to maintain this [48, 49]. There are precise and

diverse mechanisms enabling Ca^{2+} to enter the cytosol, involving chemical signals or changes in the membrane potential. The two main sources of entry for free Ca^{2+} into cells are via the extracellular space and from internal stores [49].

Differences in Ca^{2+} concentration across the cell membrane creates an electrochemical gradient which is exploited by various types of calcium channels located on the plasma membrane. The best characterised channels are voltage operated channels (VOCs) such as L-type channels (described in more detail in section 1.4.2) and receptor operated channels (ROCs), which respond to various external signals. There are also other less well characterised entry mechanisms such as store operated channels (SOCs) [50]. When the Ca^{2+} channels open there is a rise in cytosolic Ca^{2+} concentration, which triggers various physiological responses. Upon entry into the cytosol the Ca^{2+} binds to a wide array of calcium binding proteins, for example in humans there are approximately 200 genes encoding such proteins which act as Ca^{2+} buffers and effectors [51].

Release of Ca^{2+} from internal stores in the ER/SR is regulated mainly by two channel proteins, inositol 1,4,5 triphosphate receptors (IP_3Rs) and RyRs. IP_3Rs rely on the secondary messenger molecule inositol 1,4,5 triphosphate (IP_3) for activation [48, 52] and play numerous roles in cells during development. RyRs are closely related to IP_3Rs , however their regulation and function differs substantially [53, 54]. The IP_3Rs , like RyRs, are homomeric tetramers, however they are smaller than RyRs, with approximately 2700 amino acids per sub-unit [55]. There is a high degree of conservation between IP_3Rs and RyR transmembrane regions, with over 30% amino acid identity [56]. RyRs are also essential for normal body development and function [57] (described in more detail in section 1.3.3).

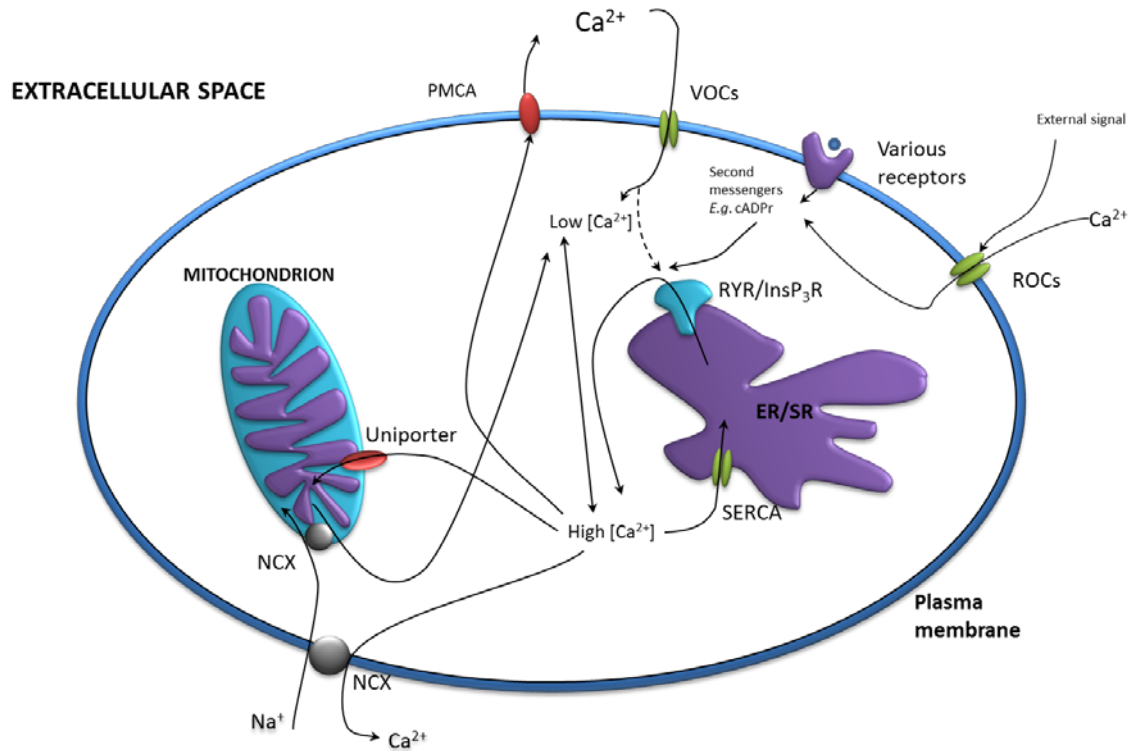


Figure 3 Diagrammatic representation of the main components involved in free Ca^{2+} entry into, and removal from, the cell cytosol. NCX –sodium calcium exchanger, VOCs- voltage gated channels. PMCA – plasma membrane calcium pump, ER/SR-endoplasmic / sarcoplasmic reticulum, cADPr - cyclic adenosine diphosphate ribose.

The removal of Ca^{2+} from cells is facilitated by a number of pumps and exchangers and is a crucial step to maintain the low resting Ca^{2+} concentration required for activation of different cellular processes like exocytosis, contraction, transcription, metabolism, and proliferation. There are four mechanisms which facilitate this, the $\text{Na}^+/\text{Ca}^{2+}$ exchanger (NCX), the plasma membrane Ca^{2+} ATPase pump (PMCA), Ca^{2+} ATPase located on the sarco(endo)plasmic reticulum (SERCA) and the mitochondrial uniporter [49]. The high concentration of Ca^{2+} inside the ER/SR lumen is maintained by SERCA and Ca^{2+} sequestering proteins located inside the ER such as calsequestrin (CSQ) [58].

Because free Ca^{2+} is an important secondary messenger, micro and macro changes of local, or global, concentrations, as well as the spatial distribution of Ca^{2+} triggers different physiological responses which are essential for a number of cellular functions, such as the activation of ion channels, neurotransmitter release, neuronal degeneration, gene transcription, cell apoptosis and cell proliferation [22, 48, 58]. All

of these functions exhibit different response dynamics ranging from less than a millisecond (in the case of exocytosis) to hours (transcription or proliferation). The kinetics of ion transport for proteins involved in the Ca^{2+} mediated processes are tailored to the required rates, and the level of expression of individual protein components is important as well as the types of isoforms present. For example various types of PMCAs respond differently to a sudden increase in Ca^{2+} [59]. Most of our knowledge of Ca^{2+} homeostasis comes from studies of vertebrates, but some aspects of calcium signalling have been studied in insects, predominantly the model organism *D. melanogaster*, which offers a simpler system with a wide range of genetic and molecular tools for manipulation of different components of calcium signalling. Unlike mammals, *D. melanogaster* tends to have only one homologue for each of the major calcium signalling components [60].

1.3.2 Overview of RyR isoforms

There are 3 RyR isoforms in mammals, with tissue specific distributions. RyR1 (skeletal) is highly expressed in striated skeletal muscle cells in the gap between the transverse tubule of the sarcolemma and the sarcoplasmic reticulum (SR) [61], RyR2 (cardiac) is found in cardiac muscle cells and RyR3 (brain) is present at relatively low levels (no more than 5% of the total number of RyRs in the cell) in striated muscles as well as neurons and other tissues [58]. The receptors were first identified on electron micrographs of frog twitch fibres as ‘foot’ structures located in the triads between the T-tubules and the SR [62]. Since their discovery, they have been isolated and purified from muscle membrane fractions and their Ca^{2+} release channel properties verified experimentally [63, 64]. Advance in molecular biology has allowed the cloning and expression of genes encoding RyRs [65] and an overview of methods and published records of the first successful attempts to clone various RyR genes is described in chapter III section 3.1. Non-mammalian vertebrates have only two isoforms known as α -RyR and β -RyR whose functions can be compared to RyR1 and RyR3 respectively and are expressed in equal amounts in muscle cells [66, 67].

In humans the 3 *RyR* genes are present on different chromosomes, *RyR1* on 19q13.2, *RyR2* on 1q43 and *RyR3* on 15q13.3-14. All 3 are complex genes with over 100 exons (104-RyR1, 102-RyR2, 103-RyR3) encoding the full-length cDNA of

approximately 15Kb [68]. The three mammalian RyRs share approximately 65% amino acid identity. It is well established that RyR1 and RyR2 are essential for normal body function and development, with knockout mice lacking the gene encoding either of the receptors either dying in embryonic development (in the case of RyR2) due to heart abnormalities [69] or immediately after birth (RyR1), due to muscle defects [61, 70]. Interestingly RyR3 does not seem to be critical for normal body function, since knockout mice do not exhibit developmental abnormalities and are able to reproduce normally [54]. All the RyRs are also expressed in non-muscle related body tissues such as the liver or nerve cells [58] and the different isoforms of RyR have different properties depending on which tissue they are expressed in. In addition splice variation can occur within isoforms, and these also show tissue specific expression [52]. All this leads to receptor diversity and variability in the response of different cells to the same factors, which may cause variable results in studies of RyRs.

1.3.3 Excitation contraction coupling (ECC)

Excitation contraction coupling is the process linking the electrical stimulation of skeletal and cardiac muscle to muscle contraction. The mechanisms of ECC vary between skeletal and cardiac muscle but both involve the release of free Ca^{2+} into the cytosol from SR stores via RyRs. Free Ca^{2+} is directly responsible for the activation of the myo-filaments that cause contraction [65, 71].

In skeletal muscle cells, ECC occurs by a "mechanical coupling" mechanism involving protein-protein interaction between RyR1 and L-type Ca^{2+} channels (also called dihydropyridine receptors DHPRs) located on transverse (T-) tubules of the plasma membranes. Action potential leads to activation of voltage sensing DHPRs [72] and direct interaction of DHPR α -subunit intracellular loops II and III with the cytosolic domain of RyR1 during successful depolarisation triggers a release of luminal Ca^{2+} by RyR1. This increases the speed of receptor response to exogenous stimuli leading to faster muscle contraction [58]. In the case of RyR2 a significant Ca^{2+} elevation in the cytosol, is required for its activation [52]. There is substantial experimental evidence that apart from free Ca^{2+} cyclic adenosine diphosphate (ADP)-ribose is also an endogenous RyR activator, regulating sensitivity threshold for CICR, a phenomenon first described in sea urchin eggs [49, 73].

In cardiac muscle cells there is no association of L-type Ca^{2+} channels and RyRs and activation occurs via calcium induced calcium release (CICR). Small amounts of Ca^{2+} enter the cell through DHPRs, bind to the nearest RyR2 channel and result in activation. Two to four calcium ions are enough to trigger a full RyR2 response and neighbouring channels are activated either by elevated local Ca^{2+} concentrations or by a coupling/gating within the RyR2 array (see more section 1.3.5.4) [71].

There is still no consensus regarding the termination of Ca^{2+} release during ECC. Various mechanisms have been proposed but none have been proven experimentally to be correct. The shutting down of Ca^{2+} release is imperative for muscle relaxation and in the case of the heart, the diastole phase [65]

1.3.4 Role of RyRs in disease

To date the majority of research on RyRs has focused on mammalian isoforms, particularly RyR1 and RyR2, due to their involvement in human disease and the search for potential therapeutic agents. Mutations and small in-frame deletions in genes encoding these RyRs are associated with an array of clinically distinct diseases. It has been shown that these are clustered in 3 major hot spots on both RyRs: the N-terminus, the central domain and the C-terminus [74]. Although RyRs are also expressed in neurons and smooth muscles, in these they control Ca^{2+} release in tandem with IP_3Rs , and their dysfunction does not appear to lead to adverse effects [75].

1.3.4.1 RyR1

In humans, point mutations in the *RyR1* gene can cause severe myopathies such as malignant hypothermia (MH), central core disease (CCD), multi-minicore disease (MmD), core-rod myopathy (CRM) and centronuclear myopathy (CNM) [70]. The most widespread and best characterized are MH and CCD. MH is a disorder triggered by volatile anaesthetics, resulting in sustained and uncontrolled Ca^{2+} release from SR, which leads to elevated muscle metabolism causing lactate accumulation and heat production [76]. CCD, a rare disorder resulting in a various degree of muscle weakness during infancy which may persist through adolescence, is recognised by altered morphology of muscle fibres containing “core” lesions, which can vary in intensity and localization [77]. A considerable number of mutations, over

160 for MH and over a 100 for CCD, have been identified and linked to the clinical onset of the disorders, and some are linked with the onset of both MH and CCD. It has been hypothesized that mutations in genes encoding RyR accessory proteins, such as calsequestrin, can also lead to a disease phenotype [78]. There are no clear molecular mechanisms which explain the effects of mutations on RyR1 function in MH, or with the abnormalities in muscle structure seen in CCD [75]. Recently, a number of these mutations have been mapped *in silico* onto known *RyR1* alternative splicing sites, domains involved in channel gating regulation, accessory protein binding sites and regions involved in inter-domain interactions, helping to link disease phenotype with particular RyR regulation mechanisms [79]. Also, knock-in mouse models with mutations inducing both the MH and CCD disorders have been developed and analysed. Various hypotheses regarding the underlying causes of these diseases have emerged from these studies, including oxidative stress due to RyR1 Ca^{2+} leak [80] and ‘mechanical’ stress from abnormal Ca^{2+} release created by formation of wild type/mutant heterotetrameric RyRs [81].

1.3.4.2 RyR2

Mutations in genes encoding RyR2 cardiac channels lead to exercise- and emotional stress- induced Catecholaminergic Polymorphic Ventricular Tachycardia (CPVT) [82]. CPVT causes arrhythmias, which if not treated promptly lead to sudden cardiac death (SCD); the mutations responsible are mainly autosomal and recessive [83]. The main mechanism underlying CPVT is the increased likelihood of delayed after-depolarisations (DADs). During heart relaxation (diastole) DADs can be initiated by a Ca^{2+} leak from the SR through RyRs. If sufficient Ca^{2+} is released into the cytosol after repolarization, but before the next action potential, it causes the sodium calcium exchanger NCX to operate in reverse leading to depolarization, which can spread to neighbouring cells and results in an unsynchronised beat [65].

Heart failure is also caused by dysfunctional RyR2, however the mechanism of Ca^{2+} leak differs from CPVT and it is proposed to be associated with altered Ca^{2+} sensitivity and hyperphosphorylation of the RyR2 [65]. There have been over 150 mutations identified to date in *RyR2* associated with CPVT (<http://www.fsm.it/cardmoc/>). As in the case of the skeletal RyR channelopathies

there is no consensus on the exact molecular mechanism that leads to the clinical manifestations and several hypotheses are proposed [75].

1.3.5 RyR protein structure and function

For the purpose of clarity, the remaining part of Sections 1.3 and 1.4 relate to functional aspects of RyRs and are described collectively for all mammalian isoforms. The available information on invertebrate RyRs is discussed separately in section 1.5.

RyRs form homotetrameric channels, with each individual monomer having a molecular mass of approximately 560kDa (depending on the isoform and species), making them the largest ion channels known to date, with approximately 5000 amino acids per subunit. In comparison its close relative IP3R has only approx. 2600 amino acids per subunit and an entire sodium channel consists of approx. 2000 amino acids [84].

Due to the large size and the intrinsic association with membranes, the crystal structure of an entire receptor has not been resolved. However, there are single particle electron microscopy (EM) density maps at 14Å resolution of an entire RyR1 channel available [85], which were based on results from previous lower 20-30Å resolution studies [86]. Also, a cryo-EM study of the closed state of the RyR1 pore forming domain at 10Å resolution identified some of the secondary structures, although it did not allow the assigning of individual amino acid side chains [87]. Although RyR1 remains the most extensively analysed isoform, there are also electron density maps for RyR2 and RyR3 isoforms [88]. Despite potential structural differences resulting from the 65% amino acid identity between all 3 isoforms, low resolution (23-30Å) EM density maps of all 3 mammalian RyRs look virtually identical [89]. A number of small crystal structures of individual domains were solved which were recently summarized in the attempt to map a 3D model ryanodine receptor macromolecular complex [90]. A more recent crystal structure became available for larger cytosolic domain of of RyR which is associated with diseasecausing mutations [91].

1.3.5.1 Cytosolic domain

It is established that the cytosolic part of RyRs is responsible for the regulation of calcium release; however the precise mechanisms involved in linking cytosolic regulatory sites with modulation of channel gating are yet to be fully determined. Mutations associated with MH in RyR1, especially in the N-terminal and central part of the protein, lead to “unzipping” of the channel and leaky openings, suggesting that these two regions come together in the 3D structure and may regulate channel gating [92]. The cytosolic part of RyRs does not form a rigid structure; instead it has groups of individually folded domains, separated by solvent-filled cavities. In the receptor, the cytosolic parts of four RyR subunits co-assemble to create a central cavity leading to the channel pore [93]. Although RyRs do not bind IP₃, there are structural similarities between the N-terminal part of RyR and the IP₃ binding and the suppressor domains in IP₃Rs, suggesting a conserved regulatory mechanism [94]. It has been demonstrated that co-expression of the transmembrane region of the RyR2 protein with a series of separate regulatory cytoplasmic parts restored some of the channel’s regulatory ability [95]. The cytosolic part acts as scaffold for a number of regulatory proteins and it contains many binding sites for small molecular weight modulators, described in more detail in sections 1.4.1 and 1.4.2

1.3.5.2 The transmembrane domain

RyRs are internal membrane-embedded proteins with a majority of their mass (approximately 4/5ths) found in the cytosol, with the transmembrane (TM) domain accounting for the last 1/5th of the full-length protein [65]. The cytosolic region functions as a regulatory domain with multiple binding sites for various ligands, whilst the TM region incorporates the channel pore (see more detail in the following section) [96]. The TM region of skeletal RyR can be expressed autonomously and forms a functional Ca²⁺ channel sensitive to ryanodine and activation by Ca²⁺; however the regulation of the truncated protein is impaired, for example the channel does not close at high Ca²⁺ concentrations [97]. The functioning and regulation of the TM region of cardiac RyR2 has also been studied by expressing two truncated proteins [95].

The lack of a solved crystal structure for RyR means that the exact number of TM helices has not been confirmed and the precise topology is still disputed. It has been shown that RyRs have an even number of TM helices, since both the N- and C-

termini lie in the cytosolic domain [53, 98]. Different topology models have been proposed with a varying number of TM helices (Figure 4). Early studies suggested that a RyR subunit had 4 TM helices [99]. Subsequently up to 12 TM helices were proposed [100]. A more complicated model with one of the predicted helices forming a loop and the total number of TM helices being 6-8 was also suggested [98]. The most recent cryo-electron microscopy study of a single receptor identified only 5 TM helices and suggested that the additional helices predicted in previous studies are closely associated with the membrane but not integrated within it [53, 87]. It is currently accepted that 6 TM helices are most likely present, making the RyR comparable to IP₃R. Such a 6 TM model was also hypothesised with the first isolation of a cDNA encoding human RyR2 [101]. The TM helices of 4 monomers arranged within a functional tetrameric unit create a central ion-conducting pore through which ions are transported from the SR lumen to the cytosol [99].

The extreme end of the C-terminus of the TM region is important in the formation of fully functional tetrameric channels and expression of the last 100 amino acids of RyR2 shows an ability to create tetramers [102]. Furthermore, deletion of the last 15 amino acids of RyR1 abolishes the ability to form stable channels in lipid bilayers, most probably due to lack of tetramerization [103].

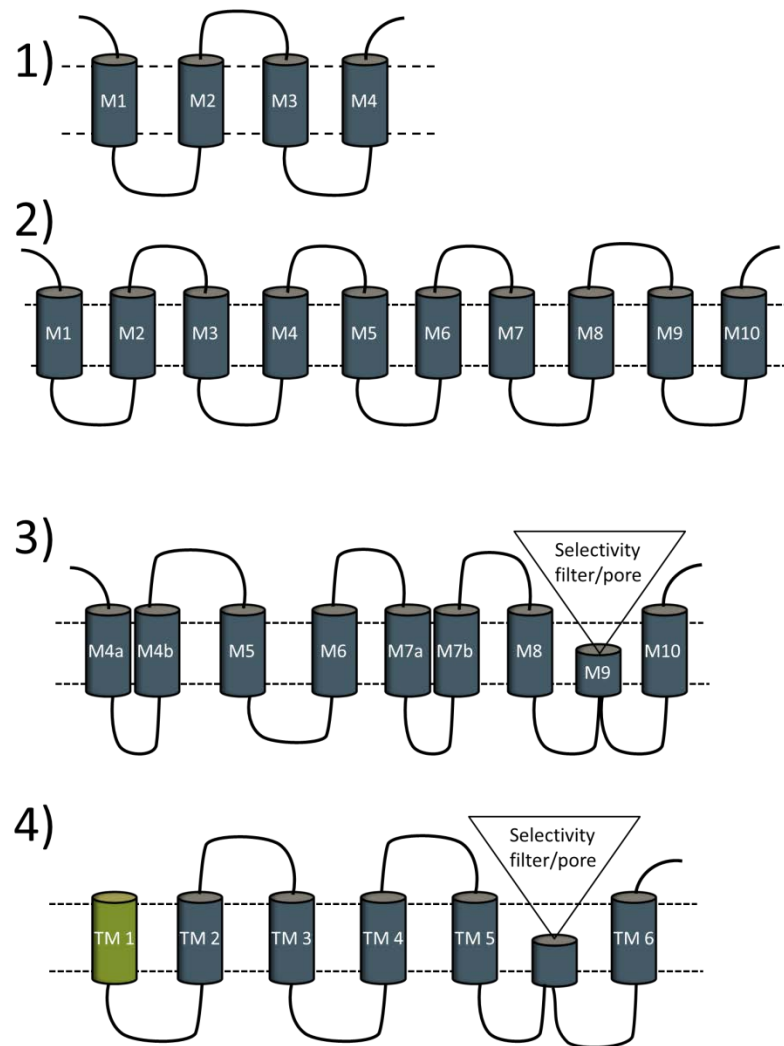


Figure 4 Progress of TM helix prediction in mammalian RyR from (1) the four transmembrane helices in Takeshima *et al.* 1989 [99] (2) much less stringent TM helix assignment in Zorzato *et al* [100] (3) the most complex model in Du *et al.* [98] (4) High-resolution electron microscopic images of single channels identified 5 main TM helices in the channel [87, 96]. TM1 is inconsistently predicted in various models.

1.3.5.3 The pore forming domain

Most experiments to understand RyR structure-function relationships have been done on RyR1, due to its high expression levels in skeletal muscles and relative ease of purification [104]. The first characterization of purified rabbit skeletal RyR showed that the channel is selective toward divalent cations [105]. More detailed studies of RyR2 indicated that the channel was permeable to a wide range of both monovalent and divalent cations, with an approx. 6.5-fold greater preference for divalent [106]. Although direct comparison of different isoforms is difficult, it is

considered that the pore forming regions are largely the same and that they all exhibit a remarkably high rate of ion translocation, approximating to 1ns for monovalent cations [104]. The pore forming region forms an autonomous part of the protein; in the case of RyR1 it was possible to successfully express the pore peptide on its own (amino acids 4829-5037) to generate a functional tetrameric cation channel, albeit lacking regulatory elements [107].

The pore forming domain of RyRs is believed to be made up of the last 3 helices of the TM region of each monomer. In the TM model of Du *et al* [100], helices 8 and 10 correspond to the inner and outer pore lining helices, whilst helix 9 forms a P-loop with a selectivity filter sequence GGGIGD. The selectivity filter was first identified in RyR1 through investigation of an I4898T substitution linked with CCD. The amino acid region surrounding this substitution has distinct similarities to the selectivity filter of bacterial potassium channels such as KcsA [108]. The 3D structure of KcsA has been solved (PDB accession 1BL8), enabling direct comparison with RyRs and allowing a pore homology model for RyR to be produced [109]. Although the overall structures of the RyR and the K⁺ channel pore are somewhat comparable, the ion selectivity mechanisms seem to work in different ways. The selectivity filter of the K⁺ channel is able to distinguish between similar ions like Na⁺ and K⁺, whilst RyR is permeable to various cations. However, such comparative modelling needs to take account of other studies, based on single particle cryo-EM imaging, that suggest that the RyR pore is more similar to another bacterial potassium channel MthK (pdb 1LNQ) [87]. The mechanisms of pore opening and closing are not fully understood. In a recent study, a series of mutations were introduced to pinpoint critical amino acids responsible for the channel gating without altering ion permeation [110].

The importance of other amino acids in the P-loop and neighbouring helices for ion conductance has been studied extensively in RyR1 and RyR2, using site directed mutagenesis. The terminal aspartic acid (D) in the selectivity filter plays a crucial role in ion selectivity [111]. As in potassium channels, the lumenally-orientated part of the RyR pore is negatively charged; however the net potential is much higher in RyRs which may contribute to the very high unitary conductance rate (1nS for RyR against 50-250 pS for K⁺ channel) [70, 109].

1.3.5.4 RyR arrays

Electron microscopy of skeletal and cardiac mammalian muscle tissue reveal that RyR1 and RyR2 form organized 2D arrays; for RyR1 this leads to the formation of tetrads of voltage gated L-type Ca^{2+} channels (DHPRs), through physical interaction with RyR1 receptors. The RyR2 isoform is not physically coupled with plasma membrane Ca^{2+} channels, although it forms 2D arrays, whilst RyR3 fails to create any arrays at all. An absence of RyR1 in the cell stops the organization of DHPRs into tetrads, which implies that RyR1 is an essential component of this structure [58, 112]. The function of array formation is not fully understood but it has been suggested that a specific pattern of organization helps with the regulation and coordination of RyR function. It was speculated that monomers of one channel are allosterically coupled with neighbouring channels [58, 113, 114]. RyR2 forms regular arrays made up of approximately 70-260 individual channels, the number depends on the type of organism; species with a faster heart rate have larger arrays, as was shown in the case of rat and human cardiac myocytes [65, 115].

1.4 Modulation of RyRs

1.4.1. Ryanodine receptor macro molecular complex components

RyRs act as a target and a scaffold for a number of regulatory proteins which interact with the receptor by either direct binding, anchoring other proteins, or covalent modification of the receptor itself (Figure 5). These regulatory proteins can be localized to different parts of the cell including the intra-luminal space (Calsequestrin-CSQ), ER or SR membrane (Triadin and Junctin) and cytoplasm (Calmodulin, FKBP12, protein kinases and phosphatases). The large number of different regulatory proteins creates a very complex picture of RyR regulation and studies of individual components often lead to contradictory results.

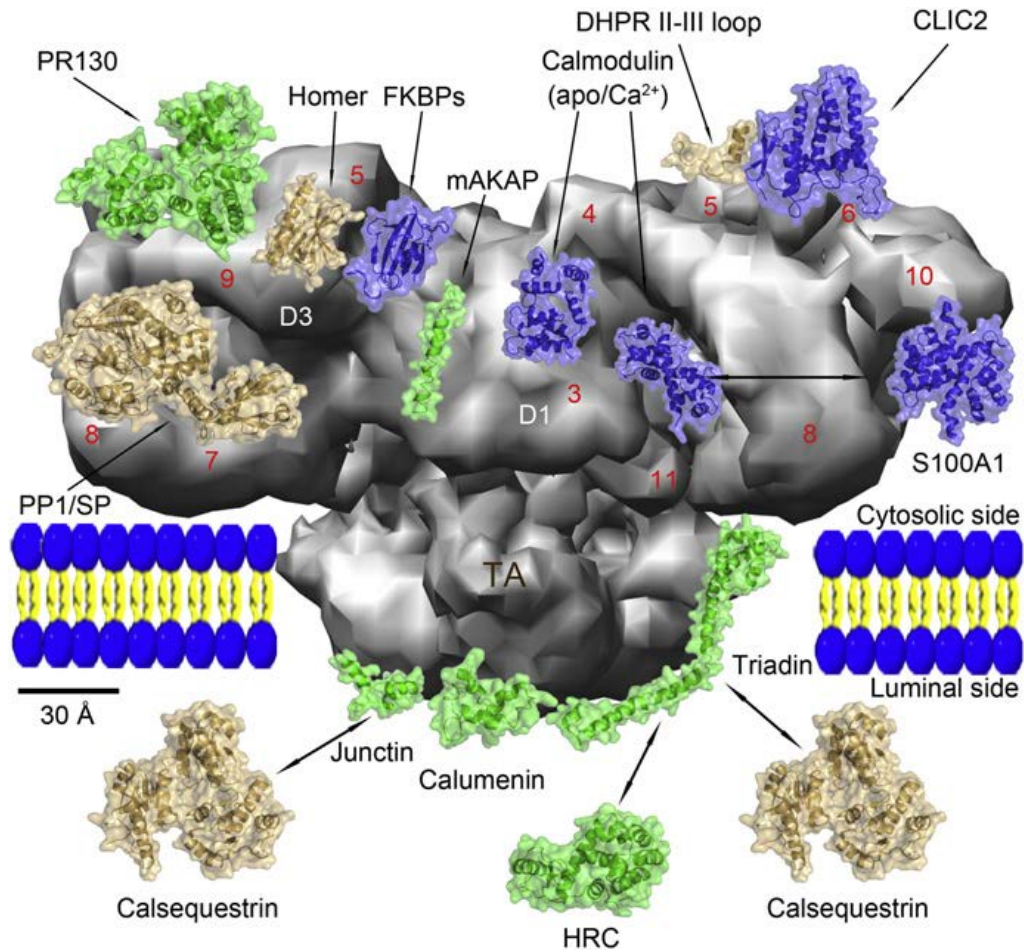


Figure 5 Ryanodine receptor macromolecular complex (adapted from Song *et al* [90]) showing the predicted sites of protein interaction with the closed rabbit RyR1 superstructure (seen from the side). PP1/SP- Protein phosphatase 1/Spinophilin; DHPR – dihydropyridine receptors, CLIC2 -Chloride intracellular channel 2. D1-D3 represent divergent regions associated with RyR channelopathies, red numbering indicate individual domains, described in detail in Song *et. al*. The TA indicates transmembrane domain. For further information on proteins not mentioned in the text (PR130, CLIC2, HRC, Homer, SA100A1, mAKAP, PP1/SP, Calumenin) see [90].

1.4.1.1 Protein kinases and phosphorylation of RyR1 and 2

Phosphorylation of RyRs by different protein kinases has important regulatory functions. Phosphorylation by Protein Kinase A (PKA) leads to an increase in binding of ryanodine [116], and increases the probability of the channel being in the open state by decreasing the binding affinity of FKBP (in RyR1 and 2) [117, 118]. One PKA phosphorylation site (S2809) has been identified in RyR2 and there is a

similar site (S2843) in RyR1 [70, 118]. It is proposed that PKA and CaMKII (Ca²⁺ and CaM dependent) kinases are associated with RyRs through specialized anchoring proteins such as mAKAP (A-kinase anchoring proteins), SP (spinophilin) and PR130 and conserved leucine zippers on the surface of the receptor [52]. Activation of PKA is the outcome of a signalling pathway which begins by activation of β -adrenergic receptors [70]. The CaMKII kinases can phosphorylate both RyR1 and RyR2 at S2843 and S2809 respectively, but there is also a unique site on RyR2 at S2814 [93]. Research suggests that a cardiac isoform CaMKII δ , like PKA, is associated with the RyR2 isoform through accessory proteins and conserved leucine zipper domains [119, 120]. The effects of CaMKII kinases are not fully understood; studies of RyR2 phosphorylation by CaMKII δ showed that it is a potent channel activator, however unlike PKA it does not abolish binding of calstabin (FKBPs) to the receptor [70]. PKA and CaMKII phosphorylation can also protect RyR1 channels from Mg²⁺ inhibition, but also decrease the open state probability of the channel [119]. There is considerable controversy regarding mis-regulation of phosphorylation and its involvement in the symptoms of heart failure. Transgenic mice which overexpress PKA develop cardiomyopathy and arrhythmias [121]. Some studies found that the RyR2 is hyper-phosphorylated in the heart failure animal models; however some found that it remains unchanged. There is also no clear explanation how phosphorylation by PKA and CaMKII δ actually modifies RyR2 gating [65].

1.4.1.2 Calstabins and calmodulin

RyRs have binding sites for the calstabins (FKBP12 and FKBP12.6) and binding of these proteins to the receptor ensures proper transition of the channel from open to closed states. Abolishing FKBP12 binding leads to a prolonged channel sub-conductance state and Ca²⁺ leakage [122]. Unlike RyR1 and RyR3, which interact with both FKBP12 and FKBP12.6, RyR2 binds selectively to the latter [123] and deficiency of FKBP12.6 in heart tissue causes severe cardiac myopathy [119]. Cellular toxicity, caused by expression of RyR2 protein, can be rescued by co-expression of FKBP12.6, further indicating an inhibitory effect of the protein on spontaneous Ca²⁺ release through deregulated RyR2 [124]. It was shown that co-expression of rabbit RyR1 and FKBP12 in insect Sf9 cells leads to stabilisation of

the channel into closed or open states, abolishing the sub-conductance states, whilst also decreasing the channels' sensitivity to caffeine activation. FKBP inhibitors such as rapamycin and FK506 lead to dissociation of FKBP from the RyRs and reversal of the FKBP effects on channel gating [125].

Calmodulin (CaM) is a 17kDa Ca^{2+} binding protein which regulates a number of proteins including RyRs, where one CaM molecule binds to one RyR subunit [126]. Calcium-free calmodulin (apoCaM) act as a channel activator whilst calmodulin with Ca^{2+} bound (CaCaM) is an inhibitor. CaM enhances channel activation at low Ca^{2+} (nanomolar) concentrations and increases channel inhibition as levels of cytosolic Ca^{2+} rise (micromolar) [127]. The calmodulin binding domain on the RyR is located in the cytosolic region, spanning amino acids 3614–3643 in RyR1 and 3583–3603 in RyR2. Mutations in these regions abolish CaM binding [128]. Calmodulin also regulates RyR1 indirectly by binding to DHPR, leading to dissociation of the α -subunit from RyR1 [52]; scorpion toxins also disrupt DHPR-RYR interactions by binding to the same site [70]. Calmodulin binding to RyR2 is important for normal channel function, as demonstrated in a mouse model with mutations within the CaM binding domain where the mice died prematurely due to abnormalities in heart function [129]. Increased dissociation of calmodulin was also found to be one of the mechanisms responsible for heart failure in dogs [130].

1.4.1.3 Triadin, Junctin, Calsequestrin and Sorcin

Triadin (Tr) and Junctin (Jn) bind to the luminal region of RyRs and are involved in anchoring them to Calsequestrins (CSQ), the main Ca^{2+} binding proteins in the SR lumen [131]. CSQs are potent Ca^{2+} chelators; in skeletal muscle one molecule of CSQ-1 is capable of binding 40-50 calcium ions [132]. In vertebrates there are two genes encoding CSQs, associated with skeletal (CSQ-1) and cardiac (CSQ-2) muscles respectively [133]. Interaction between Tr, Jn and RyR is Ca^{2+} independent [134]. CSQs have regulatory effects on RyR channel function; increasing concentration of Ca^{2+} in the lumen leads to saturation of Ca^{2+} binding sites on CSQ and dissociation of the CSQ protein from the RyR complex, which then leads to an induction of free calcium efflux from the SR to the cytosol upon RyR channel activation. At low luminal Ca^{2+} concentrations ($<100\mu\text{M}$) some CSQ remains bound to the Tr/Jn complex, decreasing RyR activity [131, 135]. It is hypothesised that Tr,

Jn and CSQ are all vital for RyR channel regulation and the failure of CSQ to interact with RyR leads to regulation abnormalities. For example, when exposed to isoproterenol a CSQ-2 (cardiac) deficient mouse model displays CPVT-like symptoms, with unchanged basal heart function, increased diastolic Ca^{2+} leak and arrhythmogenic beats [136]. Similarly a CSQ-1 (skeletal) null mutant exhibits malignant hypothermia symptoms upon exposure to anaesthetics [137]. Interestingly, studies of mouse models showed that CSQs are not required for luminal Ca^{2+} sensing, which is contradictory to one of the proposed RyR regulation hypotheses [138].

Another protein involved in RyR2 regulation is Sorcin, which interacts with both RyR and L-type Ca^{2+} channels (DHPRs). The exact site of interaction is unknown, but Sorcin seems to have an inhibitory effect on the channel and it only interacts with cardiac RyRs when free Ca^{2+} levels in the cytosol are high. Calcium binding to Sorcin induces conformational changes in the protein which may increase its interaction with RyR2, leading to channel closure [52, 139]. PKA phosphorylation of Sorcin reverses its effect on cardiac RyRs [140].

1.4.2. Low molecular weight modulators

RyRs are also modulated by a number of low molecular weight compounds (Table 1).

Table 1 Summary of low molecular weight pharmacological modulators affecting RyRs

| Chemical | Effect | Comments |
|--|--------------------------------|--|
| Caffeine and its derivatives e.g. sulmazole | Agonist | Well known channel activator, increasing sensitivity to free Ca^{2+} [141]. |
| Ryanodine | Modulator of ion translocation | Complex effect depending on concentration, encompassing activation (at nM levels) to closure (at μM levels) [141]. Has insecticidal activity. |
| Ruthenium Red | Channel blocker | Acts in a voltage-dependent manner, blocking the pore |
| Dantrolene | SR calcium release inhibitor | Muscle relaxant used to treat malignant hypothermia [142]. |
| Heparin | SR calcium release activator | Activates the channel, possibly by causing a local increase in Ca^{2+} [143]. |
| Peptide toxins | Channel gating modulators | Different effects depending on the toxin, for example, IpTx _a inhibits DHPR-RyR1 interaction [144]. |
| 4-Chloro-m-cresol | Agonist | RyR1 agonist, with evidence of similar effects on other isoforms [145]. |

1.4.2.1 Common RyR modulators

Caffeine, a RyR activator, is found in leaves and seeds of certain plants including coffee and tea, and is used as a popular mild stimulant. It induces Ca^{2+} release by increasing sensitivity of the channel toward Ca^{2+} even at nanomolar concentrations [146], and is responsible for increasing channel open probability in a dose-dependent manner [141]. Some other compounds like sulmazole and its derivatives, e.g. EMD 41000 affect RyRs in a similar way, but their potency is much higher [141]. 4-Chloro-m-cresol (4-CMC) also activates Ca^{2+} release via RyRs. Detailed effects of this ligand have been studied mainly in RyR1, although there is evidence it can modulate other isoforms as well [141, 145]. Like caffeine, it increases the frequency and duration of the channel open state and ryanodine binding, however its potency is approximately 10 times lower, and unlike caffeine it has an ability to modulate the channel from both the luminal and cytosolic sides [145]. Adenine triphosphate (ATP) is also known to be an activator of RyR1 in the presence of micro-molar Ca^{2+} ,

as shown in single-channel bilayer experiments [147]. Recently, 3 regions of the RyR protein were identified to be involved in ATP binding; the N-terminus, central region and C-terminus [148]. In RyR2 it was possible to express the central region independently while retaining the ATP binding capabilities [149]. The only currently used clinical drug targeting RyR is Dantrolene, which is used to treat patients with symptoms of MH. These include sustained uncontrolled release of Ca^{2+} triggered by certain anaesthetics, leading to rapid increase in body temperature, contracture and degeneration of muscles leading to death if untreated. At therapeutic concentrations dantrolene inhibits the uncontrolled release of Ca^{2+} from SR mediated via RyR, and relieving the symptoms of the MH episode [150]. Dantrolene appears to preferentially bind to RyR1, however its lack of apparent effect on other RyR isoforms is inconclusive [141]. It was demonstrated that it can inhibit the activation of RyR1 via Ca^{2+} and CaM [142] and that it has the ability to rescue RyR1 channels containing the R615C MH mutation [151].

1.4.2.2 Ryanodine and its analogues

Ryanodine (figure 6) is the best characterised pharmacological probe binding specifically to RyRs. The dissociation kinetics of ryanodine binding are slow enough for the binding to be considered irreversible in most experimental channel recordings [152]. It has complex effects on channel function, either decreasing or increasing Ca^{2+} permeability depending on concentration [141]. At nanomolar concentrations it increases channel open probability and causes the continuous leak of Ca^{2+} from ER/SR lumen into the cytosol. At micromolar concentrations it causes the channel to close and inhibits the release of calcium [141]. Synthetic ryanodine derivatives (which were an attempt to create insecticides based on the natural product - see Section 1.2.1) resulted in the discovery of compounds with altered association and much faster dissociation kinetics to RyR channels [153].

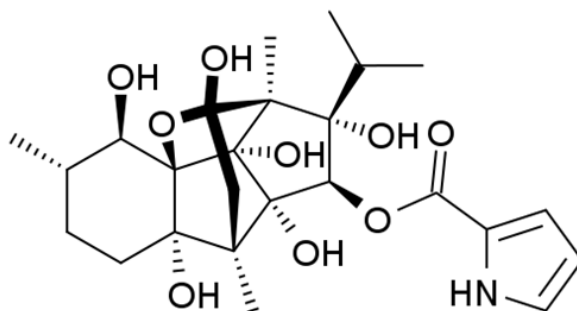


Figure 6 Chemical structure of ryanodine

The binding of ryanodine to RyRs relies on the presence of Ca^{2+} as it can only bind to the open state, and its binding is enhanced by agonists propagating opening of the channel such as caffeine [154], whilst binding is inhibited by Mg^{2+} and Ruthenium red [155]. The investigation of ryanodine binding using radio-labelled ligand has suggested the presence of both high- and low- affinity sites [156], and experiments with photo-affinity probes and proteolysis have located the high-affinity site to the transmembrane region of the protein. Modification of cardiac RyR2 by site directed mutagenesis around the predicted TM 10 region of the Zorzato model (see Section 1.3.5.2) abolished ryanodine binding whilst maintaining sensitivity to caffeine. The alanine to glutamine substitution at position 4863 did not significantly alter the single channel sensitivity to physiological ligands and ion handling properties but did change the affinity of ryanodine and the synthetic ryanoids [157, 158]. Despite an extensive amount of experimental data the exact sites of the ryanodine binding sites remain unknown.

1.4.2.3 Free Ca^{2+} ions

Free Ca^{2+} ions are primary regulators of RyRs and are responsible for calcium induced calcium release (CICR), a phenomenon observed in all isoforms of RyRs, with low (μM) Ca^{2+} concentration stimulating opening of the channel and high ($\leq 0.1\text{mM}$) concentrations shutting down open channels [159]. There is evidence that RyRs contain two types of Ca^{2+} binding site; stimulatory high affinity sites and inhibitory low affinity sites [160]. However there is much controversy regarding exactly how CICR is regulated [71]. Inhibitory concentrations of free Ca^{2+} differ for various RyRs, being higher for RyR2 and RyR3 (5mM) compared to RyR1 (0.6-1mM) [58]. Some evidence suggests that termination of CICR does not occur via

elevated levels of cytosolic free Ca^{2+} but by decrease of free Ca^{2+} and Ca^{2+} disassociation from SR luminal facing sites on the receptor and associated proteins [70, 161].

1.5 Invertebrate RyRs

There is very little information regarding the organisation of invertebrate RyR within muscle cells, although one electron microscopy study concluded that the organisation within invertebrate dyads is similar to the vertebrate ones [162].

1.5.1 Gene

In contrast to the wide range of literature available on vertebrate RyRs, there is considerably less information available on the RyR in invertebrates. What is known is that all the invertebrates studied to date have only one gene encoding RyR, with the translated RyR protein having approximately 45% similarity (at the amino acid level) to mammalian homologues [163]. However, the C-terminus region of the invertebrate receptor, containing the TM domain and the channel pore, is much more conserved, sharing around 70% amino acid similarity with mammalian RyRs [164]. The overall level of sequence conservation is much higher between different insect species (see Table 2); thus *B. mori* and *D. melanogaster* RyRs show 79% amino acid identity [30], with similar values found for the *P. xylostella* isoforms (78%) [165]. A RyR gene has also been identified and cloned from the nematode *Caenorhabditis elegans* [166]; it has approximately 47% identity to the *D. melanogaster* RyR and approximately 40% identity to mammalian isoforms [167].

Table 2 Comparison of RyR protein sequences of various insects shown as % identity

| | <i>D. melanogaster</i> | <i>P. xylostella</i> ¹ | <i>B. mori</i> ² | <i>A. pisum</i> ² | <i>A. gambiae</i> | <i>B. tabaci</i> | <i>C. medinalis</i> | <i>S. exigua</i> | <i>A. mellifera</i> ² |
|-----------------------------------|------------------------|-----------------------------------|-----------------------------|------------------------------|-------------------|------------------|---------------------|------------------|----------------------------------|
| <i>D. melanogaster</i> | X | 77.8 | 78.9 | 75.6 | 82.4 | 77.1 | 79.3 | 78.9 | 78.8 |
| <i>P. xylostella</i> ¹ | | x | 91.2 | 77.0 | 78.5 | 78.7 | 92.0 | 92.1 | 80.7 |
| <i>B. mori</i> ² | | | x | 77.7 | 79.6 | 79.3 | 93.8 | 94.6 | 81.7 |
| <i>A. pisum</i> ² | | | | x | 76.9 | 82.3 | 78.3 | 78.3 | 79.7 |
| <i>A. gambiae</i> | | | | | x | 77.9 | 80.2 | 80.0 | 79.4 |
| <i>B. tabaci</i> | | | | | | x | 79.9 | 79.9 | 82.4 |
| <i>C. medinalis</i> | | | | | | | x | 95.0 | 82.3 |
| <i>S. exigua</i> | | | | | | | | x | 82.3 |
| <i>A. mellifera</i> ² | | | | | | | | | X |

¹First published sequence; ² Automatic computational prediction done by NCBI

There is a considerable variation in the number of exons found in insect *RyR* genes. The *D. melanogaster* gene has 26 exons making up the coding sequence [168]. However, members of other insect orders such as *Acyrtosiphon pisum* (pea aphid) and *B. mori* have over 100 exons within the *RyR* gene, similar to the number present in human *RyR* genes (Davies TGE, unpublished). There is evidence of alternative gene splicing in insect *RyR*s, although the function of this is unknown. Alternative splicing often appears to be associated with tissue distributions or different stages of insect development. Analysis of the C-terminal part of the *H. virescens* *RyR* confirmed the presence of at least two splice forms [169], and more recent sequencing of *RyR*s from the economically important pests *P. xylostella* and the rice leafroller *Cnaphalocrocis medinalis* (Guenee) detected the presence of multiple splice forms (as well as a number of single nucleotide polymorphisms) [165, 170].

1.5.2 Functional studies

Expression and functional analyses of an insect *RyR* has been best described in detail for *D. melanogaster*, showing that the *RyR* is expressed both during early embryonic development and in the muscle cells, digestive tract and nervous system of adult flies [171, 172]. It has also been demonstrated that ryanodine sensitive internal calcium stores located in *D. melanogaster* photoreceptors are essential for

phototransduction [173]. Analysis of a *D. melanogaster* RyR deletion mutant, lacking the entire first exon of the gene, showed that the receptor is essential for correct insect development, since the first instar larvae died 4 to 7 days after hatching. Lack of the correct protein resulted in reduced heart rate, body wall contraction and impaired feeding and digestion; however the function of the photoreceptor cells and the development of the larval brain were not impaired [174]. Interestingly the RyR is not essential for ECC in nematodes and the null mutants of the channel, although exhibiting impaired motility and partial flaccid paralysis, are able to develop to adults and reproduce [175]. Electrophysiological measurements of transiently expressed *D. melanogaster* RyRs have shown fast opening and closing kinetics similar to the rabbit skeletal RyR, but with a much larger conductance [22, 163]. More detailed characterization of the functionally expressed carboxyl-terminal calcium release channel part of the protein confirmed a much larger conductance of inward and outward currents through the insect channel when compared to its mammalian counterparts under the same experimental conditions [163]. Single channel recordings of insect RyR were also obtained from sucrose gradient purified native membrane preparations from the thoracic muscles of *H. virescens*. Like its mammalian counterpart, this channel showed an irreversible modification with ryanodine and was sensitive to ruthenium red and to ATP [176]. The role of RyR in halothane-mediated anaesthesia has also been investigated using *D. melanogaster* and it is thought that the fly glial and neuronal specific RyR protein is responsible for halothane sensitivity and may have a significant role in the anaesthetic effects observed *in vivo* [177]. The presence of RyRs has also been confirmed in *P. americana* neurons through radio-labelled ryanodine binding studies [178] and antibody detection has localized RyR to photoreceptors and muscle tissue in the honeybee *Apis mellifera* [179, 180].

ECC studies on muscle have also been used to demonstrate different activation kinetics between *A. mellifera*, *D. melanogaster* and vertebrate RyRs [179], and electron microscopy of flight muscles from dragonflies (unknown species) and tail muscles from *Centruroides sculpturatus* (Arizona bark scorpion) suggests an indirect activation of RyRs during ECC, similar to that seen in mammalian cardiac muscle [181]. Calcium currents during EC coupling have been measured in isolated muscle fibres from *A. mellifera*, *D. melanogaster* and other insect species, where it was

shown that the Ca^{2+} current kinetics were much faster (5-20ms at V_{max}) when compared to vertebrate skeletal muscle (>100ms) [179]. Also the myotoxic effects of ryanodine and a synthetic pyrethroid allethrin have been characterized in adult *A. mellifera*, showing that differences in EC function may be related to structural differences between vertebrate and invertebrate muscle fibres, and the expression patterns of RyRs [179]. There is limited evidence on how many of the vertebrate accessory proteins (section 1.4.1) are conserved in insects and if their role in regulation of the invertebrate RyR channel is comparable to the mammalian models. Similarly, there is very little information on the impact of differences between insect and mammalian RyRs on channel function; studies with diamide insecticides, which are highly specific for certain insect RyRs, suggests that channel differences do affect ligand binding and may play a key role in the specificity of these new insecticides [30].

1.6 Aims of this project

The overall aims of this project were to better understand the mode of action and selectivity of diamide insecticides, and to determine the molecular basis of any resistance occurring in pest insects. This would be achieved by:

- 1) The creation of a database of DNA sequences encoding RyRs, and a separate database of RyR protein sequences, from a range of insect and mammalian species. To use these databases to identify divergent regions within the insect RyR receptors that could account for the specificity of the diamides towards certain insect species and the contradictory action of different diamides towards sucking and chewing pests. (Chapter 3)
- 2) Using these RyR cDNA sequences to design primers to amplify RyRs from a sucking pest (*Myzus persicae*) and a chewing pest (*Plutella xylostella*), and to clone these into expression vectors. (Chapter 3)
- 3) Expressing full-length cDNAs encoding the *M. persicae* and *P. xylostella* RyRs in cell lines. (Chapter 4)
- 4) Using the expressed RyRs for binding studies with RyR modulators in order to identify their site(s) of interaction. (Chapter 4)
- 5) Site-directed mutagenesis of the insect RyR cDNAs to identify amino acids involved in ligand binding. (Chapter 5)
- 6) Determining the molecular basis of any resistance to diamides arising in field populations of pest insects (potentially mutations in *RyR* genes). (Chapter 5)

Chapter II: General methods

This chapter describes the standard methods used routinely in the project. Additional methods, developed for specific tasks, are presented in the research chapters (III-V).

2.1 General

All centrifugations were done in either a model 5415D, 5415R (when temperature control was needed) or a 5810R (for volumes larger than 50ml) table top centrifuge (Eppendorf, Hamburg, Germany).

All enzyme reactions were set up on ice and incubations for restriction digests and reverse transcriptions were done in a G-Storm GS-482 thermo cycler (Labtech International, UK).

All PCR reactions were set up on ice and done in a G-Storm GS-1 thermo cycler (Labtech International, UK). Room temperature was $22 \pm 2^{\circ}\text{C}$.

2.2 Insect material

Myzus persicae clones 4106A and 4191A were reared in Blackman boxes on Chinese cabbage (*Brassica rapa* spp.) leaves at $18 \pm 1^{\circ}\text{C}$ with 16h light / 8h dark photoperiod and 70% relative humidity. 4106A is a susceptible population collected in Scotland and 4191A is a neonicotinoid-resistant strain collected in Greece.

The Rothamsted (Roth) strain of *Plutella xylostella* originated in the UK and has been reared in the laboratory for over 30 years on Chinese cabbage (*Brassica rapa* spp.) plants in fan-ventilated Perspex cages with 16h light / 8h dark photoperiod, 70% relative humidity and a constant room temperature of $21 \pm 1^{\circ}\text{C}$.

Mixed populations of *P. xylostella* larvae and adults were collected in 1.5ml Eppendorf tubes and flash frozen in liquid nitrogen prior to RNA extraction. Frozen insect stocks were kept at -80°C .

2.3 RNA extraction

2.3.1 E.Z.N.A® mollusc RNA kit

RNA extractions from insects were carried out using an E.Z.N.A® Mollusc RNA kit (Omega Bio-Tek, GA, USA) on no more than 35mg of flash frozen *M. persicae* or *P. xylostella*, following the manufacturer's recommended protocol.

Flash frozen insects were ground up in a 1.5ml eppendorf tube kept on dry ice using a pre-cooled plastic pestle. 350µl of MRL buffer/β-mercaptoethanol was subsequently added to the insect powder and the tube vortexed. 350µl of chloroform : isoamyl alcohol (24:1) was added to the homogenate, the tube contents mixed thoroughly and centrifuged at 10,000g for 2 minutes at room temperature. Following centrifugation the upper aqueous layer was collected and transferred to a fresh tube. RNA was precipitated by adding 1 volume of isopropanol, the tube contents mixed and centrifuged at 10,000g for 2 minutes. The supernatant was carefully removed and the pellet briefly air dried (1 minute) and then re-suspended in 100µl of pre-heated (65°C) RB buffer. 350µl of RB buffer/β-mercaptoethanol and 250µl of absolute ethanol were added to the re-suspended RNA and the mixture loaded onto aHiBind® RNA column assembled in a 2 ml collecting tube. Resin bound RNA was washed twice with 500µl of wash buffers I and II and centrifugation at 10,000g for 1 minute and the RNA subsequently eluted from the column in 50µl DEPC-treated water.

Potential DNA contamination was removed from the RNA eluate using a DNA-free™ DNase kit (Ambion®, Life Technologies, CA, USA), following the manufacturer's recommended protocol. A 0.1 sample volume of 10x reaction buffer was added to the RNA together with 1µl of DNase I enzyme (2u/µl), the solution mixed gently and incubated at 37°C for 30 minutes. The reaction was terminated by adding 0.1 sample volume of Stop solution and incubating for 2 minutes at room temperature with occasional mixing. The mixture was then spun at 10,000g for 2 minutes in a bench top micro-centrifuge. After centrifugation the RNA solution was transferred to a fresh 1.5ml eppendorf tube.

2.3.2 Isolate RNA mini kit

For RNA extractions from individual *M. persicae* or *P. xylostella*, an Isolate RNA mini kit (Bioline, London, UK) was used, following the manufacturer's recommended protocol. Flash-frozen insects were ground in 450µl of Lysis Buffer in a 1.5ml eppendorf tube, centrifuged at max speed for 1 minute and the supernatant transferred to a spin column R1. Eluate was retrieved from the column by a 2 minute centrifugation at 10,000g and the column discarded. One volume of 70% ethanol was added to the filtrate supernatant, mixed, transferred to spin column R2 and centrifuged for 2 minutes at 10,000g. The column was then washed by a 1 minute centrifugation at 10,000g with 500µl of buffer AR followed by a second wash with 700µl of buffer BR. The column was then further centrifuged at 10,000g for 2 minutes to remove any residual liquid. RNA was eluted from the column into a 1.5ml eppendorf tube using 40µl of RNase-free water and 1 minute centrifugation at 6,000g.

2.3.3 TRIzol® reagent RNA extraction

TRIzol® reagent extraction was employed for RNA isolation from larger pools of insect material, following the manufacturer's recommended protocol. Flash frozen samples were homogenised as described previously (2.3.1) and 1ml of TRIzol® reagent (Life Technologies, CA, USA) was added per 50mg of insect material. The homogenized mixture was centrifuged at 12,000g for 10 minutes at 4°C to remove parts of the insect exoskeleton and other insoluble materials. The supernatant was transferred to a fresh centrifuge tube, chloroform added in a ratio of 0.2ml per 1ml of TRIzol®, the tube shaken and incubated at room temperature for 3 minutes and then centrifuged at 12,000g for 15 minutes at 4°C. The upper phase was collected into a new tube (approximately 50% of the original volume) and 0.5ml of isopropanol added per 1ml of TRIzol® used, the solution mixed and incubated at room temperature for 10 minutes followed by centrifugation at 12,000g, 4°C for 10 minutes. The RNA pellet obtained was washed with 1ml of ice-cold 75% ethanol per 1ml of initial reagent volume and centrifuged at 7,500g for 5 minutes. The supernatant was then removed, the RNA pellet briefly air-dried and re-suspended in 50µl of RNase-free water.

All RNA samples were stored at -80°C . The quality of RNA was checked using a NanoDrop1000 spectrophotometer (Thermo scientific, MA, USA). Samples were considered pure if the A260/A280 and A230/A260 ratios were above 1.8. RNA degradation was checked for by incubating $1\mu\text{l}$ of the RNA mixed with $1\mu\text{l}$ RNA loading dye (New England Biolabs, MA, USA) and $4\mu\text{l}$ of RNase free water at 65°C for 5 minutes and then running the sample on a 1% (w/v) TAE agarose gel at 70V/200mA for 50 minutes using buffers made up with double distilled water.

2.4 Synthesis of cDNA

2.4.1 SuperScript® III

SuperScript® III Reverse Transcriptase (Life Technologies, CA, USA) was used to synthesize cDNA to be used as a template for PCR amplification of RyR fragments for cloning. The cDNA synthesis was carried out in $20\mu\text{l}$ reactions in 0.2 ml thin walled PCR tubes as follows: $4\mu\text{g}$ of total RNA (various concentrations), $2\mu\text{l}$ dNTPs (10mM), $1\mu\text{l}$ Oligo_dT25 (100pmol, Thermo-Fermentas, MA, USA) and up to $13\mu\text{l}$ of RNase free water. For synthesis of *M. persicae* cDNA, $1\mu\text{l}$ of a gene specific primer (20pmol) was occasionally added to the reaction. Reaction mixtures were pre-incubated at 65°C for 10 minutes to resolve any RNA secondary structure and then the following reagents were added: $1\mu\text{l}$ of DTT (0.1M), $1\mu\text{l}$ of RNaseOUT™ (40U/ μl Life Technologies, CA, USA), $4\mu\text{l}$ of 5x first strand Buffer and $2\mu\text{l}$ reverse-transcriptase enzyme (200U/ μl). The tube contents were mixed and incubated at 55°C for 1 hour. The reactions were terminated by incubating the tubes at 70°C for 15 minutes. To remove any DNA/RNA hybrids, $1\mu\text{l}$ of RNaseH (2U/ μl Life Technologies, CA, USA) was added and the reactions incubated at 37°C for 20 minutes. The synthesised cDNA was subsequently used as a template in downstream PCR reactions.

2.4.2 RevertAid™

RevertAid™ Premium Reverse Transcriptase (Thermo-Fermentas, MA, USA) was used to synthesize cDNA to be used as a template for PCR amplification of fragments close to the 5' end of genes. The cDNA synthesis was carried out in a total volume of $20\mu\text{l}$ with the reaction set up similar to SuperScript® III: $4\mu\text{g}$ of total RNA (various concentrations), $2\mu\text{l}$ dNTPs (10mM), $1\mu\text{l}$ Oligo_dT25 (100pmol)

(Thermo-Fermentas, MA, USA) and up to 14µl RNase free water. The tube contents were mixed and incubated at 65°C for 10 minutes, to resolve any RNA secondary structure, and then the following reagents added: 4µl of 5x RT buffer, 1µl of RiboLock™ RNase inhibitor (40U/µl) and 1µl reverse-transcriptase enzyme (200U/µl). The reactions were mixed and incubated at 55°C for 45 minutes, then heat inactivated at 85°C for 5 minutes.

2.5 Polymerase Chain Reaction (PCR)

2.5.1 Primer design

All gene specific primers were designed according to the sequence to be amplified. At least one Guanine or Cytosine was present at the 3' end of the primer and the properties of the primers, including melting temperature (T_m) and secondary structures, were checked using an online service OligoCalc (<http://www.basic.northwestern.edu/biotools/oligocalc.html>) [182]. Primers were synthesised by Sigma–Aldrich (Haverhill facility, UK) and shipped desalted and dry. Primers for mutagenesis reactions were ordered with further purification using HPLC or reverse phase cartridge purification. 100µM primer stocks were stored at -20°C. Before use primer stocks were diluted to give 20pmol working concentrations.

2.5.2 PCR with proof reading enzymes

All PCR reactions using cDNA as a template were set up in thin walled 0.2ml PCR tubes with 25µl reaction volumes, unless stated otherwise. The enzymes used for amplification of fragments for cloning were *Pfu* (Promega, WI, USA) and Long Range PCR mix (Thermo-Fermentas, MA, USA). A typical reaction mix included: 2.5µl 10x Buffer with MgCl₂, 0.5µl dNTPs mix (10mM), 0.5µl forward primer (20pmol), 0.5µl reverse primer (20pmol), 0.5µl DNA polymerase enzyme (2-3 u/µl), 1-2µl of template cDNA, nuclease free water to 25µl. Cycling conditions were individually tailored according to the fragment to be amplified by varying the annealing temperatures and extension times. Further details are provided in appropriate sections of the research chapters.

2.5.3 Colony PCR

Prior to propagation of *E. coli* transformants in liquid cultures, PCR was used to test for the presence of inserts in the bacterial plasmids using small samples taken from colonies of the plasmid containing bacteria (colony PCR). PCRs were usually done with gene specific primers where there was existing sequence information. Primers based on vector sequences were used when there was no sequence information for the cloned fragment and the insert did not exceed 2Kb. For large inserts only a small portion was PCR amplified to avoid false negative results. No colony PCRs were designed to amplify fragments that exceeded 3Kb in length.

The PCR reactions used one of two standard x2 *taq* master-mixes RED*taq*@mastermix (Sigma, MO, USA) and Dream*taq*TMmastermix (Thermo-Fermentas, MA, USA). Both of these contain a dye which can be seen in agarose gels. The templates were cells remaining on a pipette tip following colony transfer on to a fresh LB agar plate containing antibiotic. Cells were re-suspended in 5µl of DHCP treated water. The PCR reactions were set up in a total volume of 25µl as follows: 12.5µl of 2x mastermix, 0.5µl of forward primer (20pmol), 0.5µl of reverse primer (20pmol), 9.5µl of sterile water and 2µl of template. Typical PCR cycling conditions were: 95°C for 5 minutes followed by 28-35 cycles of 95°C for 20 seconds, 50°C for 30 seconds and 72°C for 1-4 minutes, with a final extension step of 72°C for 5 minutes. The extension time used was dependant on the anticipated size of the PCR product allowing 1minute per 1kb. The number of cycles was also dependant on the size of the colonies on the plate; small colonies needed more amplification cycles to avoid false negatives. 5µl of product from each PCR reaction was run on a 1% (w/v) TAE agarose gel to confirm the presence of the product. Typically 8 colonies were screened for small inserts and 12-16 colonies for larger inserts. If the clones screened showed no positive results additional clones were tested.

2.5.4 Analytical agarose gel electrophoresis

All PCR reactions were checked for the presence of the desired product by analytical TAE agarose gel electrophoresis. Gels were made from molecular grade agarose (Fisher Scientific, Loughborough, UK). Typically 0.8% w/v (for large fragments

>4kb) or 1.1% w/v (for smaller fragments <1Kb) gels were cast. A 1Kb GeneRuler™ DNA ladder (Thermo-Fermentas, MA, USA) was typically loaded onto a single lane of each gel, in a total sample volume of 6µl (1µl of ladder, 1 µl 6x DNA loading dye, 4 µl water). 5µl of each PCR reaction mixed with 1µl of 6x DNA loading dye (containing bromophenol blue), or 5µl of PCR master-mixes which included the dye, was loaded onto gels. Typical voltage and current settings were 70V/200mA for 50ml gels and 100V/ 200mA for 100ml gels. Average run times were between 50 to 70 minutes. All cast gels were pre-stained with 2.5µl (50ml gels) or 5µl (100ml gels) 10mg/ml ethidium bromide and then visualised on a 302nm UV trans-illuminator (Syngene, MD, USA) using the Gene Genius Bio-Imaging System.

2.6 Purification of PCR products

2.6.1 Gel purification

PCR products were run on either a 0.75% or 1% w/v 50ml TAE-agarose gel (depending on the fragment size) in TAE buffer at 50V/200mA for at least 1hour. DNA fragments were subsequently purified from excised gel slices using QIAquick® (Qiagen, Hilden, Germany) or GeneJET™ (Thermo-Fermentas, MA, USA) gel extraction kits. Gel slices were excised quickly under low emitting UV light to avoid excess DNA damage and the gel slices weighed. Extraction of DNA was carried out following the manufacturer's recommended protocols. Binding buffer was added to a gel slice placed in a 2ml eppendorf tube in 3:1 (QIAquick®) or 1:1 (GeneJET™) w/v ratios. Samples were mixed, incubated at 60°C until the agarose was completely dissolved, then 10 µl of 3M NaOAc (pH 5.5) was added to adjust the solution pH. A volume of isopropanol equivalent to the volume of the gel slice was then added and the whole mixture was transferred to a DNA binding column (pre-assembled in a 2 ml collection tube) and centrifuged at 10,000g for 1 minute. 0.7ml of wash buffer was added to the column and the column re-centrifuged at 10,000g for 1 minute. The flow-through was discarded and the column spun again at max speed for 1 minute to remove any residual ethanol. DNA was eluted from the column after a 5 minutes pre-incubation of the column resin with 30µl of pre-warmed (at 50°C) EB buffer (provided in the kit), followed by a 1 minute centrifugation at 10,000g.

2.6.2 Column purification

For PCR fragments which did not need gel purification (single products) a MinElute® PCR purification kit (Qiagen, Hilden, Germany) was used to recover the DNA following the manufacturer's protocol. Five volumes of Buffer PB were added to each PCR reaction and mixed. If the resulting mixture did not turn yellow in colour then 10 µl of 3M NaOAc (pH 5.5) was added to adjust the solution pH. The entire sample was then loaded onto a MinElute® column and the column assembly centrifuged for 1 minute at 10,000g. Column bound DNA was washed with 0.75 ml of PE buffer, centrifuged for 1 minute at 10,000g and then the column re-centrifuged at max speed again for 1 minute to remove any residual wash buffer. DNA was eluted in 10µl of EB buffer following a 1 minute pre-incubation of the column.

2.6.3 Phenol-chloroform purification

For RACE products and for column-based purifications which did not give entirely clean DNA preparations, an adaptation of the phenol-chloroform extraction method described by Sambrook *et al.* [183] was used to remove unwanted contaminants. Each DNA sample was mixed with 0.1 volume of 5M EDTA and 1 volume of water, then 1 volume of phenol and 1 volume of chloroform was added. After thorough mixing, the sample was spun at 12,000g for 4 minutes at room temperature. The upper aqueous phase was then carefully collected and transferred to a fresh 1.5ml eppendorf tube for further extraction with 1 volume of chloroform. The sample was mixed and centrifuged at 12,000g for 4 minutes at room temperature. The upper aqueous phase was again collected and transferred to a fresh eppendorf tube. 0.1 volume of 3M NaOAc and 2.5 volumes of absolute ethanol were added to precipitate the DNA and the mixture was incubated at -20°C for a minimum of 1hour. The sample was then spun at 12,000g at 4°C for 20 minutes and the pellet washed with ice-cold 70% ethanol. The recovered pellet was briefly air dried and then re-suspended in DEPC-treated water. The quality of the DNA was checked by measuring the A260/280 absorbance ratio using a NanoDrop1000 (Thermo Scientific, MA, USA).

2.6.4 Precipitation with NH₄OAc

This protocol was mainly used for the purification of large PCR products (over 4Kb) for direct sequencing. 20µl of a PCR reaction was transferred to a 1.5ml eppendorf tube and 1 volume of 4M NH₄OAc and 200µl of absolute ethanol were added, the tube contents were mixed well and immediately centrifuged at max speed for 20 minutes at room temperature. The supernatant was removed, the DNA pellet washed with 250µl of 70% ethanol and the tube re-centrifuged at max speed for 5 minutes. The majority of the supernatant was again removed and the DNA pellet briefly air dried. The DNA pellet was then re-suspended in 30µl of EB buffer (provided in Qiagen kits) and the quantity of DNA checked by measuring absorbance ratio A₂₆₀/A₂₈₀ using NanoDrop1000 measurements (Thermo Scientific, MA, USA).

2.7 Molecular cloning and Bacterial transformation

2.7.1 pCR-XL TOPO kit

Ligations with the pCR-XL TOPO vector (Life Technologies, CA, USA) were done following the manufacturer's recommended protocol. 4µl DNA (with TA overhangs) and 1µl pCR-XL-TOPO vector were mixed and incubated for 5 minutes at room temperature then 1µl of 6X TOPO cloning Stop solution was added and the reaction placed on ice.

One vial of competent TOP10 *E. coli* cells supplied with the TOPO kit was thawed on ice then 2µl of the prepared ligation reaction was added to the cells and incubated on ice for a further 30 minutes. Cells were then heat-shocked for 30 seconds at 42°C and immediately put on ice for another 2 minutes. 250µl of room temperature S.O.C. medium (supplied with the kit) was added to the cells and the cells were allowed to recover by shaking at 250rpm for 2 hours at 30°C. The cells were then plated onto two (75µl/150µl) LB agar plates containing 50µg/ml kanamycin and placed in an incubator overnight at 30°C.

2.7.2 CloneJET™ PCR cloning kit

Most DNA fragments were ligated into the pJET1.2 blunt vector, which is a part of the CloneJET™ PCR cloning kit (Thermo-Fermentas, MA, USA). PCR products generated with *pfu* enzyme were ligated directly into the vector in 20µl reactions as

follows: 10 μ l of 2x reaction buffer, 1 μ l of pJET vector (50ng/ μ l), 1 μ l of T4 DNA ligase (5U/ μ l), 150ng of insert DNA, and nuclease-free water up to 20 μ l. A 3:1 insert:vector molar ratio was used in each reaction, as recommended by the manufacturer. Where only small quantities of insert DNA were available the amount of vector used in the reaction was halved. PCR products produced by enzymes generating TA overhangs were incubated at 70°C for 5 minutes with 1 μ l of blunting enzyme (provided with the CloneJET kit) before the DNA ligase was added. Ligations were incubated at room temperature for 30 minutes and then subjected to bacterial transformation as described below (2.7.3).

2.7.3 Bacterial transformations

35 μ l of XL-1 blue super-competent cells or 25 μ l of XL-10 gold ultra-competent cells (Agilent, CA, USA) were used per reaction. Cells were thawed on ice in 14ml Falcon tubes, gently mixed with 0.59 μ l of 1.72M β -mercaptoethanol (XL-1 blue kit) or 1.2 μ l of XL-gold β -mercaptoethanol and incubated on ice for a further 10 minutes. Typically 2 μ l of ligation reaction was added to the cells and the mixture incubated on ice for a further 30 minutes. Cells were then heat-shocked at 42°C for 45 seconds (XL-1 blue) or 30 seconds (XL-10 gold) and immediately placed on ice for a further 2 minutes. 250 μ l of pre-warmed S.O.C. medium was then added to each tube and the tubes placed in a shaking incubator for 2 hours at 30°C and 250 rpm. 150 μ l (XL-1 Blue) or 100 μ l (XL-10 gold) of cells were then plated onto two LB agar plates containing 50-100 μ g/ml of antibiotic for colony selection and incubated at 30°C for approximately 30 hours.

2.7.4 Propagation of expression vectors

Empty pcDNA3.1(-) and pIZ/V5-his expression vectors (Life technologies) were propagated in *E. coli* XL-1 blue competent cells (Agilent, CA USA) to provide large quantities of vector DNA. 0.42 μ l of 1.72M β -mercaptoethanol was added to 25 μ l of thawed XL-1 blue competent cells and the cells incubated on ice for 10 minutes. 1 μ l of vector DNA (20 μ g in TE buffer, pH 8.0) was then added to the cells, which were incubated for a further 30 minutes on ice, followed by a heat shock at 42°C for 45 seconds. Cells were allowed to recover for 2 minutes on ice, then 250 μ l of S.O.C. medium added and the transformations incubated at 37°C, 250rpm for 1 hour. 50 μ l

of transformed cells were plated out onto two (75µl/150µl) LB agar plates containing 100µg/ml of ampicillin (pcDNA) or Zeocin™ (pIZ) and incubated at 37°C overnight. Vector DNA from 4ml liquid cultures was later purified using mini prep kits.

2.8 Analysis of transformants

2.8.1 Plasmid purification (mini-preps)

QIAprep® Spin Miniprep Kit (Qiagen) or GeneJET™ mini-prep kit (Thermo-Fermentas) were used for purification of plasmid DNA from small volumes of liquid culture. Both kits follow a similar protocol involving alkaline lysis of bacterial cells and binding of DNA to silica membrane columns. Prior to plasmid DNA purification, liquid cultures of *E. coli* containing plasmid DNA were set up in 15 ml Falcon tubes containing 4ml of low salt LB broth and 50 µg/ml of appropriate antibiotic and incubated for at least 18 hours in a shaking incubator at 250rpm, 30-37°C.

Cells were harvested by centrifugation at 4000g for 15 minutes at 10°C, the supernatants removed and the pellets re-suspended (by pipetting and vortexing) in 250µl re-suspension buffer. Cell suspensions were transferred to sterile 1.5ml eppendorf tubes and cell lysis was performed by adding 250µl of lysis buffer to each tube followed by gentle mixing until a homogenous solution was obtained. Each lysis reaction was terminated by adding 350µl of Neutralisation solution. The mixtures were then centrifuged for 8 minutes at 10,000g at room temperature to pellet the cell debris and denatured proteins. Supernatants were then transferred to DNA binding columns. A brief 1 minute centrifugation at 10,000g allowed DNA to bind to the column resin which was then washed once with 700µl of wash buffer (QIAGEN) or twice with 500µl of wash buffer (Thermo-Fermentas). Columns were then spun for a further 1 minute at max speed to remove any residual wash buffer. DNA was eluted from the columns with 50µl of EB buffer. The quality of the DNA was checked by A260/A280 measurements using a NanoDrop1000 (Thermo Scientific) spectrophotometer. For inserts over 8Kb analytical agarose gel electrophoresis was used to check the recovered DNA (see 2.5.4).

2.8.2 Restriction digests

All plasmids containing inserts larger than 8Kb were checked for possible rearrangements using restriction enzyme digests. Expected restriction fragment sizes were predicted *in silico* using Vector NTI v10.5 (Life Technologies) or Geneious v.6.6.5 (Biomatters Ltd., Auckland, NZ) software. Typical diagnostic BglIII or SalI (Promega, WI, USA) digests were set up in a 20 μ l reaction as follows: 2 μ l 10x buffer D (Promega), 2 μ l 10x BSA, 1 μ l BglIII or SalI (10U/ μ l), 1 μ g of plasmid DNA, nuclease free water up to 20 μ l. Reactions were briefly vortexed and then incubated in a PCR block at 37°C for at least 1 hour, 15 minutes. Products were run on 0.8-1% w/v agarose TAE electrophoresis gels for visualization and analysis.

2.8.3 Sequencing

Sequencing done in-house at Rothamsted utilized the Big Dye Terminator v1.1 kit (Applied Biosystems®-Life Technologies, CA, USA) and an ABI 3100 genetic analyser (Hitachi, Tokyo, Japan). A typical 20 μ l sequencing reaction was set up as follows: 4 μ l Big Dye v1.1 reaction mix, 2 μ l 5x BigDye Sequencing buffer, 1 μ l sequencing primer (20pmol), 500ng Plasmid DNA (or 100ng purified PCR product), nuclease-free water up to 20 μ l. The PCR block cycle conditions were 25 cycles of: 96°C for 30 seconds, 50°C for 30 seconds 60°C for 4 minutes with the temperature ramp set at 1°C per second.

Dye labelled DNA was precipitated from the reaction mix by the addition of 2 μ l of 125mM EDTA, 2 μ l of 3M NaOAc (pH 5.5) and 71 μ l of absolute ethanol, brief vortexing, then incubation at room temperature for 15 minutes. The precipitated DNA was pelleted by 20 minutes centrifugation at 10,000g, the supernatant removed and the pellet washed with 100 μ l of 70% ethanol. Following another centrifugation at 10,000g for 5 minutes, as much of the supernatant as possible was decanted by inverting the tube, and the DNA pellet was allowed to air dry in the dark until all the residual ethanol had evaporated. The DNA was then re-suspended in 20 μ l of Hi-Di™ formamide (Life technologies) and transferred into an individual well on a 96 well plate. Prior to sequencing all reactions were briefly incubated at 90°C for 2 minutes.

In some cases sequencing was done commercially by MWG ERUOFINS DNA (Eurofins Scientific group, Brussels, Belgium).

2.8.4 Maxi preps

2.8.4.1 Liquid cultures

A colony of *E. coli* with desired plasmid was inoculated into a 2.5ml starter culture of LB broth (containing 50µg/ml of antibiotic) and propagated in a shaking incubator at 30°C, 250rpm. After approximately 8-10 hours, 1ml of the starter culture was used to inoculate two 200ml LB broth cultures (containing 50µg/ml of antibiotic) and incubated with shaking overnight at 30°C, 250rpm. Before harvesting the OD of the culture at 600nm was checked and if the absorbance value was approximately 1.0 the cells were transferred to 250ml Beckman centrifuge bottles and spun down at 6000g, 4°C for 15 minutes in a JA-14 rotor / Avanti 28 Centrifuge (Beckman, CA, USA).

2.8.4.2 DNA purification

The pelleted *E. coli* cells were processed with a Plasmid Plus maxi kit (Qiagen, Hilden, Germany) using a modification of the manufacturer's protocol. Pellets were re-suspended in 8ml of Qiagen kit resuspension buffer P1, containing lysate-blue and RNase A. Cells were lysed by adding 8ml of lysis buffer P2 and gently mixing the solution until the colour of the lysate turned blue. 8ml of neutralization buffer S3 was then added to stop the lysis reaction and the contents of the tube gently mixed until all the blue colour disappeared. The mixture was then centrifuged at 4500g and 10°C for 5 minutes and the supernatant from two 200ml cultures was transferred into one QIAfilter cartridge. The lysate was gently pushed through the cartridge filter (using the plunger provided) and collected in a fresh sterile 50ml tube. 10ml of binding buffer was added to the filtrate, the solution mixed, and the entire contents of the tube applied to a DNA binding column placed on a vacuum manifold. After all the liquid had passed through the column, it was washed with 0.7ml of ETR buffer to remove endotoxins, centrifuged for 1 minute at 10,000g and then washed with 0.7ml of buffer PE and re-centrifuged for 1 minute at 10,000g. The column was then spun again at max speed for 1 minute to remove any residual wash buffer. DNA was eluted from columns using 400µl of EB buffer and a 2 minutes centrifugation at

8,000g. The quality and quantity of the DNA was checked by NanoDrop1000 spectrophotometry and by restriction digests (see 2.8.1 and 2.8.2 for details).

2.9 Site-directed mutagenesis

All mutagenesis experiments were carried out using the Quikchange Site-directed mutagenesis (SDM) kit (Agilent, CA, USA) and the manufacturer's recommended protocol. Primers for the PCR reaction were designed so that the target / primer mismatch was at least 10 base pairs from either end of the primer with a determined T_m for each primer of over 75°C, calculated using the following formula:

$$T_m = 81.5 - 0.41(GC\%) - \frac{675}{N} - \%mismatch$$

Where N = number of bases

SDM reaction conditions were: 5 μ l *pfu* 10x Turbo buffer, 1 μ l dNTPs (kit mix), 1 μ l forward primer (125ng), 1 μ l reverse primer (125ng), 1 μ l plasmid DNA (diluted to 50ng/ μ l), 41 μ l nuclease-free water, 1 μ l *pfu* Turbo (2.5U/ μ l). PCR thermo-cycler conditions were initial denaturation at 95°C for 30 seconds followed by 16-18 cycles of: 95°C for 30 seconds, 55°C for 1 minute, 68°C for 2 minutes, 30 seconds per 1Kb of plasmid. The number of cycles depended on the type of modification: 16 cycles for a single mutation and 18 cycles for multiple mutations.

PCR products were treated with 1 μ l of DpnI (provided with the kit) for 1 hour at 37°C to remove template DNA. After the digest, 2 μ l of the reaction was transformed into competent *E. coli* (either XL-1 blue or XL-10 gold) cells following standard procedures (see, 2.7.3). The success of each mutagenesis reaction was checked by direct sequencing of isolated plasmid DNA.

2.10 Insect cells

2.10.1 Starting insect cell cultures from frozen stocks

Frozen stocks of Sf9 cells (Life Technologies) were stored under liquid nitrogen in 1.5ml aliquots of approximately 1.5×10^7 cells suspended in Sf-900 II SFM media containing 10% FBS and 10% DMSO. In order to initiate new cultures, a frozen stock aliquot was gently thawed at 37°C and transferred to T-25 culture flasks. Flasks were placed in a 27°C incubator and left for 1 hour for cells to attach to the bottom surface. The SFM medium containing DMSO was then removed and replaced with 5ml of fresh pre-warmed SFM media containing 10% FBS and 50µl of a penicillin-streptomycin cocktail (50U/100µg/ml). The cells were kept in the flask until they reached confluence. The cells were then passaged as described below, halving the FBS concentration until it reached 0.6% and the cells were ready to use for downstream applications. Sf9 cells were maintained in a sterile dedicated incubator at a constant 27°C.

2.10.2 Propagation of insect cell cultures

Media in near confluent (90-95% cell coverage) T-25 flasks was removed and 4ml of fresh Sf-900 II™ media added. Cells were detached from the bottom of the flask by sloughing and tapping the side of the flask. 1ml of detached cells was transferred to a new T-25 flask containing 5ml of fresh media containing 0.6% FBS. Near confluent cell cultures were passaged every 2-3 days, with the typical number of passages not exceeding 30. To scale up the cell cultures 3ml of detached cells from the T-25 flask were seeded into a T-75 flask containing 12ml of fresh Sf-900 II SFM media and the desired concentration of FBS.

Stocks of low passage cultures were made by collecting cells from near confluent T-75 flasks into fresh media and transferring the detached cells from each flask into a 50ml tube (Greiner Bio-One, Kremsmünster, Austria). The number of cells present was determined by transferring 10µl of the cell suspension to a hemocytometer for counting. The 50ml tube was then centrifuged at 500g for 5 minutes, the supernatant removed and the cell pellet gently re-suspended in Sf-900 II media containing 10% FBS and 10% DMSO, at a density of 1×10^7 cells/ml. These cells were split into 1.5ml

aliquots and placed in a -80°C freezer for 24 hour before being transferred to liquid nitrogen in a storage container for long term storage.

2.11 Propagation of HEK 293 cell cultures

All experiments with HEK 293 cells were done at Cardiff University with cultures initiated and maintained by members of Alan Williams' research group. The HEK 293 cultures were maintained in complete high glucose Dulbecco's Modified Eagle Medium (DMEM) (Gibco®-Life Technologies, CA, USA) containing 10% FBS and penicillin-streptomycin (50U/50µg/ml), in a sterile dedicated 37°C, 5% CO₂ incubator. For cell propagation, the media surrounding cells grown to near confluence in T-75 flasks was removed from the flask and the cells washed once with 3ml of phosphate-buffered saline pH 7.4 (PBS). To detach the cells from the flask, 2ml of DMEM media (containing 0.05% trypsin-EDTA (Life Technologies), pre-warmed to 37°C was added, spread out to coat all the cells and left for 2 minutes. 10ml of DMEM at 37°C was then added to stop the reaction; cells were pipetted up and down to break up any clumps and the cells transferred to a 50ml sterile centrifuge tube. The total number of cells was determined using a hemocytometer. Cells were centrifuged at 500g for 5 minutes at 18°C, the supernatant removed and the cells re-suspended in fresh complete DMEM at a density of 1x10⁶ cells/ml. One ml of cells was then seeded into a new T-75 flask in a total volume of 15ml complete DMEM.

Chapter III: Molecular cloning and characterization of insect ryanodine receptors

3.1 Introduction

The main challenge posed for cloning the full-length ryanodine receptor (RyR) is the size of its mRNA. The average length of its coding sequence is approximately 15,000 base pairs, depending on the organism and, in the case of vertebrates, the isoform. Despite this, RyRs have been cloned successfully from a range of organisms. The first was a full-length rabbit skeletal muscle isoform (RyR1), obtained by cDNA library screening, with the final expression construct being made through a series of ligations of digested fragments from the library into the vector pRRS7 for expression in CHO cells [99]. This was followed by the cloning of the rabbit cardiac receptor (RyR2) [184] and brain isoform (RyR3) [185]. All 3 isoforms have now been cloned successfully from various mammals including mice and humans [186].

In peer reviewed publications there are only two reports of successful attempts to clone and express insect RyRs. The first full-length insect channel was cloned from the common fruitfly, *Drosophila melanogaster* (a model organism). The coding sequence was obtained through a combination of RT-PCR (to give six overlapping cDNA fragments) and cDNA library screening. Final assembly of the full-length cDNA was made in the mammalian expression vector pcDNA3.1, using a series of specific restriction digests and ligations. However, only two deletion mutants, lacking most of the cytosolic domain, were sufficiently expressed in CHO cells to allow detailed functional analysis [163]. The second insect RyR successfully cloned and expressed was isolated from the silkworm, *Bombyx mori*. Again, the RyR cDNA was obtained by a combination of RT-PCR (to give overlapping fragments) and cDNA library screening, with the final full-length cDNA being assembled in the expression vector pcDNA3.1 using PCR-based techniques [30]. For both constructs an N-terminal eGFP tag was added to monitor protein expression. A patent WO/2004/027042, filed by the DuPont Corporation in 2004, gave details of the isolation and expression of four additional insect RyR genes; from peach-potato aphid (*Myzus persicae*), corn planthopper (*Peregrinus maidis*), cotton melon aphid

(*Aphis gossypii*) and tobacco budworm (*Heliothis virescens*). Each of the four genes were amplified as a single large cDNA in a two-step nested PCR, sub-cloned into pCR-XL-TOPO vector and then transferred into the insect expression vectors pIBV5His and pFastBac1 [187]. Since the beginning of this project a number of additional studies have been published detailing the sequencing of RyR genes from economically important pests such as the rice leaf folder, *Cnaphalocrocis medinalis* (Guenee) [170] and the diamondback moth, *Plutella xylostella* [165, 188, 189]. These papers will be discussed in more detail towards the end of this thesis.

This chapter presents a detailed strategy for the successful amplification and cloning of two insect RyRs. *In silico* analysis of the obtained sequences, and comparison to other insect and mammalian RyRs is also described. The RyR cDNAs isolated were from the two economically important pest species, *Myzus persicae* and *Plutella xylostella*. Both of these insects have the potential to cause damage to commercial crops resulting in severe yield losses, and both can be controlled with diamide insecticides. Both species are also notorious for developing resistance to insecticides [190, 191]. *M. persicae* is the most economically important agricultural pest in the UK and a major pest in temperate climates. It is polyphagous, feeding on a wide range of plants including potatoes, tomatoes and fruit trees. It causes damage through both feeding and, more importantly, the transmission of over a hundred different plant viruses [192]. *P. xylostella* is one of the most widely distributed lepidopteran species on the planet [190]. Its larval stage is a major pest of cruciferous crops, causing feeding damage to the leaves, decreasing the quality of the produce and in extreme cases may be responsible for up to 100% loss in yield [193].

3.2 Methods and results

3.2.1 Creation of databases of available RyR protein and cDNA sequences

A database of invertebrate and mammalian RyR sequences was constructed, to help identify conserved domains and regions of interest within the insect RyRs as well as to pin point regions of dissimilarity between vertebrate and invertebrate channels which could be important for the selectivity of diamide insecticides. The cDNA database was also used as a guide for primer design for the amplification of *P. xylostella* RyR. The database was updated during the project to include newly

published invertebrate RyRs. Table 3 lists all of the sequences currently present in the database. Sequence alignments were made initially using VectorNTI 10.1 and later using Geneious 6.1.4. The database does not include all the available mammalian RyR sequences.

Table 3 List of species with available RyR protein and DNA sequence

| Species (invertebrates) | GenBank Accession number | cDNA size (bp) | Protein size (aa) |
|---|---|---------------------------|------------------------------|
| <i>Heliothis virescens</i> ² | DuPont patent ¹ | 15429 | 5142 |
| <i>Myzus persicae</i> | DuPont patent ¹ | 15845 | 5101 |
| <i>Aphis gossypii</i> | DuPont patent ¹ | 15315 | 5099 |
| <i>Peregrinus maidis</i> | DuPont patent ¹ | 15384 | 5127 |
| <i>Acyrtosiphon pisum</i> ³ | XP_003246190.1 | 15306 | 5101 |
| <i>Drosophila melanogaster</i> ² | NM_057643.3 | 15384 | 5127 |
| <i>Aedes aegypti</i> ⁴ | XP_001657320.1 | 15357 | 5118 |
| <i>Bombyx mori</i> ³ | XP_004924916.1 | 15375 | 5124 |
| <i>Bemisia tabaci</i> | AFK 84957.1 | 15429 | 5142 |
| <i>Apis mellifera</i> ³ | XP_392217.4 | 15426 | 5082 |
| <i>Anopheles gambiae</i> ³ | XP_318561.3 | 15330 | 5109 |
| <i>Nasonia vitripennis</i> ³ | XP_003425568.1 | 15240 | 5079 |
| <i>Cnaphalocrocis medinalis</i> | AFI80904.1 | 15264 | 5087 |
| <i>Plutella xylostella</i> ⁴ | AET09964.1 | 15576 | 5164 |
| <i>Spodoptera exigua</i> | AFC36359.1 | 15357 | 5118 |
| <i>Nilaparvata lugens</i> | KF306296.1 | 15423 | 5140 |
| <i>Pediculus humanus</i> ⁴ | XP_002424547.1 | 15177 | 5058 |
| <i>Laodelphax striatella</i> | AFK84959.1 | 15348 | 5115 |
| <i>Pieris rapae</i> | AGI62938.1 | 15324 | 5107 |
| <i>Brugia malayi</i> | XP_001900491.1 | 15219 | 5072 |
| <i>Caenorhabditis elegans</i> | BAA08309.1 | 15146 | 5071 |
| <i>Daphnia pulex</i> ³ | EFX89429.1 | 15471 | 5119 |
| Species (vertebrates) | | | |
| <i>Homo sapiens</i> RyR1 | AAC51191.1 | 15117 | 5038 |
| <i>Homo sapiens</i> RyR2 | CAA66975.1 | 14904 | 4967 |

| | | | |
|-----------------------------------|------------|-------|------|
| <i>Homo sapiens</i> RyR3 | CAA04798.1 | 14613 | 4870 |
| <i>Mus musculus</i> RyR2 | AAG34081.1 | 14904 | 4967 |
| <i>Oryctolagus cuniculus</i> RyR1 | CAA33279.1 | 14907 | 5037 |

¹DuPont patent US2007/0105098A1; ²Four splice variants available; ³cDNA obtained from genome sequence by Dr TGE Davies at the beginning of the project; ⁴Sequence published during the project and was not used during amplification and assembly of *P. xylostella* RyR

3.2.2 Amplification of *Myzus persicae* RyR gene fragments

A reference cDNA sequence for *M. persicae* RyR was sourced from DuPont patent US2007/0105098A1 [187]. However, it proved to be impossible to re-amplify the full-length *M. persicae* RyR cDNA using a single nested PCR reaction as described in the patent. A new strategy was therefore employed, whereby short fragments which could be easily amplified were obtained by PCR, sub-cloned and joined together by overlap extension PCR to create a full-length coding sequence for insertion into expression vectors for protein production in cell lines.

Initially, five overlapping fragments were amplified in a single round of PCR (Figure 7, Gel1), using *pfu* proofreading polymerase (Promega) and primer pairs matching the patented sequence (Table 4). All reactions were set up as described in Chapter II, section 2.5.2. The PCR reaction involved an initial incubation in the temperature cyclor at 94°C for 2 minutes, followed by 35 cycles of: 94°C for 10 seconds, 50°C for 30 seconds, 68°C for 20 minutes, with a final 20 minutes extension step at 68°C. The N6a and N6b fragments were amplified using cDNA made with RevertAid® premium reverse transcriptase (Thermo-Fermentas); this enzyme is capable of producing cDNA products of up to 20Kb, and this considerably improved the yield of PCR reactions covering the 5' end of the RyR gene. All other fragments, C4Kb, LNK1 and LNK2, covering the remaining portion of the gene, were amplified from Superscript™ III (Life Technologies) generated cDNA. The RNA used for the cDNA synthesis was a pooled sample of RNA extracted from various life stages of two aphid clones (4601a and 5191a) using an E.Z.N.A mollusc® RNA kit (Omega bio-Tek), as described in Chapter II, section 2.3.1.

Table 4 List of primers used for amplification of *M. persicae* RyR fragments

| Primer Name | Sequence 5'-3' | name | Length (bp) |
|----------------|------------------------------|------|-------------|
| FLn-F* | GCGATGGCCGACAGCGAGGGCAGTTCG | N6a | 3140 |
| N3Kb-R2 | GTGCGGACTGTTTCGCTTGCTGTATCTC | | |
| N3Kb-F | GCTAATAGAGATACAGCAAGCGAAAC | N6b | 2684 |
| 6Kb-R* | CCCCCAATGGGATCTCTATTATGAACC | | |
| LNK1-F | CTTGAGGAAGCCGTATTAGTTAACCAGG | LNK1 | 3056 |
| LNK1-R | CCTCTATTGTTCAAAGGTGCATCGTTC | | |
| LNK2-F | GGATGGAGTATTGAACATTCAGAGAACG | LNK2 | 2522 |
| LNK2-R | GCGTGGAGTGAGAGTTGTCGGAAACA | | |
| C4Kb-F2 | GCCGTAATTGCTTGTTCGACAAC | | |
| FLn-R | TCAGACGCCTCCTCCGCCGCGAGCT | C4Kb | 4083 |

*Primers used for N6Kb overlap extension PCR

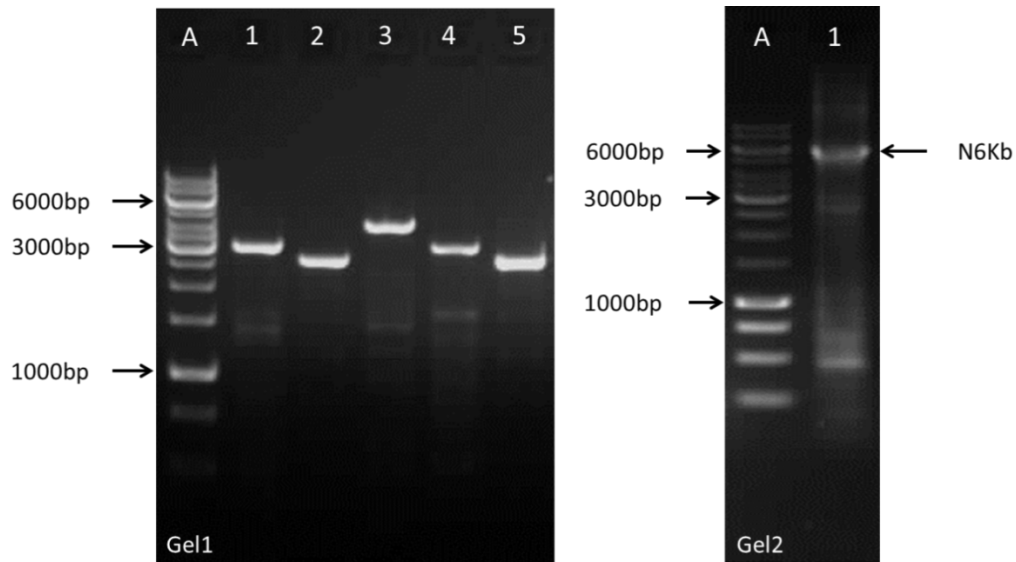


Figure 7 left- Five overlapping PCR fragments of the *M. persicae* RyR run on a 1% (w/v) TAE-agarose gel. Lanes: A) GeneRuler™1Kb DNA ladder, 1) N6a 2) N6b 3) C4Kb 4) LNK1 5) LNK2 **right** – N6Kb overlap extension PCR. Lanes: A) GeneRuler™ 1Kb DNA ladder, 1) N6kb.

The N6a and N6b PCR fragments were excised from a 1% (w/v) TAE-agarose gel (Figure 7, Gel1) and purified using a QIAquick® gel extraction kit, as described in Chapter II, Section 2.6.1. Both fragments had a 33bp overlap which was utilized in an overlap extension PCR reaction to create a single large product, N6Kb (Figure 7, Gel2). The primers used to make the fusion were Fln-F (a forward N6a primer) and 6kb-R (a reverse N6b primer). Gel purified N6a and N6b PCR fragments were combined in a 1:1 w/w ratio, and the template DNA (not exceeding 20ng) added to a

25µl reaction utilizing *pfu* enzyme. The temperature cycler conditions were an initial incubation at 94°C for 2 minutes followed by 35 cycles of: 94°C for 10 seconds, 50°C for 30 seconds 68°C for 20 minutes, and a final 20 minutes extension step at 68°C.

3.2.3 Sub-cloning *M. persicae* RyR fragments

Two sub-cloning vectors were used for propagation of the final 4 RyR fragments: pCR XL-TOPO (Life Technologies) for C4Kb and LNK1 fragments and pJET1.2 (Thermo-Fermentas) for LNK2 and N6kb. Vector maps are included in Appendix B. Both are positive selection vectors and are able to propagate large inserts of up to 10Kb. Successful insert ligation disrupts a lethal gene within the vector and allows propagation of the recombinant plasmid; as a result only bacteria containing the insert are able to grow on the antibiotic selective media and blue/white colony screening is not required. pJET1.2 carries a lethal restriction enzyme *eco47IR* and ligates blunt-ended products. pCR XL-TOPO carries a lethal *E. coli ccdB* gene [194] and has 3' end thymine (T) overhangs for TA cloning. It was the vector of choice for the sub-cloning described in the DuPont patent US2007/0105098A1. LNK2 and N6kb were ligated into pJET1.2 (as described in Chapter II, section 2.7.2) and transformed into XL-1 blue super-competent cells following the protocol described in Chapter II, Section 2.7.3. Products generated by *pfu* amplification are blunt ended; therefore, an additional step to create 3' end adenine (A) overhangs was required for the LNK1 and C4Kb PCR products prior to ligation with the pCR XL-TOPO vector. After gel purification both fragments were incubated at 72°C for 20 minutes with a standard DNA polymerase; a 50µl reaction was set up containing: all the recovered DNA, 10µl of 5x reaction buffer, 1µl dATP (100mM), 6µl MgCl₂ (25mM), 0.25µl Flexi® *taq* enzyme (5U/µl, Promega), and nuclease free water up to 50µl. After incubation, DNA fragments were ethanol precipitated and used in TOPO ligation as described in Chapter II, Section 2.7.1 and transformation into *E. coli* TOP10 cells. Positive colonies were checked for the presence of inserts via colony PCR (Chapter II, section 2.5.3), and liquid cultures were set up for purification of plasmid DNA using the protocol described in Chapter II, section 2.8.1. Plasmid DNA (isolated from at least two colonies for each RyR fragment) was checked by sequencing using the primers listed in the Appendix C, section 2.

3.2.4 *M. persicae* RyR fragment assembly

Due to the lack of suitable restriction sites, it was decided that the four cloned RyR PCR products would be joined together to create larger fragments through overlap extension PCR. All fragments had an overlap of at least their original primer length. In the first step towards creating a full-length cDNA, all 4 fragments were individually PCR amplified using *pfu*, in 50µl reactions using the original amplification primers, and plasmid DNA containing the relevant insert as a template. The temperature cycler conditions were an initial incubation at 95°C for 2 minutes followed by: 20 cycles of 95°C for 10 seconds, 50°C for 30 seconds, 68°C for 14 minutes, and a final 10 minutes extension step at 68°C. The number of cycles was reduced to 20 to minimize the possibility of PCR errors during the amplification. All of the products from the first step PCR were gel purified using a Qiagen gel extraction kit following the protocol described in Chapter II, Section 2.6.1. Four overlap extension PCR reactions were then set up to create fusions of two or three fragments (Table 5). An attempt was also made to create a full-length *M. persicae* RyR by simultaneous fusion of all four RyR fragments in a single PCR. The reactions were set up using *pfu* in a total volume of 25µl, with 50ng of each gel purified fragment and 5' and 3' primers corresponding to the ends of the desired final product. The new assemblies were named: N6L1, N6L2, L2C4 and L1C4 (Figure 8). Temperature cycler conditions were 95°C for 2 minutes followed by 25 cycles of: 95°C for 10 seconds, 50°C for 30 seconds, 68°C for 20 minutes, and a final 10 minutes extension step at 68°C. It was possible to create fusions of up to 3 fragments, all of which were gel purified using this approach; however, the subsequent assembly of a full-length *M. persicae* RyR coding sequence cDNA through overlap extension PCR was not possible when using *pfu*. Other *taq* blends were also tried including a Long PCR mix (Thermo-Fermentas) and Extensor PCR mix (Sigma), but did not yield positive results. Overlap extension PCRs were also set up with an increased number of PCR cycles (up to 35) and altered timings, using different combinations of existing fusions and fragments as templates: N6L1 with L2C4, N6L2 with C4Kb, N6kb with L1C4, but none produced satisfactory products.

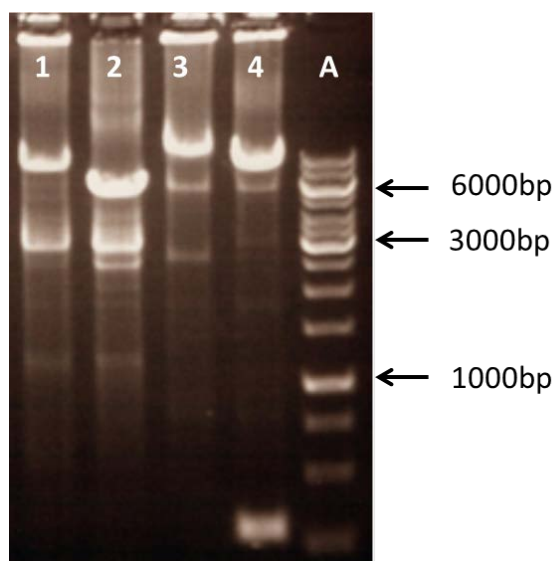


Figure 8 1% (w/v) TAE agarose gel of 4 overlap extension PCR products (as described in Table 2).

Table 5 Summary of *M. persicae* RyR fusion PCRs

| Assembly name | Templates | Primer pair | Gel lane | Product size (bp) |
|---------------|------------------|---------------|----------|-------------------|
| N6L1 | N6kb and LNK1 | Fln-F/ LNK1-R | 4 | 8865 |
| N6L2 | N6kb, LNK1, LNK2 | Fln-F/ LNK2-R | 3 | 11387 |
| L2C4 | LNK2 and C4Kb | LNK2-F/ Fln-R | 2 | 6605 |
| L1C4 | LNK1, LNK2, C4Kb | LNK1-F/ Fln-R | 1 | 9661 |

3.2.5 Sub-cloning and analysis of *M. persicae* RyR PCR fusions

Two fusion fragments, N6L1 and L1C4 (Figure 8) were individually ligated into pJET1.2 and transformed into XL-1 blue super-competent cells, following the protocol described in Chapter II, Section 2.7.3. At least 12 colonies from each transformation were screened using colony PCR. Plasmid DNA was purified from at least 5 colonies for each fusion fragment. To check for possible rearrangements of inserts within the plasmid, 1µg of plasmid DNA from all of the samples was restriction digested with BglII and run on a 1% (w/v) TAE-agarose gel to check that the expected restriction digest fragments were obtained. Orientation of the inserts within each plasmid was checked by sequencing using vector specific primers (see Appendix C, section 1). Additionally, one clone for L1C4 and one clone for N6L1 were fully sequenced and analysed before the final full-length RyR cDNA assembly.

Sequencing of L1C4 revealed the presence of 268bp of the pCR-XL vector, positioned immediately after the RyR STOP codon. The 268bp comprised the 5' end

of the multiple cloning site (MCS), containing a number of restriction sites including EcoRI, the M13 reverse primer binding site, and a portion of the Lac Z promoter. The origin of this 268bp was difficult to explain, since only insert-specific primers were used to amplify the fragment from the vector for the overlap extension PCR. *In silico* analysis of this portion of pCR-XL, using Vector NTI, gave a 92.6% match to the Fln-F primer sequence at the 3' edge of the 268bp carry over. It is possible that contamination of the PCR reaction with the Fln-F primer occurred and this, coupled with low annealing temperatures during the thermal cycling, gave a partial amplification of the vector sequence. However, the inadvertent presence of this 268bp was fortuitous as the EcoRI site was later utilized for the assembly of the full-length RyR in the mammalian expression vector pcDNA 3.1(-). Further sequencing of L1C4 also revealed an insertion of a thymine (T) at position 9717 (of the predicted full-length *M. persicae* RyR) which was not present in the original fragments used for making L1C4. This thymine insertion caused a frame-shift, resulting in the premature termination of the protein coding sequence, and had to be removed by site directed mutagenesis using the primer pair: Mz.mutdel-F / Mz.mutdel-R and the protocol described in Chapter II, section 2.9, before assembly of the full-length RyR could be attempted. Successfully mutagenized (corrected, in-frame cDNA) clones of L1C4 were identified through plasmid DNA sequencing.

3.2.6 Assembly and propagation of the *M. persicae* RyR in pcDNA 3.1(-)

The overall strategy for cloning the full-length RyR is shown in Figure 9. The expression vector pcDNA 3.1(-) (vector map in Appendix B) was chosen for propagation of the full-length *M. persicae* RyR, as it gives constitutive high-level protein expression using the immediate-early human cytomegalovirus promoter (CMV), and has been used successfully to express a number of RyR proteins in mammalian cell lines [186]. Empty vector was propagated in XL-1 blue *E. coli* as described in Chapter II, section 2.7.4. A strategy was devised to accommodate the full-length RyR into pcDNA 3.1(-), based on the *M. persicae* RyR sequence in the DuPont patent (US2007/0105098A1) and data from sequencing of the individual fragments and the two large fusions N6L1 and L1C4 generated in this work. *In silico* analysis showed that the *M. persicae* RyR contained only a single ApaI site (at position 7352), and that this ApaI site was present in both N6L1 and L1C4 fusion

fragments so could be used for ligating together the full-length sequence. NotI and EcoRI sites within the pcDNA 3.1(-) MCS were used to incorporate the fusion fragments into the vector. Both of these restriction sites were also present in the sub-cloned fusion fragments. The NotI site was located at the 5' end of the MCS of the pJET1.2 vector which was used to sub-clone N6L1, and the EcoRI site was present immediately after the STOP codon in the L1C4 pCR-XL carry over (as discussed in 3.2.5) (Figure 9). Some modifications of N6L1 and L1C4 were required before final ligation was possible. The correctly orientated N6L1, with a translation initiation START codon close to the MCS NotI site, had to have a 5'-ACG-3'Kozak consensus sequence created by site-directed mutagenesis. An additional START codon, which was created during ligation of the insert's 5' end and the vector, also needed to be removed. A single G to A substitution was introduced 3 base pairs upstream of the native RyR START codon using Mz.N12-F / Mz.N12-R primer pair. The final mutagenized plasmid was named N6L1a. L1C4 had an additional EcoRI site present 1067 bp upstream of the STOP codon, which was removed by introduction of a silent mutation using Mz.Eco-F / Mz.Eco-R primer pair. This new plasmid was named L1C4a. Both mutagenesis reactions were carried out following the protocol described in Chapter II, section 2.9. Positive clones containing correctly mutagenized inserts were identified and confirmed by DNA sequencing.

Prior to their ligation, 2µg of N6L1a, L1C4a, and the empty vector, were double digested with appropriate restriction enzymes (N6L1a: NotI, ApaI; L1C4a: ApaI, EcoRI), and the digested fragments were run on 0.75% (w/v) TAE-agarose gels, excised from the gels and purified using a gel extraction kit (see Chapter II, section 2.6.1). The ligation reaction was set up in a total volume of 20µl including: 40ng of each DNA fragment in a 1:1:1 weight ratio, 2µl of ligation buffer and 1µl T4 DNA ligase (Thermo-Fermentas), and incubated overnight at 15°C. Before transformation, 10µl of the ligation reaction was run at 70V/200mA on a 0.8% (w/v) TAE-agarose gel for 50 minutes to confirm that successful ligation of all three fragments had been achieved. 2µl of the ligation was then used to transform 30µl of XL-10 gold cells, as described in Chapter II, section 2.7.3. Transformed cells were allowed to recover at 30°C for 2 hours, with shaking at 250rpm. The transformation mixture was then plated out on low salt LB plates containing 100µg/ml Ampicillin, and incubated at 30°C for 24 hours, and then at room temperature overnight. This allowed enough

time for colony size discrimination to become apparent on the plates; small colonies were more likely to contain an intact insert-containing plasmid and these were preferentially selected for screening. Positive transformants were identified with two separate colony PCR reactions, using primer pairs N1-F / N2kb2-R and C2kbF / C1-R, amplifying fragments close to the 5' and 3' end of the insert respectively. Only clones which gave the correct PCR product with both primer pairs were set up as overnight liquid cultures, maintained in a shaking incubator set at 30°C and 250 rpm. Plasmid DNA was extracted and purified using column-based kits (following methods described in Chapter II, section 2.8.1) and checked for possible rearrangements by restriction digests with BglII (Promega). The ligation sites and the entire RyR cDNA insert were then checked by direct sequencing. The large quantities of plasmid DNA required for subsequent transfections were obtained using modified maxi-prep purification, as described in detail in Chapter II, section 2.8.4.

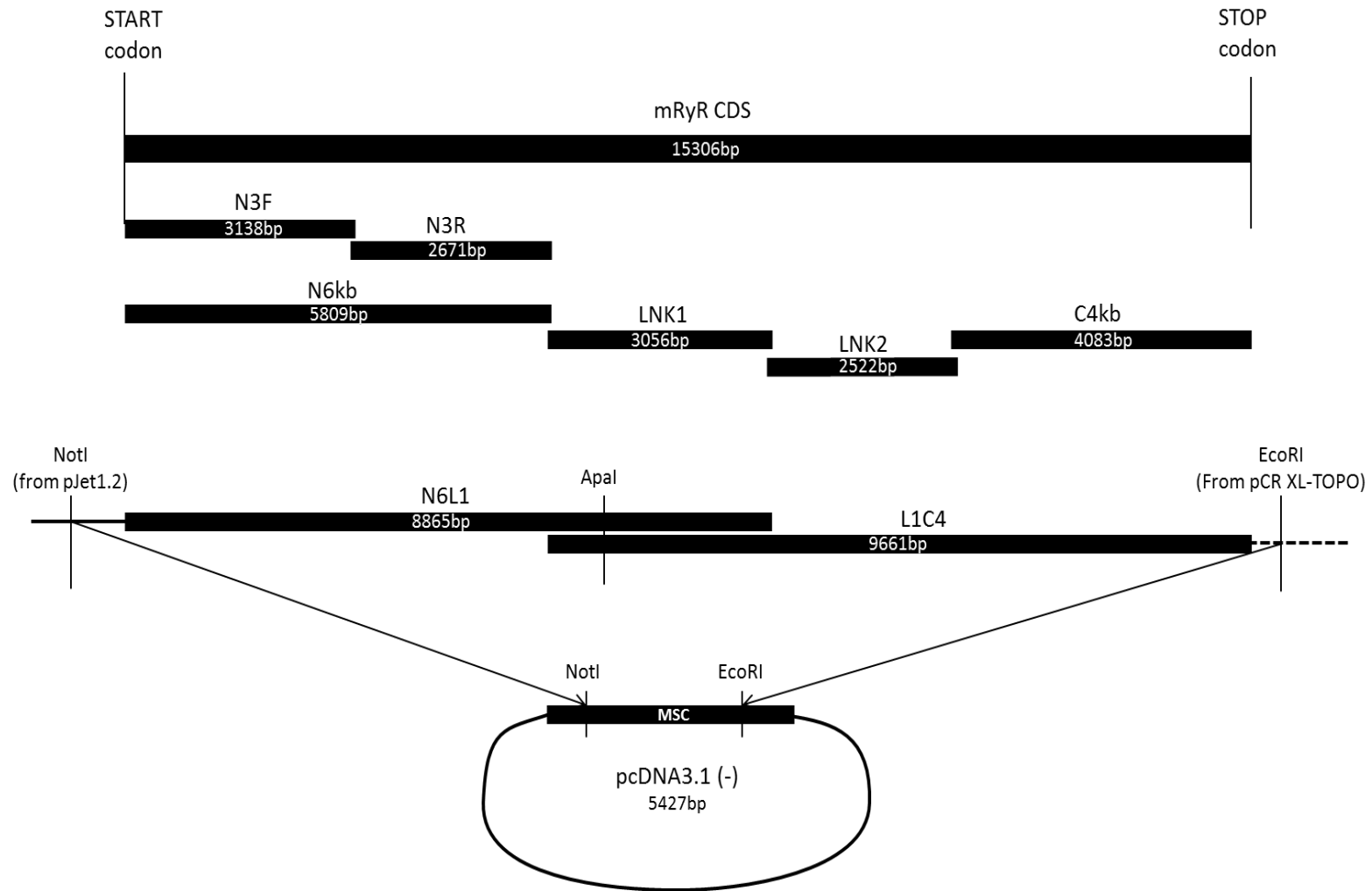


Figure 9 Summary of the cloning strategy used for assembly of full-length *M. persicae* RyR in the expression vector pcDNA 3.1(-).

3.2.7 Modification of pcDNA 3.1(-) to insert eGFP sequence

In order to be able to monitor the expression of the *M. persicae* RyR cDNA in live cells, a vector was made with an enhanced Green Fluorescent Protein (eGFP) coding sequence incorporated in a position that would allow for the production of N-terminally tagged protein fusions. Addition of eGFP would also allow detecting expressed channels in membrane preparations using anti-eGFP antibody in western blots. The eGFP was incorporated into the empty pcDNA 3.1(-) vector by ligation of a cassette, made from PCR-amplified and fused vector CMV promoter and eGFP coding sequence, between MluI and NotI sites (following a method described for the human RyR2 construct [195]). The eGFP sequence was amplified from a human wild type (WT) RyR2 construct provided by Prof. Tony Lai, Cardiff University. The human RyR2 construct was first propagated in XL-10 *E. coli* as described for *M. persicae* RyR in section 3.2.6. The forward eGFP amplification primer (eGFP-F) contained a 5' end overhang with a small overlap with the pcDNA 3.1(-) vector CMV promoter's 3' end, whilst the reverse primer (eGFP-R) had a functional NotI site incorporated. The CMV promoter forward primer (pcDNA-CMV F) had a MluI site incorporated, and the reverse primer (pcDNA-CMV R) had an overlap with the beginning of the eGFP sequence. Both eGFP and the CMV promoter were PCR amplified separately using *pfu*. The human RyR2 plasmid was used as a template in the eGFP reaction and the empty pcDNA3.1(-) vector was the template for obtaining the CMV promoter. After successful PCR amplification, both products were gel purified and used in a second round of PCR to create a single fused CMV - eGFP cassette (using *pfu* and pcDNA-CMV-F / eGFP-R primer pair), which was ligated into pJET1.2 vector and transformed into *E. coli*. Following the selection of successful transformants, the fusion cassette was sequenced to check for potential PCR errors. The cassette was then cut out of the pJET1.2 vector, using the restriction enzymes MluI and NotI, and ligated (using T4 DNA ligase) into empty pcDNA3.1(-) plasmid previously digested with the same restriction enzymes. Successful transformants were selected by colony PCR using eGFP-F / eGFP-R primer pair. Stocks of purified plasmid DNA were made for future use. The new plasmid was called pcDNA3.1-eGFP.

3.2.8 Modification of *M. persicae* RyR and assembly of eGFP fusion in pcDNA

3.1(-)

Direct NotI / EcoRI ligation of the digested, untagged RyR construct with the modified pcDNA3.1-eGFP vector would be expected to give a 36 base pair linker between the end of the eGFP sequence and the RyR START codon, consisting of residual pJET1.2 vector sequence. Additionally, the ACG Kozak consensus sequence from the untagged RyR construct would also be present, and could potentially interfere with eGFP-RyR protein expression. It was therefore decided that the linker would be shortened to remove the Kozak and pJET1.2 vector sequences. The new construct would have only 3 amino acids between the eGFP and the RyR sequence (Figure 10). In order to achieve this, site-directed mutagenesis was used on the pJET1.2 plasmid containing the N6L1 fragment, to introduce a novel AfeI site 204bp downstream of the RyR START codon. The mutagenesis involved a silent substitution which would not alter the predicted amino acid sequence. The reaction was done with primers Mz.Afe-SDM-F / Mz.Afe-SDM-R, following the protocol described in Chapter II, section 2.9. The mutagenized plasmid, named N6L1-Afe, was identified by sequencing and used as a template for amplification of a short cassette using *pfu* and primers Mz.NotI-F / Mz.AfeI-R (primers sequence in Appendix C, section 3). The forward primer contained a functional NotI site immediately upstream of the RyR START codon and the reverse primer contained the newly introduced AfeI site. The cycling conditions were an initial denaturation at 95°C for 1 minute followed by: 35 cycles of 95°C for 20 seconds, 50°C for 35 seconds, 72°C 1 minute 30 seconds, and a final extension of 72°C for 2 minutes. The product was gel purified, double digested with NotI and AfeI restriction enzymes and purified again using a Qiagen PCR purification kit (Chapter II, section 2.6.2). The cassette was then ligated into pJET1.2 N6L1-Afe plasmid, pre-digested with NotI and AfeI, using T4DNA ligase. The ligation product was transformed into XL-1 blue *E. coli* and the modification of the plasmid was confirmed by sequencing. The new plasmid was named N6L1b. The final assembly of the full-length *M. persicae*

RyR was performed as described in section 3.2.6, using pcDNA3.1-eGFP, N6L1b and L1C4a plasmids (Figure 9).

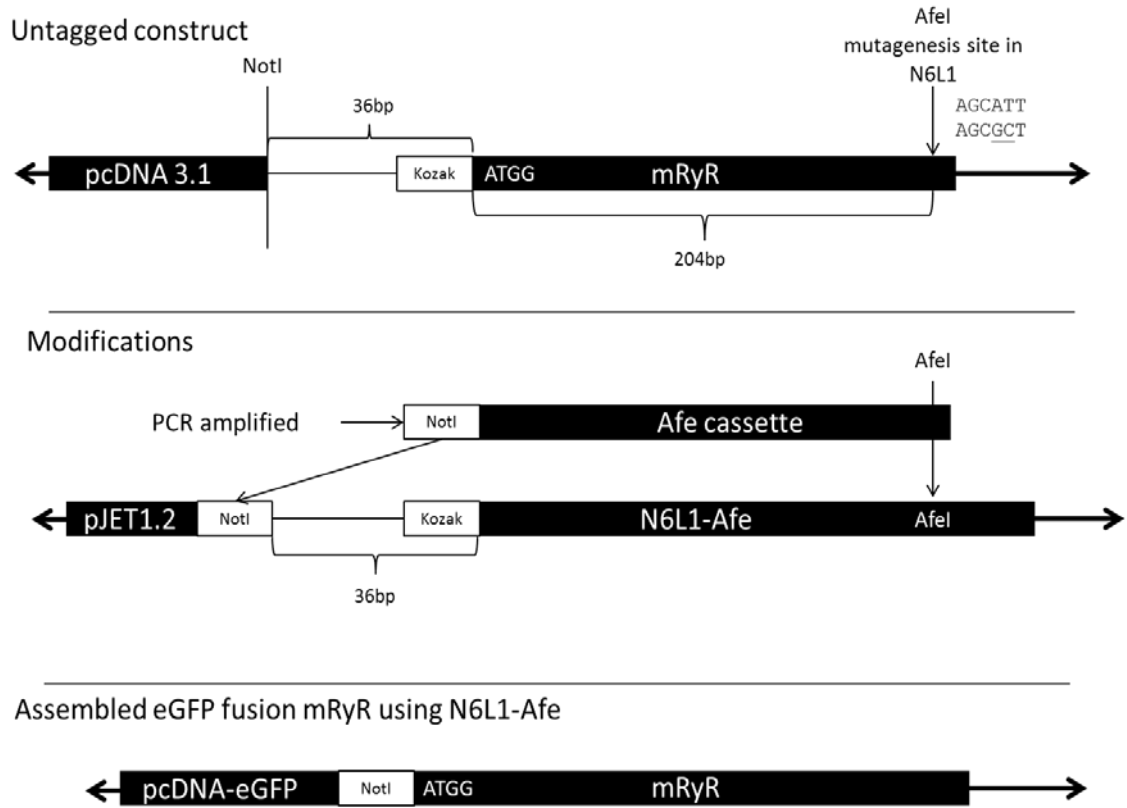


Figure 10 Summary of techniques used to remove the Kozak sequence and generate a short linker between the *M. persicae* (mRyR) START codon and eGFP sequence in the pcDNA-eGFP fusion construct.

3.2.9 Assembly of eGFP tagged *M. persicae* RyR construct in a vector for expression in insect cells

A pIZ/V5-His (Life Technologies) plasmid was used to accommodate the *M. persicae* eGFP tagged RyR coding sequence. This vector gives constitutive expression of a target protein, through baculovirus immediate-early promoter OpIE2, in a range of insect cell lines. Unlike a baculovirus expression system it does not cause cells to lyse, and gives an option to use Zeocin™ (Life Technologies) selection to isolate stable cell lines. The vector contains a single Zeocin™ resistance gene, used for selection of both *E. coli* clones and successfully transfected insect cells. The pIZ/V5-His has two tags for protein purification, both on the 3' end of the MCS, meant to be used as C-terminal fusion tags.

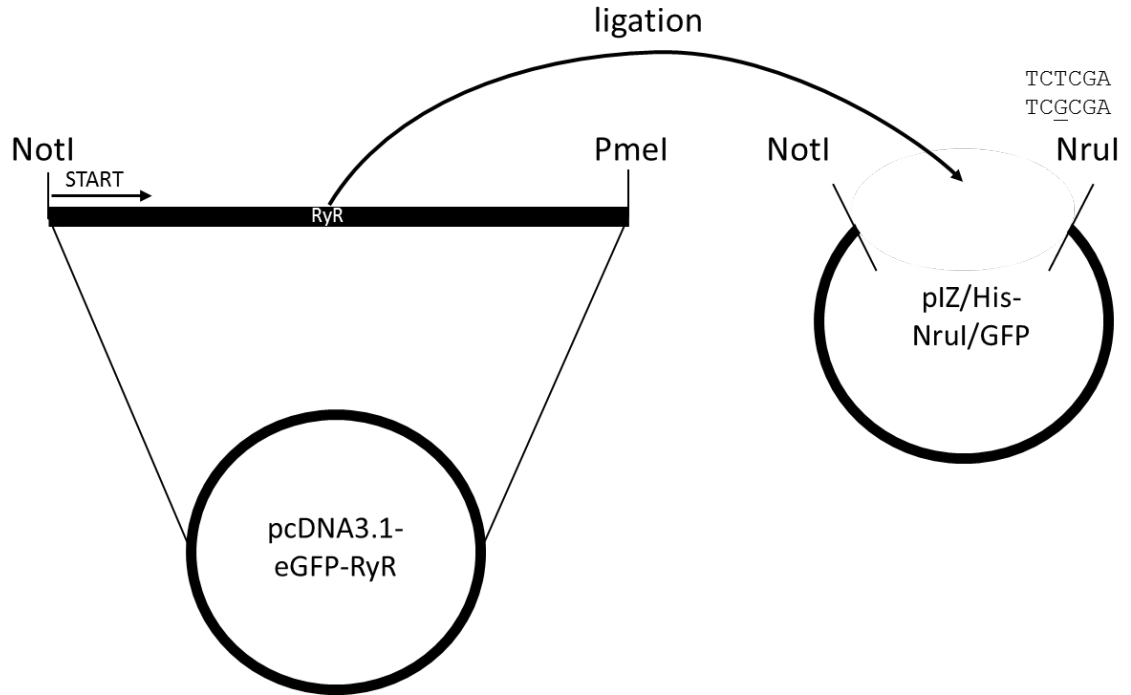


Figure 11 Summary of the strategy used to introduce insect RyRs into a modified pIZ vector for expression in insect cell lines. The NruI site had to be engineered into the empty pIZ vector.

Removal of the full-length RyR insert from the pcDNA3.1-eGFP vector requires the use of NotI and PmeI restriction sites. This is not ideal because PmeI digestion creates a blunt ended product. There is no site present in the pIZ/V5-His vector which would give a blunt end and allow insertion of the RyR in the correct position and desired orientation. The pIZ/V5-His vector was therefore modified prior to use for propagation and expression of insect RyRs through the introduction of a novel restriction site, NruI. The NruI site was engineered in such a position as to allow the removal of most of the V5 tag from the vector upon restriction digest and insert ligation. The site was created by site-directed mutagenesis of the thymine (T) at vector position 694 to guanine (G), using primer pair pIZ/His-NruI SDM-F and pIZ/His-NruI SDM-R (Appendix C, section 1), following the protocol described in Chapter II, section 2.9. Successfully mutagenized clones were identified by sequencing and the modified vector, named pIZ/NruI, was propagated in XL-1 blue cells. The eGFP sequence was then inserted into the modified vector: the eGFP sequence was amplified from pcDNA3.1-eGFP using *pfu* and primer pair eGFP-EcoRI-F / eGFP-R. The forward primer had a 5' end overhang with an EcoRI site and the insect 5'-CAAA-3' Kozak consensus sequence incorporated. The cycling

conditions were 95°C for 2 minutes followed by: 30 cycles of 95°C for 10 seconds, 50°C for 30 seconds, 72°C for 2 minutes, and a final extension at 72°C for 5 minutes. Amplified product was gel purified, double digested with EcoRI / NotI and purified again using a Qiagen PCR purification kit. The cassette was then inserted between the EcoRI and NotI sites of the pIZ/NruI vector. The new vector was propagated in XL-1 blue cells, and successful transformants were selected by colony PCR and sequencing. The final assembly of the *M. persicae* RyR was then attempted: the entire insert was cut out from the eGFP tagged pcDNA3.1 construct using NotI / PmeI, and ligated overnight at 15°C into the NotI / NruI digested pIZ/eGFP vector in 1:1 weight ratio, using T4DNA ligase (figure 11). Prior to *E.coli* transformation, 10µl of the ligation reaction was run on a 0.8% (w/v) TAE agarose gel to confirm the success of the ligation. XL-10 gold cells were used for transformation following the standard protocol described in Chapter II, section 2.7.3, and positive transformants were selected exactly as described previously for the two pcDNA3.1 constructs (see 3.2.6). The integrity of ligation sites within the plasmid DNA containing the RyR-eGFP insert were checked by sequencing, and the integrity of the construct as a whole was checked by BglII restriction digest.

3.2.10 Quantitative RT-PCR

Quantitative RT-PCR was used to examine the relative levels of expression of the RyR in four different life stages of *M. persicae* clone 4106; apterous adults, winged adults and nymphal stages L1/L2 and L3/L4. The primers were designed to amplify a fragment of 90-150bp, and are listed in Table 6.

Table 6 *M. persicae* qPCR primers

| Primer | Sequence 5'-3' | Expected amplicon size |
|------------|----------------------|------------------------|
| Mz.qPCR3-F | CGAACTTGCATTAGCGTTGA | 125bp |
| Mz.qPCR3-R | CTGGATCCCAGCCTAAATCA | |
| Mz.qPCR4-F | CAATTGGGAATCGCAGTTCT | 127bp |
| Mz.qPCR4-R | CGCTGCACGAGTTCATTA | |

Total RNA was prepared as described (Chapter II section, 2.3.2) and 750ng used for cDNA synthesis using Superscript III (Life Technologies) and random hexamers (Life Technologies, CA, USA), according to the manufacturer's recommended protocol. PCR reactions (15µl) contained: 4µl cDNA (20ng), 7.5µl SensiMix SYBR Kit (Bioline, London, UK) and 0.25 µM of each primer. Samples were run on a Rotor-Gene 6000™ (Corbett Research) using temperature cycling conditions of 10 minutes at 95°C followed by 40 cycles of: 95°C for 15 seconds, 57°C for 15 seconds, 72°C for 20 seconds. A final melt-curve step was included post-PCR (ramping from 72°C-95°C by 1°C every 5 seconds) to confirm the absence of any non-specific amplification. The efficiency of PCR for each primer pair was assessed using a serial dilution of 100ng to 0.01ng of cDNA. Each qRT-PCR experiment consisted of three independent biological replicates with two technical replicates for each. Data were analysed according to the $\Delta\Delta$ CT method [196], using the geometric mean of two selected housekeeping genes (actin and the *para* gene which encodes the voltage-gated sodium channel) for normalisation according to the strategy described previously [197]. In this analysis the reference life stage was adult apterous aphids.

3.2.11 Amplification and cloning of *Plutella xylostella* RyR fragments

At the start of this project there was no *P. xylostella* RyR sequence published, or available in online sequence depositories, so attempts were made to amplify small fragments of *P. xylostella* RyR using degenerate PCR primers designed to conserved regions of other Lepidopteran (*Bombyx mori* and *Heliothis virescens*) RyR genes, near to their 5' and 3' ends and also around the middle of the coding sequence. Four primers per fragment were designed (two forward and two reverse, see Table 7) to amplify fragments of less than 1kb in length. All possible primer combinations were used in PCRs.

Table 7 List of degenerate primers used for amplification of *P. xylostella* RyR fragments

| Primer Name | Sequence 5'-3' | Description |
|-----------------|---|---------------------------------------|
| Px.NA df | TTYY <u>T</u> NC <u>G</u> DAC <u>S</u> GAAGAYATGG | Forward primers for 5' end N fragment |
| Px.NB df | GAAGG <u>H</u> TT <u>Y</u> GG <u>H</u> AA <u>Y</u> CGDCAYTG | Reverse primers for 5' end N fragment |
| Px.N1 dr | GGT <u>W</u> T <u>N</u> GT <u>N</u> ARRCAYTCRTCDCC | Forward primers for 3' end C fragment |
| Px.N2 dr | CC <u>N</u> GCCCA <u>Y</u> TTDGT <u>N</u> CKVGC <u>B</u> AG | Reverse primers for 3' end C fragment |
| Px.CA df | GG <u>A</u> RTTYGACGG <u>N</u> CTGTWCATYGC | Forward primers for middle M fragment |
| Px.CB df | AA <u>Y</u> HTGYTB <u>G</u> GBATGGARAAGAC | Reverse primers for middle M fragment |
| Px.C1 dr | TC <u>W</u> CC <u>N</u> AC <u>N</u> GGGAARAAGTCCC | Forward primers for 5' end N fragment |
| Px.C2 dr | GGTCACG <u>V</u> AGCTC <u>D</u> CCGA <u>A</u> VGC | Reverse primers for 5' end N fragment |
| Px.MA df | G <u>A</u> RA <u>A</u> RTTGATCC <u>A</u> BTACAT <u>N</u> GAYAGDGC | Forward primers for 3' end C fragment |
| Px.MB df | GACTTCCTGAG <u>V</u> TT <u>Y</u> TG <u>Y</u> GTTTGGG | Reverse primers for 3' end C fragment |
| Px.M1 dr | CCAG <u>H</u> AR <u>B</u> TGCCAGTCTTCTTGTATCTG | Forward primers for middle M fragment |
| Px.M2 dr | GCRTAGTTCTC <u>R</u> GC <u>Y</u> TCGTTGTAGA | Reverse primers for middle M fragment |

Degenerate residues are underlined.

All degenerate PCRs were done in 25µl reactions with: 1µl cDNA (made with RevertAid premium transcriptase), 12.5µl of REDtaq® master mix and varying amounts of primers and nuclease free water. During reaction optimisation, 10 to 40 pmole of each primer were tested. The cycling conditions tested were 95°C for 2 minutes followed by: 35 cycles of 95°C for 20 seconds, 45-50°C for 45-60 seconds, and 72°C for 2-3 minutes, with a final extension time of 72°C for 5 minutes. This gave 3 fragments: CA-1 (3' end), MB-2 (middle) and NA-1 (5' end), obtained when a long annealing time (1minute) at 50°C was used in combination with high primer concentrations. Bands of the expected size were purified by gel extraction and ligated into p.Jet1.2 vector, using the insert's sticky-ends protocol. All 3 fragments were transformed into XL-1 blue cells following the protocol described in Chapter II, section, 2.7.3. Positive transformants were selected by colony PCR using vector specific primers, the plasmid DNA purified, and the insert sequenced (using the same vector specific primers) to confirm the identity of the cloned fragments. The RyR sequences obtained were then used to design *P. xylostella* gene specific primers to amplify fragments covering the large gaps (approximately 7Kb) between the CA-1, MB-2 and NA-1 fragments (Figure 6). A long PCR mix (Thermo-fermentas) was used to successfully amplify both 7Kb fragments after initial attempts with *pfu* failed. Two sets of PCR reactions were set up following standard protocols (Chapter II, section 2.5.2), but with additional amount of 10mM dNTPs (1µl) included in the reaction mix and gradient cycles with different extension times. Primer pair Px.M1f / P.C2R was used to amplify between CA-1 and MB-2 to generate fragment N7Kb.

Primers Px.N1f / Px.M1r were used to amplify between NA-1 and MB-2 to generate fragment C7Kb. The cycling conditions for both PCR reaction sets were an initial denaturation at 94°C for 2 minutes followed by: 35 cycles of 94°C for 10 seconds, 45-55°C for 20 seconds, 68°C for 14 or 25 minutes, followed by a final extension of 68°C for 15 minutes. The best amplification results were obtained with a 50°C annealing temperature and a 25 minute extension time for C7Kb, and 45°C annealing with 25 minutes extension time for N7Kb. Both PCR fragments were then gel purified, cloned into p.Jet1.2 vector following the sticky ends protocol (Chapter II, section 2.7.2), and transformed into XL-1 blue cells. Transformation reactions were recovered at 30°C for 2 hours, and then transferred to low salt LB 100µg/ml ampicillin plates. The LB plates were also incubated at 30°C for 24 hours to increase the likelihood of getting intact, non-rearranged plasmids. Due to the large insert size and lack of sequence information it was impossible to select positive clones by colony PCR. Instead 16 colonies for both fragments (C7Kb and N7Kb) were taken and grown overnight in 4ml of LB broth with 50µg/ml ampicillin, their plasmid DNA purified using a mini- prep kit, and 400ng of the undigested plasmid DNA run on a 1% (w/v) TAE-agarose gel, which allowed a size discrimination of plasmids containing the insert to be visualized. Two positive clones for C7Kb and N7Kb were chosen for sequencing; initially vector specific primers were used to sequence the insert ends, and then this new sequence data was used to design the initial forward and reverse primers to allow for sequential sequencing through the whole insert, as illustrated in Figure 14. Primer sequences are in Appendix C, section 4.

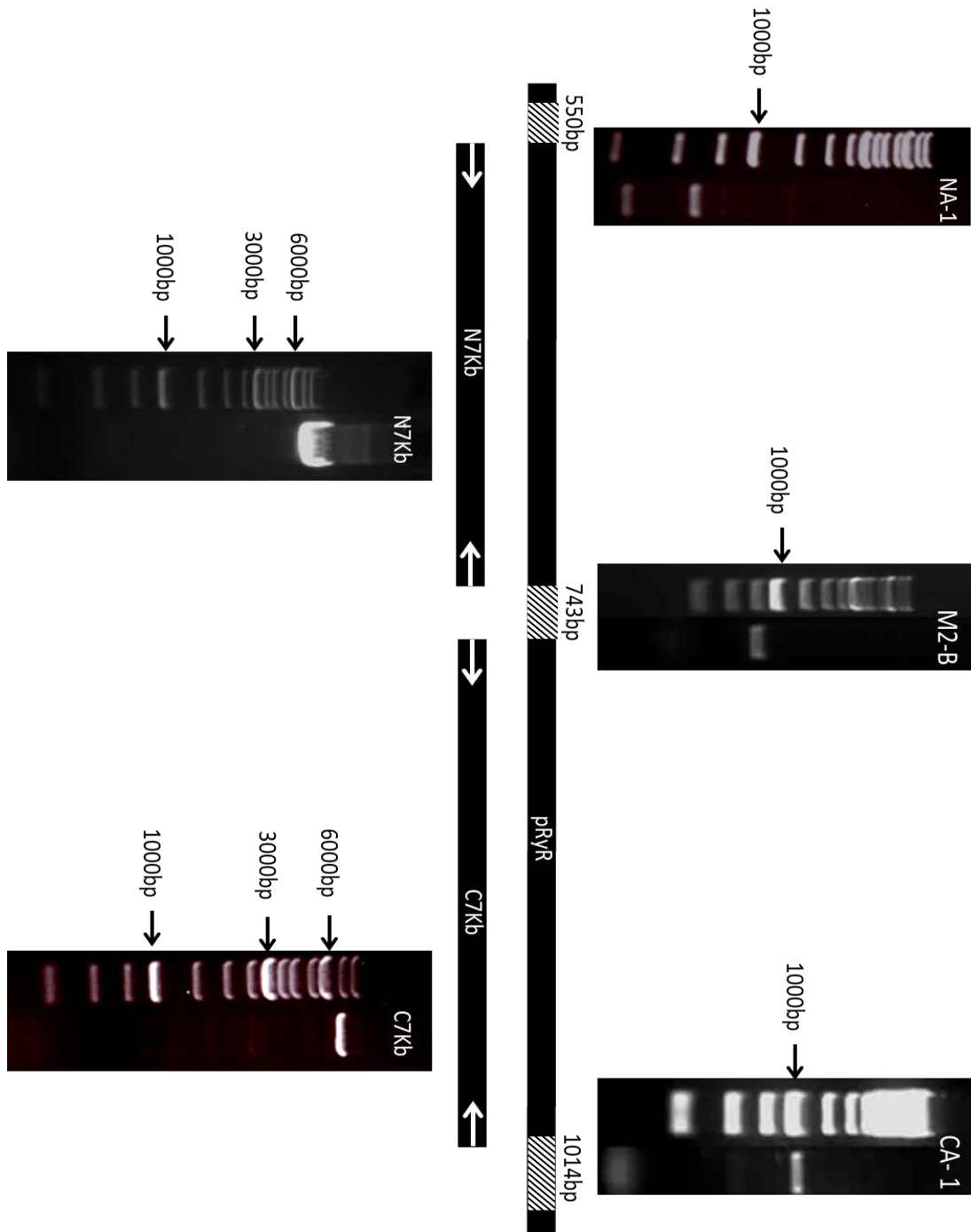


Figure 12 Summary of the amplification of *P. xylostella* RyR in order to obtain sequence of the receptor to device cloning strategy. Top: The 3 initial small fragments amplified by degenerate PCR, which were cloned and sequenced to provide information for gene specific primer design for. (Bottom) 2 large fragments spanning the gaps between the initial small fragments. The extreme 5' and 3' ends missing approximately 100bp were obtained through RACE.

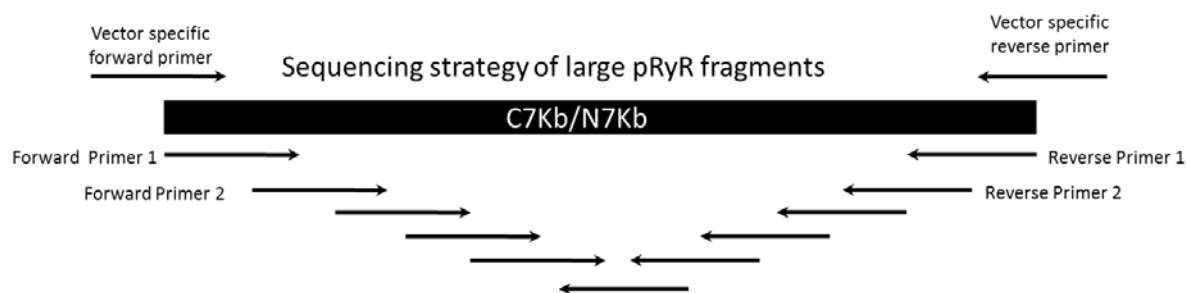


Figure 13 Diagram of the sequencing strategy for the two large *P. xylostella* RyR fragments. Fragments were first cloned and initially sequenced using vector specific primers. All subsequent overlapping primers were designed based on collected information for the sequencing results using upstream (for the 5' end) and downstream (for the 3' end) primers, until entire fragment have been sequenced.

A consensus sequence for both fragments was then assembled using Contig Express, part of Vector NTI 10 (Invitrogen) suite of programs.

3.2.12 Obtaining *P. xylostella* RyR gene ends by RACE

It was estimated that there were between 50 to 100 bps missing between the amplified fragments NA-1 and CA-1 and the START and STOP codons of the *P. xylostella* RyR coding sequence, respectively. In order to obtain information on the entire coding sequence, a 5' and 3' Rapid Amplification of cDNA Ends (RACE) was done, using a First Choice® RLM RACE kit (Ambion®-Life Technologies, CA, USA). A set of RACE primers was designed according to the kit manufacturer's recommendations (see Table 8).

Table 8 List of RACE primer sequences

| Primer name | Sequence 5'-3' | position |
|---------------------|--------------------------|-------------|
| Px.3'RACE inner-1F | GAGTCCAATTGCTTCATCTGTGGC | 15103-15126 |
| Px.3'RACE outer-2F | CATCGGAGACGAACTGGAGCC | 14928-14948 |
| Px.5'RACE inner -1R | CGCTCAGTAGCGACAGACACGAGG | 498-521 |
| Px.5'RACE outer-2R | GTACCGCTCAGTAGCGACAGACAC | 502-525 |
| Px.5'RACE F | GATATGGTGTGCCTGTCTGCACG | 63-84 |

Freshly extracted *P. xylostella* RNA was used for both 5' and 3' end reactions. For 5' end RACE, 8µg of total RNA was first treated with calf intestine alkaline phosphatase (CIP) at 37°C for 1 hour to remove free 5'-phosphates. The reaction was

terminated with ammonium acetate, the RNA extracted with phenol:chloroform and precipitated with isopropanol. The RNA was then treated with tobacco acid pyrophosphatase (TAP) at 37°C for 1 hour, to remove the 5' end caps from the full-length mature messages. The 5' end RACE adapter was then ligated to CIP/TAP treated RNA in a 1 hour incubation at 37°C with T4 RNA ligase. The reverse transcription reaction was then set up in a total volume of 20µl using: 2µl of treated RNA, 2µl random decamers, 4µl dNTP mix (10mM), 1µl RNase inhibitor and 1µl M-MLV reverse transcriptase which was provided with the kit. The 3' end RACE used a cDNA synthesis reaction: 1µg of non-treated RNA with 4µl dNTPs (10mM), 2µl 3' adapter, 1µl RNase inhibitor and 1µl of M-MLV transcriptase in a total reaction volume of 20µl. Both reactions were incubated at 42°C for 1 hour and were terminated with a 5 minute incubation at 70°C. The cDNA was then used for a series of gradient PCR reactions, set up in total volume of 25µl using: REDtaq® mastermix, RACE outer primer (20pmol) pairs and 1µl of cDNA as a template. The PCR cycle was 95°C for 3 minutes followed by 35 cycles of: 95°C for 30 seconds, a temperature gradient of 55-65°C for 30 seconds, 72°C for 2 minutes and a final 5 minutes extension at 72°C. Results of the first PCR cycle gave no, or very weak amplification, therefore 1µl of the first reaction was used as a template for a secondary nested PCR using RACE inner primer (20pmol), REDtaq® mastermix and the same cycling conditions. Two fragments with the best amplification in the secondary reaction (at 65°C for the 5'RACE and 55°C for the 3' RACE) were gel purified, ligated into p.Jet1.2 vector and transformed into XL-1 blue cells. 12 colonies were tested for the presence of insert using vector specific primers. Four clones from each RACE reaction were grown in liquid culture for plasmid DNA isolation. Cloned fragments for both reactions were confirmed to be part of the *P. xylostella* RyR gene by sequencing, which also provided information on the 5' and 3' UTR regions of the gene.

3.2.13 Amplification and sub-cloning fragments of full-length *P. xylostella* RyR

The initial sequence information obtained for the *P. xylostella* RyR facilitated the design of a strategy to clone a full-length coding sequence. It was decided that the *P. xylostella* gene would be cloned as 4 overlapping fragments. However, unlike for the *M. persicae* RyR, individual fragments would be joined together by ligation using

unique restriction sites. It was assumed that the initial *P. xylostella* RyR sequence contained an unknown number of introduced errors, due to the use of a low-fidelity *taq* in the PCR. Therefore, for amplification of the 4 overlapping fragments a high fidelity proofreading polymerase enzyme was used.

Initially, a set of *P. xylostella* gene-specific primers were designed to amplify four fragments named Nterm, M1, M2 and Cterm, using *pfu* in a standard reaction set up as described in Chapter II, section 2.5.2. PCR conditions were 95°C for 2 minutes followed by 35 cycles of: 95°C for 10 seconds, 50°C for 20 seconds, 68°C for 20 minutes and a final extension at 68°C for 10 minutes. This strategy gave a good yield of products for M1 and M2, which were gel purified and cloned into p.Jet1.2 vector (Chapter II, section 2.7.2). Despite attempts to optimise the PCR reactions for the other fragments (by increasing the amount of dNTPs and extending the annealing and extension times to 35 seconds and 25 minutes, respectively) PCR reactions to amplify Nterm (4kb) gave only very weak amplification, not suitable for purification and cloning, and PCR reactions to amplify Cterm (6Kb) did not produce any product of the expected size. Replacing *pfu* with other high fidelity enzymes such as fusion® (New England Biolabs) did not improve this; in fact fusion *taq* failed to amplify any large RyR fragments, following the manufacturers recommended protocols (data not shown).

Four additional primers were designed to sub-divide PCR amplification of Nterm and Cterm into smaller overlapping fragments which could be easily amplified using *pfu* and joined together in an overlap extension PCR (Figure 15). Primers Px.Ntm2F and Px.Ntm1R were designed to amplify (in conjunction with the two previous primers - see above) two 2Kb fragments named N1 and N2, and primers Px.Cv1-F and Px.Cv2-F to amplify two 3Kb fragments, C1 and C2. Extended temperature cycler conditions were used (50°C annealing for 35 seconds and a 25 minutes extension step at 68°C) to amplify all 4 sub-fragments (see Figure 7). These were gel purified and used as a template (in 1:1 weight ratios) for two secondary overlap extension PCRs using primers Px.NtermF / Px.NtermR for the Nterm fragment and Px.CtermF / Px. CtermR for the Cterm fragment. The secondary PCR cycle was 95°C for 2 minutes followed by 35 cycles of: 95°C for 10 seconds, 50°C for 35 seconds, 68°C for 24 minutes and final extension at 68°C for 15 minutes. The fused

N and C fragments were then cloned into p.Jet1.2 as described in Chapter II, section 2.7.2.

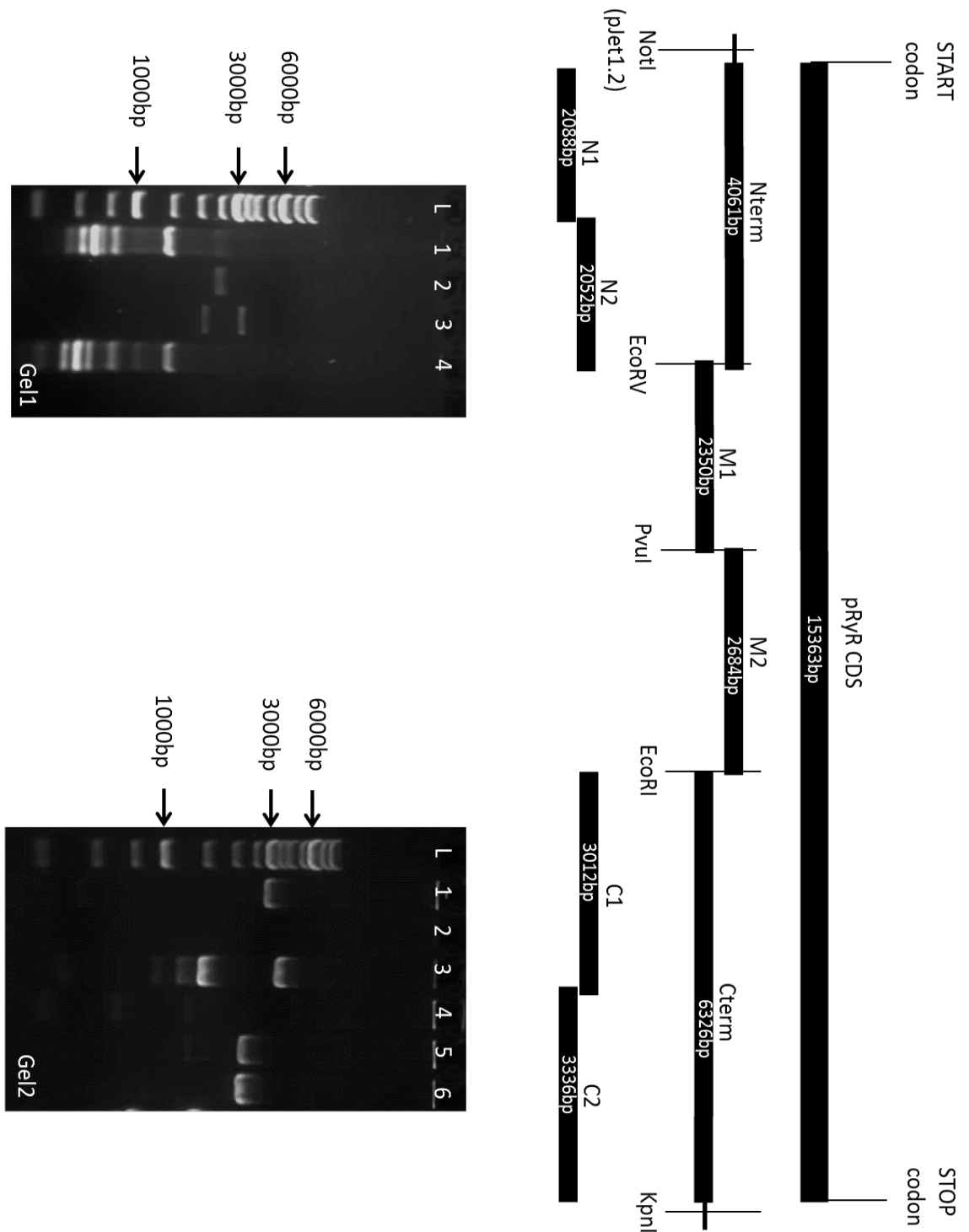


Figure 14 Summary of *P. xylostella* RyR fragments used for the full-length assembly. Nterm and Cterm fragments were generated as initial sub-fragments fused together using overlap extension PCR to give the final product. Gel images: L - GeneRuler 1Kb ladder.

Gel 1: lanes 1 and 4 = positive controls (REDtaq®), lane 2 = fragment M1, lane 3 = fragment C2. Gel 2: lane1 = fragment M2, lane 3 = fragment C1, lane 5= fragment N1, lane 6 = fragment N2

Positive transformants were selected by colony PCR, using insert specific primers. Four clones for each of the sub-cloned fragments were grown in liquid culture for purification of plasmid DNA and sequencing (using already existing primers from section 3.2.11, Appendix C, section 4) to confirm the presence of the required restriction sites within the constructs and to rule out the presence of any possible PCR errors.

3.2.14 Modification of sub-cloned *P. xylostella* RyR fragments

Sequencing revealed significant sequence diversity in the cloned *P. xylostella* RyR fragments (see discussion section, 3.3.2), including the presence / absence of alternative splice sites (table 9). It was therefore decided that the full-length *P. xylostella* RyR would be assembled from fragments which had the best alignment to the *B. mori* RyR cDNA which had previously been functionally expressed [30]. Unfortunately the number of SNPs present in the different fragments made it difficult to use the restriction site cloning strategy originally planned to ligate together the full-length cDNA.

Table 9 List of sequenced splice sites

| Name | Position (cDNA) | Length (bp) | type |
|----------------|------------------------|--------------------|-------------|
| Nterm-1 | 261-276 | 15 | insertion |
| Nterm-2 | 2596-2896 | 300 | deletion |
| M1-1 | 4065-4197 | 132 | deletion |
| Cterm-1 | 13536-13578 | 42 | insertion |

For the four C6 clones, all four clones had a Kpn1 site, two had an EcoRI site and one of these also had an insertion. For the four M2 clones, only two contained PvuI sites and only one had an EcoRI site. None of the clones contained both restriction sites. It was decided that the M2 fragment with the EcoRI site would be mutagenized to introduce the PvuI site needed for the final ligation, by introducing a silent polymorphism that would not change the amino acid sequence. The M2 fragment was small enough that the PCR needed to engineer the restriction site was unlikely to introduce any new errors. A site directed mutagenesis kit was used with primer pair

Px.M2pvu-SDM-f / Px.M2pvu-SDM-r, (Appendix C, section 5) following the protocol described in Chapter II, section 2.9. The mutagenized plasmid was propagated in XL-1 blue cells and clones carrying the PvuI site were identified by sequencing.

The Nterm fragment was re-amplified twice from the selected plasmid using *pfu* and two modified forward primers. The first fragment generated was amplified with primer Px.NotI-F which contained a NotI restriction site overhang immediately upstream of the START codon, and was to be used for introducing the Nterm fragment into the pcDNA3.1-eGFP construct containing an N-terminal eGPG tag and short linker sequence (as seen in the *M. persicae* RyR plasmids). The second fragment generated was to be introduced into the untagged pcDNA3.1 construct, and was amplified using primer Px.No-tag-F containing an overhang incorporating a NotI site and 5'-ACC-3' Kozak sequence upstream of the START codon. The PCR conditions used for both reactions were 95°C for 2 minutes followed by 35 cycles of: 95°C for 20 seconds, 50°C for 45 seconds, 72°C for 10 minutes, and a final extension at 72°C for 20 minutes. Both fragments were ligated into pJET1.2 vector, transformed into XL-1 blue cells, and positive clones were sequenced to confirm the presence of the modification and that no PCR errors had been introduced

3.2.15 Assembly of *P. xylostella* RyR in expression vectors

Before the final ligations to generate full-length cDNA containing constructs, 2µg of each of the pJET 1.2 plasmids containing the sub-cloned fragments described above were double digested using appropriate Fastdigest® restriction enzyme pairs (Figure 15), run on a TAE gel and purified using gel extraction.

The first assembly was done in the pcDNA3.1-eGFP vector by simultaneous ligation of all four required fragments with the NotI / KpnI digested plasmid. A 30µl ligation contained 3µl 10x buffer, 50ng of each cDNA fragment (1:1 weight ratio), 1µl of T4DNA ligase, and nuclease free water up to 30µl. The reaction was incubated at room temperature for at least two hours, and prior to transformation 15µl of the reaction was run on a gel to confirm the success of the ligation (Figure 16). 50µl of XL-10 gold cells, treated with 2µl of β-mercaptoethanol, were used for the transformation with 2µl of the ligation reaction added, as described in Chapter II section 2.7.3. Transformed cells were allowed to recover in 250µl of pre-warmed

SOC, in a 30°C incubator with shaking for 2 hours at 250 rpm. The cells were then plated out on two LB-agar plates containing 100µg/ml ampicillin. Positive transformants were selected after 30 hours incubation at 30°C by double colony PCR, as described for the *M. persicae* RyR (section 3.2.9). Out of the 12 clones screened, one clone gave a positive amplification of both PCR fragments and the expected banding pattern for a full-length *P. xylostella* RyR construct using a diagnostic Sal I restriction digest. All ligation sites were also sequenced to confirm that there were no ligation errors. Large quantities of the selected plasmid were obtained by Maxi-prep following the protocol described earlier.

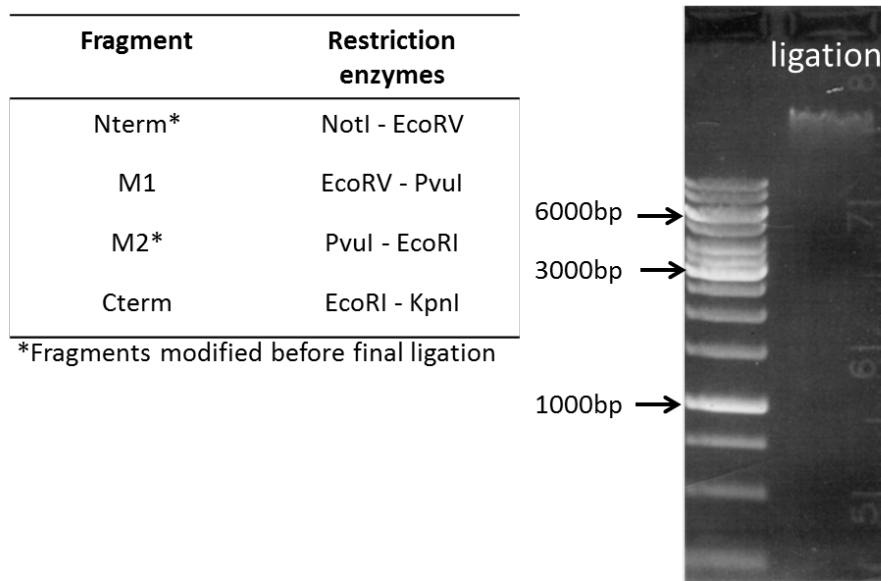


Figure 15 Summary of the restriction enzymes used to recover *P. xylostella* RyR fragments from the pJET1.2 vector (table) and a gel image of a ligation of all 4 fragments with the pcDNA-eGFP vector.

The second construct made was for the expression of *P. xylostella* RyR in insect cells using the modified eGFP-pIZ vector. The full-length coding sequence was cut out of the pcDNA-eGFP construct using NotI / PmeI, and the insert was then ligated between the NotI / NruI sites in the vector (as for the *M. persicae* RyR, see 3.2.9). The 20µl ligation reaction was set up using T4DNA ligase and a 3:1 insert to vector (w/w) ratio. After overnight incubation at 15°C, 10µl of the ligation reaction was run on a 0.8% (w/v) TAE gel to check for the presence of a single ligation product, and 2µl of the ligation was used to transform 35µl of XL-10 gold cells (Chapter II, section 2.7.3). Positive transformants were identified by double colony PCR. Out of

the 20 clones screened, 2 contained the intact *P. xylostella* RyR, as confirmed by diagnostic SalI restriction digest and sequencing.

3.2.16 Deletion mutants of the *P. xylostella* RyR

Two deletion mutants were made for the expression of the C-terminal pore-containing region of *P. xylostella* RyR in both insect and mammalian cell lines. Both the pcDNA3.1-eGFP and eGFP-pIZ constructs were digested with XbaI (which only cuts within the RyR sequence), which allowed the creation of a fusion of the N-terminus and the transmembrane domain without introducing a frame shift (Figure 17). Functional deletion mutants of *D. melanogaster* and *B. mori* RyR channels which were successfully cloned and expressed were based on similar mammalian deletion mutants [97].

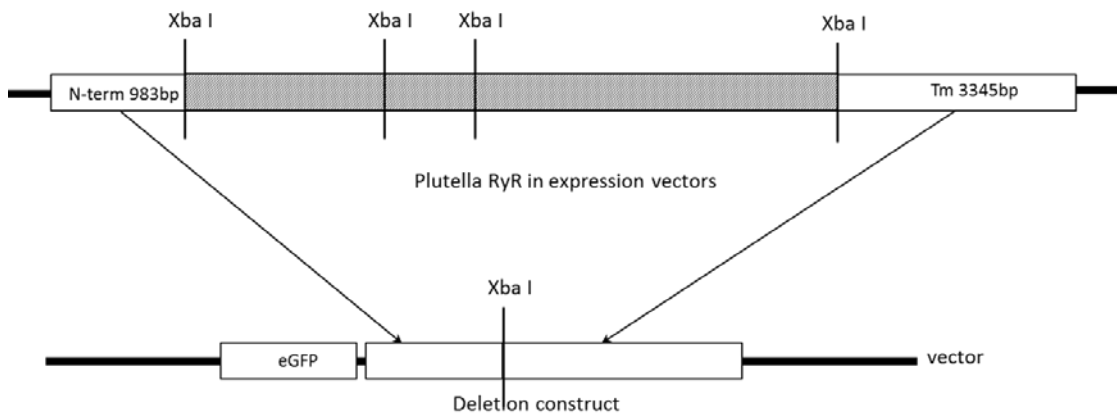


Figure 16 Summary of the construction of *P. xylostella* RyR deletion mutants containing 963bp of the N-terminus (N-term) of *P. xylostella* RyR fused to the transmembrane (Tm) domain, using digestion with XbaI.

One of the products of XbaI digestion contained the vector sequence together with a portion of the N-terminus of the RyR protein and the entire transmembrane region. This fragment was gel purified and re-ligated using T4DNA ligase. Both pcDNA3.1 and pIZ deletion constructs were transformed into 25 μ l of XL-10 cells (Chapter II, section 2.7.3). After transformation, cells were allowed to recover in 250 μ l of S.O.C medium at 30°C, with shaking at 250rpm for 1 hour 30 minutes, and then plated out on two LB plates containing antibiotics (100 μ g/ml ampicillin for pcDNA and 50 μ g/ml of Zeocin for pIZ). Positive clones were selected by colony PCR, using N-terminus specific and transmembrane-specific primers. The ligation site within each

construct was sequenced to rule out the possibility of a frame shift having been introduced.

3.3 Discussion

3.3.1 *M. persicae* RyR

Sequencing of the *M. persicae* RyR constructs and sub-cloned PCR fragments generated in this study highlighted 44 randomly distributed single nucleotide polymorphisms (SNPs) compared to the sequence data in the DuPont patent (US2007/0105098A1). 27 of these SNPs would be predicted to result in amino acid substitutions (Table 10) and might therefore affect the function of the receptor. Multiple alignments of 30 available RyR sequences from various organisms (insects and vertebrates) indicated that the translation of our sequence has a better match to other RyRs than does the DuPont sequence. The presumed PCR errors in the DuPont sequence were most likely the result of using a lower fidelity *taq* and a high number of PCR cycles to amplify the entire coding sequence in a two-step nested PCR reaction, as described in the patent methods.

Table 10 SNPs in the *M. persicae* RyR sequence (DuPont data versus experimental results)

| Nucleotide residue | DuPont | experimental | AA change |
|--------------------|--------|--------------|-----------|
| 453 | C | A | N---K |
| 479 | C | G | P---R |
| 675 | C | T | |
| 1892 | A | C | Q---P |
| 2137 | A | G | N---D |
| 2195 | G | A | G---E |
| 2454 | C | T | |
| 2549 | G | A | G---D |
| 2712 | G | A | |
| 2972 | G | A | G---E |
| 3696 | C | T | |
| 3721 | G | A | A---T |
| 3756 | G | A | |
| 3923 | G | A | G---D |
| 3943 | G | A | G---R |

| | | | |
|-------|---|---|-------|
| 4019 | G | A | R---Q |
| 4414 | C | T | P---S |
| 4771 | G | A | G---R |
| 4854 | A | G | |
| 5531 | N | A | X---N |
| 5548 | T | C | |
| 6287 | G | A | R---K |
| 6817 | G | A | V---M |
| 6830 | T | C | P---L |
| 7577 | A | G | Y---C |
| 7842 | G | A | |
| 7938 | G | T | K---N |
| 7988 | G | A | G---D |
| 9166 | C | T | H---Y |
| 9733 | G | C | D---H |
| 10031 | C | T | T---M |
| 10592 | G | A | S---N |
| 10973 | G | A | R---Q |
| 11004 | C | T | |
| 11347 | G | A | V---M |
| 11394 | A | G | |
| 12221 | T | A | L---Q |
| 12546 | T | A | |
| 12819 | G | A | |
| 13227 | T | C | |
| 13398 | T | C | |
| 14241 | A | G | |
| 14414 | C | T | S---L |
| 15033 | G | A | |

The full-length coding sequence of the *M. persicae* RyR is 15,306bp long, which corresponds to a 5101 amino acid protein with a mass of 580 kDa. The deduced amino acid sequence has 46.2% identity with human RyR2 (accession number: CAA66975.1) and 75.5% homology to the *D. melanogaster* RyR (accession number NP_476991). The predicted protein sequence shares features with other invertebrate and vertebrate RyRs, including retention of commonly occurring domains such as MIR (212-293), SPRY (663-801, 1091-1214, 1539-1682) and RIH (440-648, 2219-2450). One potential EF-hand Ca²⁺ binding domain pair (4198-4248) was also identified; this domain is also partly conserved in recently characterized *P. xylostella*

RyR sequences [165]. Transmembrane (TM) helix prediction using hidden Markov approach [198] indicated 6 potential helices close to the C-terminal end of the *M. persicae* RyR sequence, with the probable pore forming domain localized between TM5 (4897-4919) and TM6 (4977-4996). The selectivity filter motif GXRXGGGXGD, critical for RyR ion conductance, is also fully conserved in the *M. persicae* sequence [199]. The amino acid residue Q(4863), found in mouse RyR2 and thought to be a prerequisite for sensitivity of the channel to ryanodine, is also present [200]. Overall, this confirms that a true *M. persicae* RyR has been obtained.

Three constructs were made for expression of *M. persicae* RyR: an untagged and an N-terminal eGFP tagged RyR for expression in mammalian (HEK) cells, and an N-terminal eGFP tagged RyR for expression in insect (Sf9) cells. All 3 constructs were stable when propagated in *E. coli*, and it was possible to obtain large quantities of highly pure plasmid DNA for cell line transfections. Attempts were also made to clone and express the *M. persicae* RyR using a Bac to Bac® baculovirus expression system (Life technologies), but despite successful cloning of the full-length RyR into the pFastbac1 shuttle vector, it proved impossible to isolate recombinant bacmid DNA from DH10 Bac *E. coli* cells (data not shown).

3.3.1.1 Expression of the *M. persicae* RyR in different life stages

The level of expression of the *RyR* gene was measured in different developmental stages of *M. persicae* (clone 4106A); a mixed pool of first and second instar larvae, mixed third and fourth instar larvae, apterous and winged adults, but these showed no significant differences (Figure 17).

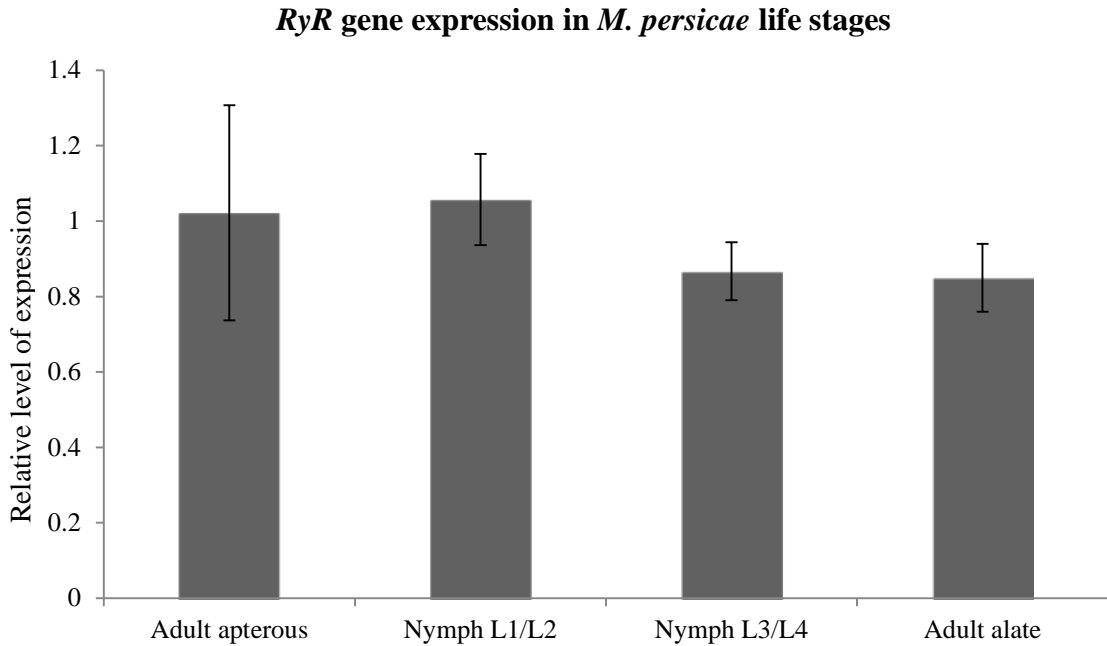


Figure 17 Summary of the relative expression of the RyR gene in different life stages of *M. persicae* clone 4106A. The apterous adult stage was used as a reference. There was no significant difference observed between all tested life stages. The data is presented as a mean of 3 biological and technical replicates with 95% confidence intervals.

This finding is in contrast with other insect species which have been shown to have differential expression of RyR during development. For example, in *P. xylostella* the expression of RyR is significantly different between larval, egg, pupal and adult stages, and also in various body parts of the adult moth, being higher in the thorax and lower in the abdomen [165]. Differences were also found in expression of RyRs in isolated tissues of fourth instar larvae in another *P. xylostella* study [188]. Differential expression of the *RyR* gene was also found in *Nilaparvata lugens* (brown planthopper) between macropterous female adults and other developmental stages [201]. Tissue specific analysis of expression levels of RyR in *M. persicae* would be difficult to examine due to the aphids morphology; tissue dissection in such a soft bodied insect being a challenging undertaking.

3.3.2 *P. xylostella* RyR

The cloned *P. xylostella* RyR cDNA sequence reported here consisted of 15,354bp, corresponding to a 5,118 amino acid protein with a molecular mass of 579 kDa. The

deduced amino acid sequence has 77.3% identity with the cloned *M. persicae* RyR, 91.7% with *B. mori* (unpublished), 78.3% with *D. melanogaster* (accession number NP_476991) and 45.8% with human RyR2 (accession number CAA66975.1). As found for the *M. persicae* channel, the *P. xylostella* RyR shares all of the characteristics of ryanodine receptors including: the highly conserved transmembrane region, the GXRXGGGXGD selectivity filter motif required for cation selectivity, RIH (2232-2454), MIR (212-393) and SPRY domains (664-803, 1091-1214, 1551-1693). It also has a partly conserved calcium binding EF hand domain pair (4222-4271). The seven amino acid residues found in the rice leafroller (*Cnaphalocrocis medinalis*) RyR transmembrane region, which are thought to be lepidopteran specific, are also found in the *P. xylostella* RyR sequence at positions N(4953), N(4955), N(4966), L(4981), L(5012), N(5044), T(5095) [170]. It is speculated that these residues may play a part in diamide insecticide selectivity towards Lepidopteran species. Overall this confirms that a true *P. xylostella* RyR has been obtained.

In contrast to the *M. persicae* RyR, sequencing of the *P. xylostella* fragments used for full-length cDNA assembly revealed many variations in the RyR coding sequence (Figure 18, encompassing: 4 splice sites: - a 15bp insertion and a large 300bp deletion in one of the Nterm fragments, deletion of 132bp in one M1 fragment, and a 41bp insertion in one of the Cterm fragments. Additionally, a large number (over 200) silent SNPs were found, with a clustered distribution suggesting that they are not a result of PCR errors (Figure 18). This *P. xylostella* RyR sequence variability and the presence of alternative splice sites were also reported independently [165], with all four of the splice sites identified in this study being confirmed, along with another additional 7 sites which were probably not identified in this current study due to limited clone coverage. Comparison of this current study's assembled RyR sequence with the reported frequency of all 11 splice sites (in 10-20 sequenced clones) suggests that our cDNA construct is most likely the most prevalent form of the receptor in *P. xylostella*.



Figure 18 Sequence alignment (using Geneious v6.05) of all of the *P. xylostella* RyR fragments generated for RyR cDNA assembly versus the initial sequencing results obtained early in the project. Gray bars represent sequence covered; names of individual cloned fragments are shown on the left. Black vertical lines represent individual SNPs, some of these could be attributed to the errors made by a low fidelity taq used to generate the reference sequence. Black horizontal lines represent individual splice sites. Top bar shows the scale numbering individual positions every 1000bp.

Initially two constructs were made for the expression of the full-length *P. xylostella* RyR: an N-terminal eGFP-RyR fusion in pcDNA3.1(-) for expression in mammalian (HEK) cells, and an N terminal eGFP-RyR fusion in pIZ/V5 for insect (Sf9) cell expression. Two deletion constructs, with only a small portion of the cytosolic domain and the entire transmembrane region, were also subsequently made. All four constructs were stable in *E. coli* and easily propagated.

3.3.3 General remarks

This chapter reports the successful cloning of RyRs from *M. persicae* and *P. xylostella*. During PCR initial amplifications of *M. persicae* RyR it was found that better yields were obtained if the cDNA synthesis reaction was spiked with a gene specific primer binding to the 3' UTR. Spiking had no apparent effect for amplification of *P. xylostella* RyR. It was also noted that PCR reactions using *pfu* polymerase and RyR cDNA as template needed extremely long extension times to achieve successful amplification. In the case of the LNK1 and LNK2 fragments, extension times as long as 5 minutes per kb were required if the reaction was to yield any product. Interestingly, despite the long extension times and the low annealing temperatures, primer binding remained specific with little evidence of artefacts. Propagation of all insect and mammalian RyRs (and sub-cloned fragments) in *E. coli* was done under lower growth temperatures than normal, in order to avoid plasmid rearrangements and colony growth suppression as the cloned fragments were toxic to the bacteria at higher temperatures. It was noted that lowering the temperature and extending the cell's recovery time increased the efficiency of cloning for all DNA fragments above 2kb. In contrast, maintaining the cells at 37°C greatly decreased the chances of selecting successful transformants when cloning large DNA fragments. Additionally the density of the liquid cultures was critical for obtaining high yields of plasmid DNA. The highest yields of pure plasmids were obtained when the optical density measured at 600nm was between 0.8-1. During the expression experiments described in Chapter IV, an additional two *P. xylostella* constructs were made (one in pcDNA3.1(-), one in pIZ) without the eGFP tag and with 3 modified amino acids (which were potential PCR errors identified by aligning our sequence with other reported *P. xylostella* RyRs (details in chapter IV, section 4.3.3)).

Chapter IV: Functional expression of insect ryanodine receptors

4.1 Introduction

The main challenges for successful expression of RyRs are the complexity of the functional unit (a combination of four monomers), the large size of the individual subunits, and the intracellular membrane localization. In early studies conducted on mammalian RyR channels it was found that the purified RyR tetramers are very stable, allowing functional and structural analyses to be carried out [202, 203]. All 3 mammalian RyR isoforms (isolated from different species, including *Homo sapiens*, *Mus musculus* (mouse) and *Oryctolagus cuniculus* (rabbit)) have been successfully expressed in various cell lines, including Chinese hamster ovary (CHO), Human embryonic kidney (HEK) 293, and Monkey kidney derived COS-1 and COS-7 [186]. The ability to achieve a good level of expression in cell lines has proven particularly useful for studying RyR mutations associated with different disease states, in understanding different domain interactions within the receptor, and in identifying the location of the binding sites for various ligands and accessory proteins [186].

To date there have been very few attempts to express and functionally analyse insect RyRs. The first analysis was done on native protein purified from *H. virescens* thoracic tissue [176]. The RyR from *D. melanogaster* was the first insect channel to be successfully expressed in CHO cells, but the level of expression obtained allowed only very basic electrophysiological measurements to be made, and a further limited electrophysiological analysis of a truncated channel containing only the C-terminal TM region to be carried out [163]. The same CHO expression system was also used for confirming that the receptor is the target protein for the diamide insecticide flubendiamide, through calcium release assays on full-length RyR using fluorescent calcium imaging techniques [31]. More recently the full-length *B. mori* RyR and a series of deletion mutant constructs were expressed successfully in HEK293 cells. The expression level was sufficient for *in vivo* measurements of ER Ca^{2+} mobilisation through the RyR by caffeine, ATP, and by flubendiamide. Functional analysis of the deletion mutants pinpointed the binding region of flubendiamide to the TM part of the protein (see more detail in Chapter I section 1.2.1, figure 19) [30].

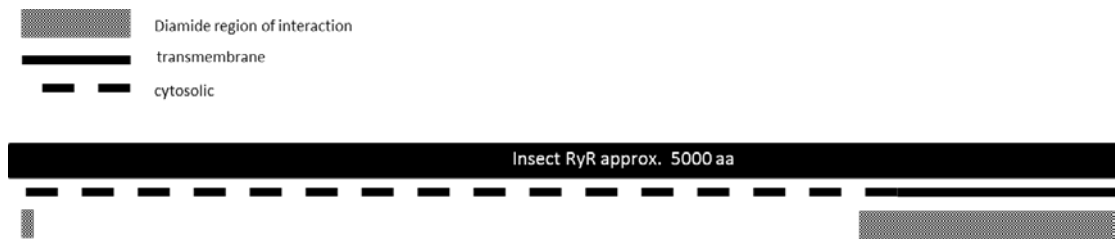


Figure 19 Graphical representation of known diamide sites of interaction on the model insect ryanodine receptor based on *B. mori* RyR expression.

Sf9 and Sf21 are insect cell lines established from pupal ovarian tissue of *Spodoptera frugiperda* (fall army worm) and they are primarily used for protein expression using the baculovirus system [204]. Insect cells are often used for the production of mammalian proteins since they have eukaryotic processing capabilities, being deficient only in the ability to glycosylate the final protein products. In many cases this glycosylation deficit has been overcome by modifying the cell lines to incorporate mammalian glycosylation genes, which allows the production of ‘human-like’ glycoproteins [205]. In the past both Sf9 and Sf21 cells have been used to express rabbit skeletal RyRs using the baculovirus system. Both cell lines were able to produce large quantities of fully-functional protein, which was almost identical to the isolated native channels [125, 206]. So far there have been no published reports of invertebrate RyRs being expressed in insect cell lines.

In this chapter a detailed overview of methods and optimization approaches used to successfully express two insect RyRs in mammalian HEK 293 and in insect Sf9 cells is described and evaluated.

4.2 Methods

In the course of this project various approaches were tested to try and achieve optimal transfection and protein expression in two cell lines: insect Sf9 and mammalian HEK 293 (growth and maintenance of both cell lines are described in Chapter II sections 2.10 and 2.11). Since the primary objectives of this chapter was to find optimal expression conditions for both insect RyRs, experiments showing poor expression and lack of function were not replicated more than two or three times in order to save resources and time. This methods section outlines the general protocols used, and the optimised conditions empirically achieved through a series of modifications of the initial protocols are discussed in the Results and Discussion

section. Experiments which produced poor expression or no receptor function were not rigorously quantified and GFP construct expression experiments were compared visually to the mammalian RyR2 positive controls, without fluorescent signal quantification, since there was no access to appropriate software tools.

4.2.1 Transfections

4.2.1.1 Calcium phosphate transfections of HEK 293 cells

Calcium phosphate was the initial method of choice for transfecting large quantities of HEK 293 cells. A typical transfection was done in twenty 90mm cell culture dishes (Sigma-Corning, MA, USA). The protocol used was optimised for expressing the mammalian RyR2 cardiac channel (Cardiff University), transfecting batches of 10 dishes at a time. Twenty-four hours prior to transfection, cells were harvested and counted (as described in Chapter II, section 2.11), and 1×10^6 cells were seeded into each dish containing 9ml of complete DMEM media (Life technologies, CA, USA). The transfection mixture used was: 5ml of 2xHEPES solution pH 6.95 (recipe in the Appendix A, section 2) in one 50ml Falcon tube and 1.24ml of 1M CaCl₂ together with plasmid DNA (12µg per plate) in a second 50ml Falcon tube, the total volume of this tube being brought to 5ml using sterile distilled water. The DNA-calcium solution was then added drop-wise into the 2xHEPES solution (tube 1) with shaking. This ensured the formation of the fine precipitate required for good transfection efficiency [207]. 1ml of the precipitate solution was then dispensed into each culture dish and the dishes were placed in a 37°C / 5% CO₂ incubator. Fresh complete DMEM media was added to the cells 24 hours later and all cells were harvested 48 hours post transfection.

4.2.1.2 Cellfectin™ II transfections of Sf9 cells

Cellfectin™ II (Life Technologies, CA USA) is a lipid based reagent designed for transfecting insect cells and is recommended by the supplier as a “superior” method of transfection. Initial experiments with Cellfectin were done in 6-well plates and later, larger scale, transfections in 60mm cell culture dishes (Sigma-Corning, MA, USA). The protocol for the 6-well plates was as follows: 8×10^5 cells in 3ml of Sf-900 II medium containing 0.6% FBS (no antibiotic) were seeded into each well and left overnight to attach to the bottom of the plate. On the day of transfection at least

1µg of DNA was diluted in 100µl of Sf-900 II medium (non FBS supplemented) in a 1.5ml tube, and 8µl of the Cellfectin reagent was diluted in the same volume of medium in a second 1.5ml tube. Both tubes were vortexed and incubated at room temperature for 15-30 minutes, then the contents of both tubes were combined, vortexed and incubated for a further 5-10 minutes. In the meantime, the FBS-containing medium was removed from the attached cells in each well, the cells washed once with 2ml of fresh medium (to remove any traces of FBS) and the wells filled with 2ml of un-supplemented Sf-900 II. After incubation, the transfection mixture was added drop-wise to the cells, the plate gently rocked to evenly distribute the solution, and left to transfect in a 27°C incubator for 4h. The medium containing the transfection solution was then removed and replaced with 3ml of fresh Sf-900 II containing 0.6% FBS.

For the large scale transfections at least ten 60mm dishes were transfected at a time. One day prior to transfection 2.5×10^6 (approximately 65-70% confluence) cells were seeded into each dish containing 5ml of unsupplemented Sf-900II media. The exact amounts of DNA, Cellfectin reagent and incubation times for each step were first determined in the small scale transfections and are discussed in section 4.3.2.3. The transfections were set up similarly to the small scale ones: desired amounts of DNA and Cellfectin were first diluted in two tubes containing 500µl Sf-900 II medium (no FBS) for each 60mm dish, and after appropriate incubation time, the contents of both tubes were mixed together. After further brief incubation, transfection solutions were gently (to avoid disturbance of the monolayer) applied to each 60mm dish and cells were placed at 27°C for 48-72h.

4.2.2 Optimization of transfection methods

4.2.2.1 HEK 293 cells

For calcium phosphate transfections, the efficacy of using differing amounts of plasmid DNA (12µg, 16µg or 20µg per plate) was investigated. The effect of adding 1.7mM sodium butyrate (a known transfection and translation up-regulation agent [183, 208, 209]) 15-25h post transfection was also tested. Other commercially available transfection reagents were also assessed, including Effectene® (Qiagen, Hilden, Germany) and JetPrime® (PolyPlus™ transfections SA, Illkirch, France), following the manufacturer's recommended protocols.

4.2.2.2 Sf9 cells

In order to achieve the highest possible transfection and expression efficiency, various amounts of plasmid DNA and PLUS™ reagent (Life technologies, CA, USA) were equilibrated together prior to incubation of the DNA with Cellfectin II reagent (see Table 11). Addition of PLUS™ reagent (a transfection enhancer) was according to the manufacturer's recommended protocol (5µl per well in 6 well-plates). Various DNA / reagent incubation times were also investigated: 15, 30 and 45 minutes for the DNA / PLUS™ reagent and 5, 10 and 15 minutes for the DNA mixture / Cellfectin reagent. The effect on cell viability of maintaining Sf9 cells in the transfection medium after 4h incubation was also looked at. The efficacy of adding 1-1.7mM sodium butyrate 4h and 24h post-transfection was also assessed. Expression efficiencies and expression levels were analysed 24h, 48h and 72h post transfection by imaging with a Leica M205 FA microscope using GFP2 filters.

Table 11 Composition of transfection reactions

| Cellfectin™ (µl) | Plasmid DNA (µg) | PLUS™ reagent (ul) |
|------------------|------------------|--------------------|
| 10 | 20 | 0 |
| 20 | 20 | 0 |
| 30 | 20 | 0 |
| 15 | 8 | 0 |
| 15 | 10 | 0 |
| 15 | 12 | 0 |
| 15 | 15 | 0 |
| 15 | 20 | 0 |
| 15 | 1 | 5 |
| 15 | 8 | 5 |

Additionally, different transfection methods were analysed including calcium phosphate and FectoFly® (Polyplus-transfection SA, Illkirch, France) reagent, following the manufacturer's recommended protocol.

4.2.3 Analysis of transfected cells

4.2.3.1 Mixed-membrane preparation

To make a mixed-membrane preparation, cells were collected from the culture dishes (60mm-Sf9, 90mm-HEK 293) by gentle tapping and pipetting. Cells were then counted using a hemocytometer and then re-suspended in hypo-osmotic buffer (see Appendix A section 3) at a density of 1×10^6 cells (HEK 293) or 2×10^6 cells (Sf9) per ml of buffer. Cell aliquots of 10-15ml were homogenised using a glass homogeniser kept on ice (around 10 even strokes), and each aliquot was then passed at least 10 times through a 23G gauge needle attached to a 10ml syringe. The homogenate was centrifuged at 2700rpm (1500g) and 4°C for 15 minutes to remove broken cells and nuclei. The supernatant was carefully removed and then centrifuged at 28,000rpm (100,000g) in a Beckman Optima–L90K centrifuge, using a 50.2 Ti rotor, for 1h at 4°C. The pellet was then transferred to a 1ml glass homogeniser kept on ice, resuspended in 0.4M sucrose, 20mM HEPES solution (20µl per 1×10^6 (HEK 293) cells or 2×10^6 (Sf9) cells) and homogenised to give a fine suspension. Mixed-membrane preparations were first flash frozen in liquid nitrogen and stored in 100µl aliquots in a -80°C freezer.

4.2.3.2 Protein assays

A micro BCA™ (bicinchoninic acid assay) protein assay (ThermoScientific, MA, USA) was used to quantify protein. The mixed-membrane sample was diluted 1:50, 1:100, 1:200 in double distilled water, mixed well, and 100µl of the diluted protein was loaded into a 96 well (flat bottom) plate, either in duplicate or triplicate. 200µl of working reagent (a mixture of kit reagents A, B and C) was then added to each well and the plate incubated in the dark for 15 minutes. The absorbance of each well at 595nm was measured using a UV max kinetic micro-plate reader (Molecular Devices, CA, USA). The protein concentration of each mixed-membrane preparation was then calculated by fitting the average absorbance values of each duplicate or triplicate sample onto the BSA (bovine serum albumin) standard curve.

Alternatively, a Bradford reagent (Bio Rad, CA, USA) assay was used. The mixed-membrane preparation was diluted 1:2, 1:4, 1:8, 1:16 in double distilled water and measured against a set of BSA standards in a 96 well (flat bottom) plate. 200µl of Bradford reagent and 5µl of the diluted mixed-membrane sample were added to each well. All concentrations were prepared in duplicate. Readings were taken after a 10 minute incubation by measuring the absorbance at 590nm, using a SpectraFluor Plus

(Tecan, Dorset, UK) micro-plate reader, and the protein concentration in each well was determined by the Magellan™ data analysis software (Tecan) associated with the plate reader.

4.2.3.3 Radio-ligand binding assays

Two different methods were used for the radio-ligand binding assay experiments; a glass micro-fibre GF/B filter disc (GE Healthcare-Whatman®, Little Chalfont, UK) assay, which was used for testing the expression levels of the RyRs, and a 96 well GF/B filter plate (PerkinElmer, MA, USA) based assay which was used to determine the binding kinetics of ryanodine to the receptors.

The glass micro-fibre filter disc assay protocol was as follows: The binding buffer (recipe in Appendix A, section 5.1) was made up on the day of the experiment. Experiments were done in duplicate or triplicate for hot (total binding) and cold (non-specific binding) reactions. For the hot reaction, samples were set up in 3ml vials (VWR, PA, USA) in a total volume of 500µl, consisting of 100µg of the mixed-membrane preparation, 20µl of [³H] ryanodine (0.1mCi/ml) (PerkinElmer, MA, USA) (final concentration of [³H] ryanodine 8nM) and binding buffer up to 500µl. The cold reaction had 100µg of mixed-membranes, 20µl of [³H] ryanodine, 5µl of cold ryanodine (final concentration 5µM) and binding buffer up to 500µl. Samples were thoroughly mixed by vortexing and incubated in a 37°C water bath for 90 minutes. The filter discs were pre-soaked in binding buffer and, after the sample incubation was completed, the samples were loaded onto the glass micro-fibre filters using a vacuum manifold. The glass vials were then washed with 500µl of binding buffer to recover any residual sample. Following sample binding, filter discs were washed with an additional 500µl of binding buffer. After the vacuum pump filtration was completed all discs were transferred to individual scintillation vials containing 5ml of Ultima gold™ MV scintillation fluid (PerkinElmer, MA, USA), and loaded onto a Packard Bioscience (now PerkinElmer) 2100TR TriCarb Liquid Scintillation Analyzer for counting. Obtained dpm values were then processed to calculate the amount of specific binding using Office Excel 2010 (Microsoft, CA, USA).

The 96 well filter plate assays were carried out as follows: the mixed-membrane preparation was diluted in buffer A (all the buffers recipes can be found in Appendix A, section 5.2) to a final concentration of 0.25mg/ml. Both total and non-specific

reactions were set up in a 96 well flat bottom microtiter plate in a total volume of 250 μ l. For each reaction 48 μ l of Buffer B containing 0.01% Pluronic (Sigma, MA, USA) was added together with 2.5 μ l of DMSO (for total reaction) or 1mM ryanodine (final concentration 10 μ M) in DMSO (for non-specific reaction), 100 μ l of diluted mixed-membrane preparation and 100 μ l of diluted [3 H] ryanodine (to the desired final concentration). Empty wells on the plate were filled with buffer B and diluted (old) membrane preparation. The plates were shaken gently and left to incubate at room temperature for 2h. The 96 samples were then loaded onto the filter plate (with each well pre-soaked with 50 μ l of 0.1% polyethylenimin in wash buffer) using a 96 well plate harvester (Brandel, MD, USA). The filter plate was then washed 3 times with 250 μ l wash buffer and left overnight at room temperature to dry. Each well on the plate was then filled with 50 μ l MicroScintTM-O (PerkinElmer, MA, USA) and the filter plate loaded into a TopCount NXTTM Micro-plate Scintillation counter (PerkinElmer, MA, USA). Specific binding and binding kinetics values (equilibrium dissociation constant K_d and Binding capacity/receptor density B_{max}) were calculated using GraphPad Prism v5.5 (GraphPad, CA, USA).

4.2.3.4 Western Blotting

Mixed-membrane preparations from HEK 293 cells transfected with *P. xylostella* or *M. persicae* RyR-eGFP fusion constructs were run on 5% (w/v) polyacrylamide gels (recipe in Appendix A, section 4) and blotted onto nitrocellulose membranes using an iBlot 7 minute blotting system (Life technologies, CA, USA) following the manufacturer's recommended protocol. The nitrocellulose membranes were then blocked with 5% (w/v) powdered skimmed milk (VWR, PA, USA) in TBS-T (recipe in Appendix A, section 4) for 1h at 4 $^{\circ}$ C, washed with TBS-T and then incubated overnight at 4 $^{\circ}$ C with primary mouse monoclonal anti-eGFP antibody (Santa Cruz biotechnology, TX, USA) at a 1:5000 dilution in 1% (w/v) powdered milk/TBS-T. After removal of unbound primary antibody with 3 washes of TBS-T buffer, the blot was incubated for two hours with 1:5000 diluted secondary goat anti-mouse horseradish peroxidase conjugated antibody (Sigma, MA, USA) in milk/TBS-T. After a further 3 washes with TBS-T buffer, the antibody attached peroxidase activity was detected by breakdown of a luminol (ECL) substrate (GE Healthcare, Little Chalfont, UK) and exposure of the blot to X-ray film. The protein was

visualised after a 30 minutes exposure by developing the X-ray film using an X4 Automatic X-ray Film Processor (Xograph, Stonehouse, UK).

4.2.4 Microscopy

The efficiency of transfection was checked by examining fluorescence images of transfected Sf9 cells expressing eGFP-RyR fusion constructs using a Leica M205 LA light microscope with GFP2 filter (Leica, Wetzlar, Germany), and similarly transfected HEK 293 cells with a Zeiss Axio Vert fluorescence microscope x10 objective (Zeiss, Oberkochen, Germany). This step was omitted for untagged RyR constructs. High magnification images were taken using either a Leica SP5 x63 oil immersion lens or Zeiss 780LSM x63 and x40 water immersion lenses. HEK 293 and Sf9 cells were imaged both *in vivo* in culture dishes and fixed onto coverslip with 0.4% formaldehyde.

4.2.4.1 Calcium release assays for HEK 293 cells

Expression of full-length *P. xylostella* and *M. persicae* constructs, and the *P. xylostella* deletion mutant in HEK 293 cells, was determined by monitoring the release of calcium from internal stores with a calcium sensitive fluorescent dye after addition of RyR agonists. 1×10^5 HEK 293 cells were seeded onto glass bottom dishes (MatTek, MA, USA) (12mm diameter) and transfected with plasmid DNA containing the RyR cDNA using Effectene[®] as follows (protocol to prepare 7 dishes): plasmid DNA (0.8 μ g) was diluted with 6.4 μ l of enhancer in 100 μ l of EC buffer (both supplied with Effectene[®]) and the mixture was incubated for 5 minutes at room temperature. After 5 minutes, 20 μ l of Effectene[®] was added and the mixture incubated for a further 10 minutes. In the meantime cells were washed with complete DMEM medium (cDMEM, containing 10% FBS and penicillin/streptomycin 100U/100 μ g/ml). Then 600 μ l of cDMEM was added to the plasmid DNA / Effectene[®] mixture and thoroughly mixed by vortexing. 100 μ l of this solution was then applied to each dish and the cells were returned to the 37°C / 5% CO₂ incubator.

HEK 293 cells expressing human RyR2 were used as a positive control for the calcium imaging experiments and Fluo-3 AM (Life technologies, CA, USA) loaded un-transfected HEK 293 cells were used to test for potential excitation of endogenous calcium stores. Cells in 200 μ l DMEM were loaded with 2 μ l of a 1mM

solution (final conc. 10 μ M) of Fluo-3 AM calcium sensitive dye, 24 and 48 hours post transfection, and incubated for 45 minutes at 30°C / 5% CO₂ to avoid dye compartmentalization. After the loading was completed, cells were incubated for 10 minutes with 2ml of fresh DMEM media. Calcium release events were imaged using an SP5 confocal microscope (Leica, Wetzlar, Germany) with the cells in 200 μ l of fresh DMEM. 60 second recordings were made, one recording per dish per agonist, measuring excitation at 488nm and capturing emissions at 525 nm every 70ms.

4.2.4.2 Calcium release assays in Sf9 cells

Fura 2-AM dye (Life technologies, CA, USA) was used for monitoring calcium release in Sf9 cells transfected with the untagged *P. xylostella* RyR. Glass coverslips (1cm diameter glass) coated with Poly-L-lysine (Sigma, MA, USA) were placed in a 4 well plate. Each well was then filled with 500 μ l of Sf-900 II medium and each coverslip was seeded with 2.5x10⁵ cells. Cells were allowed to attach to the coverslips for 1h and then they were transfected in 4 well plates using the optimised Cellfectin™ II method (discussed later in section 4.3.2.3). 24h, 48h, 72h and 96h post transfection cells were loaded with 1mM of Fura 2-AM. Cells on coverslips in 4 well plates were first put into 500 μ l of fresh SF-900 II medium and then 2 μ l of the dye stock solution (5mM) was added. Cells were left to incubate at 27°C for 45-60 minutes, followed by 3 washes with 500 μ l of fresh un-supplemented Sf-900 II medium. Prior to imaging, coverslips with Fura 2 loaded cells were placed in standard Ringer's solution (recipe in Appendix A, section 8). All imaging was done using an Axio Vert.A1 microscope with a LD Plan-Neo Fluar x20/0.4 lens (Zeiss, Oberkochen, Germany), measuring the ratio of excitation at 340/380nm (calcium free/calcium bound indicator) every 180ms and capturing emission at 510nm for at least 60 seconds. Cells on the coverslip were placed into a perfusion chamber of approximately 0.5 ml volume mounted on the microscope stage which was connected to a peristaltic pump, allowing for a constant fluid exchange (flow rate 3 ml/min). Test solutions were applied using 3-5 seconds bursts via a glass u-tube (Figure 20).

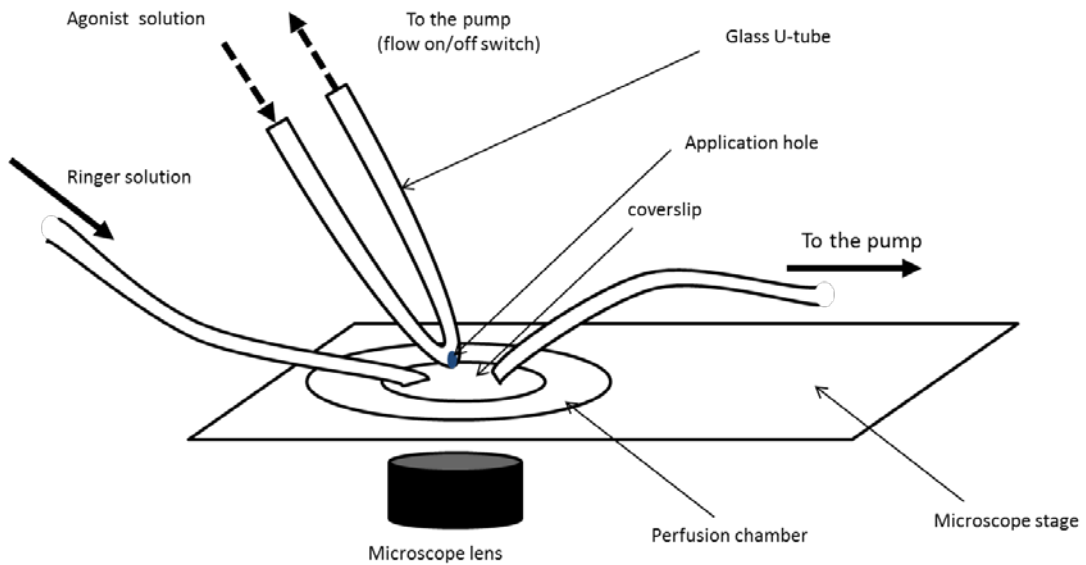


Figure 20 Perfusion chamber setup with a glass U-tube applicator for recording of multiple agonist applications. Black arrows indicate flow of Ringer's solution, which allows for a constant replacement of solution in the perfusion chamber. Agonist solutions are applied via the glass U-tube, where flow is controlled by recording software (VisiView[®]) or the electrical switch on the the peristaltic pump. When the U-tube flow is stopped, agonist present inside the tube diffuses over the cells by seepage through the application hole.

Experiments were recorded using VisiView[®] software (Visitron Systems, Puchheim, Germany) and the numerical data analysed using Microsoft Excel 2010 and SigmaPlot v.12 (Systat Software). The data were normalized using the equation: R/R_0 , where R is a fluorescence ratio value recorded for individual time points and R_0 is an average fluorescence ratio calculated over the first 5 seconds prior to addition of the agonist. Data points on graphs are presented as the mean values of individual cell responses for each independent experiment and standard errors compared to the mean. The normalized amplitude responses of individual cells were calculated by estimating the highest value subtracted from the basal level ($R_{\max} - R_0 = \Delta R_{\max}$) and normalizing with the equation: $\Delta R_{\max}/R_0$. Final amplitude data was presented as a mean value of all cells in the individual experiment and the standard deviation of the mean.

4.2.5 Membrane solubilisation and sucrose gradient purification

Mixed-membrane preparations of known protein concentration were diluted 1:4 with 0.4M KCl, and centrifuged at 50,000rpm (approximately 100,000g) for 30 minutes at 4°C using an OPTIMA TLX (100.4 Ti Rotor) Beckman ultra-centrifuge. The supernatant was discarded and the pellet was re-suspended in solubilisation buffer to a final protein concentration of 2mg/ml (recipe in Appendix A, section 6) and CHAPS/PC (3-[(3-Cholamidopropyl)dimethylammonio]-1-propanesulfonate hydrate / phosphatidylcholine) added to a final concentration of 0.6% (v/v) from the freshly prepared stock solution of 10% (w/v) CHAPS in double distilled water. The pellets were passaged through a 23G gauge needle attached to a 10ml syringe and transferred to 1.5ml eppendorf tubes and the mixture was incubated at 4°C for 1h. The membrane lysate was centrifuged in an Eppendorf 5415R centrifuge at 11,500 rpm for 30 minutes at 4°C and the supernatant collected and kept on ice.

Sucrose gradients were prepared using two mixing chambers connected to a peristaltic pump. 40%, 35% and 5% (w/v) sucrose solutions prepared in gradient buffer were incubated in a cold room on a rolling platform for 1h. 5ml of the 40% (w/v) sucrose solution was added to 2 high speed 36ml centrifuge tubes (Beckman) as a cushion. Chamber A and the chamber connector channel was filled with 40ml of the 5% (w/v) sucrose solution, and chamber B was filled with 25ml of the 35% (w/v) sucrose solution while being stirred by a magnetic stirrer. Once the two chambers were filled, the peristaltic pump was turned on and the tap between the two chambers was opened allowing a gradient to form and the sucrose mixture to migrate to fill the 2 centrifuge tubes.

4mg of solubilized membrane lysate (2mg/ml) was then gently pipetted as a layer on top of formed gradients and the tubes centrifuged at 28,000 rpm for 16 to 18h at 4°C using a Beckman OPTIMA L100 XP (rotor 32 Ti) centrifuge. Gradient fractions were collected in 2ml aliquots using a fraction collector (Pharmacia Biotech-GE Healthcare, Uppsala, Sweden) and their sucrose concentration checked using a refractometer. Ryanodine receptors were found in fractions containing 27-29% (w/v) sucrose.

4.2.6 Single channel recordings

Both mixed-membrane preparations and sucrose-gradient purified full-length RyR of *P. xylostella*, *M. persicae*, and the *P. xylostella* deletion mutant, were tested for channel activity in an artificial bilayer system held under voltage clamp. The planar phospholipid bilayers were formed from a suspension of synthetic 1-palmitoyl-2-oleoyl-*sn*-glycero-3-phosphoethanolamine (Avanti Polar Lipids, AL, USA) in *n*-decane (35 mg/ml) painted across a 200 μ m-diameter hole in a partition separating the *cis* (0.5 ml) and *trans* (1.0 ml) chambers. The *trans* chamber was held at ground and the *cis* chamber was clamped at relative holding potentials. Current flow was measured using an operational amplifier as a current-voltage converter [210]. Bilayers were formed in symmetrical solutions containing 210 or 610 mM KCl, 20 mM HEPES, pH 7 in *cis* and *trans* chambers. To measure single channel currents, aliquots of RyR2-containing fractions and 3M KCl were added to the *cis* chamber creating favourable conditions for channel incorporation in a fixed (cytosolic side at the *cis* chamber, luminal face to the *trans* chamber) orientation [211]. Unincorporated channels and the osmotic gradient were removed by perfusion and the single channel P_o (open probability) was increased following the addition of 100 μ M EMD 41000 [212] to the *cis* chamber. For the deletion mutant mixed-membrane preparation, a 250mM and 3M Caesium gluconate with 20mM HEPES solution was used instead of standard KCl, following methods described for characterization of *D. melanogaster* C-terminal RyR [163].

4.3 Results and Discussion

4.3.1 Expression of the *Myzus persicae* RyR

Table 12 summary methods of individual transfection experiments done for *M. persicae* constructs in HEK 293 cells

| Construct | Trasfection method | Number of experiments | Analysis of function |
|----------------------------|------------------------|-----------------------|--|
| WT <i>M. persicae</i> RyR | Calcium phosphate | 3 | [³ H] ryanodine binding artificial bi-layers |
| GFP <i>M. persicae</i> RyR | Calcium phosphate | 4 | Western blot, [³ H] ryanodine binding |
| | JetPrime [®] | 3 | Calcium release assay |
| | Effectene [®] | 3 | Calcium release assay |

4.3.1.1 Untagged RyR in HEK 293 cells

Initial expression of the untagged *M. persicae* RyR construct in HEK 293 cells gave a high yield of protein in the mixed-membrane preparation (between 18-36mg/ml when tested with the micro-BCATM assay) from cells harvested 48 hours after a standard calcium phosphate transfection, but there was no evidence of specific [³H] ryanodine binding. Additionally, no RyR channel activity was detected in artificial bilayers, using either mixed-membrane preparations or sucrose gradient purified RyR. Lack of an insect RyR-specific antibody or a fluorescent tag on the RyR protein made it impossible to determine whether this was due to poor expression of the cDNA or protein miss-folding.

4.3.1.2 eGFP-RyR in HEK 293 cells

The modified construct with an N-terminally-fused eGFP sequence allowed visual monitoring of the expression and efficiency of RyR transfections in HEK 293 cells. Localization of fluorescence in individual cells, and the assessment of the amount of RyR channels present, was done using high-magnification confocal imaging and eGFP-specific antibody detection on Western blots. The *M. persicae* eGFP-RyR construct gave a poor level of expression 48h post transfection using calcium phosphate as a transfection reagent, with no more than 5% of the cells displaying a GFP signal per field of view (Figure 21).

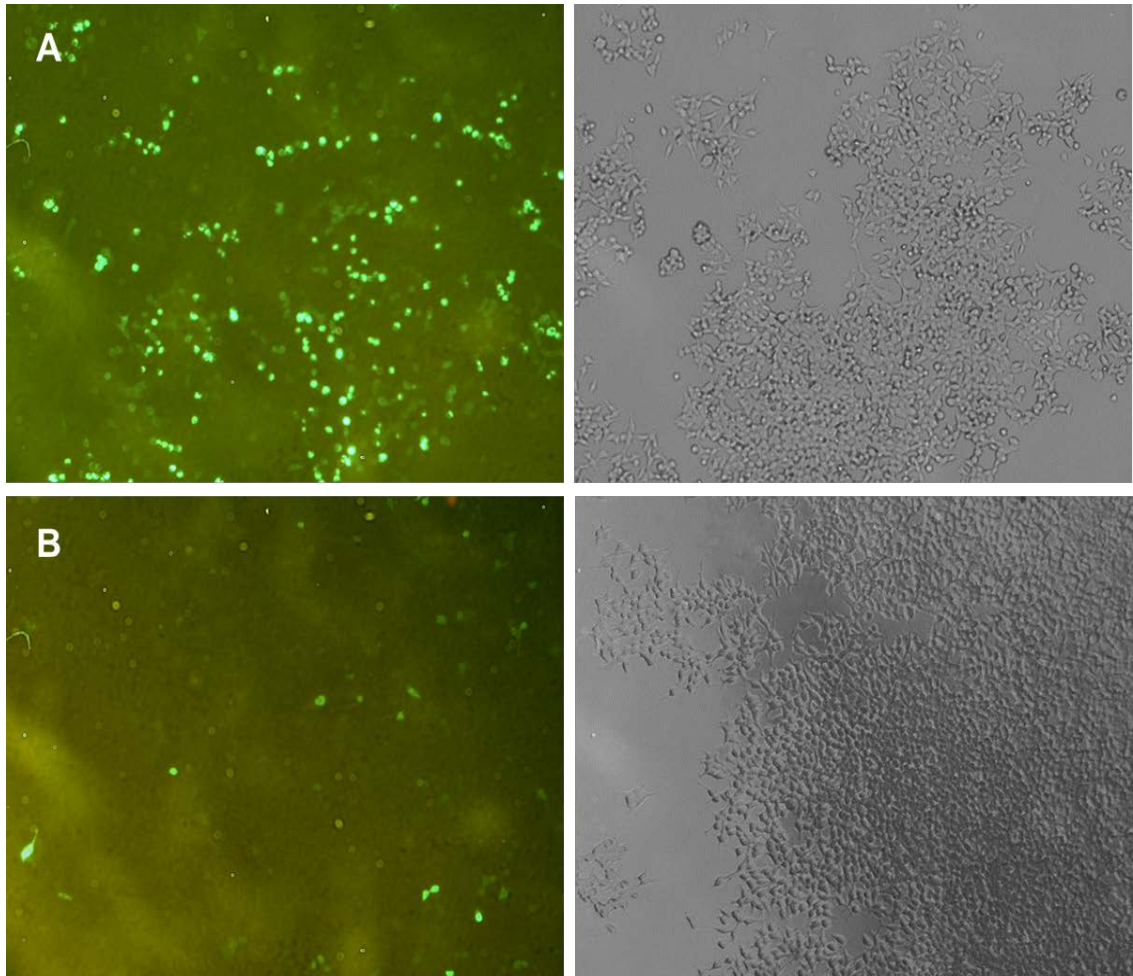


Figure 21 Low magnification images, using a Zeiss Axio Vert microscope (x10 objective), showing HEK 293 cells calcium phosphate transfected with **A**: human e-GFP-RyR2 fusion plasmid and **B** *M. persicae* eGFP-RyR plasmid. Images on the right are of the bright field view.

After further attempts at optimization (4 independent transfection experiments) it was concluded that calcium phosphate transfection does not give satisfactory amounts of *M. persicae* RyR protein. The addition of 1.7mM sodium butyrate, 4h and 24h post transfection, did not increase the number of fluorescing cells or the strength of the signal in individual cells per field of view. Further experiments using JetPrime® or Effectene® did not give a visual improvement over the calcium phosphate transfection method. In an attempt to optimise the transfection using Effectene®, two concentrations of plasmid DNA (protocol recommended and a higher than recommended quantity) were used; however it was apparent that even when very high (32µg) amounts of plasmid DNA were added the overall efficiency

and expression level was still low in comparison to the human RyR2 control (Figure 22).

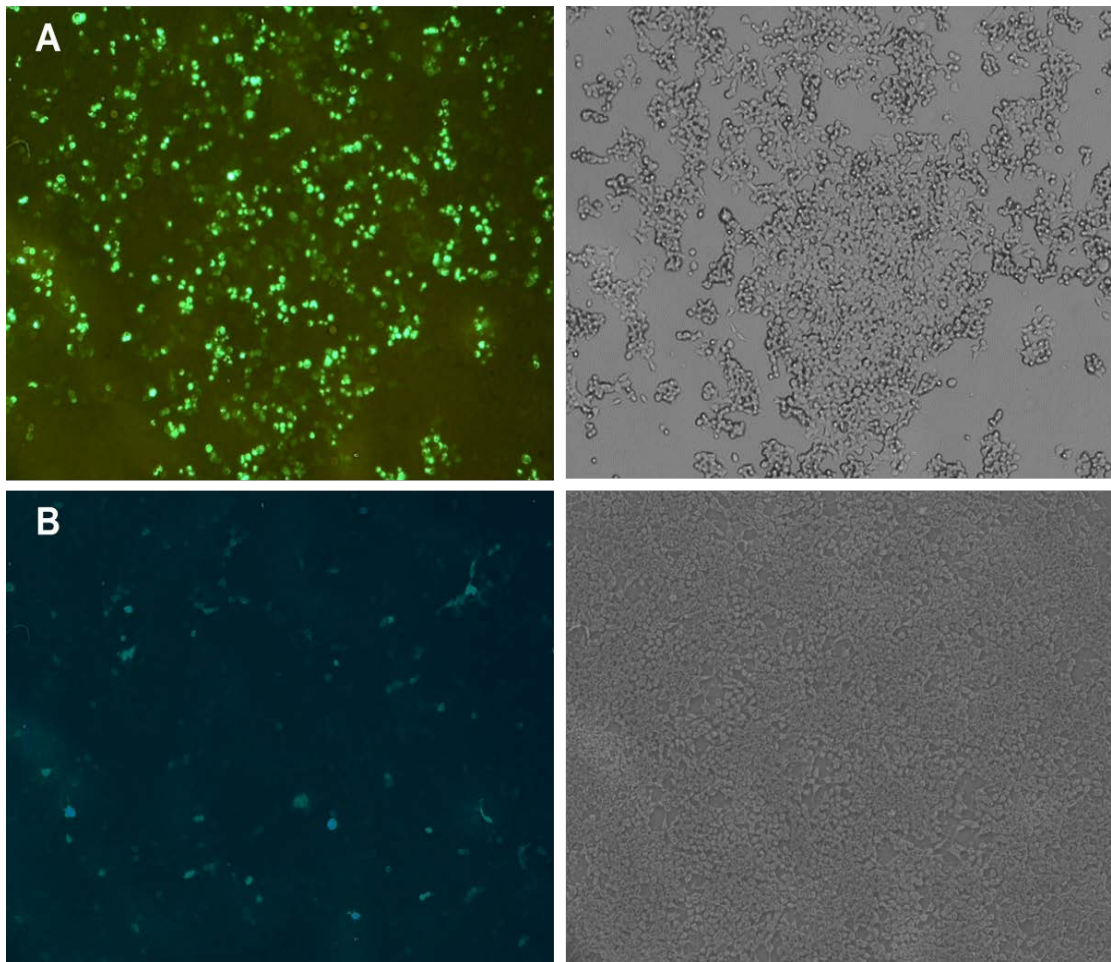


Figure 22 Low magnification images, using Zeiss Axio Vert microscope (x10 objective), showing HEK 293 cells Effectene[®] transfected with **A:** human eGFP-RyR2 fusion plasmid **B:** *M. persicae* eGFP-RyR fusion plasmid. Images on the right show the bright field view.

Transfections with JetPrime[®] showed a relatively good efficiency compared to mammalian RyR2 controls, with approximately 30-40% of cells fluorescing per field of view. However, the expression level in individual cells was very low (data not shown). Extending the post transfection incubation time from 24 to 48 hours did improve eGFP expression; however Western blots of membrane preparations showed no protein band of the expected size after labelling with anti-eGFP primary antibody, suggesting a very low expression level or miss-targeting of the protein. Calcium release assays on HEK 293 cells transfected with Effectene[®] or JetPrime[®] and *M. persicae* eGFP-RyR plasmid DNA showed no release of calcium in response to 10mM and 30mM caffeine (tested in 3 independent experiments, 6 dishes each).

4.3.1.3 eGFP-RyR in Sf9 cells

The N-terminal eGFP fusion construct of *M. persicae* RyR was expressed in Sf9 cells using two different transfection reagents; CellfectinTM II and Fectofly®, but as in the HEK 293 cells the efficiency of expression (approx. 5-10% of cells) and strength of the signal in individual cells were poor. Modifying the amount of reagent, plasmid DNA and addition of transfection enhancer (PLUSTM reagent) had no visual effect. As for HEK 293 cells, the calcium release assays with Fluo-3 AM dye and 20mM caffeine showed no activation of calcium release after addition of the agonist.

4.3.2 Expression of the *P. xylostella* RyR

4.3.2.1 eGFP-RyR in HEK 293 cells

As for the *M. persicae* RyR, the calcium phosphate transfection method proved to be unreliable in achieving a high-level of expression of *P. xylostella* RyR. Although the overall transfection efficiency appeared to be higher when compared to the aphid, it did not reach the levels seen in the human RyR2 control. Reagent-mediated transfections also did not produce satisfactory results; the reproducibility of transfection was greatly increased in comparison to using calcium phosphate, but the expression level (assessed visually) was still not as good as the human RyR2 control (data not shown). However, for membrane preparations isolated from *P. xylostella* RyR / JetPrime® transfected cells it was possible to detect both the full-length RyR and the deletion mutant proteins on Western blots. For the deletion mutant a comparable level of expression to the human RyR2 control was achieved (Figure 23).

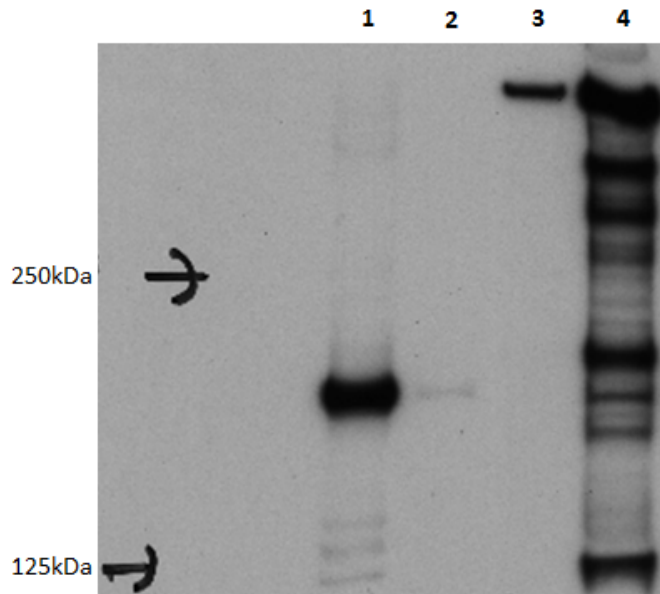


Figure 23 Western blot of membrane preparations from HEK 293 cells expressing 1) the *P. xylostella* eGFP-RyR deletion mutant transfected with calcium phosphate, 2) *M. persicae* eGFP-RyR transfected with calcium phosphate 3) *P. xylostella* eGFP-RyR 4) human eGFP-RyR2 transfected with calcium phosphate (positive control). Ladder markers are indicated with arrows. The result shows a large molecular weight band in lane 3, similar in size to the human RyR2 control and the expected molecular weight for the deletion mutant protein in lane 1. 50 μ g of mixed-membrane preparation was loaded onto each lane.

Fluorescent imaging of fixed HEK 293 cells expressing the *P.xylostella* eGFP-RyR fusion protein, revealed a diffused cytosolic eGFP signal, which was excluded from the nucleus and plasma membrane. This contrasts with images obtained for the eGFP-tagged human RyR2 channel in HEK 293 cells imaged *in vivo*, which show a more ‘spider web’ like pattern associated with the eGFP expression being targeted exclusively into ER membranes (Figure 24). The *P.xylostella* RyR deletion mutant, however, showed a more reticular eGFP expression pattern, comparable to the mammalian RyR2 control (data not shown). The cytosolic expression of the full-length insect eGFP-RyR fusions is comparable to the expression of eGFP protein on its own, as was demonstrated in earlier attempts to express *D. melanogaster* eGFP-RyR fusion proteins in CHO cells [163].

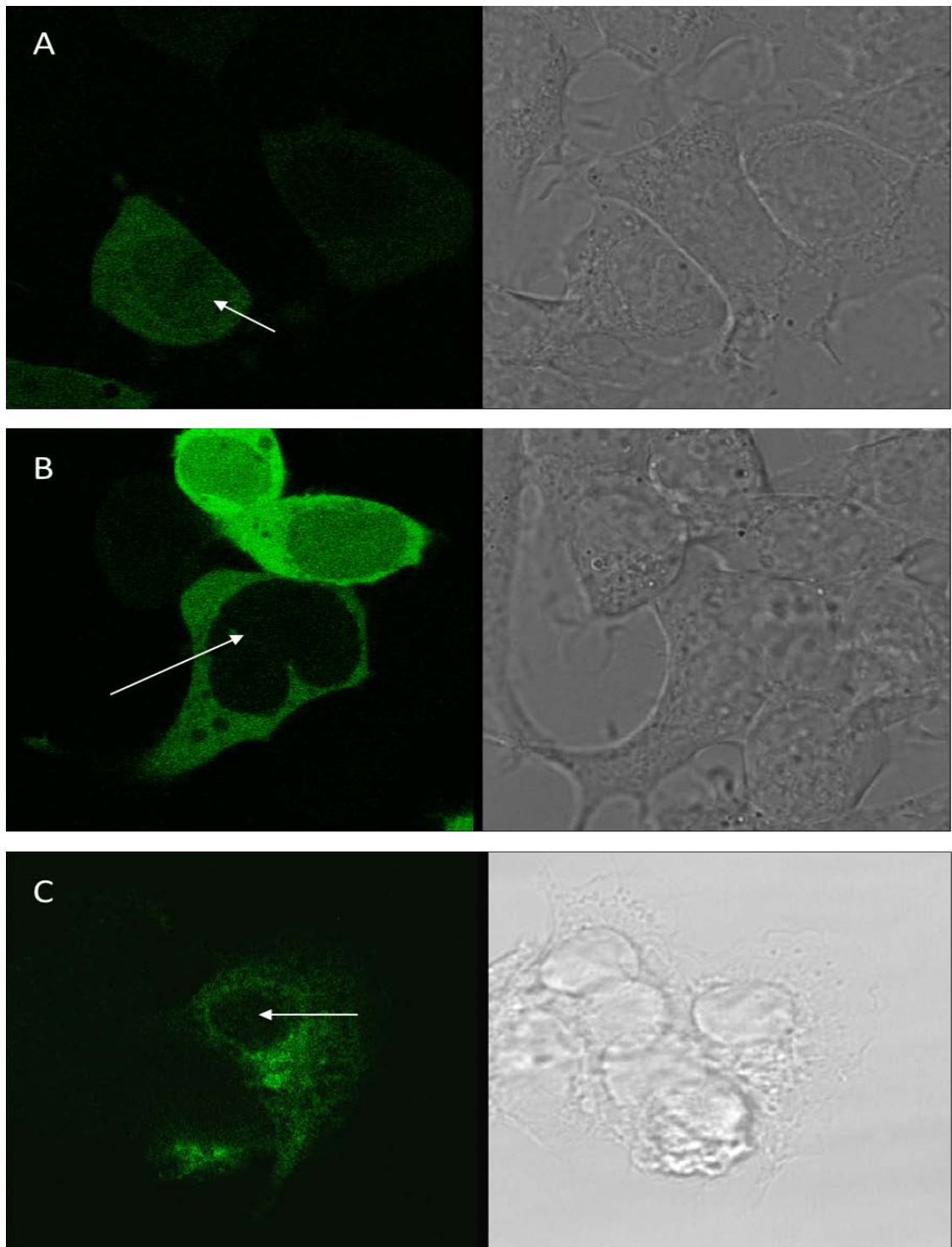


Figure 24 *In vivo*, high magnification, images, obtained using x63 lenses on a Leica SP5 microscope, of HEK 293 cells expressing **A)** *P. xylostella* eGFP-RyR fusion protein, **B)** *M. persicae* eGFP-RyR fusion, **C)** human eGFP-RyR2 fusion (kindly provided by Dr Lowri Thomas, Cardiff University) (pictures on the right show bright field view of imaged cells). The eGFP signal is excluded from the nucleus (white arrows) in all 3 images; however the cells expressing insects RyRs do not exhibit the “spider-web” like pattern of expression seen with the human RyR2 construct (C).

4.3.2.2 Functional analysis of *P. xylostella* eGFP-RyR expressed in HEK 293 cells

Out of 8 experiments set up to measure the response of the full-length *P. xylostella* eGFP-RyR to 20mM caffeine, only three cells in one dish gave a positive response. This is in direct contrast to the control imaging done on transfected cells not loaded with fluo-3 AM dye, showing at least 1-2 eGFP fluorescing cells per field of view at high magnification. It appears that the functioning of the channel is abolished or severely impaired when expressed in HEK 293 cells. In the case of the *P. xylostella* deletion mutant, it was assumed that the caffeine binding site would no longer be present, so caffeine was not used. Out of 8 dishes transfected with the deletion construct, half were tested with 20 μ M ryanodine and the other half with 30 μ M flubendiamide. No responses were recorded for either agonist. It was speculated that most cells expressing the deletion protein did not survive the dye loading procedure. As in the case of the *M. persicae* RyR constructs no [³H] ryanodine binding was detected for either the *P. xylostella* full-length or deletion construct RyR and no channels were incorporated and recorded in the lipid bilayers.

4.3.2.3 eGFP-RyR in Sf9 cells

Expression of the *P. xylostella* eGFP-RyR fusion construct in Sf9 cells showed lower efficiency to eGFP only controls (Figure 25), with the strength of the signal in individual cells being significantly weaker. Basic calculation of the efficiency by selection of a small portion of the image containing approximately 100-200 cells showed values for GFP only of 56-58% and for the *P. xylostella* approx. 20% without PLUS™ reagent and approximately 35% with the reagent.

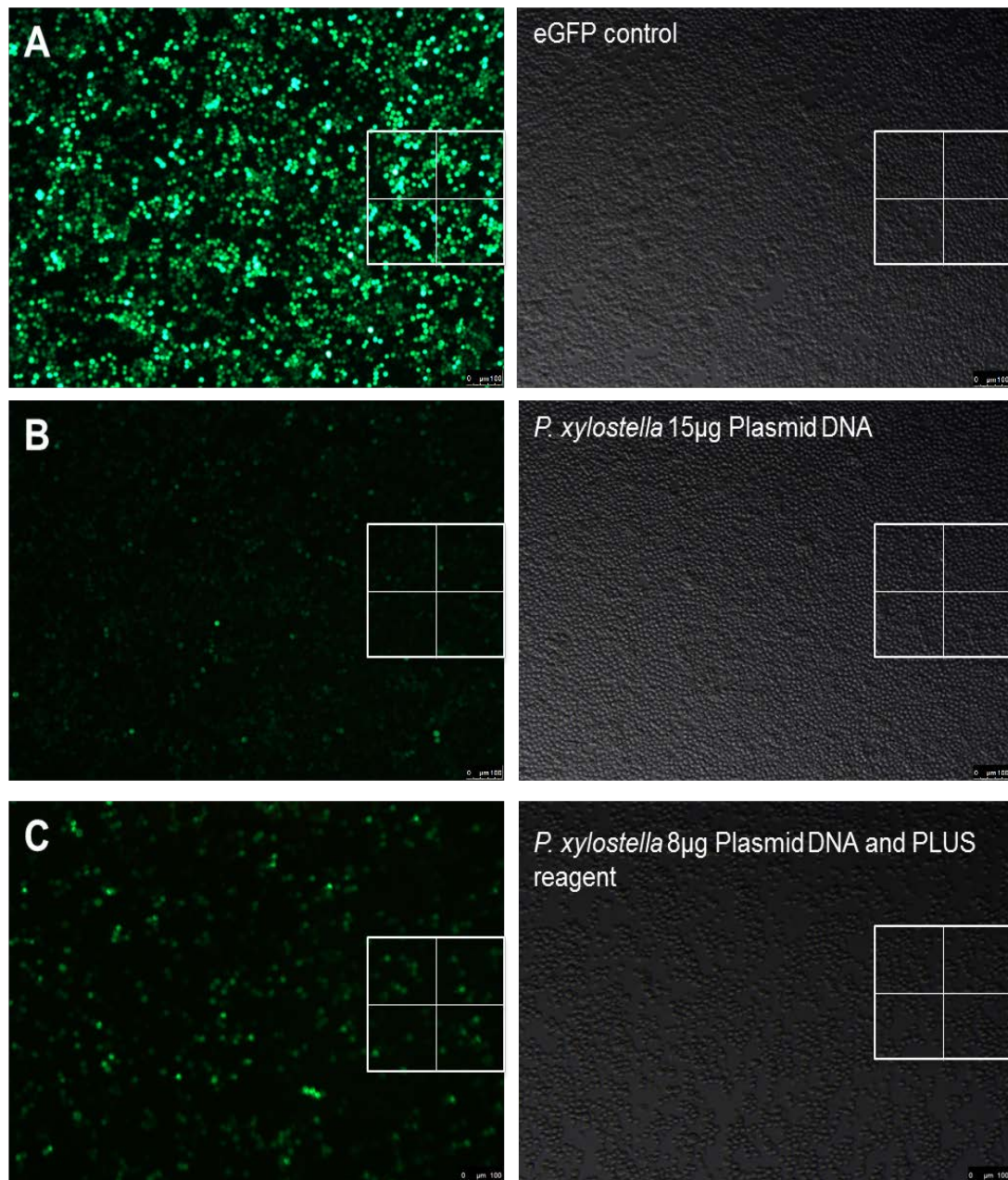


Figure 25 Low magnification images of transfection experiments for the expression of the *P. xylostella* eGFP-RyR fusion protein in Sf9 cells (bright field view showed on the right). Panels: **A**) control plasmid carrying only the eGFP sequence (1µg of DNA), **B**) large amounts (15 µg) of plasmid DNA were required to achieve good transfection efficiency, **C**) addition of PLUS™ reagent improved the efficiency and decreased (8 µg) the amount of plasmid DNA needed. White square indicate the size of the imaged used for counting the efficiency.

After optimisation of transfection conditions the best results were achieved when 10-12µg of plasmid DNA was used with Cellfectin™ II treated cells. Higher amounts of DNA did not improve the success of the transfection, and higher quantities of Cellfectin™ II (<15µl) had a detrimental effect on cell viability. Addition of PLUS™ reagent to the plasmid DNA mix did improve the transfection efficiency

and gave good results with much lower amounts of DNA (1 μ g), with the best results being achieved using 8 μ g of plasmid (Figure 25). The PLUSTM reagent also reduced variability across transfection experiments and seemed to make the procedure less dependent on the overall condition of the cells prior to transfection. It was observed that when CellfectinTM II was used exclusively, transfection efficiency fluctuated between 5-50%, despite the same batch of media, plasmid DNA and FBS being used. In order to scale up the transfection experiments it was decided, based on the obtained results, that 3 μ g of plasmid DNA in the presence of PLUSTM reagent is sufficient to achieve the desired level of eGFP-RyR expression in 60mm culture dishes. It was also noted that altering the length of time of incubation of DNA and lipid reagent prior to applying to the Sf9 cells had no apparent effect on the experimental outcome. Keeping the cells in contact with the transfection mixture for longer than 4h also did not have any negative effects. Although most experiments were imaged 48h post transfection, it was noted that individual cells were able to reach a high level of expression (bright cells) after 24h incubation. Extending the post transfection imaging analysis to 72h showed no positive effects on the level of expression seen. It was impossible to achieve good expression for the eGFP-RyR deletion mutant in Sf9 cells, regardless of the conditions used. In contrast to the HEK 293 cells, the expression of the truncated protein seems to cause the insect cells to die at an early time point post transfection. High magnification, *in vivo* imaging of Sf9 cells expressing the *P. xylostella* eGFP-RyR fusion protein, using a Zeiss 780LSM microscope, confirmed good transfection efficiency. Two populations of cells were observed expressing the eGFP-tagged RyR; some cells having a diffused cytosolic signal (also seen in the HEK 293 cells expressing both insect RyRs) and some a more reticular expression, with a more concentrated 'globular signal (Figure 26).

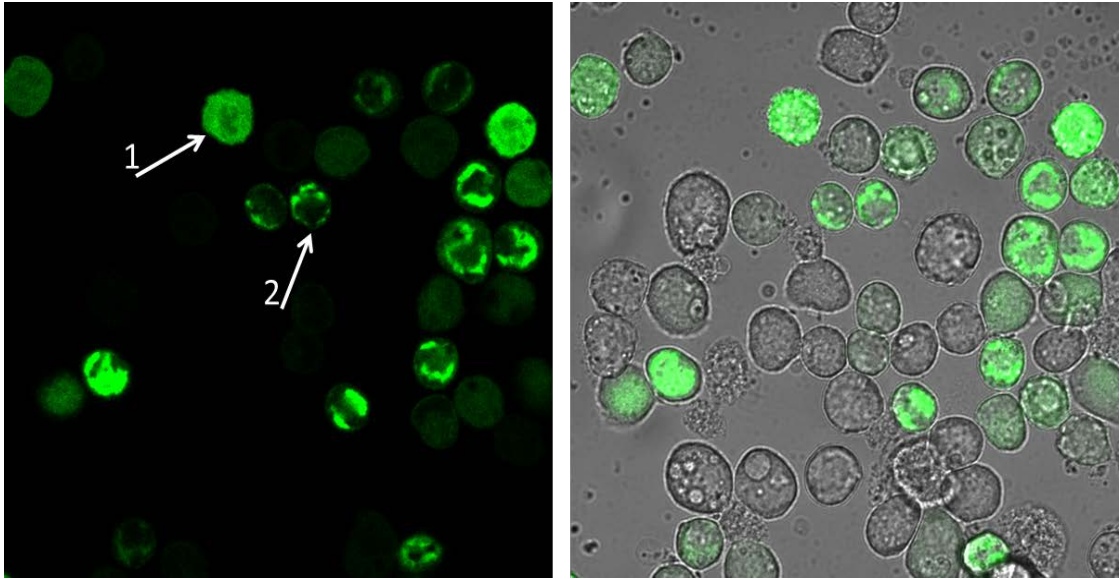


Figure 26 High magnification in vivo images of Sf9 cells expressing the *P. xylostella* eGFP-RyR fusion protein, using a Zeiss 780LSM microscope (x63 lens). Arrows indicate two populations of cells with (1) a diffused cytosolic signal and (2) a more reticular globular signal distribution. The image on the right shows a fluorescent-bright field overlay showing that the expression efficiency is good, with approximately 46% of cells containing eGFP signal.

4.3.2.4 Functional analysis of the *P. xylostella* eGFP-RyR expressed in Sf9 cells

Western blots of mixed-membrane preparations obtained from Sf9 cells expressing the eGFP-RyR fusion showed no protein band of the expected size. It was speculated that the most probable cause for the negative results was that there was not enough eGFP-RyR fusion protein to detect on the blot, due to the transfections being limited to ten 60mm culture dishes (compared with twenty 90mm dishes for HEK 293s), which was dictated by the cost of the transfection reagent and difficulty in obtaining sufficient numbers of Sf9 cells for transfection. Unfortunately, the calcium release assays using Fluo-3 AM also gave negative results, as for HEK 293 expression, despite the good transfection efficiency in Sf9 cells. It was concluded that although it was theoretically possible to obtain good transfection efficiency for *P. xylostella* RyR, the expressed protein did not form a functional channel.

4.3.3 Modification of the *P. xylostella* RyR constructs

Despite a relatively good expression (strong eGFP signal and production of protein of the correct size in HEK 293 cells) there was no evidence that the expressed eGFP-RyR channel was functional, as no specific [³H] labelled ryanodine binding was detected (in the filter disc assay from HEK 293 mixed-membrane preparations) and transfected cells loaded with a fluorescent calcium sensitive dye failed to evoke a calcium release response after exposure to 30mM caffeine in both HEK 293 and Sf9 cells. This non-functionality was probably due to either the presence of the N-terminal eGFP tag or errors in the RyR coding sequence. The cloned *P. xylostella* RyR sequence was therefore aligned with newly available *P. xylostella* RyR sequences to look for possible PCR errors (since the beginning of the project different groups have published *P. xylostella* RyR sequences independently; these were not available during the initial sequencing and assembly of the *P. xylostella* RyR constructs). An alignment with 5 sequences found in GenBank (accession numbers: JF927788.1, JN801028.1, JQ769303.1, JF926694.1 and JF926693.1) showed 3 base differences in the cloned sequence which resulted in 3 amino-acid substitutions unique to the cloned sequence: S815T, Y2834H and M4291I. It was assumed that these 3 substitutions do not occur naturally and were generated during PCR amplification. Since the errors were present in different regions of the gene, the easiest way to obtain modified (corrected) constructs was to mutate the original sub-cloned fragments, Nterm, M2 and Cterm, using site-directed mutagenesis (Chapter II, section 2.9). Only the Nterm fragment generated for the untagged *P. xylostella* RyR construct, which contained the 5'-ACC-3' Kozak consensus sequence immediately upstream of the START codon, was modified and used in the final full-length ligation. The assembly of a new modified untagged *P. xylostella* RyR in pcDNA3.1 (-) was done as described in Chapter III, section 3.2.15. After selecting the correct plasmid DNA by colony PCR and sequencing, the full-length *P. xylostella* RyR was excised from the pcDNA3.1- untagged RyR construct with NotI and PmeI restriction enzymes and ligated into a modified pIZ vector containing an NruI site as described in section 3.2.15. Both new plasmid constructs were tested for potential rearrangements, and the ligation sites were sequenced to check for possible ligation errors. Large quantities of the plasmids were then prepared for multiple transfections in HEK 293 and Sf9 cells.

4.3.4 Expression of untagged modified *P. xylostella* RyR in HEK 293

Calcium release assays were used to test for functional expression of the modified construct in HEK 293 cells. In 5 independent experiments, at least 1-2 cells per field of view showed an increase in intracellular calcium in the presence of 20mM caffeine, 48 hours post transfection. Normalized to the baseline, individual cell responses were consistent with caffeine activation of the RyRs, displaying sharp increases in intracellular Ca^{2+} which returned to basal levels over time (Figure 27).

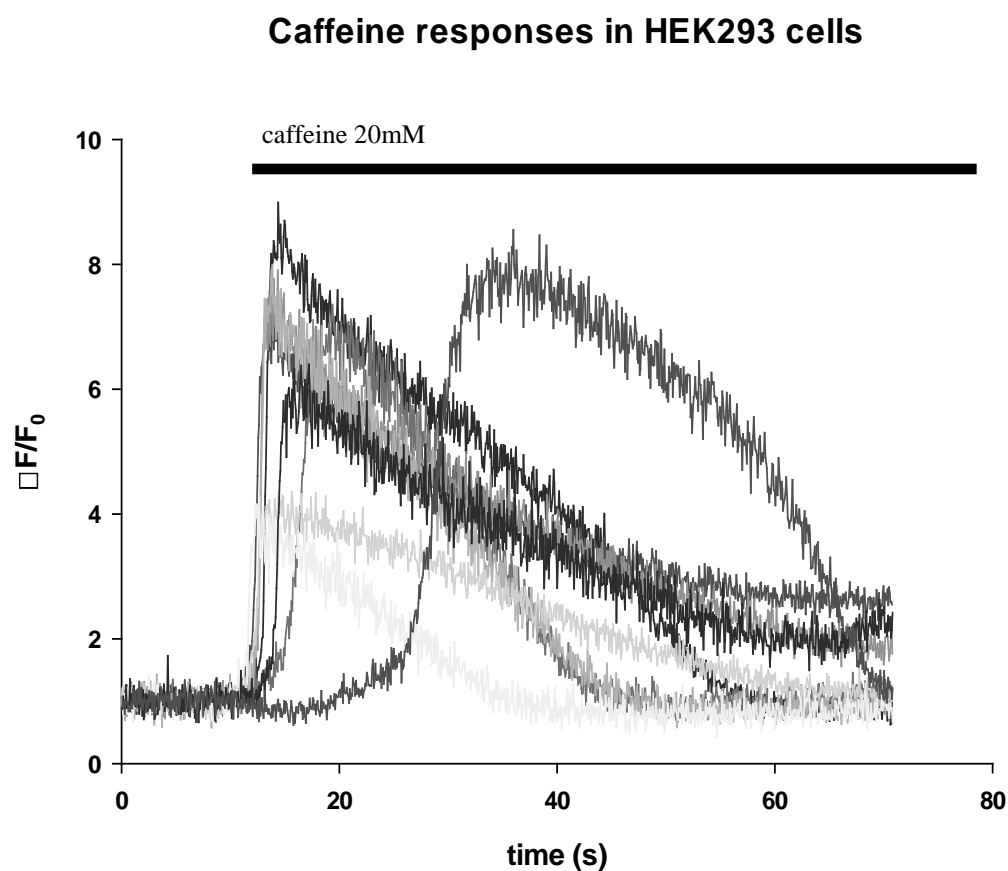


Figure 27 Responses in individual HEK 293 cells transfected with *P. xylostella* - untagged RyR and loaded with Fluo-3 AM dye, after addition of 20mM Caffeine dissolved in DMEM. Data collected from a single experiment represents one field of view using x63 lenses.

Untransfected HEK 293 cells gave no such positive responses (in two separate dishes tested, data not shown), indicating that the response seen with the *P. xylostella* RyR resulted from successful channel expression. No positive responses were recorded when the transfected cells were challenged with diamide insecticides (10 μ M flubendiamide or 10 μ M chlorantraniliprole) when using Fluo 3-AM dye. Due to the

low solubility of diamide compounds in water, DMSO (Dimethyl sulfoxide) was used as a diluent; this proved problematic since DMSO triggers an increase in fluorescence in all imaged cells, making it impossible to determine the origin of the fluorescent signal following diamide application, even when the final concentration of the solvent was not exceeding 1% (v/v) of the total solution. The assays done with 20mM caffeine confirmed that modifying the constructs had a positive effect on the channel function. However, subsequent binding assays with [³H] ryanodine on membrane preparations from two large scale transfections (at least 10 plates), using JetPrime® or calcium phosphate, showed no specific binding. It was concluded that although it is possible to express functional *P. xylostella* RyR channels in HEK 293, the level of expression is insufficient for detailed binding studies to be performed.

4.3.5 Expression of untagged modified *P. xylostella* RyR in Sf9 cells

4.3.5.1 Calcium release assays

The modified construct pIZ WT *P. xylostella* RyR was tested first for functionality in calcium release assays using cells loaded with fluo-3 AM dye in simple experiments without the perfusion system. As with the HEK 293 expression system, it was possible to observe responses in 2-3 cells per field of view to 20mM caffeine, 48h post transfection. However unlike with the HEK 293 cells, over the course of the 60 second recordings the signal was not returning to the baseline level, possibly because of the high concentration of caffeine remaining in solution or different Ca²⁺ handling capabilities of the insect Sf9 cells (Figure 28). Untransfected cells failed to evoke any caffeine mediated responses in the four dishes tested. This result indicates that, as for HEK 293 cells expressing the modified *P. xylostella* RyR construct, the Sf9 cells were expressing a functioning RyR channel.

Individual cell responses to 10mM caffeine

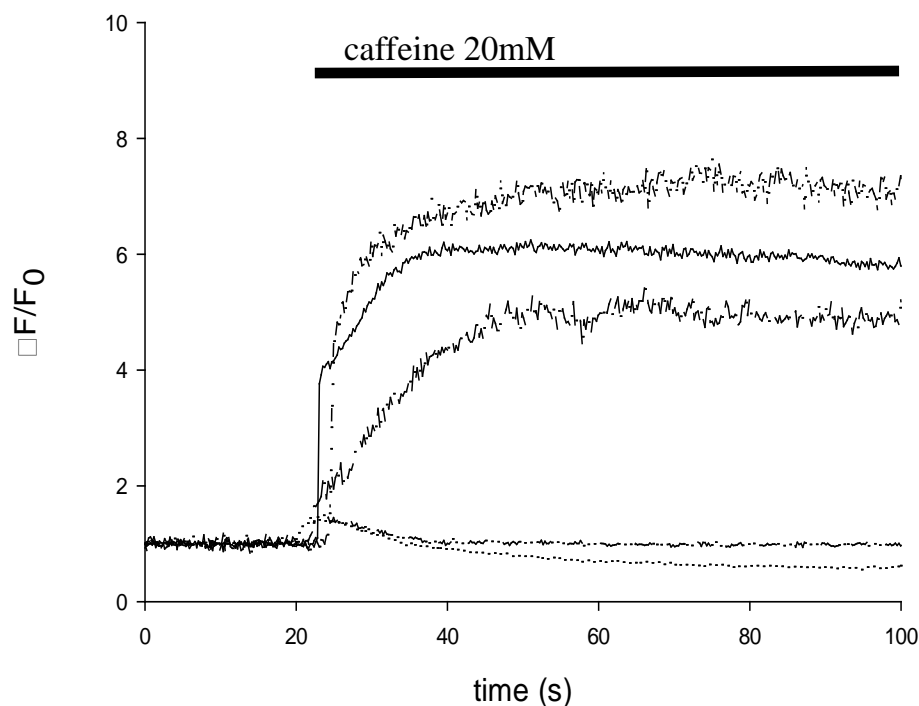


Figure 28 Activation of individual Sf9 cells expressing modified *P.xylostella* RyR using 20mM caffeine. Cells were loaded with FLUO-3 AM and the spike in fluorescent 20mM caffeine dissolved in Sf-900 II media was added to the dish. Like HEK cells cells did not show fast return of the signal to the baseline level. Data collected from a single experiment represents one field of view using x63 lenses.

In subsequent experiments a perfusion system was employed, such that once a suitable patch of caffeine responsive cells was found, the cells could be challenged with a number of different agonists. A typical experiment consisted of one or two application of caffeine (30mM and/or 10mM) followed by either 30 μ M of a diamide analogue (a reversible agonist capable of being washed out of the binding site) or 10 μ M of flubendiamide or chlorantraniliprole insecticide, followed by 30mM caffeine. The initial exposure to caffeine resulted in a typical brief elevation of intracellular Ca²⁺ which usually returned to basal level over time. A similar cellular response was also seen with 30 μ M of the diamide analogue. However, the fluorescence level remained elevated in the cells exposed to 10 μ M flubendiamide or chlorantraniliprole and it was impossible to evoke any further caffeine responses in the same cells, which suggest that the binding of both insecticides was irreversible over the time course of the experiment (Figure 29). In contrast, it was possible to

record further responses to 30mM caffeine in cells exposed to the diamide analogue. Lower concentrations (0.5 μ M, 1 μ M, 5 μ M) of flubendiamide and the diamide analogue were also tested, showing no 'measurable' responses; however, flubendiamide, even at low concentrations (0.5 μ M and 1 μ M), abolished further caffeine responses even if no Ca²⁺ mobilization was recorded (data not shown). This lack of a recorded response to lower concentrations of insecticide is likely due to experimental setup limitations such as a short release time for each compound (3-5 seconds), or distance to and size of the U-tube aperture. It was previously demonstrated that in *H. virescens* neurons less than 1 μ M of flubendiamide can evoke an EC₅₀ (effective concentration) response [31]. The initial high concentration of flubendiamide used (10 μ M) was previously reported to cause a maximum response in calcium release assays in CHO cells expressing *D. melanogaster* RyR [31]. The experimental setup might also have a negative effect on measured responses to 10mM caffeine, resulting in false negatives during some experiments.

The functional expression was also tested at different time points (48h, 72h and 96h), to determine if channel activity decreased with time, and if cells were showing cytotoxic effects typically associated with RyR overexpression [186]. Interestingly, receptor activity in Sf9 cells did not appear to diminish over time. Also, unlike with the mammalian HEK 293 cells, Sf9 cells did not show cytotoxic effects, and many cells expressing the protein were able to divide. In total, from all time points and separate transfections investigated, the response of 71 cells to 30mM caffeine was monitored in 12 separate recordings; 16 cells (3 recordings) with 10mM caffeine; 43 cells (8 recordings) with 30 μ M of the diamide analogue, and 2 recordings for both chlorantraniliprole (10 cells) and flubendiamide (13 cells). The average amplitude with 30mM caffeine was 0.22 ± 0.095 SEM ($\Delta R/R_0$), from 8 independent experiments (n=30 cells) over different time points. Cells with normalized response values lower than 0.05 were excluded from the final calculation. The duration of the response (from excitation to return to the resting state) varied between individual cells in any given experiment and between different experiments, and ranged between 12 to 22 seconds (as seen in Figure 29), or lasted until the end of the recording - suggesting a very slow decrease of signal to the baseline (a result also seen with fluo 3-AM imaging, Figure 28). As these were preliminary experiments designed to assess channel functionality, all of the calcium release assays omitted the

initial dye calibration step which allows for Ca^{2+} quantification. It was therefore not possible to assess the resting Ca^{2+} concentration and to quantify the amount of Ca^{2+} released following agonist exposure in cells expressing *P. xylostella* RyRs from this particular dataset.

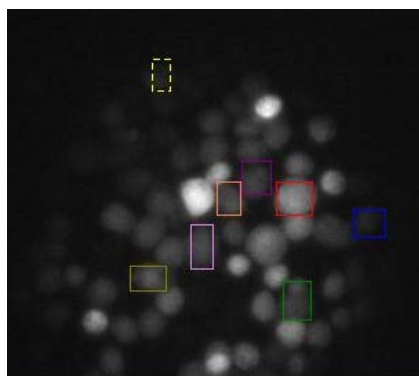
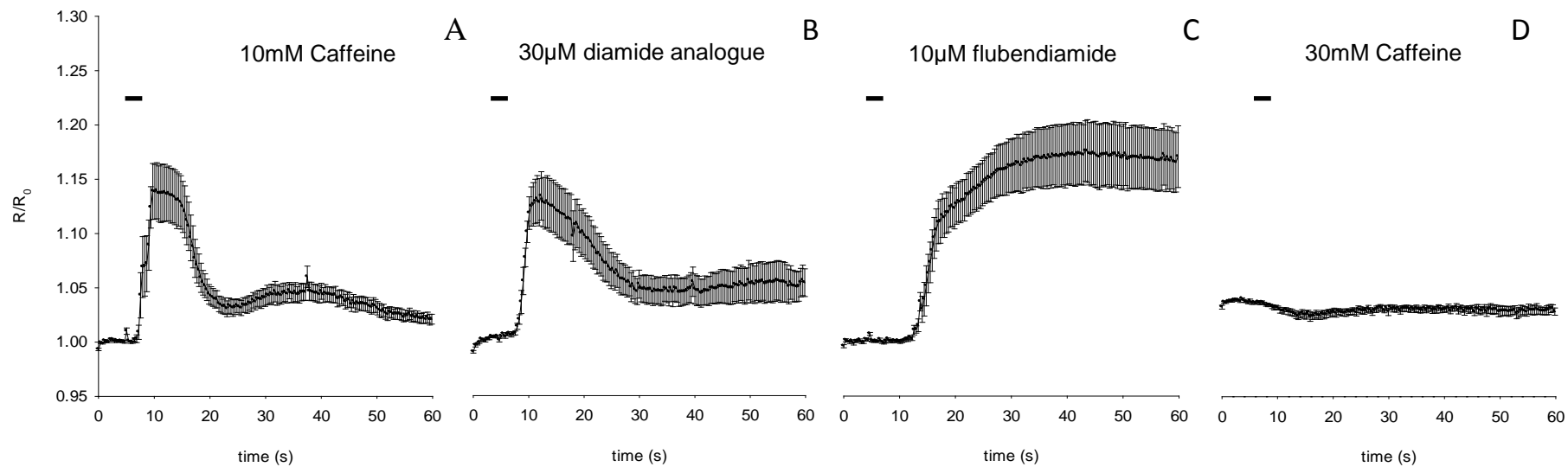


Figure 29 Fluorescence ratios measured over time in single calcium release experiment using Fura 2 AM. Panels A-D show mean \pm standard error responses of the same cells ($n=8$) to **A** 10mM caffeine, **B** 30 μ M diamide analogue, **C** 10 μ M flubendiamide and **D** 30mM caffeine - application of flubendiamide abolishes further caffeine responses, suggesting an irreversible binding. The picture on the left shows a snapshot of cells during fluorescence ratio measurement, using x40 lens and an excitation wavelength of 380nm.

4.3.5.2 Ryanodine binding assays and single channel recordings

The preliminary filter disc binding assays on mixed-membrane preparations from large scale transfection experiments (at least 15 x 60mm dishes) using Sf9 cells, indicated positive binding of ryanodine to the *P. xylostella* RyR receptor in the presence of 800 μ M of free Ca²⁺ (3 independent experiments, done in duplicate). The calculated average specific binding was 0.72 pmol/mg of protein, with a standard deviation of \pm 0.16. The specific binding for all 3 experiments was greater than 90% of the total binding value (Table 13).

Table 13 Results for individual filter discs titrated [³H] ryanodine binding assay

| Total (dpm) | Non-specific (dpm) | Specific binding (dpm) | Protein (μg) | Specific binding (pmol/mg) |
|--------------------|---------------------------|-------------------------------|------------------------------------|-----------------------------------|
| 13714.7 | 684.12 | 13030.58 | 100 | 0.617855856 |
| 15269.8 | 624.61 | 14645.19 | 100 | 0.69441394 |
| 16277.2 | 811.8 | 15465.4 | 100 | 0.733304884 |
| 16974.4 | 844.82 | 16129.58 | 100 | 0.764797534 |
| 9268.78 | 1275.4 | 7993.38 | 100 | 0.379012802 |
| 18996.1 | 1242.24 | 17753.86 | 100 | 0.84181413 |

Grey/white backgrounds highlight experimental duplicates. All discs contain membrane preparations from Sf9 expressing untagged *P. xylostella* RyR.

Additionally the Sf9 mixed-membranes incorporated into artificial bilayers resulted in incorporation and brief recordings of ‘ryanodine-like’ channels (Figure 30). However, it was impossible to record responses to any agonists, since the (non-purified) mixed-membrane preparation compromised the integrity of the artificial bilayer, causing it to break down upon perfusion. Further purification of the channels through sucrose gradient centrifugation will be required before more detailed experiments can be done.

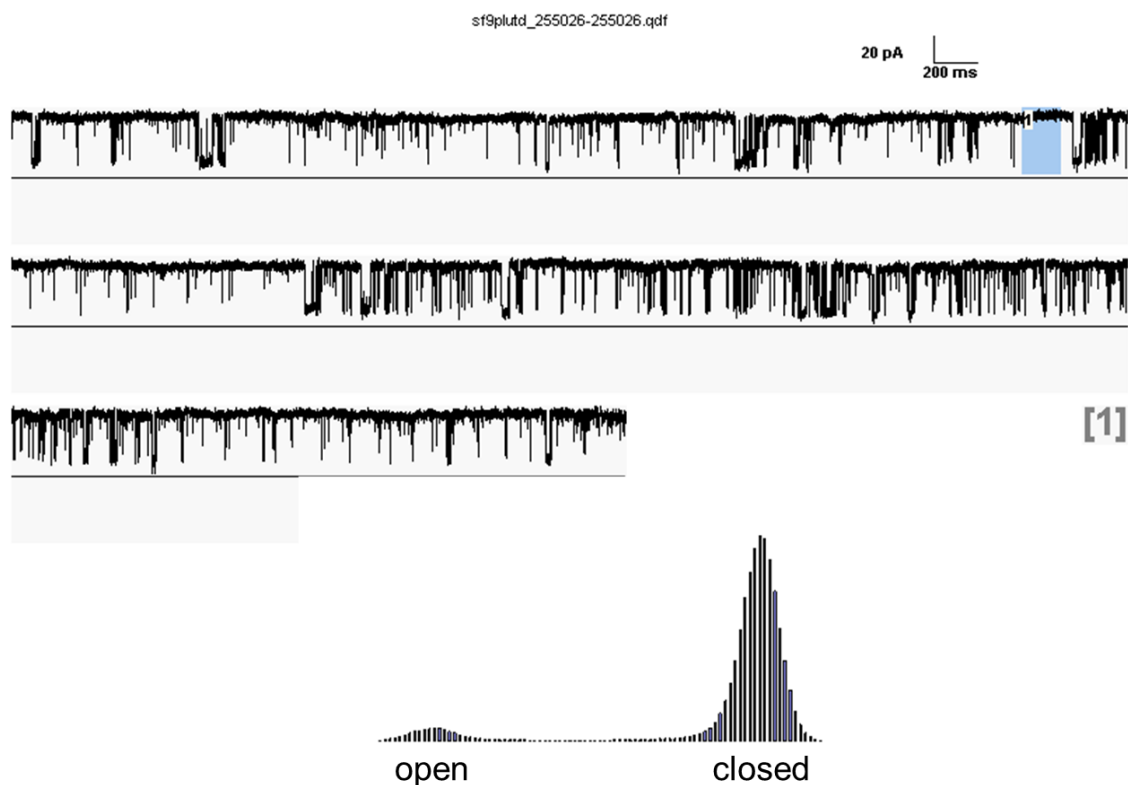


Figure 30 A single channel trace obtained from a bi-layer experiment showing a ‘ryanodine receptor-like’ channel incorporated into a membrane. The recording was done in a 4:1 KCl (~850:210mM) gradient between cis and trans chambers when a mixed membrane preparation from Sf9 cells expressing WT *P. xylostella* RyR was applied. The currents seen are due to the chemical gradient rather than holding potential, no agonists were tested. Histogram analysis of the trace indicated that the channel was mostly in a closed state with no visible sub-conductance states. Graph represents a single experiment. No further studies were attempted. The graph represents a single experiment; no further replications were conducted.

A binding saturation experiment was also done, using the 96 well filter plate format, with a minimum of 3 replicates per plate for each ryanodine concentration. Although specific binding was significantly lower (only approx. 40% of the total binding) in comparison to the previous filter disc assays, binding for 11 ryanodine concentration points was recorded and a curve was fitted to the data using GraphPad prism (Figure 31).

Binding of [³H] ryanodine to WT *P. xylostella* RyR channel

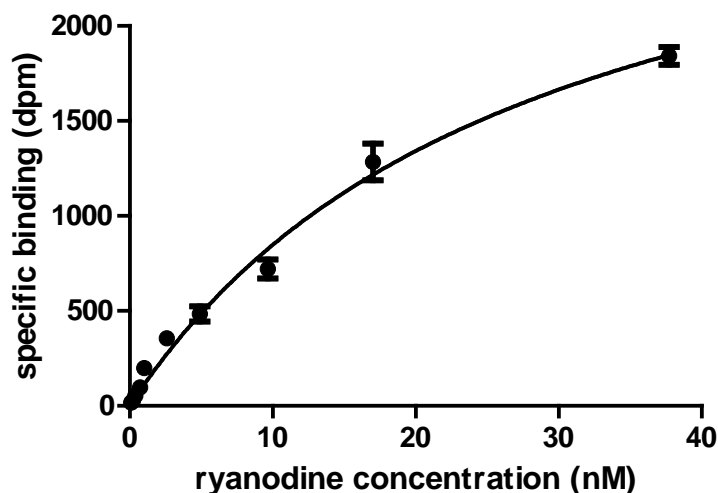


Figure 31 Binding saturation curve for WT *P. xylostella* RyR (expressed in Sf9 cells) challenged with titrated ryanodine. Each point on the graph represents the average of 3 replicates \pm S.E.M.

The density of binding sites B_{\max} (2447 ± 425 dpm (244.9 ± 42.5 fmol/mg)) and the dissociation constant K_d value (12.89 ± 4.5 nM) for ryanodine binding to *P. xylostella* RyR were calculated using this software. The K_d value is higher than seen for native preparations of rabbit skeletal muscle RyR (2.04 ± 0.12 nM) and *H. virescens* RyR (3.82 ± 0.39 nM), which also have much higher B_{\max} values; 4.57 ± 0.32 pmol/mg (rabbit) and 2.41 ± 0.17 pmol/mg (*H. virescens*) [176]. In another study however, the K_d value for *H. virescens* native membrane preparations was 13.9 ± 3.8 nM, making it comparable to the Sf9 expressed *P. xylostella* RyR, while the B_{\max} values were between 1-1.5 pmol/mg [29]. It is apparent that the filter plate experiments require further optimization to reduce the non-specific binding, which may influence the K_d and B_{\max} values of the currently obtained binding data. However, these preliminary results clearly indicate that there is sufficient functional receptor density in mixed-membrane preparations of Sf9 cells expressing the *P. xylostella* RyR to allow meaningful binding assays to be carried out.

4.3.6 General remarks

The work reported here used expression vectors (pcDNA3.1(-) and pIZ/V5-His) with constitutive promoters in non-lytic systems for the expression of insect RyRs, with the aim of achieving a good level of expression, as has been previously demonstrated for a number of mammalian RyR constructs [186]. The pcDNA family of vectors (Life technologies) has been used in the past to express insect RyRs from *D. melanogaster* and *B. mori* [30, 163]. In the case of expression in Sf9 cells, there have been no reports in peer reviewed literature on attempts to express RyRs by any other means other than recombinant baculovirus [125, 206]. The use of non-lytic vectors is mentioned in the DuPont patent WO/2004/027042, but there is very little detail on the associated methodology [187]. Both HEK 293 and Sf9 cell lines have been shown by different groups to be able to express functional mammalian RyR channels indicating that, theoretically, they may have the capability to express insect RyR channels as well. All expression studies were initially done in HEK 293 cells, as the Cardiff University laboratories have had considerable success in using these cells for expression and study of mammalian RyR2 channels [95, 195, 213]. Calcium phosphate transfection although the most cost effective method, gave very variable results across different experiments using HEK 293 cells and between different plates set up alongside each other on the same day. This method also proved unsuitable for transfection of insect Sf9 cells, as the addition of the DNA precipitate resulted in complete cell lysis within a few hours. Modifications made to the *P. xylostella* cDNA constructs resolved the lack of function seen early on in both expression systems; however, the HEK 293 cells gave inadequate (low level) expression of RyR protein, so could not be used for more detailed receptor characterization. It is possible that in the mammalian cell line chosen for this study, some insect RyR accessory proteins required to overcome the cytotoxic effects of RyR expression are not available. In studies of the mammalian RyR2 channel, it was shown experimentally that co-expression of FKBP 12.6 has a positive effect on cell proliferation and decreased the cytotoxic effects associated with RyR2 over-expression [124].

In the case of *P. xylostella* RyR, it is unclear whether the modification (correction) of the 3 amino acids deduced to be PCR errors within the cDNA sequence or the removal of the N-terminal eGFP tag restored channel function. In previously expressed insect (*D. melanogaster*, *B. mori*) and mammalian RyRs, an N-terminal GFP tag had no negative effects

on overall channel function [30, 163, 195]. Introduction of the eGFP tag to the modified *P. xylostella* RyR constructs will be required to resolve this matter.

In the case of *M. persicae* RyR, it is possibly unlikely that the eGFP tag was the reason for poor expression and lack of function, since both untagged and tagged constructs were tested in HEK 293 cells and gave the same negative result. However removal of the tag from the insect (Sf9) cells expression vector (pIZ-eGFP-RyR) could be explored as a potential way of resolving the expression problems, but other factors may also need to be looked at, including codon usage. There were no PCR errors detected in the cloned aphid sequence; direct sequencing of PCR amplified *M. persicae* fragments covering portions of the receptor did not find any errors when aligned to: - the full-length cDNA incorporated into the expression vectors, - the closely related *A. pisum* RyR sequence - other available insect RyRs.

4.4 Conclusions

It was possible to achieve a good level of protein expression for the *RyR* gene from *P. xylostella* using Sf9 cells, enabling detailed functional characterization of the channel to be carried out at a future date. The expressed *P. xylostella* RyR was shown to be responsive to caffeine and diamide insecticides and was able to bind ryanodine. There was also evidence that the level of expression is sufficient to conduct single channel recording experiments.

In summary, expression of insect RyRs proved to be a difficult task and was only achieved after modification of the original constructs and optimization of the transfection method. It was not possible, however, under any of the conditions so far tested, to achieve good expression of the *M. persicae* RyR cDNA.

Chapter V: Characterization of diamide insecticide resistance in *P. xylostella*

5.1 Introduction

5.1.1 *Plutella xylostella*

Plutella xylostella is a small nocturnal moth with a high reproductive rate and short life cycle of approximately 3-4 weeks, depending on the ambient temperature (Figure 32). Short lived adults mate soon after emergence and females can lay up to 200 eggs over a period of 4 days. The emerged first instar larvae mine into leaf tissue while the later, larger larval stages, eat whole leaves; 4th instar larvae, after completing feeding undergo pupation which can last up to 15 days in cooler temperatures [193]. *P. xylostella* is a major worldwide pest of cruciferous crops (eg. cabbage) and is particularly destructive in sub-tropical parts of the world where the climate allows for year round crop production and completion of multiple life cycles of the pest [190]. The worldwide cost of control of *P. xylostella* is estimated to be 4-5 billion US dollars per annum [190].

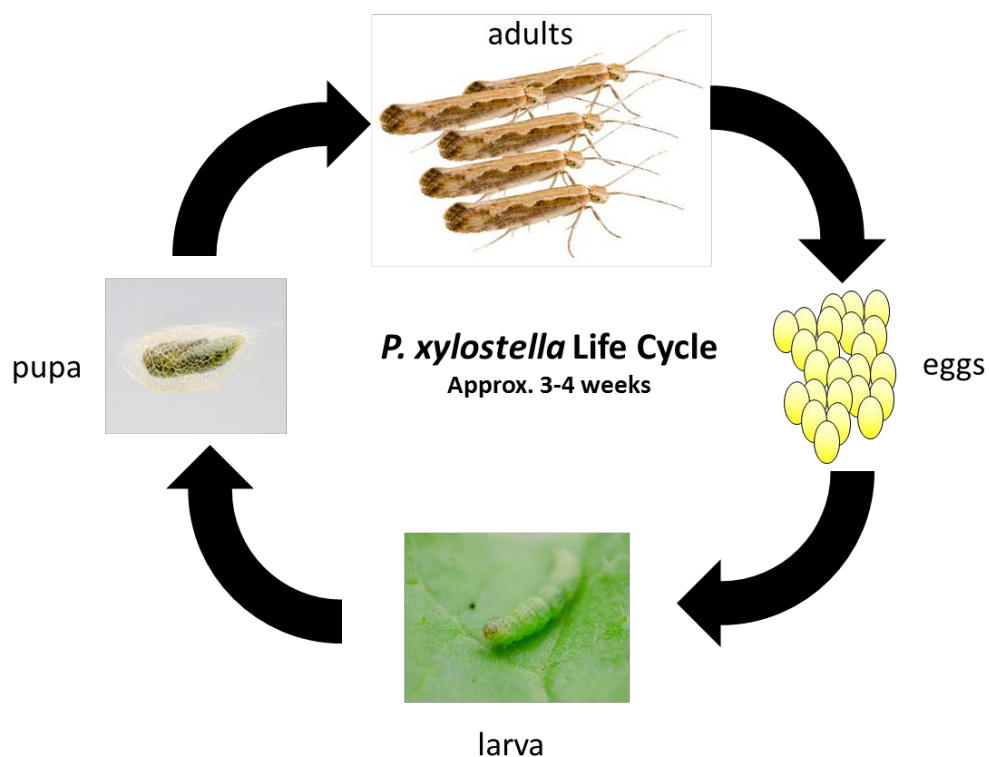


Figure 32 *P. xylostella* life cycle. Photographs provided by Mark Mallot.

5.1.2 Insecticide resistance in *P. xylostella*

Introduction of any new class of chemistry to control pests is often followed by the development of resistance to that chemistry, due to the high (unnatural) selection pressure applied to the pest population, which is often accelerated by misuse of the insecticide e.g. through application of several consecutive treatments with the same compound or by using less than the recommended application rate.

There are 3 main mechanisms of insecticide resistance:

- a) reduced insecticide uptake, usually resulting from changes in the insect's cuticle
- b) 'metabolic', which involves an increase in the rate of detoxification of the insecticide, usually by over expression and/or modification of enzymes such as cytochrome P450s, glutathione S-transferases, and carboxyl-esterases involved in the breakdown of xenobiotics
- c) modification of the target protein due to novel mutations arising in the coding sequence, especially in the vicinity of the insecticide binding site [214].

P. xylostella was the first agricultural pest to develop resistance to DDT, one of the first widely used synthetic insecticides [215], and has subsequently developed resistance to almost all chemical classes of insecticide that have been used for its control. This has involved a wide array of resistance mechanisms being induced in the pest, including target site modifications [216], increased detoxification [217] and reduced uptake [218].

The recent, in many cases exclusive, use of the new diamide insecticides on *P. xylostella* has rapidly selected for resistance in this species, and this chapter focuses on the characterization of two such diamide resistant strains. The work, which reports the first target site mutation associated with a diamide-resistant phenotype, has recently been published (see Troczka *et al.* 2013) [19]. A preliminary characterization of the effect of the target site mutation on functioning of the RyR channel, using expression in Sf9 cells (see Chapter IV for methodology), is also presented and discussed.

5.2 Methods

5.2.1 *P. xylostella* strains

Field samples of *P. xylostella* were collected from 2 geographically distinct locations where control failure with diamide insecticides had been reported. The first strain, Sudlon, was supplied by Bayer CropScience AG, and was sourced from Cebu Island in the Philippines. The second strain was supplied by Syngenta, sourced from Bang BuaThong, Thailand (ThaiR) and was subsequently selected every 2 weeks with chlorantraniliprole. Syngenta also supplied a susceptible field strain (ThaiS) which originated in an area near Chiang Mai, Thailand. Additionally two laboratory susceptible *P. xylostella* strains were available to be tested, the Roth strain (Rothamsted) and the HS strain (provided by Bayer CropScience AG).

5.2.2 Sequencing of TM region of *P. xylostella* RyRs

RNA from pools of 5 larvae (mixed instar's) from ThaiS, ThaiR, Sudlon and HS strains was extracted as described in Chapter II, section 2.3.2, and cDNA synthesised using Superscript™ III (described in Chapter II, section 2.4.1). Three short (approximately 1Kb) overlapping DNA fragments were amplified by PCR in 25µl reactions incorporating: 2x Dreamtaq™ PCR master mix (Thermo-Fermentas, MA, USA), 1µl of cDNA, and primer pairs (20pmol each primer) covering the entire TM region (assuming the 6 TM model) of the channel (Table 14). A portion of the receptor close to 5' end, which was previously reported to be important for channel sensitivity to flubendiamide in *B. mori* [30], was also PCR amplified. The PCR temperature cycle used was 95°C for 2 minutes followed by 35 cycles of: 95°C for 20 seconds, 50°C for 30 seconds, 72°C for 1 minute 30 seconds, and final extension step at 72°C for 5 minutes. All PCR products were purified by selective precipitation with 4M NH₄OAc (Chapter II, section 2.6.4) and sent for sequencing by EUROFINS DNA.

Table 14 Primer pairs used for amplification and sequencing of TM and N-terminal regions of *P. xylostella* RyR

| PCR product | Primers | Primer sequence | Size (bp) | Position (AA) ^a |
|-------------|-------------|----------------------------|-----------|----------------------------|
| F1 | Px.1Kb-F1 | GGCTATACTGATCGGGTACTACC | 1157 | 4743-5119 ^b |
| | Px.Cterm-R1 | GAGTTTGGTACCAGTGGCCCTAAGTC | | |
| F2 | Px.2Kb-F1 | CGGTTTAATGGCGGATGCGGAAG | 1087 | 4387-4749 |
| | Px.2Kb-R1 | GGTAGTACCCGATCAGTATAGCC | | |
| F3 | Px.3KbF -1 | CGGAGAGAAGAACATGCACGACGCAG | 1160 | 4008-4393 |
| | Px.3KbR-1 | CTCCGCATCCGCCATTAACCG | | |
| N | Px.N1-F | TCCTACTTCGGCATCTCAACAGTG | 1252 | 104-521 |
| | Px.N1-R | GCGGAGATCATCTCCAGCTCTG | | |

^aPosition based on Accession number JX467684, ^bReverse primer outside coding region

5.2.3 DNA extractions and *TaqMan* assay

Genomic DNA was extracted from at least 10 individual insects from each *P. xylostella* strain, using DNAzol® reagent. Each larva was ground to a powder in a 1.5ml eppendorf tube containing 200µl of DNAzol® reagent on dry ice. The homogenate was then centrifuged at 10,000g, 4°C for 20 minutes in an Eppendorf 5415R centrifuge to remove insoluble tissue fragments, RNA and polysaccharides. The supernatant was then transferred to a fresh 1.5ml tube and the DNA was precipitated by the addition of 100µl of 100% ethanol, the tube contents mixed and maintained for 3 minutes at room temperature. The samples were then centrifuged for 20 minutes in an Eppendorf 5415R centrifuge at maximum speed to pellet the DNA. The supernatant was subsequently removed and the pellet was washed with 200µl of 70% ethanol, followed by a 5 minute centrifugation at maximum speed. After the wash step the ethanol was removed and the pellet left to air dry for 5-10 minutes. The DNA was then re-suspended in 20µl of nuclease free water and used straight away in PCRs and *TaqMan*® assays.

Prior to the *TaqMan*® assay, small PCR fragments covering the region where the potential resistance mutation was identified by sequence analysis (Section 5.2.2) were PCR amplified from the genomic DNA isolated from the ThaiS, ThaiR and Roth strains, in 25µl reactions incorporating: 1µl of genomic DNA, 2xDreamtaq® mastermix, and primer pair Plut.Mut1-F / Plut.Mut1R (20pmol) (sequences in Appendix C, section 5), using the PCR cycle conditions described in section 5.2.2. The obtained PCR products were gel purified, and then sequenced in order to identify if any introns were present in close proximity to the mutation site.

A *TaqMan*[®] assay (Life Technologies), using the primers/ fluorescent probes described in Table 15, was designed to amplify across the region of interest, i.e. where a resistance-associated mutation had been found in the RyR gene.

Table 15 *TaqMan* assay probe and primer sequences

| Primer/Probe | Sequence |
|---------------------|------------------------|
| PxTaqMan_F | CGCCGCTCATCTGTTGGA |
| PxTaqMan_R | GCGTGACAGACTGCAAGATAGT |
| PxTaqMan_WT | VIC-TGGCTGTTGGGTTCAA |
| PxTaqMan_Mut | FAM-TGGCTGTTGAGTTCAA |

The forward and reverse primers, and the two minor groove binding (MGB) probes (Life technologies - Applied biosystems), were designed using Primer Express[™] Software, Version 2.0 (Life technologies). Primers PxTaqMan_F and PxTaqMan_R are standard oligonucleotides with no modification. The probe PxTaqMan_WT is labelled with VIC[®] (a fluorescent reporter dye) at the 5' end for detection of the wild type (WT) allele and probe PxTaqMan_Mut is labelled with 6-FAM (Fluorescein amidite reporter dye) for detection of the resistant allele. Each probe also had a 3' non-fluorescent quencher and a minor groove binder at the 3' end. The minor groove binder provides more accurate allelic discrimination by increasing the T_M differential between matched and miss-matched probes [219]. PCR reactions (20 μ l) contained: 1 μ l of genomic DNA, 10 μ l of SensiMix[™] Probe DNA kit (Bioline), 800nM of each primer and 200nM of each probe. Reactions were run on a Rotor-Gene 6000[™] (Qiagen-Corbett Research) cycler using temperature cycling conditions of 10 minutes at 95°C followed by 40 cycles of 95°C for 10 seconds and 60°C for 45 seconds. The increase in VIC and FAM fluorescence was monitored in real time by recording each cycle on the yellow (530nm excitation and 555nm emission) and green (470nm excitation and 510nm emission) channel of the Rotor-Gene respectively.

5.2.4 Modification of the WT *P. xylostella* untagged constructs

A full-length WT *P. xylostella* RyR cDNA has been shown to be functionally expressed in both Sf9 and HEK 293 cells (details Chapter IV). This WT cDNA was modified to introduce the mutation present in diamide resistant moths. Due to the large size of the expression plasmid constructs it was not possible to use SDM on the full-length cDNA insert, so the mutation was introduced into a sub-cloned modified C4 fragment (Chapter IV), which was used to make the full-length untagged WT plasmid, using the SDM method described in Chapter II, section 2.9. The plasmid carrying the mutation (which causes a Glycine (G) to Glutamic Acid (E) substitution) was identified by sequencing, and named C4G-E. This modified cDNA was used in the assembly of the full-length RyR into pcDNA 3.1(-), as described in Chapter III, section 3.2.15. This modified cDNA was also transferred across into the pIZ/NruI vector following the procedure described in Chapter III, section 3.2.15, and the construct named pIZ-G-E RyR.

5.2.5 Expression of G-E *P. xylostella* RyR in Sf9 cells

The pIZ-G-E RyR expression plasmid was used in subsequent transfections of Sf9 cells, using the optimized conditions described in Chapter IV, section, 4.3.5. Functional expression of the mutated RyR channel was initially tested 48h, 72h and 96h post transfection with calcium mobilization assays using FURA 2 AM dye (Chapter IV, section 4.2.4.2). Mixed-membrane preparations from large scale transfections of Sf9 cells were prepared as described (Chapter IV, section 4.2.1.2). Binding assays with [³H] ryanodine were done in 96 well plates as described in Chapter IV, section 4.2.3.3. Data were analysed using SigmaPlot v.12 and GraphPad Prism v.5 software, as previously described.

5.3 Results and discussion

5.3.1 Bioassays

The initial bioassays to determine the level of resistance of the *P. xylostella* field strains to diamide insecticides were done by researchers at Bayer CropsScience AG and Syngenta. The results of these bioassays are presented in our publication [19], and are reproduced in Table 16 below. The bioassays indicate that the ThaiR and Sudlon strains are highly resistant (>200 fold) to diamide insecticides and that both strains display cross resistance between flubendiamide and chlorantraniliprole. However, the Sudlon strain has higher resistance

ratios (RR) to both diamide compounds; it was speculated that this might be due to more than one resistance mechanism being present.

Table 16 Log-dose probit-mortality data for two diamide insecticides tested against 2nd/3rd instar larvae of *P. xylostella* in a leaf-dip bioassay (72h) as presented in [19].

| Compound | Strain | LC ₅₀ -value [mg/L ⁻¹] | 95% FL ^a | Slope (±SD) | RR ^b |
|----------------------------|--------|--|---------------------|----------------|-----------------|
| Chlorantraniliprole | HS | 0.048 | 0.026-0.15 | 1.3 ± 0.068 | - |
| | Sudlon | >200 | - | - | >4100 |
| | Thai S | 0.30 | 0.25 - 0.38 | 5.1 ± 0.83 | - |
| | Thai R | >60 | - | - | >200 |
| Flubendiamide | HS | 0.15 | 0.086-0.30 | 3.8 ± 0.30 | - |
| | Sudlon | >200 | - | - | >1300 |
| | Thai S | 0.08 | 0.06 - 0.11 | 3.8 ± 0.59 | - |
| | Thai R | >60 | - | - | >750 |

^aFiducial limits, ^bRR= resistance ratio, LC= lethal concentration (LC₅₀ of Sudlon or Thai R divided by LC₅₀ of HS or Thai S, respectively)

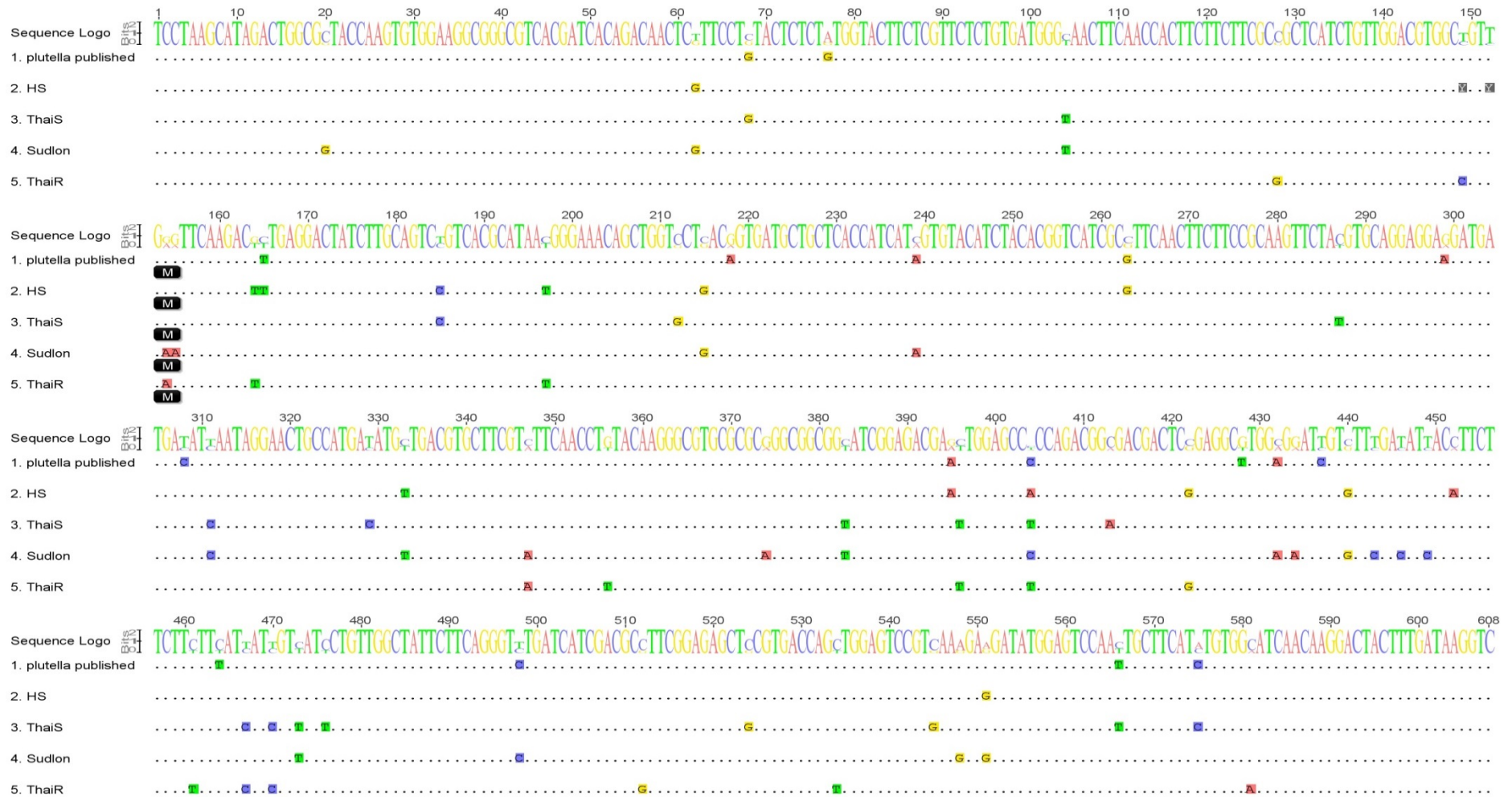
5.3.2 Sequencing of transmembrane region

PCR analysis of the field collected Thai strains was problematic, possibly due to poor storage conditions during transport from Thailand leading to some degradation of the RNA, so the cDNA synthesis was not of sufficient quality for subsequent PCR amplification of a single large fragment covering the entire TM region. It was therefore necessary to amplify the TM region in 4 fragments. In the case of the Sudlon and HS strains, the RNA isolated was of a higher quality; however the same 4 fragments were amplified by PCR in order to simplify the later data analysis by creation of multiple alignments of individual sets of fragments.

Direct sequencing of the 4 amplified fragments covering the entire TM region from both resistant and susceptible strains of *P. xylostella*, identified a mutation at position 14,837 of the cDNA predicted to cause a glycine (G) to glutamic acid (E) substitution at position 4946 (based on the first published *P.xylostella* RyR sequence [165]), or position 4900 in the cloned and expressed RyR described in this study. The mutation appears to be homozygous in all pools of individuals sequenced, for both the ThaiR and Sudlon strains. Interestingly, the nucleotide changes in the gene sequence giving rise to the G4946E substitution were different in the two resistant strains. Thus ThaiR has a single base change GGG to GAG (compared to ThaiS and Roth susceptible strains) and Sudlon potentially has an additional silent substitution GAA (Figure 33), with only the first base change being responsible for the amino

acid alteration. This finding, together with a different profile of silent SNPs (single nucleotide polymorphisms) for both resistant strains, suggests that the mutation has most likely evolved independently in both strains and has not been found at two geographically distinct locations as the result of insect migration. There are no susceptible field strains available from the region where the Sudlon strain originated, so we do not know if the susceptible population from which the resistant strain evolved carried a GGG or GGA coding triplet. In the two laboratory susceptible strains of *P. xylostella*, Roth and HS, only the GGG coding triplet was found. Once again, alignments of sequences from both Roth and HS strains showed a number of distinct silent SNPs, suggesting different geographical origins for the susceptible strains (Figure 33). Direct sequencing across the region harbouring the mutation, using as template PCR products amplified from genomic DNA extracted from at least 10 individual 3rd and 4th instar larvae, confirmed that the mutation is homozygous in ThaiR and Sudlon strains. In the susceptible Roth and HS strains, only the homozygous WT – GGG allele was found.

Chapter V



5.3.3 *In silico* characterization of the RyR G4946E substitution

The glycine to glutamic acid substitution, G4946E, which was found in diamide resistant *P. xylostella* populations, is located in a highly conserved region of the TM domain of RyRs. Amino acid alignments of RyRs (Chapter III, section 3.2.1) from different vertebrate and invertebrate species revealed that a glycine is present in most species at this position (Figure 34). More in-depth trawls of on-line databases indicated that only 6 species (to date) have a substitution of this glycine for a different amino acid. Two species, *Camponotus floridanus* (Florida carpenter ant) and *Daphnia pulex* (water flea) have an alanine at this position, and two crustaceans, *Litopenaeus vannamei* (Whiteleg shrimp) and *Homarus americanus* (Atlantic lobster) [19] along with two nematodes, *Caenorhabditis elegans* and *Brugia malayi*, have a serine substitution. Both alanine and serine are small uncharged amino acids, unlike the glutamic acid found in the resistant *P. xylostella*, and only one of them is found in the relevant position in an insect species. A BLAST search, using the highly conserved protein motif FFAAHLLDVAVE which contains the glutamic acid residue rather than glycine, returned no hits within NCBI [19].

The location of the amino acid change associated with resistance to diamide insecticides in *P. xylostella* is perhaps surprising, as the diamides chlorantraniliprole and flubendiamide are highly selective towards lepidopteran species and only a few amino acid residues within the TM region, localised distal to the immediate vicinity of the mutation, are exclusively found in Lepidoptera [170].

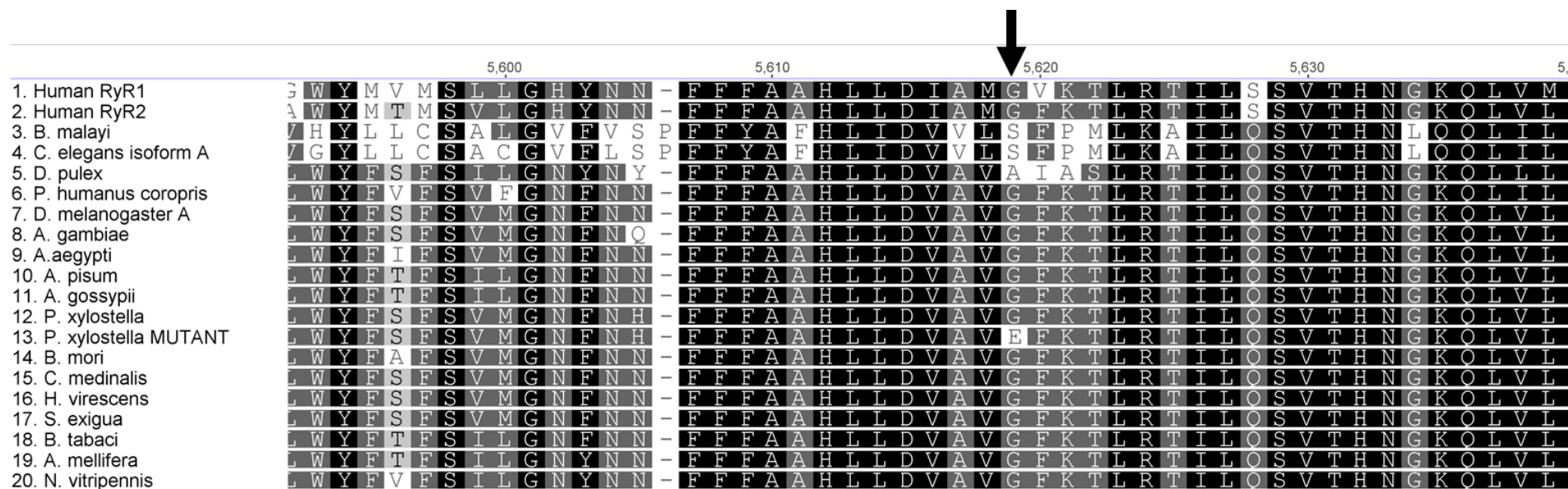


Figure 34 Amino acid alignments of the region of the RyR channel spanning the resistance-associated mutation G4946E (marked with an arrow). GenBank accession numbers for each sequence can be found in Chapter III section 3.2.1. For the purpose of clarity the alignment does not include the alternatively spliced isoforms and protein sequences available in the DuPont patent (US2007/0105098A1) and other mammalian RyRs. The glycine (G) residue is found in all species apart from nematodes and crustaceans.

Prediction of the topology of the TM domain in *P. xylostella* RyR, using a hidden Markov model approach as described in Krogh *et al.* [220], indicated the presence of 6 TM helices, in line with TM predictions for the human RyR2 channel [101] (Figure 35). The resistance-associated mutation G4946E was found to be localised close to the pore domain (in the primary structure), in the loop region between predicted TM2 and TM3 helices on the cytosolic side of the membrane (Figure 35). Since, insects have only one copy of the *RyR* gene, the RyR channel must be made-up of four identical subunits. The mutation appears to be homozygous in diamide resistant individuals, so we can presume that the substitution will be present in all four subunits that make up a single functional channel. Due to a lack of detailed 3D structure for the RyR TM region, it is difficult to speculate what the structural implications are for the substitution of a small side chain amino acid (Glycine) with a much larger polar one (Glutamic Acid) within the external cytoplasmic loop linking TM2 and TM3 helices. Mutational studies of the TM region of mammalian RyR isoforms revealed that modification of amino acids around the channel pore region usually leads to anomalies in channel function [200]. Additionally, a recent study of mammalian RyR1 gating, which introduced tryptophan substitutions at positions V4830 and T4840 (in rabbit RyR1) in close proximity (10-20 AA) to the resistance mutation site G4946, resulted in the channel being locked in either a permanently open or closed state when modifying H4832 and G4834, indicating the potential functional importance of this region in channel gating [110].

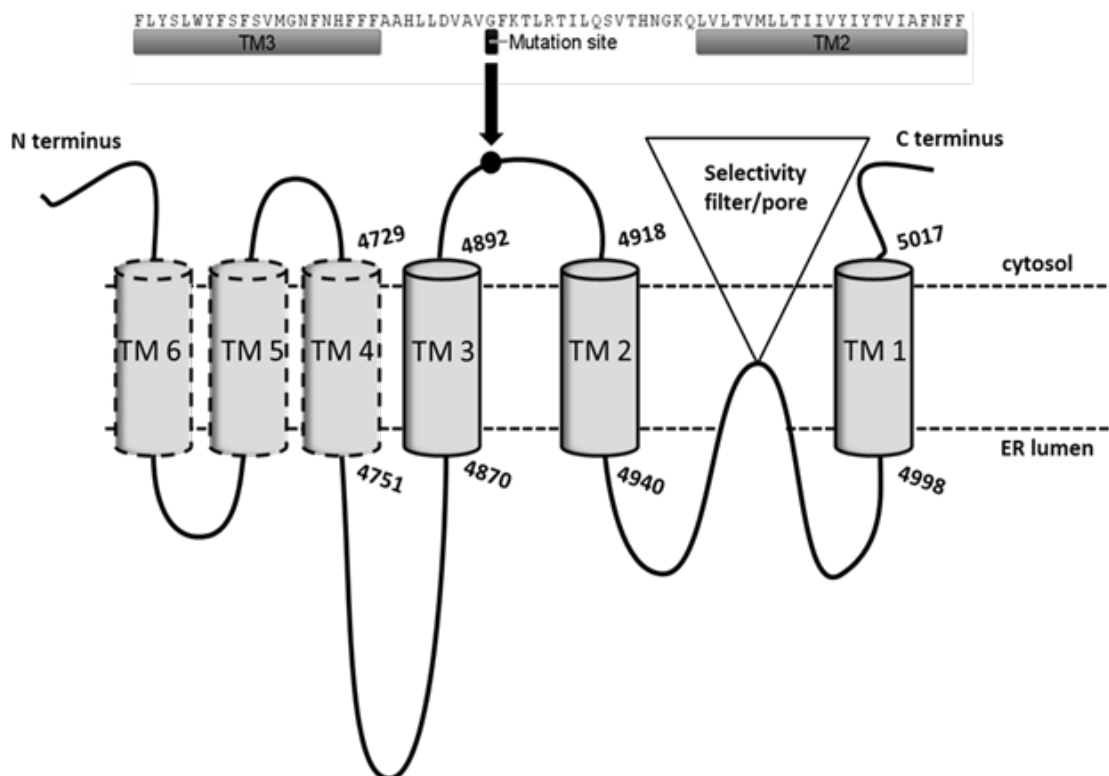


Figure 35 *P. xylostella* RyR TM domain topology map, predicted using a hidden Markov modelling approach [220]. Individual TMs are labelled as in the cryo-EM images of the pore and TM region of RyR1 [87]. The amino acid residues at each end of the helices are numbered according to the RyR cDNA sequence described in this study. The location of the resistance-associated mutation is indicated with an arrow.

5.3.4 *TaqMan* assay

A *TaqMan* assay was developed to allow for screening of individual insects for the presence of the resistance-associated mutation G4946E, and was initially done on genomic DNA from 15 individuals of the ThaiR and ThaiS strains. This mutation was found to be homozygous (n=30) in all ThaiR individuals. In the ThaiS strain, 13 individuals were homozygous for the WT allele (n=26) and 2 heterozygous for the resistance allele (n=2) (Figure 36).

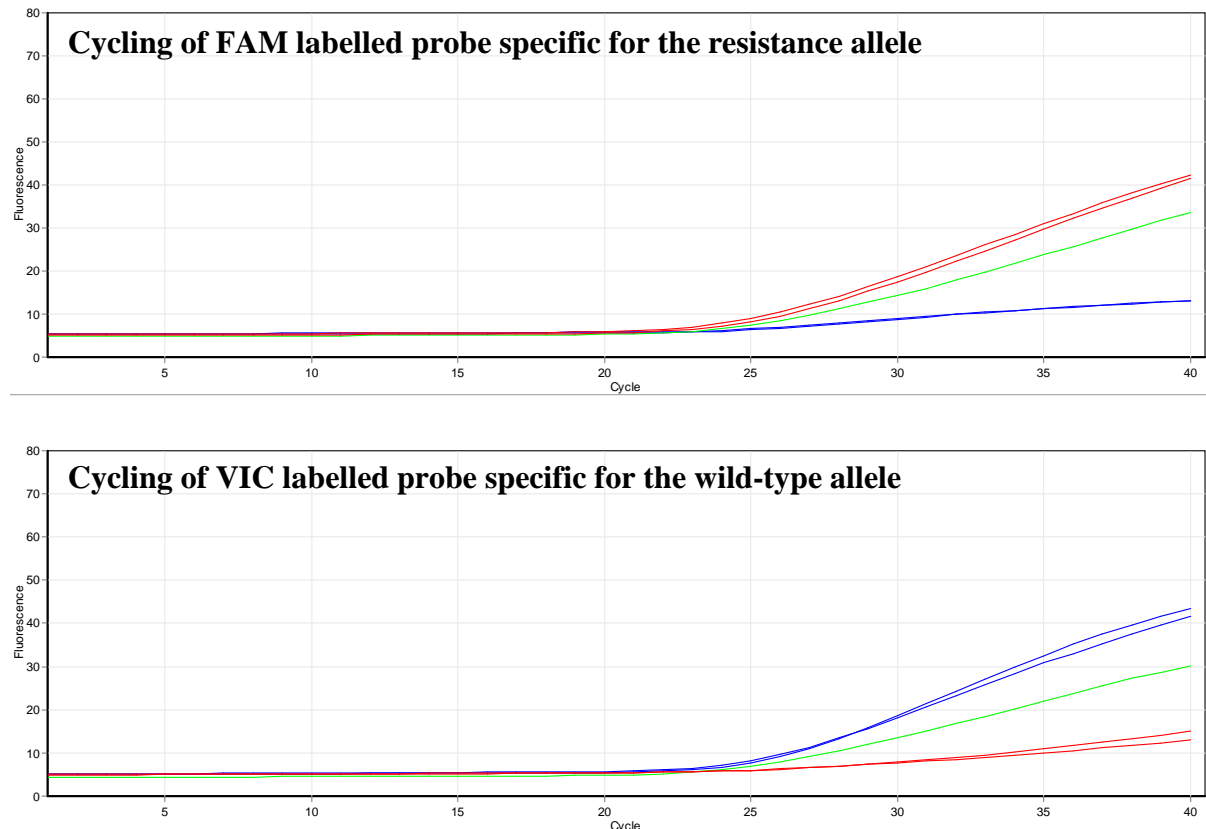


Figure 36 Representative *TaqMan* traces for the ThaiS strain showing the homozygous WT allele (blue), heterozygous resistant allele WT/resistant (green), and homozygous resistance allele (red).

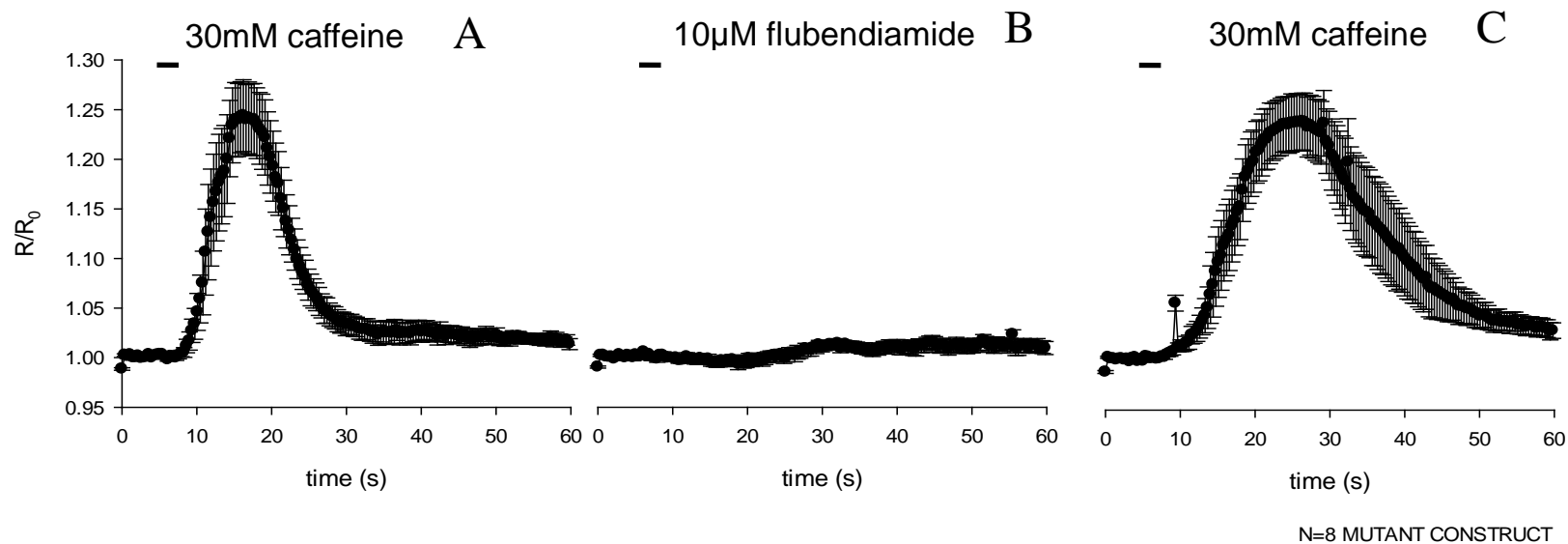
This indicated that the resistance allele is likely to be present in the susceptible ThaiS population at a low frequency (approximately 6.7% based on the number of samples tested). The assay was also used on 15 individuals of the Sudlon strain (before direct sequencing was done on these Sudlon samples) but these individuals scored very poorly, with many failed reactions (no fluorescence signal for either WT or resistance allele). It was later discovered (on direct sequencing of the samples) that silent SNPs in the Sudlon sequence, as well as a different coding triplet for the resistance mutation, were responsible for the *TaqMan* failure. It was concluded that the high number of silent SNPs present in different *P. xylostella* strains means that the *TaqMan* assay is not a viable tool for monitoring for resistance in field samples from diverse regions.

5.3.5 Expression of the *P. xylostella* RyR G4946E in Sf9 cells

Modification of the WT *P. xylostella* RyR cDNA to give an expression vector containing the resistance-associated mutation G4946E had no apparent effect on the stability of the pIZ plasmid, and large quantities of pure plasmid DNA were obtained using the methods described previously (Chapter II, section 2.8.4).

Insect (Sf9) cells expressing *P. xylostella* RyR G4946E cDNA incorporated in the pIZ vector were used for functional expression analyses. It was expected that the presence of the G4946E mutation would most likely have a significant effect on the biophysical properties of the channel, due to its location close to the channel pore [19]. Initial imaging experiments measuring the release of Ca^{2+} after exposure to 10mM or 30mM caffeine, showed multiple responses as expected for a functioning channel (Figure 6). However, no Ca^{2+} release was recorded in response to application of two diamides (10 μM flubendiamide or 30 μM diamide analogue) (Figure 6). These experiments indicate that the mutation has greatly reduced the ability of diamides to activate the modified channel, most likely by decreasing the binding affinity. As demonstrated in Chapter IV, the binding of flubendiamide to the WT channel expressed in Sf9 cells appears to be irreversible and abolishes any subsequent caffeine induced Ca^{2+} release. The ability of the Sf9 cells expressing the modified G4946E channel to respond to caffeine after exposure to flubendiamide supports the reduced binding affinity hypothesis.

There was no significant difference in the calcium signal amplitude of the response to caffeine for cells expressing WT or G4946E modified channels following 30mM caffeine induced Ca^{2+} release at different (72 or 96 hours) time points (Figure 6). However, a more detailed analysis is required, since the Ca^{2+} release assays were done without calibration of the Ca^{2+} indicator (Fura2 AM dye), therefore cytoplasmic Ca^{2+} concentrations could not be calculated.



Mean amplitude responses to 30mM caffeine

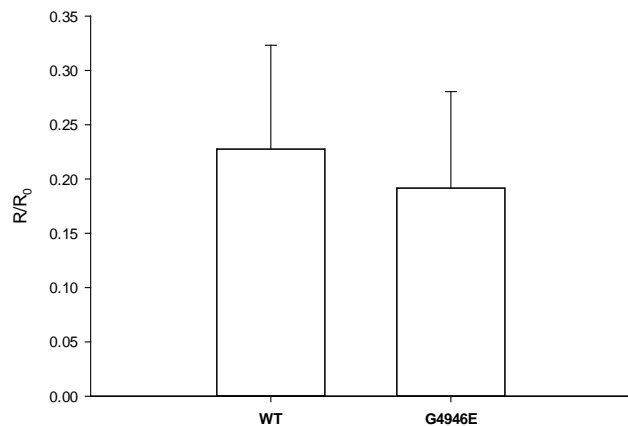


Figure 37 Normalized A340/A380 nm fluorescence intensity ratios measured for Sf9 cells expressing *P. xylostella* RyR G4946E in a single Ca²⁺ release experiment using FURA 2 AM. Panels A-C show mean \pm standard error responses of the same cells (n=8) 72h post transfection to **A** 30mM caffeine, **B** 10 μ M flubendiamide, **C** 30mM caffeine. Binding of flubendiamide appears to be abolished by the presence of the mutation.

Left: Bar chart showing that the average amplitude \pm SEM of responses to 30mM caffeine in Sf9 cells expressing WT and G4946E *P. xylostella* RyR remains the same. WT (n=30 cells), G4946E (n=30 cells). Data for G4946E RyR collected from 4 independent experiments.

An additional experiment using high concentration of chlorantraniliprole (100 μ M), which is a more water soluble diamide, indicated that it is possible to evoke Ca^{2+} release in cells expressing the G4946E channels whilst also abolishing further caffeine induced Ca^{2+} release (Figure 7), suggesting that the diamide binding is not completely abolished.

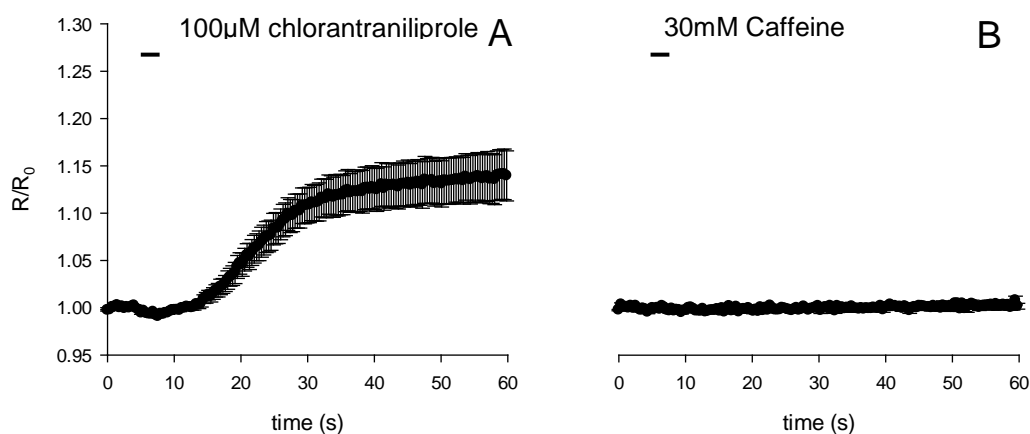


Figure 38 Normalized A340/A380 nm fluorescence intensity ratio measurements for Sf9 cells expressing *P. xylostella* RyR G4946E in a single Ca^{2+} release experiment using FURA2 AM, 96h post transfection. n=8 cells. **Panel A.** 100 μ M chlorantraniliprole, **Panel B.** 30mM caffeine after exposure to chlorantraniliprole. A high dose of chlorantraniliprole is able to induce a response in cells expressing the G4946E channel and abolish subsequent release of calcium by caffeine.

5.3.6 Ryanodine binding assay

Mixed-membrane preparations from Sf9 cells transfected with the G4946E construct were tested for their ability to bind [^3H] ryanodine. A saturation binding experiment was done to determine the kinetics of ryanodine binding, and the data compared to the results for the WT RyR (presented in Chapter IV, section 4.3.5.2). At least 3 replicates per data point were collected and, as found for WT membrane preparations, the specific binding was low (40%). However, the data obtained did allow a curve to be fitted (Figure 39) and determination of the K_d and B_{max} values for the binding of ryanodine. The K_d and B_{max} values were $14.69 \pm 4.18 \text{ nM}$ and $2671 \pm 401.1 \text{ dpn}$ ($267 \pm 40 \text{ fmol/mg}$) respectively, making them comparable to the WT channel ($12.89 \pm 4.5 \text{ nM}$ and $244.9 \pm 42.5 \text{ fmol/mg}$ respectively) and to previously

published K_d values for binding of ryanodine to *H. virescens* native membrane preparations ($13.9 \pm 3.8 \text{ nM}$) [29]. Although further optimisation of the binding assay protocol is required to reduce the non-specific background, it is clear that the presence of the G4946E mutation does not alter ryanodine binding affinity and kinetics in the diamide resistant *P. xylostella* RyR channel.

Binding of [^3H] ryanodine to MUT *P. xylostella* RyR channel

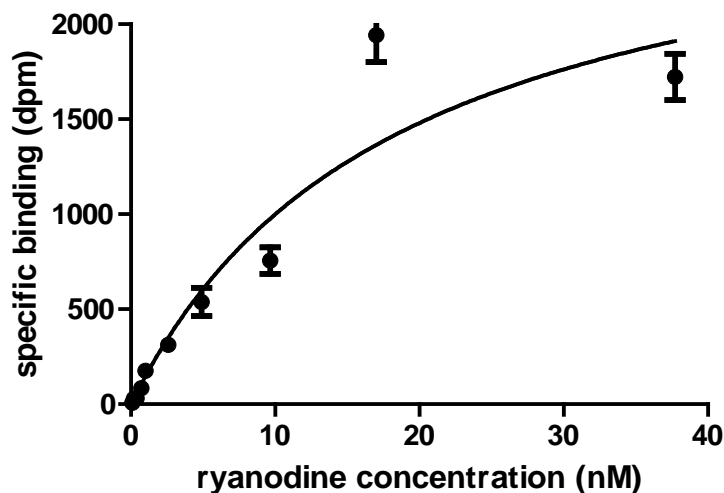


Figure 39 Saturation curve fitted to data obtained for the binding of ryanodine to *P. xylostella* RyR G4946E expressed in Sf9 cells. Each data point is a mean of 3 replicates \pm S.E.M .

5.4 General remarks

There were no apparent differences between Sf9 cells expressing the WT or G4946E RyR in terms of cell viability or RyR protein expression levels. The latter was difficult to assess directly as there was no fluorescent tag attached to the G4946E RyR channel, and no *P. xylostella* RyR specific antibodies are currently available. However, in calcium release experiments a similar number of cells were seen responding to the agonists per field of view, and the B_{\max} values obtained in ryanodine binding assays for the WT and G4946E channel were similar. This suggests that a comparable receptor density is present for both sets of cells.

The G4946E RyR channel responds to caffeine and binds ryanodine at comparable levels to the WT RyR, but does have a significantly lower sensitivity to diamide

insecticides. This is the first evidence at a molecular level that the presence of the G4946E mutation confers a high level of resistance to diamide insecticides in *P. xylostella*. More detailed experiments are however required to investigate if the G4946E mutation has any effects on the channels electrophysiological properties and whether the decreased sensitivity to diamide insecticides is the result of an allosteric effect or direct modification of the binding site.

Chapter VI: General Discussion

This chapter summarises the work done in this PhD. Suggestions and recommendations for future research- on this topic are also presented.

6.1 Identification, cloning and analysis of insect RyRs

The discovery and introduction of the diamide insecticides has led to an increased interest in insect RyRs as a target for the development of novel compounds for controlling insect pests. Since the beginning of this project a number of insect and other invertebrate RyR DNA and protein sequences have become available (see chapter III, section 3.2.1). Sequences of RyRs from economically important pests which are controlled by diamides, published on-line and in peer review journals, include the small white butterfly (*Pieris rapae*) [221], the brown planthopper (*Nilaparvata lugens*) [201], the rice leafroller (*Cnaphalocrocis medinalis*) [170] and the diamondback moth (*Plutella xylostella*) [165]. The latter was investigated by several groups, including in this study, resulting in several independent sequences being deposited in online databases. Additional sequence information from other species has come from DuPont patents associated with the discovery and marketing of chlorantraniliprole and cyantraniliprole [22, 187], and by annotation of insect genomes by International consortia and initiatives such as i5K (5000 insect genomes). To date, sequencing of 58 insect genomes has been completed and an additional 120 initiated (<http://www.arthropodgenomes.org/wiki/i5K>). During this study draft genome sequences became available for both of the species under investigation, *M. persicae* (<http://tools.genouest.org/tools/myzus/login>) and *P. xylostella* (<http://dbm.dna.affrc.go.jp/px/>) [222].

Before the commercial release of the diamide insecticides very few attempts were made to investigate insect RyRs, the most notable exceptions being the cloning and expression of the *D. melanogaster* RyR [163], *B. mori* [30] and an investigation of the C-terminus of the RyR of *H. virescens* [169]. These studies, together with information published subsequently and new sequence data available online, highlighted that insect RyRs are complex and diverse. Although all invertebrates studied to date have only one *RyR* gene (see Chapter I, section 1.5.1), there is considerable diversity in exon usage ranging between 26 (*D. melanogaster*) to over a hundred (106 - *A. pisum*) between different insect orders (Davies TGE, unpublished).

The RyRs in many insect species also appear to be polymorphic, with a number of alternative splice sites and SNPs (eg. in *Drosophila melanogaster*, *Heliothis virescens*). This was also found for the *P. xylostella* RyR investigated in this study, where a large number of SNPs were discovered together with 4 potential splice sites in the various cDNAs isolated (Chapter III, section 3.3.2). These findings were confirmed in an independent study which published the full coding sequence of the *P. xylostella* RyR [165]. Additionally, the *P. xylostella* RyR gene was found to be differentially expressed in different life stages and body parts of the moth [165, 188], and its expression modulated by exposure to sub-lethal doses of diamide insecticides [189]. Differential expression patterns of RyR mRNA were also found in *Nilaparvata lugens* and *Cnaphalocrocis medinalis* [170, 201]. In contrast, in the study reported here there were no significant changes in the expression of RyR mRNA in different life stages of *M. persicae* (Chapter III, section 3.3.1.1) and no splice sites or SNPs were found. It remains unclear why the fairly extensive RyR diversity found in other insects is not present in *M. persicae*, but it is possible that the lack of SNPs results from the asexual life cycle and clonal offspring. It is also unclear what the functional implications of differential splicing and modulated expression of insect RyRs are; it has been proposed that differential splicing introduces requisite functional diversity, as insects lack the specialised RyR isoforms found in mammals [168]. Interestingly, splicing of human RyR2 was shown experimentally to evoke different effects on cytosolic and nuclear Ca^{2+} signalling [195, 223]. Differential expression of RyR in some insects may be attributed to their biology, where the motionless egg and pupae do not require a high level of RyR protein [188]. Modification of RyR expression following exposure to diamides might be part of the insect defence mechanism, helping to protect the insect from the insecticide's toxic effects [189].

In the present study, two insect RyRs were successfully cloned and propagated in different plasmid and expression vectors. The main challenge was the initial amplification and assembly of the very large mRNA (approx. 15Kb). The size of the final vector constructs also made them difficult to modify directly using methods such as SDM. Both of the insect RyRs show a high degree of sequence similarity at the protein level, but with very different cDNA profiles, with the *P. xylostella* having

significant cDNA sequence variability (SNPs, splicing) and *M. persicae* in contrast being very conserved.

6.2 *In vitro* expression of insect RyRs

This study has reported the successful expression of the *P. xylostella* RyR in Sf9 cell lines (Chapter IV), but expression of the *M. persicae* RyR was not achieved. There is no obvious reason for this lack of expression of the aphid cDNA, since the aphid RyR sequence is very similar (almost 80% at the protein level) to that of *P. xylostella* and other successfully expressed insect RyRs (*B. mori*, *D. melanogaster* [30, 163]) and there are no obvious amino acid sequence differences in the highly conserved regions of the channel such as the transmembrane helices and pore forming region that could impair functional expression. However, RyRs are complex proteins, with many accessory proteins involved in their modulation (see Chapter I, section 1.4.1); it is possible that the cell lines tested in this study lack essential components needed for successful expression of the aphid RyR. Alternatively there may be codon usage issues that could impair successful expression of the aphid cDNA in the cell lines.

During this study it became clear that although mammalian cell lines have been used to express insect RyRs, they are not best suited for the expression of the *P. xylostella* channel. Expression of this channel was much more robust in an insect derived Sf9 cell line. The expressed *P. xylostella* RyR was shown to be sensitive to caffeine and flubendiamide in Ca^{2+} release assays, as was seen for the *B. mori* RyR expressed in HEK293 cells [30]. However, a more detailed comparison between the two systems was not possible due to the exclusion of quantification of Ca^{2+} concentration in the experiments presented in this study.

The results presented here (Chapter IV, section 4.3.5.2) also indicated that, as expected, the WT *P. xylostella* RyR is able to bind labelled ryanodine with a K_d value of $\approx 14\text{nM}$, comparable to that obtained with native channels from *H. virescens* [29] but approximately 3 times higher than that obtained with native rabbit RyR1 ($\approx 3.4\text{nM}$) [176]. This is in contrast to another study which showed that the ryanodine binding affinity of insect and mammalian RyRs is similar, with values ranging between 4.4-5.6nM for *M. domestica*, *P. americana* and mouse RyR1 [224]. This may be because in the present study the binding conditions for the *P. xylostella* RyR membrane preparation was not optimised and this resulted in low specific

binding. The differences might be also due to species-specific differences in [³H] ryanodine binding as reported for *Homarus americanus* (American lobster), *M. domestica*, *A. mellifera*, *H. virescens* and *Agrotis ipsilon* (black cutworm) [225]. The results of the ryanodine binding assays with *P. xylostella* RyR indicate that the receptor density in the Sf9 expression system is sufficient to carry out binding assays, and this was consistently repeatable across independent transfection experiments. Binding of [³H] flubendiamide to Sf9 mixed-membrane preparations was not determined due to the compound's low water solubility.

In summary, the data presented in Chapter IV shows that a good level of expression of one of the tested insect RyRs was achieved, giving a solid foundation for future optimisation of the system and a more detailed study of insect RyRs.

6.3 Emergence of resistance to diamides, identification of the diamide binding site and implications for resistance management

The results presented in Chapter V identified the first reported mutation (G4946E) in the *RyR* gene associated with a high level of resistance to both classes of diamide insecticides in *P. xylostella*. This work was published in 2012 [19]. A more detailed functional characterization of this mutation, by functional expression of modified RyRs in Sf9 cells (Chapter V, section 5.3.5), indicated a direct effect of the G4946E substitution on the channel's sensitivity to diamides, thereby confirming the involvement of the mutation in the observed resistance phenotype. Data collected from Ca²⁺ release experiments with Sf9 cells expressing G4946E RyR demonstrated a lack of channel activation at high doses (10-30µM) of flubendiamide whereas a normal sensitivity to caffeine was retained. The Ca²⁺ activation effect of diamides was observable at a very high dose of chlorantraniliprole (100µM), indicating that the *P. xylostella* RyR mutation decreases diamide binding affinity rather than totally abolishing it. This has recently been confirmed by a study showing a ≈2.5 fold shift in K_d for native membranes of *P. xylostella* with the G4946E RyR mutation, using labelled chlorantraniliprole in fluorescent polarization binding assays [226]. A complex picture of diamide binding comes from recent displacement studies using radiolabelled chlorantraniliprole and flubendiamide and native *M. domestica* RyRs, where it appeared that three distinct binding sites were present for flubendiamide, chlorantraniliprole and ryanodine respectively [28]. In a follow-up study it was

shown that the diamide binding sites in insect RyRs are likely to be species specific, with *H. virescens* and *A. ipsilon* having a single binding site for both classes of diamides and *A. mellifera* having low chlorantraniliprole binding and no flubendiamide binding. The mammalian (rabbit RyR1) and crustacean (*H. americanus*) RyRs showed no diamide binding, as expected [225].

Despite a range of studies, the location of the diamide binding site on the insect RyR remains elusive. Initial results from *B. mori* RyR, using a series of deletion mutants, narrowed it down to the TM region (amino acids 4111-5084) of the protein [30]. A recent study, using *D. melanogaster* / plant parasitic nematode (*Meloidogyne incognita*) chimeras, identified a small (45 amino acids) area within the TM region (between highly divergent residues 4610-4655) as essential for diamide binding. [227]. However, there is no clear evidence that these 45 amino acids, present between TM5 and TM6, form the actual binding site for the diamides or whether they have an allosteric effect. The G4946E mutation identified in the present study is located outside of the region identified in the chimeric *D. melanogaster* / *M. incognita* RyR, and much closer to the pore region. One of the possible explanations is that G4946E and the 45 residues form part of the binding pocket, when assembled into the functional channel but without the 3D structure of the RyR TM region or a homology model this hypothesis cannot be tested. However, mapping the location of the mutation and the chimeric region on to TM topology model (shown in Chapter V) places them on the opposite sides of the ER membrane, with the chimeric region facing the luminal side. Unlike in most insects and mammals, in nematodes such as *M. incognita* glycine 4946 is substituted with a serine; additionally adjacent amino acids are also different (see Figure 33, Chapter 5), which could be one of the contributing factors explaining the poor nematicidal properties of diamides [227].

The emergence of high level resistance to diamides in *P. xylostella* soon after their introduction for the control of Lepidopteran pests emphasises the importance of establishing good agronomic practices and integrated pest management as part of the overall pest control strategy. It is well established that over reliance on a single compound leads to a high selection pressure and the emergence of resistance. For the diamides a global integrated effort from companies marketing these compounds is currently underway to minimize and manage the spread of resistance and to monitor product efficacy in the field [228].

6.4 Future work

Overall, the results presented in this study provide a good foundation for further characterization of insect ryanodine receptors.

Potential areas for study are:

- The experiments presented in Chapters III, IV and V show that expression of the WT and G4946E *P. xylostella* RyR constructs in insect cells is at sufficient levels to allow more detailed receptor characterization to be made. It was also noted that the Sf9 cells were able to divide while expressing the *P. xylostella* RyR and that they did not suffer the severe cytotoxic effect usually associated with unregulated expression of RyRs. Since the pIZ/V5-His expression vector is suitable for the isolation of stable cell lines, an attempt should be made to isolate cells stably expressing both WT and G4946E *P. xylostella* RyR. This would eliminate the variability in protein expression associated with individual transient transfection experiments.
- In this study only a basic characterization of both WT and G4946E *P. xylostella* RyRs was possible. A more detailed study is now required involving (i) quantification of the released Ca^{2+} in the calcium release experiments and (ii) dose response measurements for caffeine and other known agonists, to identify more subtle differences between WT and G4946E channels.
- The decent level of receptor density in isolated Sf9 membranes, which has allowed the radio ligand binding assays with [^3H] ryanodine and the detection in artificial bilayers of ‘ryanodine-like’ channels (in mixed-membrane preparations), suggests that more in-depth electrophysiological experiments are possible. Purification of the expressed *P. xylostella* RyR from Sf9 cells should be attempted to determine the electrophysiological properties of the insect channels and compare them to their mammalian counterparts. The effects of diamide insecticides and other well-known agonists (such as caffeine, ryanodine) on single channel gating could also be investigated, bridging the knowledge gap between invertebrate and mammalian RyRs

- The identification and characterization of the target site mutation G4946E, conferring resistance to diamide insecticides in *P. xylostella*, will allow monitoring of resistance proliferation in field populations and could help in the identification and analysis of diamide resistant strains that may appear in other high risk insect species. e.g. *Spodoptera exigua* and *Tuta absoluta*. There is already confirmed resistance to diamide insecticides in the leafminer (*Liomyza trifolli*) in the USA and control failures in other Lepidoptera including beet armyworm (*Spodoptera exigua*) in Indonesia, rice stem borer in Malaysia and shoot borers in India and the Phillipines (source: IRAC diamide resistance group)
- Modification of the WT *P. xylostella* RyR by site-directed mutagenesis and analysis of different splice forms using the established expression system will allow the identification of structurally important parts of the channel. Analysis of single channels will identify dissimilarities between insect and mammalian RyRs and could help in understanding the specificity of diamide binding.
- The Sf9 expression system could also be used to investigate insect RyR accessory proteins identified (by their homology to known mammalian accessory proteins) from available online genomic resources e.g. KONAGAbase. This will give information on which components are important in the RyR macromolecular complex in invertebrates. In turn this could lead to the identification of novel targets for insecticidal chemistry.
- A well-established expression system for the *P. xylostella* RyR could be used in cellular screening assays for the discovery of novel compounds targeting RyRs (potential novel insecticides).

Appendix A: Media and buffers recipes

1. Bacterial media recipes

SOC medium (per 1 litre)

| | |
|----------------------------|----------|
| Tryptone | 10g |
| Yeast Extract | 5g |
| NaCl | 0.5g |
| 250mM KCl | 10ml |
| Distilled H ₂ O | up to 1L |

Autoclave at 15 psi, 121-124°C for 15 minutes, then add 5ml of sterile 2M MgCl₂ and 20ml of sterile 1M glucose.

LB (Luria - Bertani) medium and agar (per 1 litre)

| | |
|------------------------------|-----------|
| Tryptone | 10g |
| Yeast Extract | 5g |
| NaCl | 10g |
| pH adjusted to 7.0 with NaOH | |
| distilled H ₂ O | up to 1 L |

Autoclave at 15 psi, 121-124°C for 15 minutes.

To make LB agar add 15g of Bacto-agar before autoclaving.

References

2. Calcium phosphate transfection solutions

2x HEPES (500ml)

| | |
|---|-----------------|
| NaCl (280mM) | 8.18g |
| KCl (10 mM) | 0.373g |
| Na ₂ HPO ₄ x7H ₂ O(1.5 – 1.8 mM) | 0.201 g -0.241g |
| Glucose (12mM) | 1.08 g |
| HEPES (50mM) | 5.96 g |

pH 6.95 – 7.05

Make up to a final volume of 500 ml with DIW

Solution filtered through a 0.2µm sterile filter and stored at RT in a sterile sealed 50ml tube.

3. Hypo-osmotic buffer (per 1 litre)

| | |
|-------------------------------------|-------|
| Tris (20 mM) | 2.42g |
| EDTA (1 mM) | 0.29g |
| H ₂ O (double distilled) | 900ml |

pH to 7.4 with HCl and top up to 1l with double distilled H₂O. Before use add 1 protease inhibitor (EDTA free) tablet per 50ml of buffer.

4. Western blots gel/buffers

Resolving gel 5% (20ml):

| | |
|----------------------|---------|
| DIW water | 12.16ml |
| 40% (w/v) Acrylamide | 2.5ml |
| 1.5M Tris pH 8.8 | 5ml |
| 10% (w/v) SDS | 160µl |
| 10% (v/v)APS | 160µl |
| TEMED | 20µl |

References

Stacking gel (6.675ml):

| | |
|----------------------|--------|
| DIW water | 4.73ml |
| 40% (w/v) Acrylamide | 583µl |
| 0.5M Tris pH 6.8 | 1.25ml |
| 10% (w/v) SDS | 50µl |
| 10% (v/v) APS | 50µl |
| TEMED | 8.3µl |

TBS-T(Tris buffered saline (TBS) x1 (per 1 litre):

| | |
|-------------------------------------|-------|
| Tris (20 mM) | 2.42g |
| NaCl (137 mM) | 7.99g |
| 0.1% (v/v) Tween-20 | |
| H ₂ O (double distilled) | 900ml |

pH to 7.6 with HCl and adjust volume to 1l with double distilled H₂O

5. [³H] Ryanodine binding assay buffers

5.1 Filter disc assay binding buffer (per 1litre)

| | |
|-------------------------------------|--------|
| KCl (1M) | 74.55g |
| PIPES (25mM) | 7.56g |
| 1M CaCl ₂ (100 µM) | 100µl |
| H ₂ O (double distilled) | 900ml |

pH to 7.4 with KOH and adjust volume to 1l with double distilled H₂O

References

5.2 96 well filter plate assay buffers

Buffer A (per 250ml)

| | |
|-------------------------------------|---------|
| Tris (20mM) | 0.606 g |
| Sucrose (0.3M) | 25.67g |
| DTT (1mM) | 0.0385g |
| BSA (0.8%) | 2g |
| H ₂ O (double distilled) | 200ml |

pH to 7.4 with HCl and adjust volume to 250ml with double distilled H₂O

Buffer B (per 1 litre)

| | |
|---|---------|
| HEPES (10mM) | 2.383g |
| CaCl ₂ x2H ₂ O (1.38mM) | 0.203g |
| ATP (10mM) | 5.511g |
| KCl (1.5M) | 111,83g |
| H ₂ O (double distilled) | 900ml |

pH to 7.4 with KOH and adjust volume to 1 litre with double distilled H₂O

Wash buffer (per 1 litre)

| | |
|-------------------------------------|--------|
| HEPES (10mM) | 2.383g |
| KCl (150mM) | 11.18g |
| H ₂ O (double distilled) | 900ml |

pH to 7.4 with KOH and adjust volume to 1 litre with double distilled H₂O

References

6. Solubilisation and gradient buffers

Solubilisation buffer (per 250ml)

| | |
|--|----------|
| NaCl (final conc. 1M) | 14.61g |
| 1M CaCl ₂ (final conc. 0.15 mM) | 0.0375ml |
| EGTA (final conc. 0.1 mM) | 0.0095g |
| NaPIPES (final conc. 25 mM) | 1.89g |

pH to 7.4 with NaOH and adjust volume to 250ml with double distilled water. Add 1 (EDTA free) protease inhibitor tablet per 20ml.

Gradient buffer (per 100ml)

| | |
|-------------------------------------|---------|
| 2.5 M NaCl | 11.96ml |
| 1 M/ 2M Tris/HEPES | 2.49ml |
| 0.1 M EGTA | 300µl |
| 1 M CaCl ₂ | 10µl |
| 10 % (w/v) CHAPS/PC | 3ml |
| H ₂ O (double distilled) | 82.24ml |

Add 1 EDTA free protease inhibitor tablet per 25ml

7. Electrophoresis buffers

TAE x 50 agarose gel electrophoresis buffer (per 500ml)

| | |
|-------------|--------|
| Tris base | 121g |
| Acetic acid | 28.5ml |
| EDTA 0.5M | 50ml |

Adjust pH to 7.4 with acetic acid. Make up to 500 ml with DIW water.

To make 1x TAE buffer, take 20 ml of 50X stock and dilute to 1 litre with double distilled H₂O.

8. Calcium imaging solutions

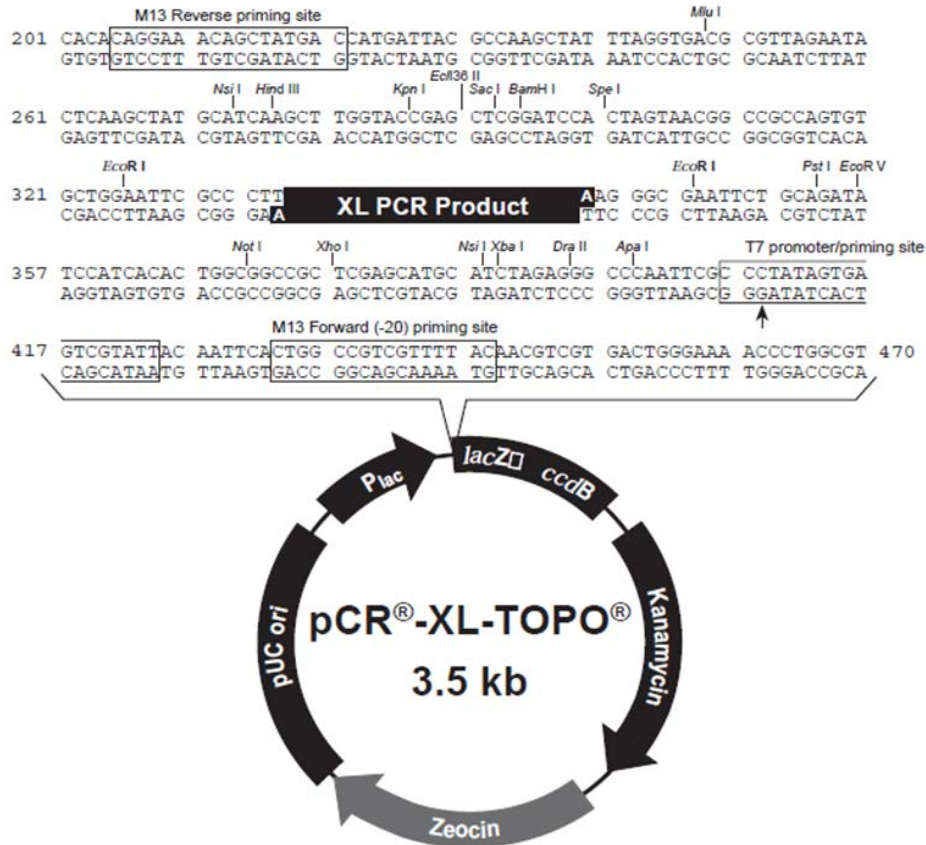
Standard Ringer's solution (per 1l)

| | |
|-------------------------------------|-------|
| 150mM NaCl | 8.76g |
| 4mM KCl | 0.29g |
| 2mM MgCl ₂ | 0.19g |
| 2mM CaCl ₂ | 0.22g |
| 10mM HEPES | 2.38g |
| H ₂ O (double distilled) | 900ml |

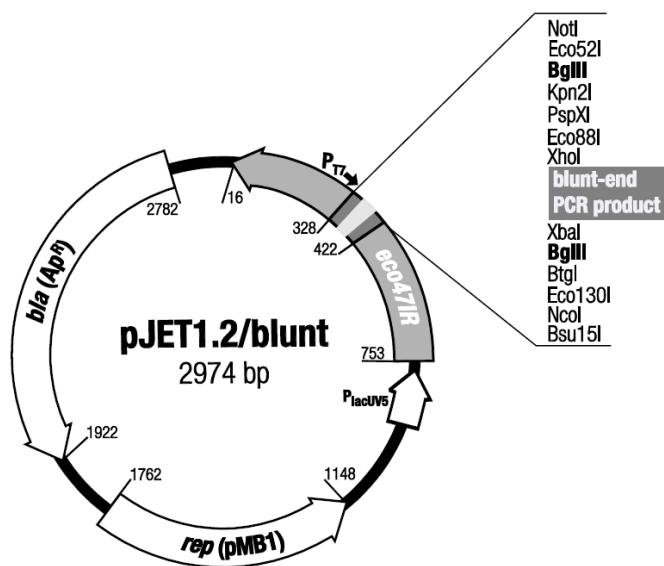
pH to 3 (with NaOH) and adjust volume to 1 litre with double distilled H₂O. Pass through a 0.22µm filter to sterilize.

Appendix B: Vector maps

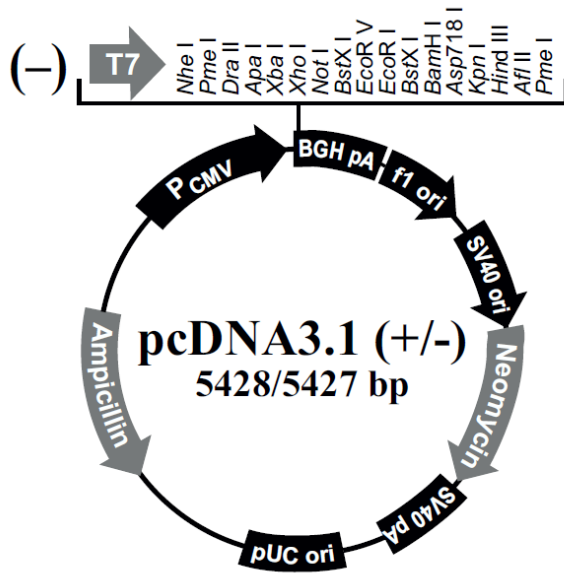
1. pCR-XL-TOPO



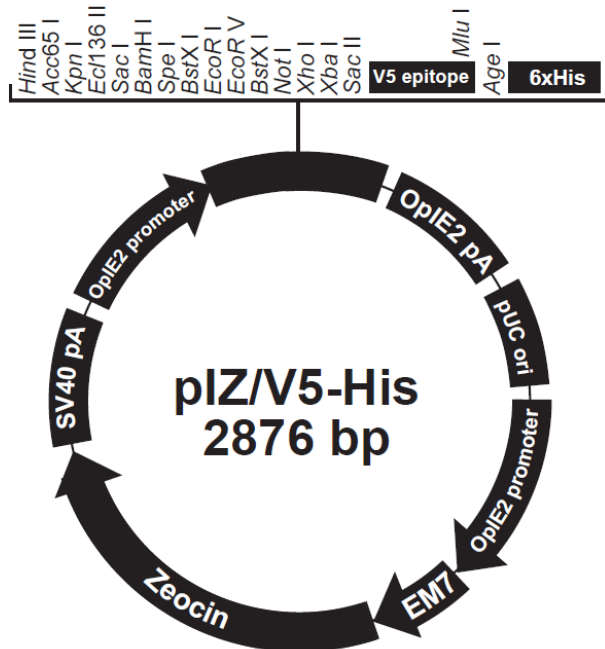
2. pJET1.2



3. pcDNA3.1(-)



4. pIZ/V5-His



Appendix C: Primer sequences

1. Vector and eGFP tag specific primers

| Vector/tag | Primer name | Sequence 5'-3' | Description |
|----------------------|---------------------|--------------------------------------|----------------------------------|
| pCR-XL-TOPO | M13(-20) F | GTAAAACGACGGCCAGT | |
| | M13(-24) R | AACAGCTATGACCATG | |
| pJET1.2 blunt | pJET 1.2 F | C GACTCACTATAGGGAGAGCGGC | Sequencing |
| | pJET 1.2 R | AAGAACATCGATTTTCCATGGCAG | |
| pcDNA3.1 | T7 universal primer | TAATACGACTCACTATAGGG | |
| | BGH R | TAGAAGGCACAGTCGAGG | |
| | pcDNA-CMV F | GGCCAGATATACGCGTTGACATTG | Promoter amplification |
| | pcDNA-CMV R | CAGCTCTGCTTATATAGACCTCCCA | |
| pIZ/V5-His | pIZ/His-NruI | CCCTCTCCTCGGTCGCGATTCTACGCG | Mutagenesis primers (NruI) |
| | SDM-F | TACC | |
| | pIZ/His-NruI | GGTACGCGTAGAATCGCGACCGAGGA | |
| | SDM-R | GAGGG | |
| | Piz-gfp-stop-R | CTAGACTCGAGCGGCCTATCTTGTACA GCTCG | Mutagenesis for pIZ eGFP control |
| | Piz-gfp-stop-F | CGAGCTGTACAAGATAGGCCGCTCGA GTCTAG | |
| GFP tag | eGFP -F | GGTAGGCGTGTACGGTGGGAGG | GFP cloning cassette |
| | eGFP -R | GCGGCCGCTCTTGTACAGCTCGTCCAT GCC | |
| | GFPseq-F | GGCATCAAGGTGAACTTCAAGATCCG C | GFP sequencing |
| | GFPseq-R | CCGGTGGTGCAGATGAACTTCAGG | |
| | eGFP-EcoRI -F | GAATTCAAAATGGTGAGCAAGGGCGA GG | GFP pIZ cassette |

2. *M. persicae* RyR sequencing primers

| Cloning fragment | Primer name | Sequence 5'-3' |
|------------------|---------------------|----------------------------|
| N6Kb | N1-F ^{1,2} | GGAACAGGACGATGTCTCGTTTCTC |
| | N3-R ² | GGTATTGTCAAACACTCGTCGCCG |
| | N6F SEQ1 | GGCGACGAGTGTTTGACAATACCG |
| | N6F SEQ2 | CATGTAAGTGGATCTGCTGTTTATAG |
| | N6F SEQ3 | CGAGGTTATTCAGATGATCCTGTTG |
| | N6R SEQ4 | GCCCACTGATGTGGTCTTAAACATTG |
| | N6R SEQ5 | GGGAACATGTGAACCTGGCCC |
| | N6R SEQ6 | GTGATAATGTTAACTTTATCAATGGC |
| | Mz.N3f | TACCAGCTGGTTCAGATACACCACC |

References

| | | |
|------------------|----------------------|-------------------------------|
| | Mz.N1r | ATGCGGGACGGTGGATTATCAATAG |
| | Mz.N2r | GGTACAAATCCTTCTCCTTGGACTTC |
| | Mz.N4r | GCACTAACACTGTGCTGTCACCATAC |
| | Mz.N5r | GCCCACATTTTCGTGAATATTCTCTGC |
| | N6F SEQ7 | GCGTGCTCACGGGTCCATGG |
| | N4KbR 2 | CATGCCTCGATAATGACCCCTTTCGTG |
| | N2KbR 2 ¹ | GCCCATCCAATGCGAATGTGCGGAT |
| | N6F SEQ8 | CCAAATAAGAGTTTCACAAATGG |
| N6Kb/LNK1 | Mz.NL1f | TAGAGTCCCATGCCACAACAATGGAGG |
| | Mz.L1r | GAAGCTCCGTATATTCTTGACCTCC |
| | Mz.L1F-1 | GAGTTCCGATGTCCACCTCGAGAAC |
| LNK1 | LNK1 seq1R | GCATTTGGCTAGTTAATGCCACC |
| | LNK1 seq3F | GGAAGGAGAGCTCAAGCCCAATCAC |
| | Mz.L1F-2 | TACGCAGGCCTGAATGTTTGG |
| | Mz.L2r | CGTTTCAAGAGTGGGCATAGTGCCTTCC |
| | Mz.L2F-3 | GGGTACATTTAGCAGGCGTTCTAG |
| | Mz.L2F-2 | CCATTCTTACCAGTTGCGGAACGAG |
| LNK2 | LNK2 seq3F | GGTCGCTAGTTTATTTTGTAAAGTTAGC |
| | L2 seq1R | CGTAACCAGTGATTGCGTTGAAG |
| | L2 seq2F | CTGCGCCCAAGACACTTGAAGC |
| LNK2/C4Kb | Mz.LC1f | CAAGCATCATTGATGGTTGCTTGTC |
| | Mz.C4f | GCCAACCGTGGTGTGCGCAGAAATGG |
| | Mz.C4r | GTCAATTAGCTCTTTGCTCGAATAATGCC |
| | C1-F ² | GCTGGGGTCACAATCACAGACAACG |
| | C1-R ^{1,2} | CGGAAACAGTCTCCCACTGGGAAGA |
| | C4F SEQ1 | CGGAGGGTTTAGGAGTAGGATCGG |
| | C4F SEQ2 | GTTGACTAACCTATCAGAACACATGC |
| C4Kb | C4R SEQ3 | GTTGCATGAGAATACGAGATATATACC |
| | C4F SEQ4 | CGCATAACGACACCGTGCATTGAG |
| | C4R SEQ5 | CAAGAGCAAGACGGTCAATAACCAGC |
| | C4F SEQ6 | CCCAACAATGATGGTTGGGTACATCC |
| | C3KbF 2 | GACACAAGCAGGAAATACCACGACTGT |
| | C2KbF 2 ¹ | CCCATTCTGAAGAGGTATACAGGCCA |

¹Used in colony PCRs, ²Primers found in DuPont patent

3. *M. persicae* RyR mutagenesis and cloning cassette primers

| Primer name | Sequence 5'-3' | Description |
|---------------------|--|-----------------------------------|
| Mz.Afe-SDM-F | GTGTTTTTGTTCATTGAACAAGCGCTATCTGTGAGGG CTTTACAAG | Introduction of AfeI site |
| Mz.Afe-SDM-R | CCCTCACAGATAGCGCTTGTTCATGACAAAAACAC ACTG | |
| Mz.N12-F | TCAGCAAGATACGATGGCCGACAGCGAGG | Removal of additional START codon |
| Mz.N12-R | GCTGTGCGGCCATCGTATCTTGCTGAAAAACTC | |
| Mz.Eco-F | GCCAGAAGATTAGAGTTCGACGGCCTCTACATTG | Removal of EcoRI site |
| Mz.Eco-R | GAGGCCGTCGAACTCTAATCTTCTGGCAATTTTC | |

References

| | | |
|--------------------|--|----------------------------------|
| Mz.mutdel-F | GATGTAATTTTGCCGGTTTTGTCATCACTTTTTGATG ATTTAGC | Removal of PCR error |
| Mz.mutdel-R | GCTAAATCATCAAAAAGTGATGACAAAACCGGCAA AATTACATC | |
| Mz.Kozak1-F | TCAGCAAGATACCATGGCCGACAGCGAGGGC | Introduction of Kozak seq. |
| Mz.Kozak1-R | GCCCTCGCTGTTCGGCCATGGTATCTTGCTGAAAAAC TC | |
| Mz.NotI-F | CAGCGGCCGCATGGCCGACAGCGAGGGCAGTTCG | Amplification of Afe cassette |
| Mz.AfeI-R | CACAGATAGCGCTTGTTCATGACA | |

4. *P. xylostella* RyR sequencing primers

| Cloning fragment | Primer name | Sequence 5'-3' | Description |
|---------------------|-------------------------------|-----------------------------------|----------------------------|
| N7Kb | Px.N1f | GCGACGTGTTGCGTTTCTTCCACG G | Amplification primers |
| | Px.M1R | CAGCAGCCGGATCACCAGGTTCG C | |
| | Px.Nseq3R | CCATCACGTTCTCGTGGACGCGGA GG | Sequencing primers |
| | Px.Nseq1f | GGACCTCATCAACTACTTCGCGCA GC | |
| | Px.N3f | TGGCTACGTCCCATAACCCAGGG | |
| | Px.N3rB | GGTCCGACTGTTTGATCTCTACGT AAC | |
| | Px.N4R | CCATGGTGGTGGCGTGCGACTCTA GATGC | |
| | Px.N-4Fa | GGCTGGATGTACGGCGAGCATCG | |
| | Px.N-4Fb | GGCAACGGAGTGGGCGACGATC | |
| | Px.N-5R ¹ | CCGTGGAACCTTCGACCGGCACT | |
| Px.N-5Fa | GAACAGCTCCGAGTCGTTCGGC | | |
| Px.N-5Fb | CTCCGGCAAGTGGTACTTTCGAG | | |
| Px.N2f ¹ | GGTGTGCCTGTCCTGCACGGCCAC G | | |
| N7Kb/M2 | Px.M2-seq1f | GCTGTGCGGCCATCTTTAAGAGG | Additional seq. primers |
| | Px.M2-seq2r | TCGTTGTTTAGAGCCACTGAAGAC G | |
| C7Kb | Px.M1f | GAACCTGGTGATCCGGCTGCTGAT CC | Amplification primers |
| | P.C2 R | GCTCCGCAATGTACAGACCGTCA AACTC | |
| | Px.Cterm-seq1F | GGCTTCTGCGACCGCTTCCACGAG | Sequencing primers |
| | Px.Cterm-seq2F | GACGGAGGCAGCGGTGAAGAAGA CG | |
| | Px.Cterm-seq3F | CCGTCGGGCTGAACCTGTTCGC | |
| | Px.Cterm-seq4F | CCGACGTCCGCATCACAGTCCG | |

References

| | | | |
|----------------------|-------------|----------------------------------|------------------------------|
| | Px.Mseq1F | CGAATGTTAACCAAGGGTCAACG TG | |
| | Px.Cseq2R | CGAAGCCGACACCGCCATCTGC | |
| | Px.Cseq-5F | TGGACGAGATCCAAGTGGCGTCG | |
| | Px.Cseq-3f | CGAGTGCTTGGACAGCTTGTCTG C | |
| | Px.Mseq2F | GTCGAGCACTCTGAAGTGGACAT CC | |
| | Px.Mseq3f | CTCGACTCATCGAACTACTTCATA GC | |
| | Px.Cseq5r | GGTCGCAGAAGCCGATGTAGTCC | |
| | Px.C5r | CTTGTCTTTGAGATGATTCAGCAT ACCC | |
| | Px.C5f | CCGTTGGCTGAGAGGGTCAGG | |
| G4946E region | Plut.Mut1-F | CCTGTACTCTCTGTGGTACTTCTC G | Amplification/ Sequencing |

5. *P. xylostella* mutagenesis and modification primers

| Cloning fragment | Primer name | Sequence 5'-3' | Description | |
|------------------|----------------|---------------------------------------|------------------------------------|----------------------------|
| Nterm | Px.mut (T-S) F | CCTGAAGGATACTCGCCGCTAGTCGAG | Correction of potential PCR errors | |
| | Px.mut(T-S) R | CTCGACTAGCGGCGAGTATCCTTCAGG | | |
| M2 | Px.mut(H-Y) F | CCAGACAACCCTCAGTACAACCCACA ACCCATC | | |
| | Px.Mut(H-Y) R | GATGGGTTGTGGGTTGTA CTGCTGG | | |
| Cterm | Px.mut(I-M) F | CTTGTCCGAGCACATGCCCAACGAACC CAG | | |
| | Px.mut(I-M) R | CTGGGTTTCGTTGGGCATGTGCTCGGAC AAG | | |
| M2 | Px.M2pvu-SDM-f | CAAGCCTGGTGCATCGGCAAGCTGTA CAAC | | Introduction of PvuI site |
| | Px.M2pvu-SDM-R | GTTGTACAGCTTGCCGATCGCACCAGG CTTG | | |
| N term | Px.NO-tag-F | GCCACCATGGCGGAAGCGGAAGGGG | | for the untagged construct |
| | Px.NotI -F | CAGCGGCCGCATGGCGGAAGCGGAAG GG | | For the eGFP fusion |

References

1. Hazell, P.B.R., *The Asian green revolution*. Proven successes in agricultural development: a technical compendium to Millions Fed, ed. D.J. Spielman and R. Pandya-Lorch. 2010, Washington: International Food Policy Research Institute. 67-97.
2. Popp, J., K. Peto, and J. Nagy, *Pesticide productivity and food security. A review*. Agronomy for Sustainable Development, 2013. **33**(1): p. 243-255.
3. FAO, *Feeding the world in 2050. World agricultural summit on food security, Rome 12-13 October 2009* 2009: p. 1-4.
4. Pingali, P.L., *Green Revolution: Impacts, limits, and the path ahead*. Proceedings of the National Academy of Sciences of the United States of America, 2012. **109**(31): p. 12302-12308.
5. Oerke, E.C., *Crop losses to pests*. Journal of Agricultural Science, 2006. **144**: p. 31-43.
6. Grube, A., et al., *Pesticides Industry Sales and Usage 2006 and 2007 Market Estimates*. U.S. Environmental Protection Agency, 2011.
7. Anonymous, *Global Markets for Biopesticides*. BCC research, 2012.
8. Carson, R., L. Darling, and L. Darling, *Silent spring*. 1962, Boston, Cambridge, Mass.: Houghton Mifflin; Riverside Press. 368p.
9. Bass, C. and L.M. Field, *Gene amplification and insecticide resistance*. Pest Management Science, 2011. **67**(8): p. 886-890.
10. Bale, J.S., J.C. van Lenteren, and F. Bigler, *Biological control and sustainable food production*. Philosophical transactions of the Royal Society of London. Series B, Biological sciences, 2008. **363**(1492): p. 761-76.
11. Schnepf, E., et al., *Bacillus thuringiensis and its pesticidal crystal proteins*. Microbiology and molecular biology reviews: MMBR, 1998. **62**(3): p. 775-806.
12. Hilder, V.A. and D. Boulter, *Genetic engineering of crop plants for insect resistance - a critical review*. Crop Protection, 1999. **18**(3): p. 177-191.
13. R. H. Phipps, J.R.P., *Environmental Benefits of Genetically Modified Crops: Global and European Perspectives on Their Ability to Reduce Pesticide Use*. Journal of Animal and Feed Sciences, 2002. **11**.
14. Knipling, E.F., *DDT insecticides developed for use by the armed forces*. Journal of Economic Entomology, 1945. **38**(2): p. 205-207.
15. *D.D.T.: New Synthetic Insecticide*. British medical journal, 1944. **2**(4362): p. 217-8.
16. Nauen, R., *Insecticide mode of action: return of the ryanodine receptor*. Pest Management Science, 2006. **62**(8): p. 690-692.
17. Cordova, D., et al., *Anthranilic diamides: A new class of insecticides with a novel mode of action, ryanodine receptor activation*. Pesticide Biochemistry and Physiology, 2006. **84**(3): p. 196-214.
18. Lahm, G.P., D. Cordova, and J.D. Barry, *New and selective ryanodine receptor activators for insect control*. Bioorganic & Medicinal Chemistry, 2009. **17**(12): p. 4127-4133.
19. Troczka, B., et al., *Resistance to diamide insecticides in diamondback moth, *Plutella xylostella* (Lepidoptera: Plutellidae) is associated with a mutation in the membrane-spanning domain of the ryanodine receptor*. Insect Biochemistry and Molecular Biology, 2012. **42**(11): p. 873-880.
20. Anonymous, *EPA R.E.D facts Ryanodine* 1999.
21. Usherwood, P.N.R. and H. Vais, *Towards the development of ryanoid insecticides with low mammalian toxicity*. Toxicology Letters, 1995. **82-3**: p. 247-254.

References

22. Sattelle, D.B., D. Cordova, and T.R. Cheek, *Insect ryanodine receptors: molecular targets for novel pest control chemicals*. Invertebrate Neuroscience, 2008. **8**(3): p. 107-119.
23. Shiomi, K., et al., *Verticillide, a new ryanodine-binding inhibitor, produced by Verticillium sp FKI-1033*. Journal of Antibiotics, 2010. **63**(2): p. 77-82.
24. Jeanguenat, A., *The story of a new insecticidal chemistry class: the diamides*. Pest Management Science, 2013. **69**(1): p. 7-14.
25. Yan, T., et al., *Design, Synthesis and Biological Activities of Novel Anthranilic Isophthaloyl Amide*. Chemical Journal of Chinese Universities-Chinese, 2011. **32**(8): p. 1750-1754.
26. Zhao, Y., et al., *Synthesis, crystal structure and biological activity of novel anthranilic diamide insecticide containing alkyl ether group*. Molecular Diversity, 2012. **16**(4): p. 711-725.
27. Hamaguchi, H., et al., *Insecticides Affecting Calcium Homeostasis*, in *Modern Crop Protection Compounds*. 2012, Wiley-VCH Verlag GmbH & Co. KGaA. p. 1389-1425.
28. Isaacs, A.K., et al., *Insect ryanodine receptor: distinct but coupled insecticide binding sites for N-C(3)H(3) chlorantraniliprole, flubendiamide, and (3)H ryanodine*. Chemical research in toxicology, 2012. **25**(8): p. 1571-3.
29. Ebbinghaus-Kintscher, U., et al., *Phthalic acid diamides activate ryanodine-sensitive Ca²⁺ release channels in insects*. Cell Calcium, 2006. **39**(1): p. 21-33.
30. Kato, K., et al., *Molecular characterization of flubendiamide sensitivity in the Lepidopterous ryanodine receptor Ca²⁺ release channel*. Biochemistry, 2009. **48**(43): p. 10342-10352.
31. Ebbinghaus-Kintscher, U., et al., *Flubendiamide, the first insecticide with a novel mode of action on insect ryanodine receptors*. Pflanzenschutz-Nachrichten Bayer, 2007. **60**(2): p. 117-140.
32. Dinter, A., et al., *Chlorantraniliprole (DPX-E2Y45, DuPont TM Rynaxypyr, Coragen and Altacor insecticide) - a novel anthranilic diamide insecticide - demonstrating low toxicity and low risk for beneficial insects and predatory mites*. IOBC/WPRS Bulletin, 2008. **35**: p. 128-135.
33. Tohnishi, M., et al., *Development of a Novel Insecticide, Flubendiamide*. Journal of Pesticide Science, 2010. **35**(4): p. 490-491.
34. Larson, J.L., C.T. Redmond, and D.A. Potter, *Comparative impact of an anthranilic diamide and other insecticidal chemistries on beneficial invertebrates and ecosystem services in turfgrass*. Pest Management Science, 2012. **68**(5): p. 740-748.
35. Goulson, D., *REVIEW: An overview of the environmental risks posed by neonicotinoid insecticides*. Journal of Applied Ecology, 2013. **50**(4): p. 977-987.
36. Ramanaidu, K., et al., *Laboratory and field susceptibility of blueberry spanworm (Lepidoptera: Geometridae) to conventional and reduced-risk insecticides*. Crop Protection, 2011. **30**(12): p. 1643-1648.
37. Wang, X., et al., *Baseline Susceptibility of the Diamondback Moth (Lepidoptera: Plutellidae) to Chlorantraniliprole in China*. Journal of Economic Entomology, 2010. **103**(3): p. 843-848.
38. Roditakis, E., et al., *Determination of baseline susceptibility of European populations of Tuta absoluta (Meyrick) to indoxacarb and chlorantraniliprole using a novel dip bioassay method*. Pest Management Science, 2013. **69**(2): p. 217-227.
39. Su, J.Y., T.C. Lai, and J. Li, *Susceptibility of field populations of Spodoptera litura (Fabricius) (Lepidoptera: Noctuidae) in China to chlorantraniliprole and the activities of detoxification enzymes*. Crop Protection, 2012. **42**: p. 217-222.
40. Wang, X. and Y. Wu, *High levels of resistance to chlorantraniliprole evolved in field populations of Plutella xylostella*. Journal of Economic Entomology, 2012. **105**(3): p. 1019-1023.
41. Tohnishi, M., et al., *Flubendiamide, a novel insecticide highly active against lepidopterous insect pests*. Journal of Pesticide Science, 2005. **30**(4): p. 354-360.

References

42. Masaki, T., et al., *Flubendiamide, a novel Ca²⁺ channel modulator, reveals evidence for functional cooperation between Ca²⁺ pumps and Ca²⁺ release*. *Molecular Pharmacology*, 2006. **69**(5): p. 1733-1739.
43. Stael, S., et al., *Plant organellar calcium signalling: an emerging field*. *Journal of Experimental Botany*, 2012. **63**(4): p. 1525-1542.
44. Knight, A.L. and L. Flexner, *Disruption of mating in codling moth (Lepidoptera: Tortricidae) by chlorantranilipole, an anthranilic diamide insecticide*. *Pest Management Science*, 2007. **63**(2): p. 180-9.
45. Lahm, G.P., et al., *Rynaxypyr (TM): A new insecticidal anthranilic diamide that acts as a potent and selective ryanodine receptor activator*. *Bioorganic & Medicinal Chemistry Letters*, 2007. **17**(22): p. 6274-6279.
46. Legocki, J., I. Połec, and K. Żelechowski, *Contemporary trends in development of active substances possessing the pesticidal properties: ryanodine-receptor targeting insecticides*. *Pesticides 2008*(3-4): p. 15-26.
47. Foster, S.P., et al., *Susceptibility of standard clones and European field populations of the green peach aphid, Myzus persicae, and the cotton aphid, Aphis gossypii (Hemiptera: Aphididae), to the novel anthranilic diamide insecticide cyantraniliprole*. *Pest Management Science*, 2012. **68**(4): p. 629-633.
48. Taylor, C.W., D.L. Prole, and T. Rahman, *Ca²⁺ Channels on the Move*. *Biochemistry*, 2009. **48**(51): p. 12062-12080.
49. Berridge, M.J., M.D. Bootman, and H.L. Roderick, *Calcium signalling: Dynamics, homeostasis and remodelling*. *Nature Reviews Molecular Cell Biology*, 2003. **4**(7): p. 517-529.
50. McNally, B.A. and M. Prakriya, *Permeation, selectivity and gating in store-operated CRAC channels*. *Journal of Physiology-London*, 2012. **590**(17): p. 4179-4191.
51. Carafoli, E., et al., *Generation, control, and processing of cellular calcium signals*. *Critical reviews in biochemistry and molecular biology*, 2001. **36**(2): p. 107-260.
52. Zalk, R., S.E. Lehnart, and A.R. Marks, *Modulation of the ryanodine receptor and intracellular calcium*. *Annual Review of Biochemistry*, 2007. **76**: p. 367-385.
53. Meur, G., et al., *Targeting and retention of type 1 ryanodine receptors to the endoplasmic reticulum*. *Journal of Biological Chemistry*, 2007. **282**(32): p. 23096-23103.
54. Takeshima, H., et al., *Generation and characterization of mutant mice lacking ryanodine receptor type 3*. *Journal of Biological Chemistry*, 1996. **271**(33): p. 19649-19652.
55. Furuichi, T., et al., *Primary structure and functional expression of the inositol 1,4,5-trisphosphate-binding protein P400*. *Nature*, 1989. **342**(6245): p. 32-8.
56. Taylor, C.W. and D. Traynor, *Calcium and inositol trisphosphate receptors*. *Journal of Membrane Biology*, 1995. **145**(2): p. 109-118.
57. Mikoshiba, K., *Role of IP3 receptor in development*. *Cell Calcium*, 2011. **49**(5): p. 331-340.
58. Fill, M. and J.A. Copello, *Ryanodine receptor calcium release channels*. *Physiological Reviews*, 2002. **82**(4): p. 893-922.
59. Caride, A.J., et al., *Delayed activation of the plasma membrane calcium pump by a sudden increase in Ca²⁺: fast pumps reside in fast cells*. *Cell Calcium*, 2001. **30**(1): p. 49-57.
60. Chorna, T. and G. Hasan, *The genetics of calcium signaling in Drosophila melanogaster*. *Biochimica Et Biophysica Acta-General Subjects*, 2012. **1820**(8): p. 1269-1282.
61. Takeshima, H., et al., *Excitation-contraction uncoupling and muscular degeneration in mice lacking functional skeletal-muscle ryanodine-receptor gene*. *Nature*, 1994. **369**(6481): p. 556-559.
62. Franzini, C., *Studies of triad .I. structure of junction in frog twitch fibers*. *Journal of Cell Biology*, 1970. **47**(2): p. 488-&.

References

63. Lai, F.A., et al., *Purification, Photoaffinity-Labeling, Structure and Functional Reconstitution of the Ca²⁺ Release Channel from Skeletal Sarcoplasmic-Reticulum*. Biophysical Journal, 1988. **53**(2): p. A469-A469.
64. Inui, M., A. Saito, and S. Fleischer, *Purification of the ryanodine receptor and identity with feet structures of junctional terminal cisternae of sarcoplasmic-reticulum from fast skeletal-muscle*. Journal of Biological Chemistry, 1987. **262**(4): p. 1740-1747.
65. Blayney, L.M. and F.A. Lai, *Ryanodine receptor-mediated arrhythmias and sudden cardiac death*. Pharmacology & Therapeutics, 2009. **123**(2): p. 151-177.
66. Murayama, T. and Y. Ogawa, *Purification and characterization of two ryanodine-binding protein isoforms from sarcoplasmic reticulum of bullfrog skeletal muscle*. J Biochem, 1992. **112**(4): p. 514-22.
67. Ottini, L., et al., *Alpha and beta isoforms of ryanodine receptor from chicken skeletal muscle are the homologues of mammalian RyR1 and RyR3*. Biochem J, 1996. **315** (Pt 1): p. 207-16.
68. Lanner, J.T., et al., *Ryanodine Receptors: Structure, Expression, Molecular Details, and Function in Calcium Release*. Cold Spring Harbor Perspectives in Biology, 2010. **2**(11).
69. Takeshima, H., et al., *Embryonic lethality and abnormal cardiac myocytes in mice lacking ryanodine receptor type 2*. EMBO Journal, 1998. **17**(12): p. 3309-3316.
70. *Ryanodine receptors: Structure, function and dysfunction in clinical disease*. Developments in Cardiovascular Medicine, ed. X.H.T.M. Wehrens, A. R. 2005: Springer 330.
71. Bers, D.M., *Cardiac excitation-contraction coupling*. Nature, 2002. **415**(6868): p. 198-205.
72. Dulhunty, A.F., et al., *Interactions between dihydropyridine receptors and ryanodine receptors in striated muscle*. Progress in Biophysics & Molecular Biology, 2002. **79**(1-3): p. 45-75.
73. Galione, A., H.C. Lee, and W.B. Busa, *Ca²⁺-Induced Ca²⁺ Release in Sea-Urchin Egg Homogenates - Modulation by Cyclic Adp-Ribose*. Science, 1991. **253**(5024): p. 1143-1146.
74. Wehrens, X.H.T., *Ryanodine receptors: An emerging therapeutic target for heart failure and cardiac arrhythmias*. Drug Development Research, 2005. **66**(3): p. 215-215.
75. Wei, L. and R.T. Dirksen, *Chapter 7 - Ryanodinopathies: RyR-Linked Muscle Diseases*, in *Current Topics in Membranes*, I.S. Irina, Editor. 2010, Academic Press. p. 139-167.
76. Larach, M.G., et al., *Clinical presentation, treatment, and complications of malignant hyperthermia in North America from 1987 to 2006*. Anesth Analg, 2010. **110**(2): p. 498-507.
77. Monnier, N., et al., *Familial and sporadic forms of central core disease are associated with mutations in the C-terminal domain of the skeletal muscle ryanodine receptor*. Human Molecular Genetics, 2001. **10**(22): p. 2581-2592.
78. Protasi, F., C. Paolini, and M. Dainese, *Calsequestrin-1: a new candidate gene for malignant hyperthermia and exertional/environmental heat stroke*. Journal of Physiology-London, 2009. **587**(13): p. 3095-3100.
79. Hwang, J.H., et al., *Mapping domains and mutations on the skeletal muscle ryanodine receptor channel*. Trends in Molecular Medicine, 2012. **18**(11): p. 644-657.
80. Boncompagni, S., et al., *Characterization and temporal development of cores in a mouse model of malignant hyperthermia*. Proc Natl Acad Sci U S A, 2009. **106**(51): p. 21996-2001.
81. Zvaritch, E., et al., *Ca²⁺ dysregulation in Ryr1(I4895T/wt) mice causes congenital myopathy with progressive formation of minicores, cores, and nemaline rods*. Proc Natl Acad Sci U S A, 2009. **106**(51): p. 21813-8.

References

82. Priori, S.G., et al., *Clinical and molecular characterization of patients with catecholaminergic polymorphic ventricular tachycardia*. *Circulation*, 2002. **106**(1): p. 69-74.
83. Ran, Y.Q., et al., *Common RyR2 variants associate with ventricular arrhythmias and sudden cardiac death in chronic heart failure*. *Clinical Science*, 2010. **119**(5-6): p. 215-223.
84. Hamilton, S.L., *Ryanodine receptors*. *Cell Calcium*, 2005. **38**(3-4): p. 253-260.
85. Serysheva, I., et al., *Structure of Ca²⁺ release channel at 14 angstrom resolution*. *Journal of Molecular Biology*, 2005. **345**(3): p. 427-431.
86. Baker, M.L., et al., *The skeletal muscle Ca²⁺ release channel has an oxidoreductase-like domain*. *Proceedings of the National Academy of Sciences*, 2002. **99**(19): p. 12155-12160.
87. Ludtke, S.J., et al., *The pore structure of the closed RyR1 channel*. *Structure*, 2005. **13**(8): p. 1203-1211.
88. Sharma, M.R., et al., *Three-dimensional structure of ryanodine receptor isoform three in two conformational states as visualized by cryo-electron microscopy*. *Journal of Biological Chemistry*, 2000. **275**(13): p. 9485-9491.
89. Hamilton, S.L. and Serysheva, II, *Ryanodine Receptor Structure: Progress and Challenges*. *Journal of Biological Chemistry*, 2009. **284**(7): p. 4047-4051.
90. Song, D.W., et al., *Ryanodine receptor assembly: A novel systems biology approach to 3D mapping*. *Progress in Biophysics & Molecular Biology*, 2011. **105**(3): p. 145-161.
91. Kimlicka, L., et al., *Disease mutations in the ryanodine receptor N-terminal region couple to a mobile intersubunit interface*. *Nature Communications*, 2013. **4**.
92. Ikemoto, N. and T. Yamamoto, *Postulated Role of Inter-domain Interaction within the Ryanodine Receptor in Ca²⁺ Channel Regulation*. *Trends in Cardiovascular Medicine*, 2000. **10**(7): p. 310-316.
93. Van Petegem, F., *Ryanodine receptors: structure and function*. *J Biol Chem*, 2012. **287**(38): p. 31624-32.
94. Serysheva, II, et al., *Subnanometer-resolution electron cryomicroscopy-based domain models for the cytoplasmic region of skeletal muscle RyR channel*. *Proceedings of the National Academy of Sciences of the United States of America*, 2008. **105**(28): p. 9610-9615.
95. George, C.H., et al., *Ryanodine receptor regulation by intramolecular interaction between cytoplasmic and transmembrane domains*. *Molecular Biology of the Cell*, 2004. **15**(6): p. 2627-2638.
96. Samsó, M., T. Wagenknecht, and P.D. Allen, *Internal structure and visualization of transmembrane domains of the RyR1 calcium release channel by cryo-EM*. *Nature Structural & Molecular Biology*, 2005. **12**(6): p. 539-544.
97. Bhat, M.B., et al., *Functional calcium release channel formed by the carboxyl-terminal portion of ryanodine receptor*. *Biophysical Journal*, 1997. **73**(3): p. 1329-1336.
98. Du, G.G., et al., *Topology of the Ca²⁺ release channel of skeletal muscle sarcoplasmic reticulum (RyR1)*. *Proceedings of the National Academy of Sciences of the United States of America*, 2002. **99**(26): p. 16725-16730.
99. Takeshima, H., et al., *Primary Structure and Expression from Complementary-DNA of Skeletal-Muscle Ryanodine Receptor*. *Nature*, 1989. **339**(6224): p. 439-445.
100. Zorzato, F., et al., *Molecular-Cloning of cDNA-Encoding Human and Rabbit Forms of the Ca²⁺ Release Channel (Ryanodine Receptor) of Skeletal-Muscle Sarcoplasmic-Reticulum*. *Journal of Biological Chemistry*, 1990. **265**(4): p. 2244-2256.
101. Tunwell, R.E.A., et al., *The human cardiac muscle ryanodine receptor-calcium release channel: Identification, primary structure and topological analysis*. *Biochemical Journal*, 1996. **318**: p. 477-487.

References

102. Stewart, R., S. Zissimopoulos, and F.A. Lai, *Oligomerization of the cardiac ryanodine receptor C-terminal tail*. *Biochemical Journal*, 2003. **376**: p. 795-799.
103. Gao, L., et al., *Evidence for a role of C-terminal amino acid residues in skeletal muscle Ca²⁺ release channel (ryanodine receptor) function*. *FEBS Letters*, 1997. **412**(1): p. 223-226.
104. Carney, J., et al., *The Ryanodine Receptor Pore: Is There a Consensus View? Structure and Function of Calcium Release Channels*, 2010. **66**: p. 49-67.
105. Smith, J.S., et al., *Purified Ryanodine Receptor from Rabbit Skeletal-Muscle Is the Calcium-Release Channel of Sarcoplasmic-Reticulum*. *Journal of General Physiology*, 1988. **92**(1): p. 1-26.
106. Tinker, A., A.R.G. Lindsay, and A.J. Williams, *A Model for Ionic-Conduction in the Ryanodine Receptor Channel of Sheep Cardiac-Muscle Sarcoplasmic-Reticulum*. *Journal of General Physiology*, 1992. **100**(3): p. 495-517.
107. Kang, G.B., et al., *Overexpression and purification of the RyR1 pore-forming region*. *Protein and Peptide Letters*, 2007. **14**(8): p. 742-746.
108. Balshaw, D., L. Gao, and G. Meissner, *Luminal loop of the ryanodine receptor: A pore-forming segment?* *Proceedings of the National Academy of Sciences of the United States of America*, 1999. **96**(7): p. 3345-3347.
109. Welch, W., et al., *A model of the putative pore region of the cardiac ryanodine receptor channel*. *Biophysical Journal*, 2004. **87**(4): p. 2335-2351.
110. Ramachandran, S., et al., *Structural Determinants of Skeletal Muscle Ryanodine Receptor Gating*. *Journal of Biological Chemistry*, 2013. **288**(9): p. 6154-6165.
111. Gillespie, D., et al., *(De)constructing the ryanodine receptor: Modeling ion permeation and selectivity of the calcium release channel*. *Journal of Physical Chemistry B*, 2005. **109**(32): p. 15598-15610.
112. Yin, C.C., L.G. D'Cruz, and F.A. Lai, *Ryanodine receptor arrays: not just a pretty pattern?* *Trends in Cell Biology*, 2008. **18**(4): p. 149-156.
113. Block, B.A., et al., *Structural evidence for direct interaction between the molecular-components of the transverse tubule sarcoplasmic-reticulum junction in skeletal-muscle*. *Journal of Cell Biology*, 1988. **107**(6): p. 2587-2600.
114. Bray, D., M.D. Levin, and C.J. Morton-Firth, *Receptor clustering as a cellular mechanism to control sensitivity*. *Nature*, 1998. **393**(6680): p. 85-88.
115. Soeller, C., et al., *Analysis of ryanodine receptor clusters in rat and human cardiac myocytes*. *Proceedings of the National Academy of Sciences of the United States of America*, 2007. **104**(38): p. 14958-14963.
116. Takasago, T., et al., *Regulation of the cardiac ryanodine receptor by protein kinase-dependent phosphorylation*. *Journal of Biochemistry*, 1991. **109**(1): p. 163-170.
117. Wehrens, X.H.T., et al., *FKBP12.6 Deficiency and Defective Calcium Release Channel (Ryanodine Receptor) Function Linked to Exercise-Induced Sudden Cardiac Death*. *Cell*, 2003. **113**(7): p. 829-840.
118. Reiken, S., et al., *PKA phosphorylation activates the calcium release channel (ryanodine receptor) in skeletal muscle: defective regulation in heart failure*. *Journal of Cell Biology*, 2003. **160**(6): p. 919-928.
119. Mackrill, J.J., *Protein-protein interactions in intracellular Ca²⁺-release channel function*. *Biochemical Journal*, 1999. **337**: p. 345-361.
120. Witcher, D.R., et al., *Unique phosphorylation site on the cardiac ryanodine receptor regulates calcium-channel activity*. *Journal of Biological Chemistry*, 1991. **266**(17): p. 11144-11152.
121. Antos, C.L., et al., *Dilated cardiomyopathy and sudden death resulting from constitutive activation of protein kinase A*. *Circulation Research*, 2001. **89**(11): p. 997-1004.
122. MacMillan, D., *FK506 binding proteins: Cellular regulators of intracellular Ca²⁺ signalling*. *European Journal of Pharmacology*, 2013. **700**(1-3): p. 181-193.
123. George, C.H., et al., *In situ modulation of the human cardiac ryanodine receptor (hRyR2) by FKBP12.6*. *Biochemical Journal*, 2003. **370**: p. 579-589.

References

124. George, C.H., et al., *Dysregulated ryanodine receptors mediate cellular toxicity - Restoration of normal phenotype by FKBP12.6*. Journal of Biological Chemistry, 2003. **278**(31): p. 28856-28864.
125. Brillantes, A.M.B., et al., *Stabilization of calcium-release channel (ryanodine receptor) function by FK506-binding protein*. Cell, 1994. **77**(4): p. 513-523.
126. Gangopadhyay, J.P. and N. Ikemoto, *Role of the Met3534-Ala4271 Region of the Ryanodine Receptor in the Regulation of Ca²⁺ Release Induced by Calmodulin Binding Domain Peptide*. Biophysical Journal, 2006. **90**(6): p. 2015-2026.
127. Rodney, G.G., et al., *Regulation of RYR1 activity by Ca²⁺ and calmodulin*. Biochemistry, 2000. **39**(26): p. 7807-7812.
128. Yamaguchi, N., et al., *Molecular basis of calmodulin binding to cardiac muscle Ca²⁺ release channel (ryanodine receptor)*. Journal of Biological Chemistry, 2003. **278**(26): p. 23480-23486.
129. Yamaguchi, N., et al., *Early cardiac hypertrophy in mice with impaired calmodulin regulation of cardiac muscle Ca²⁺ release channel*. Journal of Clinical Investigation, 2007. **117**(5): p. 1344-1353.
130. Ono, M., et al., *Dissociation of calmodulin from cardiac ryanodine receptor causes aberrant Ca²⁺ release in heart failure*. Cardiovascular Research, 2010. **87**(4): p. 609-617.
131. Beard, N.A., et al., *Phosphorylation of skeletal muscle calsequestrin enhances its Ca²⁺ binding capacity and promotes its association with junctin*. Cell Calcium, 2008. **44**(4): p. 363-373.
132. MacLennan, D.H. and P.T. Wong, *Isolation of a calcium-sequestering protein from sarcoplasmic reticulum*. Proceedings of the National Academy of Sciences of the United States of America, 1971. **68**(6): p. 1231-5.
133. Yano, K. and A. Zarain-Herzberg, *Sarcoplasmic reticulum calsequestrins: structural and functional properties*. Mol Cell Biochem, 1994. **135**(1): p. 61-70.
134. Zhang, L., et al., *Complex formation between junctin, triadin, calsequestrin, and the ryanodine receptor - Proteins of the cardiac junctional sarcoplasmic reticulum membrane*. Journal of Biological Chemistry, 1997. **272**(37): p. 23389-23397.
135. Wei, L., et al., *The Conformation of Calsequestrin Determines Its Ability to Regulate Skeletal Ryanodine Receptors*. Biophysical Journal, 2006. **91**(4): p. 1288-1301.
136. Knollmann, B.C., et al., *Casq2 deletion causes sarcoplasmic reticulum volume increase, premature Ca²⁺ release, and catecholaminergic polymorphic ventricular tachycardia*. Journal of Clinical Investigation, 2006. **116**(9): p. 2510-2520.
137. Dainese, M., et al., *Anesthetic- and heat-induced sudden death in calsequestrin-1-knockout mice*. Faseb Journal, 2009. **23**(6): p. 1710-1720.
138. Gyorke, I., et al., *The role of calsequestrin, triadin, and junctin in conferring cardiac ryanodine receptor responsiveness to luminal calcium*. Biophys J, 2004. **86**(4): p. 2121-8.
139. Bers, D.M., *Macromolecular complexes regulating cardiac ryanodine receptor function*. Journal of Molecular and Cellular Cardiology, 2004. **37**(2): p. 417-429.
140. Farrell, E.F., et al., *Sorcin inhibits calcium release and modulates excitation-contraction coupling in the heart*. Journal of Biological Chemistry, 2003. **278**(36): p. 34660-34666.
141. West, D.J. and A.J. Williams, *Pharmacological regulators of intracellular calcium release channels*. Current Pharmaceutical Design, 2007. **13**(24): p. 2428-2442.
142. Fruen, B.R., J.R. Mickelson, and C.F. Louis, *Dantrolene inhibition of sarcoplasmic reticulum Ca²⁺ release by direct and specific action at skeletal muscle ryanodine receptors*. Journal of Biological Chemistry, 1997. **272**(43): p. 26965-26971.
143. Bezprozvanny, I.B., et al., *Activation of the calcium release channel (ryanodine receptor) by heparin and other polyanions is calcium-dependent*. Molecular Biology of the Cell, 1993. **4**(3): p. 347-352.

References

144. Gurrola, G.B., et al., *Activation of ryanodine receptors by imperatoxin A and a peptide segment of the II-III loop of the dihydropyridine receptor*. Journal of Biological Chemistry, 1999. **274**(12): p. 7879-7886.
145. HerrmannFrank, A., et al., *4-chloro-m-cresol, a potent and specific activator of the skeletal muscle ryanodine receptor*. Biochimica Et Biophysica Acta-General Subjects, 1996. **1289**(1): p. 31-40.
146. Rousseau, E., et al., *Activation of the Ca²⁺ release channel of skeletal-muscle sarcoplasmic-reticulum by caffeine and related-compounds*. Archives of Biochemistry and Biophysics, 1988. **267**(1): p. 75-86.
147. Smith, J.S., R. Coronado, and G. Meissner, *Single channel measurements of the calcium release channel from skeletal-muscle sarcoplasmic-reticulum - activation by Ca²⁺ and ATP and modulation by Mg²⁺*. Journal of General Physiology, 1986. **88**(5): p. 573-588.
148. Popova, O.B., et al., *Identification of ATP-Binding Regions in the RyR1 Ca²⁺ Release Channel*. PLOS One, 2012. **7**(11).
149. Blayney, L., et al., *ATP interacts with the CPVT mutation-associated central domain of the cardiac ryanodine receptor*. Biochimica Et Biophysica Acta-General Subjects, 2013. **1830**(10): p. 4426-4432.
150. Mickelson, J.R. and C.F. Louis, *Malignant hyperthermia: Excitation-contraction coupling, Ca²⁺ release channel, and cell Ca²⁺ regulation defects*. Physiological Reviews, 1996. **76**(2): p. 537-592.
151. Zhao, F.Y., et al., *Dantrolene inhibition of ryanodine receptor Ca²⁺ release channels - Molecular mechanism and isoform selectivity*. Journal of Biological Chemistry, 2001. **276**(17): p. 13810-13816.
152. Williams, A.J. and B. Tanna, *The interaction of ryanoids with individual ryanodine receptor channels*. Biological Research, 2004. **37**(4): p. 527-538.
153. Tanna, B., et al., *Voltage-sensitive equilibrium between two states within a ryanoid-modified conductance state of the ryanodine receptor channel*. Biophysical Journal, 2005. **88**(4): p. 2585-2596.
154. Holmberg, S.R.M. and A.J. Williams, *The cardiac sarcoplasmic-reticulum calcium-release channel - modulation of ryanodine binding and single-channel activity*. Biochimica Et Biophysica Acta, 1990. **1022**(2): p. 187-193.
155. Zimanyi, I. and I.N. Pessah, *Pharmacological characterization of the specific binding of [3H]ryanodine to rat brain microsomal membranes*. Brain Research, 1991. **561**(2): p. 181-191.
156. Pessah, I.N. and I. Zimanyi, *Characterization of multiple H-3 ryanodine binding-sites on the Ca-2+ release channel of sarcoplasmic-reticulum from skeletal and cardiac-muscle - evidence for a sequential mechanism in ryanodine action*. Molecular Pharmacology, 1991. **39**(5): p. 679-689.
157. Wang, R., et al., *Residue Gln4863 within a predicted transmembrane sequence of the Ca²⁺ release channel (ryanodine receptor) is critical for ryanodine interaction*. The Journal of biological chemistry, 2003. **278**(51): p. 51557-65.
158. Ranatunga, K.M., et al., *The Gln(4863)Ala mutation within a putative, pore-lining transmembrane helix of the cardiac ryanodine receptor channel alters both the kinetics of ryanoid interaction and the subsequent fractional conductance*. Molecular Pharmacology, 2005. **68**(3): p. 840-846.
159. Ogawa, Y., *Distinct mechanisms for dysfunctions of mutated ryanodine receptor isoforms*. Biochemical and Biophysical Research Communications, 2008. **369**(1): p. 208-212.
160. Fessenden, J.D., et al., *Mutational analysis of putative calcium binding motifs within the skeletal ryanodine receptor isoform, RyR1*. Journal of Biological Chemistry, 2004. **279**(51): p. 53028-53035.
161. Sobie, E.A., et al., *Termination of cardiac Ca²⁺ sparks: An investigative mathematical model of calcium-induced calcium release*. Biophysical Journal, 2002. **83**(1): p. 59-78.

References

162. Loesser, K.E., L. Castellani, and C. Franziniarmstrong, *Dispositions of Junctional Feet in Muscles of Invertebrates*. Journal of Muscle Research and Cell Motility, 1992. **13**(2): p. 161-173.
163. Xu, X.H., et al., *Molecular cloning of cDNA encoding a Drosophila ryanodine receptor and functional studies of the carboxyl-terminal calcium release channel*. Biophysical Journal, 2000. **78**(3): p. 1270-1281.
164. Xiong, H., et al., *Identification of a two EF-hand Ca²⁺ binding domain in lobster skeletal muscle ryanodine receptor/Ca²⁺ release channel*. Biochemistry, 1998. **37**(14): p. 4804-4814.
165. Wang, X., et al., *Molecular cloning, characterization and mRNA expression of a ryanodine receptor gene from diamondback moth, Plutella xylostella*. Pesticide Biochemistry and Physiology, 2012. **102**(3): p. 204-212.
166. Sakube, Y., H. Ando, and H. Kagawa, *Cloning and mapping of a ryanodine receptor homolog gene of Caenorhabditis-elegans*, in *Molecular Basis of Ion Channels and Receptors Involved in Nerve Excitation, Synaptic Transmission and Muscle Contraction: In Memory of Professor Shosaku Numa*, H. Higashida, T. Yoshioka, and K. Mikoshiba, Editors. 1993, New York Acad Sciences: New York. p. 540-545.
167. Hamada, T., et al., *Molecular Dissection, Tissue Localization and Ca²⁺ Binding of the Ryanodine Receptor of Caenorhabditis elegans*. Journal of Molecular Biology, 2002. **324**(1): p. 123-135.
168. Takeshima, H., et al., *Isolation and characterization of a gene for a ryanodine receptor/calcium release channel in Drosophila melanogaster*. FEBS Letters, 1994. **337**(1): p. 81-87.
169. Puente, E., et al., *Identification of a polymorphic ryanodine receptor gene from Heliothis virescens (Lepidoptera : Noctuidae)*. Insect Biochemistry and Molecular Biology, 2000. **30**(4): p. 335-347.
170. Wang, J., et al., *Molecular characterization of a ryanodine receptor gene in the rice leaffolder, Cnaphalocrocis medinalis (Guenee)*. PLOS One, 2012. **7**(5): p. e36623.
171. Hasan, G. and M. Rosbash, *Drosophila homologs of 2 mammalian intracellular Ca²⁺-release channels - identification and expression patterns of the inositol 1,4,5-triphosphate and the ryanodine receptor genes*. Development, 1992. **116**(4): p. 967-&.
172. Vazquez-Martinez, O., et al., *Biochemical characterization, distribution and phylogenetic analysis of Drosophila melanogaster ryanodine and IP₃ receptors, and thapsigargin-sensitive Ca²⁺ ATPase*. Journal of Cell Science, 2003. **116**(12): p. 2483-2494.
173. Arnon, A., et al., *Calmodulin regulation of calcium stores in phototransduction of Drosophila*. Science, 1997. **275**(5303): p. 1119-21.
174. Sullivan, K.M.C., et al., *The ryanodine receptor is essential for larval development in Drosophila melanogaster*. Proceedings of the National Academy of Sciences of the United States of America, 2000. **97**(11): p. 5942-5947.
175. Maryon, E.B., R. Coronado, and P. Anderson, *unc-68 encodes a ryanodine receptor involved in regulating C. elegans body-wall muscle contraction*. The Journal of Cell Biology, 1996. **134**(4): p. 885-93.
176. Scott-Ward, T.S., et al., *Characterization of the ryanodine receptor-Ca²⁺ release channel from the thoracic tissues of the lepidopteran insect Heliothis virescens*. Journal of Membrane Biology, 2001. **179**(2): p. 127-141.
177. Gao, S.Y., et al., *Drosophila Ryanodine Receptors Mediate General Anesthesia by Halothane*. Anesthesiology, 2013. **118**(3): p. 587-601.
178. Schmitt, M., A. Turberg, and M. Londershausen, *Characterization of a ryanodine receptor in Periplaneta americana*. Journal of Receptor and Signal Transduction Research, 1997. **17**(1-3): p. 185-197.

References

179. Collet, C., *Excitation-contraction coupling in skeletal muscle fibers from adult domestic honeybee*. Pflugers Archiv-European Journal of Physiology, 2009. **458**(3): p. 601-612.
180. Baumann, O., *Distribution of ryanodine receptor Ca^{2+} channels in insect photoreceptor cells*. Journal of Comparative Neurology, 2000. **421**(3): p. 347-361.
181. Takekura, H. and C. Franzini-Armstrong, *The Structure of Ca^{2+} Release Units in Arthropod Body Muscle Indicates an Indirect Mechanism for Excitation-Contraction Coupling*. Biophysical Journal, 2002. **83**(5): p. 2742-2753.
182. Kibbe, W.A., *OligoCalc: an online oligonucleotide properties calculator*. Nucleic Acids Research, 2007. **35**(Web Server issue): p. W43-6.
183. Sambrook, J., E.F. Fritsch, and T. Maniatis, *Molecular Cloning a laboratory manual second editions Vols. 1 2 and 3*. 1989, Cold Spring Harbor, New York, USA. Illus.: Cold Spring Harbor Laboratory Press.
184. Otsu, K., et al., *Molecular-cloning of cDNA-encoding the Ca^{2+} Release Channel (Ryanodine Receptor) of rabbit cardiac-muscle sarcoplasmic-reticulum*. Journal of Biological Chemistry, 1990. **265**(23): p. 13472-13483.
185. Hakamata, Y., et al., *Primary structure and distribution of a novel ryanodine receptor calcium release channel from rabbit brain*. Febs Letters, 1992. **312**(2-3): p. 229-235.
186. George, C.H., C.C. Yin, and F.A. Lai, *Toward a molecular understanding of the structure-function of ryanodine receptor $Ca(2+)$ release channels - Perspectives from recombinant expression systems*. Cell Biochemistry and Biophysics, 2005. **42**(2): p. 197-222.
187. Casper, T., et al., *Isolation and use of ryanodine receptors*. 2010, EI du Pont de Nemours and Company.
188. Guo, L., et al., *Cloning, characterisation and expression profiling of the cDNA encoding the ryanodine receptor in diamondback moth, *Plutella xylostella* (L.) (Lepidoptera: Plutellidae)*. Pest Management Science, 2012. **68**(12): p. 1605-1614.
189. Sun, L.N., et al., *Modulation of the expression of ryanodine receptor mRNA from *Plutella xylostella* as a result of diamide insecticide application*. Gene, 2012. **511**(2): p. 265-273.
190. Furlong, M.J., D.J. Wright, and L.M. Dossdall, *Diamondback moth ecology and management: problems, progress, and prospects*. Annual Review of Entomology, 2013. **58**: p. 517-41.
191. Devonshire, A.L., et al., *The evolution of insecticide resistance in the peach-potato aphid, *Myzus persicae**. Philosophical Transactions of the Royal Society B-Biological Sciences, 1998. **353**(1376): p. 1677-1684.
192. Silva, A.X., et al., *Insecticide Resistance Mechanisms in the Green Peach Aphid *Myzus persicae* (Hemiptera: Aphididae) I: A Transcriptomic Survey*. Plos One, 2012. **7**(6).
193. Talekar, N.S. and A.M. Shelton, *Biology, ecology, and management of the Diamondback moth*. Annual Review of Entomology, 1993. **38**: p. 275-301.
194. Bernard, P., et al., *Positive-selection vectors using the F-plasmid CcdB killer gene*. Gene, 1994. **148**(1): p. 71-74.
195. George, C.H., et al., *Alternative splicing of ryanodine receptors modulates cardiomyocyte Ca^{2+} signaling and susceptibility to apoptosis*. Circulation Research, 2007. **100**(6): p. 874-883.
196. Pfaffl, M.W., *A new mathematical model for relative quantification in real-time RT-PCR*. Nucleic Acids Res, 2001. **29**(9): p. e45.
197. Vandesompele, J., et al., *Accurate normalization of real-time quantitative RT-PCR data by geometric averaging of multiple internal control genes*. Genome Biol, 2002. **3**(7): p. RESEARCH0034.
198. Krogh, A., et al., *Predicting transmembrane protein topology with a hidden markov model: application to complete genomes*. Journal of Molecular Biology, 2001. **305**(3): p. 567-580.

References

199. Zhao, M., et al., *Molecular identification of the ryanodine receptor pore-forming segment*. The Journal of biological chemistry, 1999. **274**(37): p. 25971-4.
200. Wang, R.W., et al., *Residue Gln(4863) within a predicted transmembrane sequence of the Ca²⁺ release channel (ryanodine receptor) is critical for ryanodine interaction*. Journal of Biological Chemistry, 2003. **278**(51): p. 51557-51565.
201. Wang, J., et al., *Molecular cloning and characterization of a ryanodine receptor gene in brown planthopper (BPH), Nilaparvata lugens (Stål)*. Pest Management Science, 2013: p. n/a-n/a.
202. Lai, F.A., et al., *The ryanodine receptor Ca²⁺ release channel complex of skeletal-muscle sarcoplasmic-reticulum - evidence for a cooperatively coupled, negatively charged homotetramer*. Journal of Biological Chemistry, 1989. **264**(28): p. 16776-16785.
203. Samsó, M. and T. Wagenknecht, *Contributions of Electron Microscopy and Single-Particle Techniques to the Determination of the Ryanodine Receptor Three-Dimensional Structure*. Journal of Structural Biology, 1998. **121**(2): p. 172-180.
204. Vaughn, J.L., et al., *Establishment of 2 Cell Lines from Insect Spodoptera-Frugiperda (Lepidoptera-Noctuidae)*. In Vitro-Journal of the Tissue Culture Association, 1977. **13**(4): p. 213-217.
205. Yin, J., et al., *Select what you need: A comparative evaluation of the advantages and limitations of frequently used expression systems for foreign genes*. Journal of Biotechnology, 2007. **127**(3): p. 335-347.
206. Antaramian, A., et al., *Functional expression of recombinant type 1 ryanodine receptor in insect Sf21 cells*. Cell Calcium, 2001. **30**(1): p. 9-17.
207. Jordan, M., A. Schallhorn, and F.M. Wurm, *Transfecting mammalian cells: optimization of critical parameters affecting calcium-phosphate precipitate formation*. Nucleic Acids Research, 1996. **24**(4): p. 596-601.
208. Goldstein, S., C.M. Fordis, and B.H. Howard, *Enhanced transfection efficiency and improved cell-survival after electroporation of g2/m-synchronized cells and treatment with sodium-butyrate*. Nucleic Acids Research, 1989. **17**(10): p. 3959-3971.
209. Deng, G., et al., *Transcriptional regulation of the human placental-like alkaline-phosphatase gene and mechanisms involved in its induction by sodium-butyrate*. Cancer Research, 1992. **52**(12): p. 3378-3383.
210. Sitsapesan, R., R.A. Montgomery, and A.J. Williams, *A novel method for incorporation of ion channels into a planar phospholipid bilayer which allows solution changes on a millisecond timescale*. Pflugers Arch, 1995. **430**(4): p. 584-9.
211. Sitsapesan, R. and A.J. Williams, *Gating of the native and purified cardiac SR Ca(2+)-release channel with monovalent cations as permeant species*. Biophys J, 1994. **67**(4): p. 1484-94.
212. McGarry, S.J. and A.J. Williams, *Activation of the sheep cardiac sarcoplasmic reticulum Ca(2+)-release channel by analogues of sulmazole*. British Journal of Pharmacology, 1994. **111**(4): p. 1212-20.
213. George, C.H. and A. Lai, *In situ regulation of the human cardiac ryanodine receptor (hRyR2) by intramolecular interaction*. Biophysical Journal, 2002. **82**(1): p. 624a-624a.
214. Feyereisen, R., *Molecular biology of insecticide resistance*. Toxicol Lett, 1995. **82-83**: p. 83-90.
215. Ankersmit, G.W., *DDT-resistance in Plutella-maculipennis (curt) (lep) in Java*. Bulletin of Entomological Research, 1953. **44**(3): p. 421-&.
216. Baxter, S.W., et al., *Mis-Spliced Transcripts of Nicotinic Acetylcholine Receptor alpha 6 Are Associated with Field Evolved Spinosad Resistance in Plutella xylostella (L.)*. Plos Genetics, 2010. **6**(1).
217. Sonoda, S., *Molecular analysis of pyrethroid resistance conferred by target insensitivity and increased metabolic detoxification in Plutella xylostella*. Pest Management Science, 2010. **66**(5): p. 572-575.

References

218. Noppun, V., T. Saito, and T. Miyata, *Cuticular penetration of s-fenvalerate in fenvalerate-resistant and susceptible strains of the diamondback moth, Plutella xylostella (L)*. Pesticide Biochemistry and Physiology, 1989. **33**(1): p. 83-87.
219. Afonina, I., et al., *Efficient priming of PCR with short oligonucleotides conjugated to a minor groove binder*. Nucleic Acids Research, 1997. **25**(13): p. 2657-2660.
220. Krogh, A., et al., *Predicting transmembrane protein topology with a hidden Markov model: application to complete genomes*. Journal of Molecular Biology, 2001. **305**(3): p. 567-80.
221. Wu, S., et al., *Molecular and cellular analyses of a ryanodine receptor from hemocytes of Pieris rapae*. Developmental and comparative immunology, 2013. **41**(1).
222. Jouraku, A., et al., *KONAGAbase: a genomic and transcriptomic database for the diamondback moth, Plutella xylostella*. BMC Genomics, 2013. **14**.
223. Valdivia, H.H., *One gene, many proteins - Alternative splicing of the ryanodine receptor gene adds novel functions to an already complex channel protein*. Circulation Research, 2007. **100**(6): p. 761-763.
224. Lehmberg, E. and J.E. Casida, *Similarity of Insect and Mammalian Ryanodine Binding-Sites*. Pesticide Biochemistry and Physiology, 1994. **48**(2): p. 145-152.
225. Qi, S. and J.E. Casida, *Species differences in chlorantraniliprole and flubendiamide insecticide binding sites in the ryanodine receptor*. Pesticide Biochemistry and Physiology, 2013. **107**(3): p. 321-326.
226. Guo, L., et al., *Functional analysis of a point mutation in the ryanodine receptor of Plutella xylostella (L.) associated with resistance to chlorantraniliprole*. Pest Manag Sci, 2013.
227. Tao, Y., et al., *Identification of a critical region in the Drosophila ryanodine receptor that confers sensitivity to diamide insecticides*. Insect biochemistry and molecular biology, 2013. **43**(9): p. 820-8.
228. Teixeira, L.A. and J.T. Andaloro, *Diamide insecticides: Global efforts to address insect resistance stewardship challenges*. Pesticide Biochemistry and Physiology, 2013. **106**(3): p. 76-78.